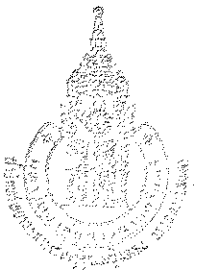

Surface Plasmon Resonance and Electrochemical Affinity Biosensors

Siriwan Suwansa-ard

A Thesis Submitted in Fulfillment of the Requirements

for the Degree of Doctor of Philosophy in Chemistry

Prince of Songkla University

2009

Thesis Title	Surface Plasmon Resonance and Electrochemical Affinity Biosensors
Author	Miss Siriwan Suwansa-ard
Major Program	Chemistry

Major Advisor

.....

(Assoc. Prof. Dr. Panote Thavarungkul)

Co- Advisor

.....

(Assoc. Prof. Dr. Proespichaya Kanatharana)

Examining Committee:

.....Chairperson

(Assoc. Prof. Dr. Wilaiwan Chotigeat)

.....

(Assoc. Prof. Dr. Panote Thavarungkul)

.....

(Assoc. Prof. Dr. Proespichaya Kanatharana)

.....

(Asst. Prof. Dr. Atitaya Siripinyanond)

The Graduate School, Prince of Songkla University, has approved this thesis as fulfillment of the requirements for the Doctor of Philosophy Degree in Chemistry

.....

(Assoc. Prof. Dr. Krerkchai Thongnoo)

Dean of Graduate School

ชื่อวิทยานิพนธ์ เซอร์เฟสพลาสมอนเรโซแนนซ์และอิเล็กโทรเคมีคัลแอฟฟินิตีไบโอเซนเซอร์
ผู้เขียน นางสาวศิริวรรณ สุวรรณสะอาด
สาขา เคมี
ปีการศึกษา 2551

บทคัดย่อ

วิทยานิพนธ์นี้พัฒนาและทดสอบประสิทธิภาพของระบบแอฟฟินิตีไบโอเซนเซอร์แบบไม่ใช้ (label-free) และใช้สารติดฉลาก (label) โดยใช้หลักการตรวจวัดด้วยเซอร์เฟสพลาสมอนเรโซแนนซ์ (surface pasmon resonance; SPR) และเคมีไฟฟ้า (electrochemical) สำหรับระบบแอฟฟินิตีไบโอเซนเซอร์แบบไม่ใช้สารติดฉลาก ในระบบดังกล่าวไบโอรีคอกนิชันอีลีเมนต์ (biological recognition element) จะถูกตรึงบนผิวทอง เมื่อเกิดการจับกันระหว่างสารที่ต้องการวิเคราะห์กับไบโอรีคอกนิชันอีลีเมนต์ สามารถตรวจวัดได้จากการเปลี่ยนแปลงค่ามุมของเซอร์เฟสพลาสมอนเรโซแนนซ์ (SPR angle) หรือค่าความจุไฟฟ้า (capacitance) หลักการตรวจวัดนี้นำไปประยุกต์เพื่อตรวจหาสารที่ต้องการวิเคราะห์ในระบบไหลผ่าน (flow injection system)

ได้ศึกษาเปรียบเทียบระบบเซอร์เฟสพลาสมอนเรโซแนนซ์และคาพาซิทิฟอิมมูโนเซนเซอร์สำหรับตรวจวัดแคนเซอแอนติเจน 125 (cancer antigen 125; CA 125) ในตัวอย่างซีรัมโดยระบบไหลผ่านแบบไม่ติดฉลาก (label-free flow-injection) โดยตรึงแอนติ-แคนเซอแอนติเจน 125 (anti-cancer antigen 125; anti-CA 125) บน เซลฟ-แอสเซมเบิลของ กรด 11-เมอแคพโตอันเดตคาโนอิค (11- mercaptoundecanoic acid) ศึกษาปัจจัยที่มีผลต่อการตอบสนองของทั้งสองระบบ ภายใต้สภาวะที่เหมาะสม ระบบเอสพีอาร์ (SPR system) มีข้อดีคือ สามารถตรวจติดตามได้ทันทีทำให้ง่ายในการติดตามขั้นตอนการตรึงและขั้นตอนการหาสภาวะที่เหมาะสมของระบบ เวลาการตอบสนองเร็ว (5 นาทีสำหรับเอสพีอาร์ และ 15 นาทีสำหรับคาพาซิทิฟ) และเวลาที่ใช้ในการทำลายพันธะระหว่างคู่แอฟฟินิตีน้อย (regeneration time) (5 นาทีสำหรับเอสพีอาร์ และ 12 นาทีสำหรับคาพาซิทิฟ) ส่วนระบบคาพาซิทิฟมีข้อดีคือมีขีดจำกัดในการตรวจวัดต่ำ (0.05 ยูนิตต่อมิลลิลิตร)กว่าระบบเอสพีอาร์ (0.1ยูนิตต่อมิลลิลิตร) เครื่องมือราคาถูกและอิเล็กโทรดทองสามารถนำกลับมาใช้ได้ใหม่ ระบบทั้งสองถูกนำไปประยุกต์ใช้ในการหาแคนเซอแอนติเจน 125 ในตัวอย่างซีรัมและเปรียบเทียบผลที่ได้กับเทคนิคทั่วไปคือเทคนิคเอนไซม์ลิงค์ฟลูออเรสเซนต์ (enzyme linked fluorescence assay; ELISA) ทั้งสองระบบให้ผลสอดคล้องกับวิธีเอนไซม์ลิงค์ฟลูออเรสเซนต์ ($P = 0.05$)

นอกจากนี้ได้ประยุกต์การตรวจวัดคาพาซิทิฟในการหาแอนติบอดี *B. pseudomllei* ในตัวอย่างซีรัมของผู้ป่วยที่เป็นโรคเมลิออยโดซิส ด้วยระบบไหลผ่าน โดยตรึงโปรตีน Bip D (Bip D protein) ที่จะจับคู่แอฟฟินิตีกับแอนติบอดีบนอิเล็กโทรดทองผ่านชั้นโมโนเลเยอร์ของกรด 11-เมอแคพโตอันเดคคาโนอิค ภายใต้สภาวะที่เหมาะสม อิเล็กโทรดสามารถแยกตัวอย่างซีรัมของผู้ป่วยที่เป็นโรคเมลิออยโดซิส (melioidosis patients) และไม่เป็นโรคเมลิออยโดซิส (non-melioidosis patients) ได้ ระบบนี้มีความไวในการวิเคราะห์หาแอนติบอดี *B. pseudomllei* โดยสามารถเจือจางตัวอย่างได้ถึง 11,000 เท่า อิเล็กโทรดสามารถนำมาใช้ใหม่ได้ 28 ครั้งและเป็นวิธีวิเคราะห์ที่รวดเร็ว (ใช้เวลา 15 นาที) กว่าวิธีการนับเซลล์ (bacterial culture) (ใช้เวลา 3-4 วัน) ที่ใช้อยู่ในปัจจุบันดังนั้นระบบที่ได้พัฒนาขึ้นนี้สามารถใช้เป็นวิธีทางเลือกในการตรวจหา แอนติบอดี *B. pseudomllei* ในซีรัมของตัวอย่างที่เป็นโรคเมลิออยโดซิส

ในการเพิ่มความสามารถของระบบแอฟฟินิตีไบโอเซนเซอร์แบบไม่ติดฉลากได้ศึกษาการใช้อนุภาคทองขนาดนาโน (gold nanoparticles; AuNPs) เพื่อเพิ่มความไววิเคราะห์ของระบบ ในการตรวจหาสารที่ต้องการวิเคราะห์ด้วยระบบเอสพีอาร์และคาพาซิทิฟอิมมูโนเซนเซอร์ (immunosensor) โดยใช้อนุภาคทองขนาดนาโนเป็นฐานในการตรึงแอนติบอดีผ่านชั้นเซลฟ์-แอสเซมเบิลของซิสทีเอมีน (cysteamine)หรือชั้นพอลิเมอร์ของพาราฟีนิลลีนไดเอมีน (*p*-phenylenediamine) บนผิวทอง ศึกษาหาความเข้มข้นของอนุภาคทองขนาดนาโนที่เหมาะสม ภายใต้สภาวะที่เหมาะสมทั้งสองระบบสามารถเพิ่มความไววิเคราะห์ประมาณสองเท่า และสามารถวิเคราะห์หาแอนติเจนที่มีความเข้มข้นต่ำได้

สำหรับระบบแอฟฟินิตีไบโอเซนเซอร์แบบติดฉลากได้ศึกษาด้วยวิธีตรวจวัดแอมเพอโรมิทริก (amperometric detection) โดยปรับปรุงเม็ดพอลีสไตรีน (polystyrene) ด้วยอนุภาคพลัสเซียนบลู (Prussian blue) ขนาดนาโนเมตรเพื่อนำมาใช้เป็นสารติดฉลากในการวิเคราะห์หาดีเอนเอ (DNA) ด้วยวิธีแซนด์วิช (sandwich assay) ดีเอนเอที่ต้องการวิเคราะห์จะจับกับดีเอนเอสายแรก (primary DNA) ที่ถูกตรึงอยู่บนอิเล็กโทรดทอง หลังจากนั้นเติมดีเอนเอสายที่สอง (secondary DNA) ที่ติดฉลากด้วยเม็ดพอลีสไตรีนที่ปรับปรุงด้วยอนุภาคพลัสเซียนบลูขนาดนาโนเมตร อนุภาคพลัสเซียนบลูขนาดนาโนเมตรจะทำหน้าที่เร่งปฏิกิริยารีดักชันของไฮโดรเจนเปอร์ออกไซด์ ระบบนี้สามารถตรวจวัดหาดีเอนเอได้ในระดับความเข้มข้น 50 เฟมโตโมลาร์ (50 fM level)

จากการศึกษาสรุปได้ว่าระบบเซอร์เฟสพลาสมอนเรโซแนนซ์ และเคมีไฟฟ้าแอฟฟินิตีไบโอเซนเซอร์ มีความไววิเคราะห์ในการตรวจหาสารที่ต้องการวิเคราะห์ได้หลายชนิดทั้งแบบไม่ใช้และใช้สารติดฉลาก เซอร์เฟสพลาสมอนเรโซแนนซ์ และเคมีไฟฟ้าแอฟฟินิตีไบโอเซนเซอร์นี้เป็นวิธีวิเคราะห์ที่มีประสิทธิภาพสามารถทำไปประยุกต์ใช้ในการวิเคราะห์หาสารอื่นๆได้

Thesis title	Surface Plasmon Resonance and Electrochemical Affinity Biosensors
Author	Miss Siriwan Suwansa-ard
Major Program	Chemistry
Academic Year	2008

ABSTRACT

This thesis focuses on the development and evaluation of the performances of surface plasmon resonance (SPR) and electrochemical transducers for label-free and labeled affinity biosensors. Label-free affinity detection was carrier out by SPR and capacitive detections. Biological recognition element was immobilized on gold substrate. During biological recognition element-analyte binding, the change in SPR angle or capacitance was detected. These measurement principles were applied for interested analytes in flow injection system.

A comparison between SPR and capacitive immunosensors was studied for a label-free flow injection detection of cancer antigen 125 (CA 125) in human serum. Anti-CA 125 was immobilized on gold surface through a self-assemble monolayer of 11- mercaptoundecanoic acid. Parameters affecting the responses of each system were optimized. Under the optimum conditions, the SPR method was superior in terms of real-time monitoring making it easy to follow and monitor the immobilization and optimization steps. It also required less time for the steady response (5 min for SPR and 15 min for capacitive) and regeneration (5 min for SPR and 12 min for capacitive). Whereas, the capacitive system showed a slightly lower limit of detection (0.05 U ml^{-1}) than SPR (0.1 U ml^{-1}). The instrument is also less complicated with lower cost and the gold rod electrode can be reuse. These immunosensors were applied to analyze CA 125 concentrations in human serum samples and compared with conventional enzyme linked fluorescent assay (ELFA). Both systems showed good agreement with ELFA ($P = 0.05$).

Further application of capacitive transducer is for the detection of *B. pseudomallei* antibody in human serum to test for melioidosis. Bip D, a protein

specific to this antibody was immobilized on gold electrode via 11-mercaptoundecanoic acid monolayer. Under appropriate regenerating solution and running solution, this modified electrode could separate between melioidosis and non-melioidosis samples with 11,000 times of dilution factor. The electrode could be reused up to 28 times. Moreover, this system provided rapid analysis for melioidosis (15 min) than the conventional analysis method based on bacterial culture (3-4 days). Thus, this developed system would be a good alternative for *B. pseudomallei* antibody analysis.

To enhance system performance label-free affinity biosensor incorporated with gold nanoparticles (AuNPs) was investigated for SPR and capacitive immunosensors. AuNPs were used as platform to immobilize antibodies via self-assembled monolayer of cysteamine or polymer layer of *p*-phenylenediamine (*p*-PD) on gold surface. The optimization of amount of AuNPs was studied. Under optimum condition, the use of AuNPs could enhance sensitivity by about 2 times and could detect interested antigens at low concentration.

Labeled affinity biosensor was also studied with amperometric detection. The polystyrene (PS) beads modified with Prussian-blue (PB) nanoparticles were developed for a labeled affinity biosensor via sandwich assay for DNA dectection. The target DNA was hybridized with immobilized primary DNA probe on the gold electrode surface and secondary DNA labeled with PB-PS beads was further added. Then catalytic activity of the captured PB tag towards the reduction of hydrogen peroxide, allows amperometric detection of the DNA target down to the 50 fM level.

The results showed that surface plasmon resonance and electrochemical affinity biosensor systems could be sensitively applied for label-free and labeled detection of various interested analytes. These surface plasmon resonance and electrochemical affinity biosensors are useful analytical methods that can be applying for other analytes.

ACKNOWLEDGEMENTS

The completion of this thesis would be quite impossible without the help of many people, whom I would like to thank.

I express my sincere thanks to my advisors Assoc. Prof. Dr. Panote Thavarungkul and Assoc. Prof. Dr. Proespichaya Kanatharana for the opportunity to work on interesting projects, for all the help, support, encouragement, advice and suggestion throughout my study. Many thanks for Prof. Dr. Joseph Wang for his advice, suggestion and financial support during my research at The Biodesign Institute and Fulton School of Engineering, Arizona State University, Arizona, USA.

I would like to thank Asst. Prof. Punnee Asawatreratanakul for her help and suggestion about the biochemistry aspect of this work. I would also like to thank Assoc. Prof. Dr. Wilaiwan Chotigeat for providing the Bip D protein, suggestion and discussion the melioidosis project. Songklanakarind Hospital and Hat-Yai Hospital provided human serum samples.

Thanks are expressed to the examination committee members of this thesis for their valuable time and all help in some technical aspects rendered by staffs of the Department of Chemistry and the Department of Physics, Faculty of Science, Prince of Songkla University. My sincere thanks are extended to The Royal Golden Jubilee Ph.D. Program (RGJ) supported by The Thailand Research Fund, Center for Innovation in Chemistry (PERCH-CIC), Graduate School and Faculty of Science, Prince of Songkla University and Trace Analysis and Biosensor Research Center for the partial support of the research fund. I wish to thank Rajamangala University of Technology Thanyaburi for opportunity for allowing me to study Doctoral degree and for financial support.

My friend in the Trace Analysis and Biosensor Research Center who helped me in many ways. Special thanks for my best friend, Mr. Tanawit Teepoo for his understanding and support.

Lastly and most importantly, I wish to thank my father, mother, brother and his family for their love and support throughout my life and leaving me free for all my decisions.

Siriwan Suwansa-ard

THE RELEVANCE OF THE RESEARCH WORK TO THAILAND

The purpose of this Doctor of Philosophy Thesis in Chemistry (Analytical Chemistry) is to develop and evaluate the performances of surface plasmon resonance and electrochemical transducers for label-free and labeled affinity biosensors. The developed surface plasmon resonance and electrochemical affinity biosensor system can be applied for the detection of several target analytes, *i.e.*, CA 125, DNA, and *B. pseudomallei* antibody etc with high selectivity, selectivity, accuracy and short time analysis. These biosensors can be applied as alternative teachniquces for the quantitative analysis of trace amounts of target analyte by, for examples, several governmental organizations in Thailand which are

- Ministry of Public Health
- Ministry of Industry
- Ministry of Environmental
- Ministry of Education

CONTENT (CONTINUED)

	Page
2.4.1.2 Surface plasmon resonance	19
2.4.1.3 Capacitive detection	20
CHAPTER 3: Optical Detection	21
3.1 Labeled optical affinity biosensor	21
3.1.1 Evanescent wave fluorescence fiber optic	21
3.1.2 Chemiluminescence measurement	24
3.2 Label-free optical affinity biosensor	25
3.2.1 Reflectometric interference spectroscopy	25
3.2.2 Interferometry	27
3.2.3 Surface plasmon resonance	30
3.2.3.1 Principle of surface plasmon resonance	30
3.2.3.2 Application of SPR for affinity biosensor	34
CHAPTER 4: Electrochemical Detection	36
4.1 Labeled electrochemical affinity biosensor	36
4.1.1 Potentiometric transducer	36
4.1.2 Amperometric transducer	38
4.1.3 Voltammetric stripping transducer	40
4.1.4 Conductimetric transducer	42
4.2 Label-free electrochemical affinity biosensor	43
4.2.1 Impedance detection	43
4.2.2 Capacitance detection	46
4.2.2.1.1 Impedimetric	52
4.2.2.1.2 Potential step	52

CONTENT (CONTINUED)

	Page
CHAPTER 5: Sensitivity Enhancement of Affinity Biosensor	55
5.1 Labeled competitive biosensor	55
5.2 Labeled sandwich biosensor	58
5.2.1 Enzyme	58
5.2.1.1 Electrochemical detection	58
5.2.1.2 SPR detection	59
5.2.1.3 Mass detection	60
5.2.2 Nanoparticle	61
5.2.2.1 SPR detection	62
5.2.2.2 Electrochemical detection	63
5.2.2.3 Mass detection	64
5.2.2.4 Fluorescence detection	65
5.2.3 Others	67
5.3 Label-Free Affinity Biosensor	68
5.3.1 Dendrimer	69
5.3.2 Nanoparticles	71
5.3.2.1 Large surface area	71
5.3.2.2 Catalysis electrochemical reactions	72
5.3.2.3 Increase optical property	73
CHAPTER 6: Performance Criteria	74
6.1 Linear range, sensitivity and limit of detection	74
6.2 Selectivity	77
6.3 Regeneration, stability and reproducibility	77

CONTENT (CONTINUED)

	Page
CHAPTER 7: Comparison of Surface Plasmon Resonance and Capacitive Immunosensors for Cancer Antigen 125 Detection in Human Serum Samples	79
7.1 Introduction	79
7.2 Experimental	81
7.2.1 Materials	81
7.3 Method	81
7.3.1 SPR immunosensor	81
7.3.1.1 Anti- CA 125 immobilization	81
7.3.1.2 SPR system	82
7.3.2 Capacitive immunosensor	83
7.3.2.1 Anti- CA 125 immobilization	83
7.3.2.2 Capacitive system	84
7.3.3 Optimization of the flow injection SPR and capacitive immunosensors	85
7.3.4 Selectivity	85
7.3.5 Determination of CA 125 in real samples	85
7.4 Results and discussion	86
7.4.1 Immobilization of anti-CA 125	86
7.4.1.1 SPR immunosensor	87
7.4.1.2 Capacitive immunosensor	87
7.4.2 Immunosensor responses	88
7.4.2.1 SPR response	88
7.4.2.2 Capacitive response	89
7.4.3 Optimization of the flow injection SPR and capacitive immunosensor systems	90
7.4.3.1 Regeneration solution	90

CONTENT (CONTINUED)

	Page
7.4.3.2 Running buffer solution	93
7.4.3.3 Flow rate	96
7.4.3.4 Sample volume	98
7.4.3.5 Linear range and detection limit	99
7.4.3.6 Selectivity	100
7.4.3.7 Reproducibility	103
7.4.3.8 Matrix effect	105
7.4.3.9 Real samples	107
7.4.3.10 Recovery	111
7.4.3.11 Limit of quantification	114
7.5 Conclusions	116
CHAPTER 8: Determination of Melioidosis using Capacitive Immunosensor	118
8.1 Introduction	118
8.2 Experimental	119
8.2.1 Materials	119
8.2.2 Serum samples	119
8.3 Method	120
8.3.1 Immobilization of Bip D protein	120
8.3.2 Capacitance measurement	120
8.3.3 Optimization of capacitive immunosensor	120
8.3.4 Reuse of modified electrode	121
8.3.5 Dilution factor	121
8.3.6 Individual serum sample analysis	121
8.4 Results and discussion	122

CONTENT (CONTINUED)

	Page
8.4.1 Immobilization of Bip D protein	122
8.4.2 Capacitance measurement	123
8.4.3 Optimization of capacitive immunosensor	124
8.4.3.1 Regeneration solution	124
8.4.3.2 Buffer solution	125
8.4.3.2.1 Concentration	125
8.4.3.2.2 pH	126
8.4.3.3 Dilution factor	129
8.4.3.4 Reuse of modified electrode	129
8.4.3.5 Individual real samples detection	130
8.5 Conclusion	135
CHAPTER 9: Sensitivity Enhancement of Label–Free Surface Plasmon Resonance and Capacitive Immunosensors using Gold Nanoparticles	136
9.1 Introduction	136
9.2 Experimental	137
9.2.1 Materials	138
9.2.2 Preparation of AuNPs	138
9.2.3 SPR immunosensor immobilization	138
9.2.4 Capacitive immunosensor immobilization	141
9.2.5 Flow-injection SPR system	144
9.2.6 Capacitive flow injection system	144
9.2.7 Optimization of amount of AuNPs immobilization for both SPR and capacitive immunosensors	145
9.2.8 Surface coverage	145
9.2.9 Immobilization yield	146

CONTENT (CONTINUED)

	Page
9.3 Results and discussion	147
9.3.1 Synthesis of AuNPs	147
9.3.2 Immobilization of antibody	148
9.3.2.1 SPR immunosensor system	148
9.3.2.2 Capacitive immunosensor system	151
9.3.2.2.1 Electropolymerization of *p*-PD	151
9.3.2.2.2 Immobilization of antibody	151
9.3.3 Optimization of amount of AuNPs	153
9.3.3.1 Surface coverage	153
9.3.3.2 Immobilization yield of antibody	154
9.3.3.3 Capacitive immunosensor	155
9.3.3.4 SPR immunosensor	156
9.3.4 Antigen detections	157
9.3.4.1 SPR immunosensors	157
9.3.4.2 Capacitive immunosensor	159
9.4 Conclusions	161
CHAPTER 10: Prussian blue Dispersed Sphere Catalytic Labels for Amplified Electronic Detection of DNA	163
10.1 Introduction	166
10.2 Experimental	166
10.2.1 Apparatus	166
10.2.2 Materials	166
10.3 Methods	167
10.3.1 Analytical protocol	167
10.3.2 Preparation of PB nanoparticles	167

CONTENT (CONTINUED)

	Page
10.3.3 Encapsulation of the PB nanoparticles within the PS beads	168
10.3.4 Effect of PB nanoparticles loading in PS beads	168
10.3.5 Conjugation of the PB-PS beads with DNA-probe 2	168
10.3.6 Immobilization, sandwich hybridization and detection	169
10.3.6.1 Immobilization of DNA probe (probe 1) on gold electrode	169
10.3.6.2 Sandwich DNA hybridization	169
10.3.6.3 Electrochemical detection	169
10.4. Results and Discussion	170
10.4.1 Characterizations of PS-PB beads	170
10.4.2 The effect of PB nanoparticles loading in PS bead	172
10.4.3 Electrochemical response	172
10.4.4 DNA hybridization detection	174
10.4.4.1 Effect of amine- DNA concentration	174
10.4.4.2 Effect of amount of probe 2 (PS-PB-amine DNA)	175
10.4.4.3 Electrochemical performance	176
10.5 Conclusions	179
CHAPTER 11: Conclusions	180
REFERENCES	224
APPENDICES	236
APPENDIX A	237
APPENDIX B	242
VITAE	265

LIST OF TABLES

Table		Page
7.1	Tested and optimum conditions of the type, pH and concentration of regeneration solution of SPR immunosensor.	92
7.2	Tested and optimum conditions of the type, pH and concentration of regeneration solution of capacitive immunosensor.	93
7.3	Comparison of CA 125 concentrations in human resume samples were obtained from SPR, capacitive immunosensors with conventional method in hospitals. (mean ± SD, n=3)	108
7.4	The Wilcoxon sign rank test for the comparison of the concentration of CA 125 in sample from the SPR immunosensor system and ELFA technique.	109
7.5	The Wilcoxon sign rank test for the comparison of the concentration of CA 125 in sample from the capacitive immunosensor system and ELFA technique.	110
7.6a	Recoveries in spiked serum samples with 100 times of dilution factor (mean ± SD, n=3).	112
7.6b	Recoveries in spiked serum samples with 1000 times of dilution factor (mean ± SD, n=3).	115
7.7	Recoveries of SPR system from real samples spiked with 10 U ml^{-1} CA 125 calculated from the detected concentration (C_1) and the original concentration in the real samples (C_2).	116
7.8	Recoveries of capacitive system from real samples spiked with 5 U ml^{-1} CA 125 calculated from the detected concentration (C_1) and the original concentration in the real samples (C_2).	116

LIST OF TABLES (CONTINUNED)

Table		Page
8.1	Tested and optimum conditions of type and concentration of regeneration solution.	125
8.2	Tested and optimized values of the capacitive immunosensor system. Capacitance change obtained from the injection of to pool positive sample at 10,000 of dilution factor with 200 µl of sample volume and 50 µl min^{-1}.	128
8.3	The Mann-Whitney Rank-Sum Test the signal obtained from negative serum sample and control serum sample.	133
8.4	The Mann-Whitney Rank-Sum Test the signal obtained from negative serum sample positive serum sample.	134
9.1	SPR immunosensors performances for antigens detection.	158
9.2	Capacitive immunosensors performances for antigens detection.	160
9.3	Immobilization yield of antibody.	161
11.1	Comparison of analytical method for CA 125 detection.	181
11.2	Comparison of analytical method for *B. pseudomallei* antibodies in serum samples detection.	182
11.3	Comparison of analytical method for DNA hybridization detection.	184
11.4	Performance of the surface plasmon resonance and electrochemical affinity biosensor systems for different analytes studied in this work.	185

LIST OF FIGURES

Figure		Page
2.1	Principle of biosensors (a) catalytic biosensor; the analyte is converted by immobilized biological sensing elements such as enzymes to products and then are detected by transducer. (b) Affinity biosensor; the analyte (e.g. antibody, antigen) is recognized by immobilized recognition molecule (e.g. antigen, antibody, receptor, and DNA) then physical property change form biomolecule binding is detected with transducer.	5
2.2	DNA hybridization events by immobilized single stranded DNA (probe) on a transducer surface to recognize its complementary (target) DNA via hybridization.	8
2.3	Structure of IgG antibody.	9
2.4	Scheme showing cells-binding Con A immobilized on the surface of a transducer.	11
2.5	Protein-based affinity biosensor for monitoring conformational change upon binding of heavy metal ions.	12
2.6	Types of labeled affinity biosensor detection (a) sandwich assay (b) competitive assay	14
2.7	Label-free affinity biosensor detection by measuring of changes in any physical property as a result of analyte-biological recognition complex.	17
2.8	Schematic of a piezoelectric crystal.	19
3.1	(a) Structure of an fiber optic and (b) a section of cladding was removed in this application for affinity biosensor (modified from Leung *et al.*, 2007; Epstein and Walt, 2003) (c) light propagates though optical fiber by total internal reflection when incident angle (θ) is more than critical angle (θ_c).	22

LIST OF FIGURES (CONTINUNED)

Figure		Page
3.2	Fluorescent fiber affinity biosensor detection; the detecting of fluorescent signal after secondary biological recognition capture with analytes by optical fiber (Modified from Lin *et al.*, 2009).	24
3.3	Chemiluminescence-based labeled affinity biosensor using enzyme oxidase.	25
3.4	Scheme of reflectometric interference spectroscopy detection; the change of the optical thinness during a binding between antibody (a) and antigen on transducer surface. The corresponding change interference spectrum is shown in (c) and the resulting binding curve is given in (d) (Modified from Proll *et al.*, 2007).	26
3.5	(a) Scheme of Mach-Zehnder interferometer (b) Real-time detection of binding curve obtained from intensity of light *vs* time (c) The cross-section of sensor channel; the cladding layer was removed to immobiliz biorecognition elements, the interaction of bimolecule take place at core-cladding interface within evanescent field region (Modified from Prieto *at el.*, 2003; Heideman *et al.*, 1993).	29
3.6	Total internal reflection phenomenon.	30
3.7	Configurations of SPR sensors (a) optical waveguide, (b) fiber optic, (c) grating prism and (d) prism coupling (Modified Hoa *et al.*, 2007; from Homola *et al.*, 1999).	31
3.8	(a) principle of surface plasmon resonance based on glass coupling and (b) a shape of reflectance minimum is produced at resonance angle (modified form Gupta and Kondoh, 2007; Green *et al.*, 2000).	32

LIST OF FIGURES (CONTINUNED)

Figure		Page
3.9	Two basic SPR detection (a) angle measurement for a fixed wavelength (b) wavelength measurement for a fixed angle.	33
3.10	(a) Surface plasmon resonance application for affinity biosensor; interaction between immobilized biological recognition element on gold substrate surface and analytes caused an increase in resonance angle (b).	35
4.1	Schematic diagram of an electrochemical cell for potentiometric measurement (Modified from Wang, 2000).	37
4.2	Potentiometric affinity biosensor detection based on sandwich assay labeled with quantum dot (Modified from Thurer *et al.*, 2007).	38
4.3	Principle of enzyme affinity biosensor by using amperometric measurement.	39
4.4	Anodic stripping voltammetry (a) the potential-time waveform, (b) along with the resulting voltammogram(Modified from Wang, 2000; Scholz, 2002).	41
4.5	Volttametric stripping detection of affinity biosensor based on metal nanoparticle label (Modified from Chu *et al.*, 2005).	42
4.6	Schematic diagram of labeled nanoparticles conductrimetric affinity biosensor assay (Modified from Valera *et al.*, 2008).	43
4.7	Randles' equivalent circuit of electrode in electrolyte (modified from Fernández-Sánchez, 2005).	44
4.8	Nyquist plot of immobilized antibody (Ab) on the surface of the electrode (a) and antibody-antigen (Ab-Ag) complex on the surface of the electrode (modified from Fernández-Sánchez 2005).	45

LIST OF FIGURES (CONTINUNED)

Figure		Page
4.9	Bode Plot that describes impedance behaviour of a simple electrochemical cell (modified from Fernández-Sánchez, 2005).	46
4.10	Schematic diagram of capacitive affinity arrangements to measure the capacitance change due to (a) the change in distance between two plates and/or the change in dielectric constant or (b) due to change in the dielectric constant using interdigitated electrode (Modified from Gebbert *et al.*, 1992; Berggren *et al.*, 2001).	47
4.11	Schematic diagram of capacitive affinity biosensor measures the change in the capacitance at the electrode/solution interface.	49
4.12	Schematic representation of (a) model of the double layer region consists of an Inner Holmholtz plane (IHP), an Outer Holmholtz plane (OHP) and a diffusion layer, C_H is the capacitance due to Holmholtz layer and C_{DL} is capacitance due to the diffusion layer; (b) potential (φ) profile in the double layer formed at a metal electrode and solution interface across the double layer; φ_m is electric potential of metal and φ_s is electric potential of solution (Modified from Scholz, 2002, Wang, 2000).	50
4.13	Affinity biosensor based electrical double layer organized on the metal electrode solution interface (Modified from Berggren *et al.*, 2001).	51
4.14	Potential step technique principle (a) applied potential pulse and (b) resulting current decay.	52
4.15	Logarithm of current *vs* time.	53

LIST OF FIGURES (CONTINUNED)

Figure		Page
5.1	The analyte-BSA conjugate was adsorbed on the working electrode surface. Analyte in the sample competes with the immobilized one to bind to AuNPs labelled antibody. Signal was amplified by electrodeposition of silver at a fixed applied potential on gold (Modified from Vig *et al.*, 2009).	56
5.2	Schematic diagram of an electrochemical competitive biosensor. Immobilized analyte–BSA conjugate on the gold electrode surface competes with free analyte in the solution to bind to a fixed amount of antibody. Secondary antibody–ALP conjugate was added followed by enzymatic silver deposition (Modified from Tan *et al.*, 2009).	57
5.3	Schematic representation of sandwich type affinity biosensor labeled with horseradish peroxidase (HRP). Analyte binds to immobilized primary biological recognition element. Addition of secondary biological recognition element conjugated with HRP followed by substrate in the present of mediator helps the transferring of electron between solution and electrode (Modified from Campas and Marty, 2007).	59
5.4	Diagram of a method to enhance the sensitivity of SPR response based on enzyme labeled sandwich assay. HRP will catalyze the oxidation of 3,3' diaminobenzidine(DAB) in the presence of H_2O_2 to generate precipitation insoluble product to enhance the SPR signal (Modified from Cao and Sim, 2007).	60
5.5	Enzymatic reaction schemes. HRP catalyzes H_2O_2 oxidation of 3,3',5,5'-tetramethylbenzidine (TMB) to form precipitation product and causes change in QCM signal (Modified from Su and Li, 2001).	61

LIST OF FIGURES (CONTINUNED)

Figure		Page
5.6	Schematic presentation of immunoassay configuration for signal enhancement based on the conjugation of AuNPs and secondary biological recognition element (Modified from Choi *et al.*, 2008).	63
5.7	AuNPs labeled enhance signal of electrochemical detection via sandwich assay. After secondary biological recognition binds with target analyte, the labeled AuNPs are dissolved with HBr solution to release gold (III) ions and detected with anodic stripping voltammetry (ASV) (Modified from Dequaire *et al.*, 2000).	64
5.8	Sensitivity enhancement based on silver-enhanced AuNPs labels, precipitation of silver on AuNPs was dissolved in H_2O_2 and detected by ion-selective electrode (Modified from Chumbimuni-Turres *et al.*, 2006).	65
5.9	Hybridization assay of target DNA with amplified QCM detection with labeled AuNPs. Primary DNA (probe 1) was immobilized on QCM gold disk surface after the binding with target DNA, secondary DNA tagged with AuNPs was then added (Modified from Mo *et al.*, 2005).	66
5.10	Scheme of fiber optic signal enhancement by AuNPs incorporation fluorophore. (Modified from Chang *et al.*, 2008).	67
5.11	Amplification of signal via polystyrene microbeads carrier many AuNPs as labeling (Modified from Kawde and Wang, 2004).	68
5.12	Structure of the fourth generation dendrimer (Modified from Lojou and Bianco, 2006).	70
5.13	Schematic illustration of immobilized polyamidoamine dendrimer on amine monolayer (Modified from Shen *et al.*, 2008).	70

LIST OF FIGURES (CONTINUNED)

Figure		Page
5.14	Sensitivity enhancement is based on immobilizing AuNPs on amine groups of self-assemble monolayer. Antibody was then immobilized on AuNPs surface by adsorption technique to enhance amount of antibody for interested analyze detection (Modified from Huang *et al.*, 2006).	71
6.1	Schematic of a calibration curve showing relationships for determining linear range, sensitivity and limit of detection (Buck and Lindner, 1994; Eggins, 1996; Thevenot *et al.*, 1999; Wang, 2000).	76
6.2	Calibration graph for LOD detection based on the signal-to-noise ratio method (modified from Miller and Miller, 1993).	78
7.1	Schematic diagram shows the flow injection SPR immunosensor system.	83
7.2	Schematic diagram shows the flow injection capacitive immunosensor system.	84
7.3	SPR sensorgram showed the change in SPR signal during anti-CA 125 immobilization steps. Arrows indicate injection of (a) 11-mercaptoundecanoic acid on cleaned gold disk, (b) NHS/EDC, (c) anti-CA 125, (d) ethanolamine hydrochloride, and (e) BSA.	87
7.4	Cyclic voltamograms of a gold electrode obtained with 5 mM $K_3[Fe(CN)_6]$ in 0.1 M KCl solution at a scan rate of 0.1 Vs^{-1} vs. Ag/AgCl reference electrode. The voltage range was −0.3 to 0.8 V. (a) Clean gold electrode, (b) self-assembled 11-mercaptoundecanoic acid layer, (c) anti-CA 125, (d) ethanolamine hydrochloride, and (e) 1-dodecanethiol treatment.	88

LIST OF FIGURES (CONTINUNED)

Figure		Page
7.5	SPR sensorgram obtained from the injections of 10 U ml^{-1} CA 125 over the anti-CA 125 immobilized SAM resulting in the increase of SPR angle.	89
7.6	Capacitive signal obtained from the injections of 5 U ml^{-1} CA 125 causing the capacitance to decrease. The binding between anti-CA 125 and CA 125 was dissociated with HCl pH 2.6 before injection of a new CA 125.	90
7.7	Response of (a) SPR immunosensor, (b) capacitive immunosensor to CA 125 using different types of buffer.	94
7.8	Response of (a) SPR immunosensor, (b) capacitive immunosensor to CA 125 using different pH of buffer.	95
7.9	Response of (a) SPR immunosensor, (b) capacitive Immunosensor to CA 125 using difference concentrations of buffer.	96
7.10	Response of (a) SPR immunosensor, (b) capacitive immunosensor to CA 125 using different flow rate of buffer.	97
7.11	Response of (a) SPR immunosensor, (b) capacitive immunosensor to CA 125 using different sample volume of buffer.	98
7.12.	Calibration curve for CA (a) SPR immunosensor and (b) capacitive immunosensor. The insets show the detection limit of each system.	100
7.13	Response change *vs* the concentration of CA 125, CEA, AFP, and blank (running buffer) in SPR (a) and capacitive (b) immunosensors.	102
7.14	Reproducibility of response of CA 125 to injection of CA 125 for SPR (a) and capacitive (b) immunosensors with regeneration steps between each individual assay.	104

LIST OF FIGURES (CONTINUNED)

Figure		Page
7.15	The standard curve and spiked curve for the study of matrices interference of human sample at dilution factor of 100 times.	106
8.1	Cyclic voltammograms of a gold electrode obtained in a 5 mM $K_3[Fe(CN)_6]$ containing 0.1 M KCl solution at scan rate of 0.1 V s^{-1}. All potentials are given *vs* Ag/AgCl reference electrode. (a) bare gold electrode, (b) self-assembled of 11- mercaptoundecanoic acid monolayer covered electrode surface, (c) Bip D protein immobilized via activated monolayer electrode, (d) ethanolamine hydrochloride, and (e) 1-dodecanethiol treatment.	122
8.2	The decrease in capacitance (ΔC) resulting from the binding between Bip D protein - *B. pseudomallei* antibody with subsequent signal increase due to dissociation under regeneration conditions.	123
8.3	Response of capacitive immunosensor to pool positive sample (10,000 dilution factor) at different concentration of Tris-HCl pH 7.00.	126
8.4	Effect of pH of 15 mM Tris-HCl buffer on response to pool positive sample (10,000 dilution factor).	127
8.5	Effect of dilution factor on capacitance change to pool negative and pool positive serum sample.	129
8.6	The reuse of the Bip D protein modified on electrode.	130
8.7	Capacitance response obtained from the analysis of blank (running buffer; B), control (number of 1-15), negative (number of 16-30) and positive (number of 30-45) serum samples.	131

LIST OF FIGURES (CONTINUNED)

Figure		Page
9.1	Schematic illustration for antibody immobilized covalently on a self-assemble cysteamine modified gold disk. (a) gold disk was modified with cysteamine, (b) amino groups of cysteamine are activated by glutaraldehyde, (c) covalent binding between aldehyde groups of the activated self-assemble monolayer and free amino groups of antibody, (d) remaining amine group deactived by ethanolamine and (e) block any pinholes on gold disk surface with BSA.	140
9.2	Schematic illustration for antibody immobilized onto gold disk via AuNPs. (a) gold disk was modified with cysteamine, (b) AuNPs were adsorbed on amino groups of cysteamine monolayer, (c) antibody was incubated on AuNPs surface, (d) modified surface were blocked with ethanolamine and (d) any pinholes were further block with BSA.	141
9.3	Structure of (a) *p*-phenylenediamine used as monomer and (b) after electropolymerization (Lakard *et al.*, 2003).	143
9.4	Schematic illustration of the immobilization of antibody onto gold electrode; (a) gold electrode covered with *p*-PD film, (b) glutaraldehyde was used to activate *p*-PD film, (c) glutaraldehyde-*p*-PD film was incubated in antibody (d) remaining amine groups were deactivated with ethanolamine and (e) 1-dodecanethiol was added to block.	143
9.5	Schematic illustration of the immobilization of antibody onto gold electrode; (a) gold electrode covered with *p*-PD film (b) AuNPs was incubated on *p*-PD film (c) antibody was introduced to immobilize on polymer film and (d) antibody-AuNPs- *p*-PD film was blocked with ethanolamine and (e) with 1-dodecanethiol.	144

LIST OF FIGURES (CONTINUNED)

Figure		Page
9.6	Cyclic votammograms of bare gold electrode and AuNPs modified electrode.	146
9.7	Characterizations of AuNPs by (a) UV–vis spectrum, (b) TEM image, and (c) histogram of size distribution.	148
9.8	SPR sensorgram showing the change in SPR signal during anti-HSA immobilization steps. Arrows indicate injection of (a) cysteamine on cleaned gold disk, (b) glutaraldehyde, (c) anti-HSA and (d) BSA.	149
9.9	SPR sensorgram showing the change in SPR signal during anti-HSA immobilization steps. Arrows indicate injection of (a) cysteamine on cleaned gold disk, (b) AuNPs, (c) anti-HSA and (d) BSA.	150
9.10	Cyclic voltammograms for the electropolymerization of 5 mM *p*-PD at a gold electrode in acetate buffer (pH 5.18) at scan rate 50 mV s^{-1}. The numbers shows the cycles.	151
9.11	Cyclic voltammograms responses obtained in 10 mM $K_3Fe(CN)_6$ solution during the immobilization of anti-HSA (a) bare gold electrode (b) electropolymerization of *p*-PD (c) glytaraldehyde (d) anti-HSA and (e) 1-dodecanethiol.	152
9.12	Cyclic voltammograms responses obtained in 10 mM $K_3Fe(CN)_6$ solution during the immobilization of anti-HSA (a) bare gold electrode (b) electropolymerization of *p*-PD (c) AuNPs (d) anti-HSA and (e) 1-dodecanethiol.	153
9.13	Effect of amount of AuNPs used in the modification of gold electrode via polymer film on effective electrode surface area.	154

LIST OF FIGURES (CONTINUED)

Figure		Page
9.14	Effect of amount of AuNPs used in the modification of gold electrode via polymer film on effective immobilization yield.	155
9.15	Sensitivity of immunosensors obtained from different amount of AuNPs.	156
9.16	Sensitivity of immunosensors obtained from different amounts of AuNPs for SPR system.	156
10.1	(a) Cubic structure of PB and (b) PB electrocatalyst of H_2O_2 reduction at 0.0 V *vs* Ag/AgCl (modified from Ricci and Palleschi, 2005; Koncki, 2002).	165
10.2	Schematic representation of the analytical protocol: (a) formation of monolayer of mixed monolayer of DNA probe on gold electrode: (b) hybridization with target DNA and (c) second hybridization with polystyrene-Prussian blue beads-labeled probe.	167
10.3	(a) SEM images of PS beads before (A) and after (B) swelling in a butanol/chloroform solution, and the resulting PS-PB beads (C), SEM parameters include an accelerating voltage of 30 kV with 50,000 magnification, (b) UV-vis absorption spectra of PS spheres (A), of PB nanoparticles (B), and of the PS-PB beads (C), Spectra were recorded in 50 mM phosphate buffer (pH 6.00), (c) FT-IR spectrum of PS (A), PB (B), and (C) incoporation of PS-PB solution in chloroform.	171
10.4	Effect of the loading of the PB particles on the PS beads on the amperometric response to 0.1 mM hydrogen peroxide.	172
10.5	Cyclic voltammograms for 0.5 mM hydrogen peroxide at the PS (a) and PS-PB (b) modified electrodes.	173

LIST OF FIGURES (CONTINUNED)

Figure		Page
10.6	Amperometric response to successive additions of 0.1 mM hydrogen peroxide at the unmodified (a) and PS-PB modified (b) gold electrodes.	174
10.7	Effect of amine- DNA concentration.	175
10.8	Effect of amount of probe 2.	176
10.9	(a) Amperometric response to different concentrations of the target DNA and noncomplementary DNA.(b) Relative current signals for the different levels of the target DNA. (c) The calibration curve of DNA concentrations *vs* response.	178

CHAPTER 1

Introduction

1.1 Background and Rationale

The determination of trace amount of toxic compounds, antibodies, antigens, and many other proteins is very important in several fields such as environment (Kawazumi *et al.*, 2005; Soh *et al.*, 2003), food control (Hohensinner *et al.*, 2007; Ramakrishnan and Sadana 2002; Xiulan *et al.*, 2006), and clinical (He *et al.*, 2008; Kumbhat *et al.*, 2007; Tan *et al.*, 2006). For instance, tumor markers that exist in blood at trace levels, if detected can be used to indicate cancer (Wu *et al.*, 2007a). Therefore, high performance analytical methods are required to achieve low concentration detection.

Affinity biosensors have evolved over the past decade as one of the more promising method capable of trace amount detection. This technique refers to a device incorporating immobilized biological molecules that can have specific interactions with analyte molecules. After biological molecule–analyte binding, the change in physical property was detected by a transducer (Rahman *et al.* 2007). Physical transducers responding to changes in mass (piezoelectric), electrical properties (amperometric, impedance, capacitance, etc.) or optical properties (reflectometric interference spectroscopy, interferometry, surface plasmon resonance, etc.) have been developed to detect affinity binding molecules (Limbut *et al.*, 2006; Liu *et al.*, 2008d; Mizuta *et al.*, 2008; Piehler and Schreiber 2001; Ricard-Blum *et al.*, 2006; Thavarungkul *et al.*, 2007; Zhang *et al.*, 2008b).

Affinity biosensors can be divided into two types, labeled and label-free. Label-free affinity biosensor detection is based on the monitoring of changes in physical properties owing to the interaction of the affinity binding pairs. It leads to many advantages such as, simple to use, rapid analysis, and low cost (Jiang *et al.*, 2008; Ramakrishnan and Sadana, 2002). The other type, labeled affinity biosensor, is based on the use of labels to amplify signal which can help the systems to reach low detection limit. Widely used labels include enzymes (Du *et al.*, 2007; Liu *et al.*,

2008d; Wu *et al.*, 2007b), radioactive isotopes (Geisler *et al.*, 2008) fluorescien (Endo *et al.*, 2005; Hong and Kang, 2006; Turiel *et al.*, 1998), and nanoparticles (Jie *et al.*, 2008; Kawaguchi *et al.*, 2008; Numnuam *et al.*, 2008a,b; Valera *et al.*, 2008).

Another key factor that can improve the detection limit of an investigated compound is a transducer. Several transducers, such as piezoelectric; quartz crystal microbalance (Ding *et al.*, 2007; Park *et al.*, 2007; Tang *et al.*, 2006b), optical; surface plasmon resonance (Mizuta *et al.*, 2008), and electrochemical; capacitive and amperometric (Limbut *et al.*, 2006a,b; Loyprasert *et al.*, 2008; Yin *et al.*, 2006; Zhang *et al.*, 2008b) have been developed for biosensor detection. Surface plasmon resonance is currently one of the most widely applied optical detection principle. It allows direct monitoring of molecular interactions provides kinetic information, is sensitive, and simple to use (Oh *et al.*, 2003; Toyama *et al.*, 1998). Electrctrochemical transducers, especially capacitive and amperometric, have also been widely investigated (He *et al.*, 2009; Ivnitski *et al.*, 2000; Vestergaard *et al.*, 2007). These are due to the fact that capacitive system provides high sensitivity, specificity, and label-free detection (Berggren *et al.*, 1999; Li *et al.*, 2005). For amperometric transducer, it also has many advantages such as fast response, simple to use, and inexpensive (Ionescu *et al.*, 2007; Walsh and Dempsey 2002; Zhang *et al.*, 2008b). Therefore, in this thesis surface plasmon resonance and electrochemical transducers, i.e. capacitive and amperometric, were investigated as transducers for label-free and labeled affinity biosensors to detect the low concentration of selected analytes.

In addition, label-free affinity biosensor incorporation with nanoparticles has also attracted considerable interests for their high sensitivity detection. Gold nanoparticles have been successfully applied in the immobilization of various kinds of biomolecules, such as antibody, DNA, and other proteins (Cui *et al.*, 2008; Feng *et al.*, 2008; Kalogianni *et al.*, 2006; Simonian *et al.*, 2005). In the present work, gold nanoparticles were used as platform to immobilize antibodies. It is expected that these nanoparticles would increase the surface area for antibodies to be immobilized, hence, improve the performances of the affinity biosensor. While, in another part of this thesis polystyrene beads modified with Prussian-blue nanoparticles was developed for a labeled affinity biosensor. The focus was to employ these particles to amplify the signal of trace level DNA detection.

1.2 Objectives of the research

The aims of this study are to develop and evaluate the performances of surface plasmon resonance and electrochemical affinity biosensors, to use these biosensors to detect analytes concentration in real samples, and to validate the results with conventional methods. To reach these objectives four subprojects using the surface plasmon resonance and electrochemical detection principle were carried out as follows;

1. Comparison of surface plasmon resonance and capacitive immunosensors for the detection of cancer antigen 125 in human serum samples
2. Determination of melioidosis by capacitive immunosensor
3. Enhancement of surface plasmon resonance and capacitive immunosensors performances by gold nanoparticles
4. Prussian blue dispersed sphere catalytic labels for amplified electronic detection of DNA

1.3 Benefits

It is expected that the developed affinity biosensors which are relatively simple to use, require short analysis time, have high sensitivity, accuracy and precision will be used as alternative methods to detect analytes at low concentration.

CHAPTER 2

Affinity Biosensors

2.1 What is affinity biosensor ?

In analytical chemistry assay, biosensors now play an important role. They provide rapid detection, high sensitive and specific assays, in many areas such as clinical chemistry (Luppa *et al.,* 2001), food quality (Mello and Kubota, 2002), and environmental monitoring (Karube and Nomura, 2000). Biosensors are by definition a combination of a biological receptor, used for the detection of a target analyte by the use of complementary structures immobilized on to a transducer, which translates a biological interaction into an electrical signal (Ziegler and Gopel, 1998).

Biosensors can be divided into two groups, depending mainly on the kind of biological recognition element used, i.e., catalytic and affinity biosensors. A catalytic biosensor uses mainly enzymes as the biological compound, catalyzing a signaling biochemical reaction (Figure 2.1a). The change from consumption of substrate or the product of the reaction is measured and related to concentration of analyte. Another type, affinity biosensor, is designed to monitor the binding event itself. It is characterized by a binding event between the biorecognition molecule and the analyte via affinity reaction. It uses specific binding proteins, lectins, receptors, nucleic acids, membranes, antibodies, and antigens for biomolecular recognition (Figure 2.1b) where the physical property change due to the binding is detected with a transducer. Affinity biosensors offer several advantages such as rapid, specific, and sensitive analytical devices (Mallat *et al.,* 2001). Affinity biosensors are now being applied in several fields such as medical (Limbut *et al.,* 2006b), environmental (Loyprasert *et al.,* 2008) and food control (Thavarungkul *et al.,* 2007). Depending on the nature of the recognition element used, affinity biosensors can be further generally classified into receptor biosensors, DNA biosensors, immunosensors, and others.

(a) Catalytic biosensor

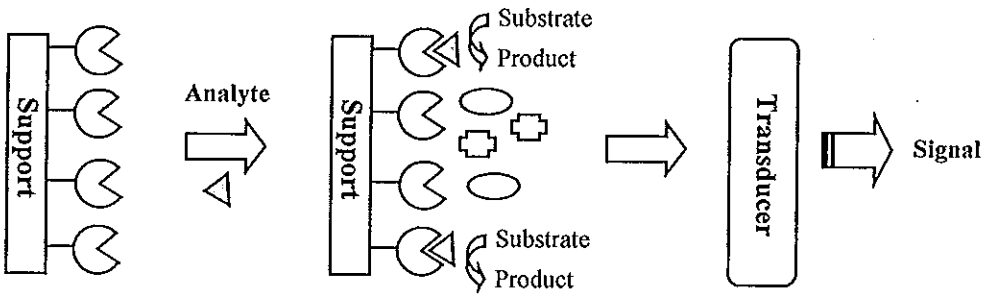

Biological recognition

-Enzyme
- Cell
- Tissue

Catalytic reaction

Transducers

- pH electrode
- Oxygen electrode
- Thermister

(b) Affinity biosensor

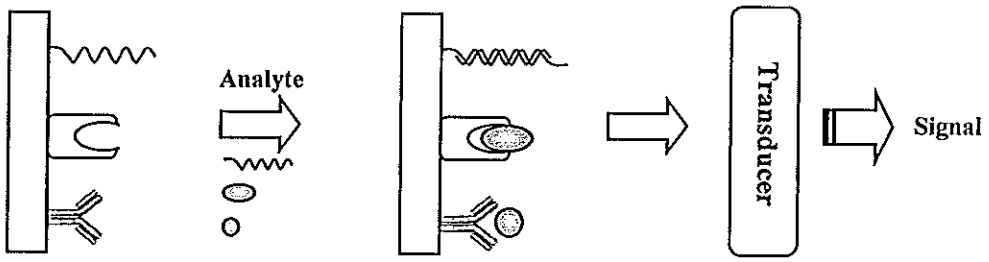

Biological recognition

-DNA
- Receptor
- Antibody

Affinity binding

Transducers

- Optical
- Eelectrochemical
- Pizoelectric

Figure 2.1 Principle of biosensors (a) catalytic biosensor; the analyte is converted by immobilized biological sensing elements such as enzymes to products and then are detected by transducer. (b) Affinity biosensor; the analyte (e.g. antibody, antigen) is recognized by immobilized recognition molecule (e.g. antigen, antibody, receptor, and DNA) then physical property change form biomolecule binding is detected with transducer.

2.2. Major affinity reactions

2.2.1 Receptor

One of the emerging application areas in biosensor technology is the use of receptors as the biological recognition element to detect target analytes (Kumbhat *et al.,* 2007). The advantage of the use of receptors as the recognition molecules is their natural affinity and specificity towards the target analyte, which can be detected by a physical transducer (Kumbhat *et al.,* 2007). Most of research into receptor has been with neuroreceptors and their recognition of neurotransmitters, neurotransmitter antagonists and neurotoxin (Eggins, 1996). Binding of a ligand to receptor triggers an amplified physiogical receptor such as (i) ion channel opening, (ii) second messenger, and (iii) activation of enzymes (Eggins, 1996). These biological receptors tend to have an affinity to specific analyte.

In a typical application protein receptors were immobilized on the surface of a transducer. The immobilization can be through several methods such as thiolated groups of receptor (Carmon *et al.,* 2005), self-assemble monolayer (Casuso *et al.,* 2008), and carboxymethylated dextran (Terada *et al.,* 2006). After the binding of protein receptor and analyte the physical properties change was detected with a suitable transducer, such as surface plasmon resonance (Kumbhat *et al.,* 2007), quartz crystal microbalance (Sung *et al.,* 2006), and electrochemical detection (Feng *et al.,* 2007a). Many receptors have been employed that is, glucose receptor (Andreescu and Luck, 2008), D3 dopamine receptor (Kumbhat *et al.,* 2007), G-protein coupled receptors (Feng *et al.,* 2007a), interleukin-1 receptor (Wu *et al.,* 2006b), and estrogen receptor (Carmon *et al.,* 2005).

Although receptors have advantages of high ligand specificity and affinity, they provided low yield and stability, are difficult to isolate and expensive. (Chambers *et al.,* 2008; Subrahmanyam *et al.,* 2002).

2.2.2 DNA

Deoxyribonucleic acid (DNA) is the genetic material that stores and encodes hereditary information in the form of genes. It is composed of two antiparallel

polynucleotide chains formed by monomeric nucleotide units. Each nucleotide is formed by three types of chemical components: a phosphate group, a sugar called deoxyribose, and four different nitrogen bases. The phosphate-deoxyribose sugar polymer represents the DNA backbone. The cellular genetic information is coded by the purine bases, adenine (A) and guanine (G), and the pyrimidine bases, cytosine (C) and thymine (T), as a function of their consecutive order in the chain. The two strands of nucleotides are twisted into a double helix, held together by hydrogen bonds between the A-T and G-C bases of each strand. A basic DNA biosensor is designed by the immobilization of a single stranded DNA (probe) on a transducer surface to recognize its complementary (target) DNA sequence via hybridization of base paring. The hybrid duplex DNA is formed on the transducer surface (Figure 2.2).

Generally, DNA biosensor detection is based on hybridization event and can be achieve by direct and indirect measurement. Direct detection, label-free, the hybridization process was measured directly by monitoring changes in the electrochemical (Li *et al.,* 2007; Park *et al.,* 2004), optical (Manera *et al.,* 2008; Zezza *et al.,* 2006) or mass properties (Caruso *et al.,* 1998; Passamano and Pighini, 2006). This allows real-time detection of the hybridization event. In contrast, indirect detection is though the detection of labeling markers, such as enzyme (Djellouli *et al.,* 2007; Hanaee *et al.,* 2007; Pan, 2007), electroactive (Dharuman *et al.,* 2006; Wei *et al.,* 2008; Zhu *et al.,* 2004), and nanoparticle (Bonanni *et al.,* 2008; Ding *et al.,* 2008a; Hanaee *et al.,* 2007). The labelling step generally enhances the sensitivity and selectivity but also increases the time, complexity and cost of the measurement (Wong and Gooding, 2006).

DNA biosensors have vast applications in various fields such as clinical diagnostics (Chen *et al.,* 2008d; Hassen *et al.,* 2008), agriculture (Mannelli *et al.,* 2003; Passamano and Pighini, 2006), and for the detection of pathogens (Csordas *et al.,* 2008). DNA biosensors provide high selectivity, high stability, and sensitivity, and the DNA can be easily synthesized in the laboratory as compared to other chemically synthesized biorecognition elements, such as antibodies (Junhui *et al.,* 1997. However, its limitation is in the immobilization process, for example in the adsorption method the whole DNA molecule may lay flat on the electrode surface

hinders the DNA's activity of hybridization and results in decrease sensitivity (Levicky *et al.*, 1998).

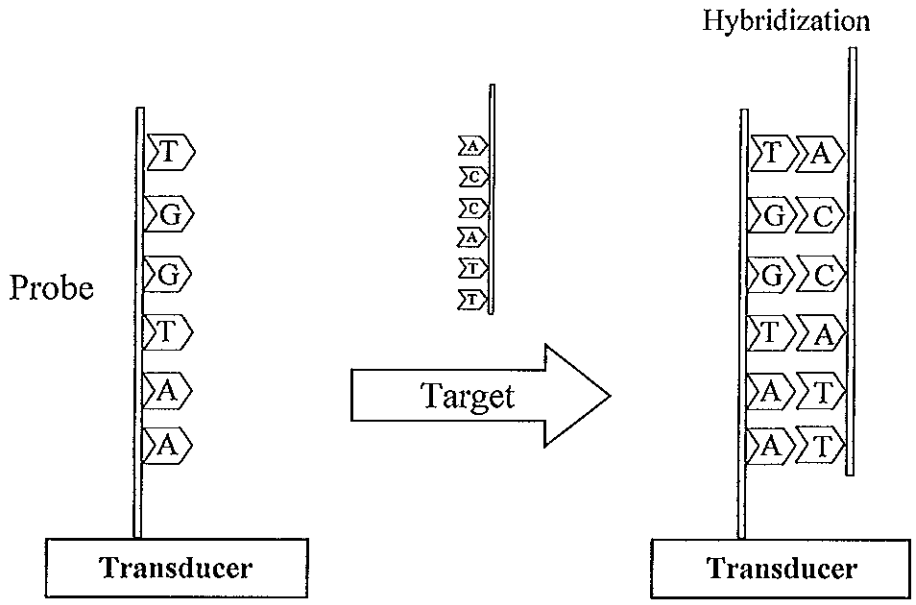

Figure 2.2 DNA hybridization events by immobilized single stranded DNA (probe) on a transducer surface to recognize its complementary (target) DNA via hybridization.

2.2.3 Antibody-antigen

The use of antibodies as specific reagents to bind with antigen targets are the principle of immunosensors. Antibodieds are gamma globulin proteins that are found in blood or other bodily fluids of vertebrates. They are five isotypes known as IgA, IgD, IgE, IgG, and IgM. Immunoglobulin G (IgG) is the most applied in biosensor application. (Anthony *et al.*, 1995). IgG molecule is a "Y" shaped that consists of four polypeptide chains; two identical heavy chains (H, MW 50,000 Da each) and two identical light chains (L, MW. 25,000 Da each) as shown in Figure 2.3. Each L chain

binds a H chain with disulfide bonds. The light and heavy chains are composed of two distinct domains: the variable region and the constant region. The variable region is located at the tip of the arms of the "Y" and serves as the antigen-binding site. An antigen fits inside the antigen binding site of an antibody because the structures match, like a key in a lock. Each antibody has antigen binding sites different from other antibodies. It leads to immunosensor give highly specific method. The antigen-antibody bond occurs through multiple non-covalent forces such as electrostatic attraction (major contribution), hydrogen bonding, hydrophobic bonding, and Van der Waals forces (Byfield and Abuknesha, 1994).

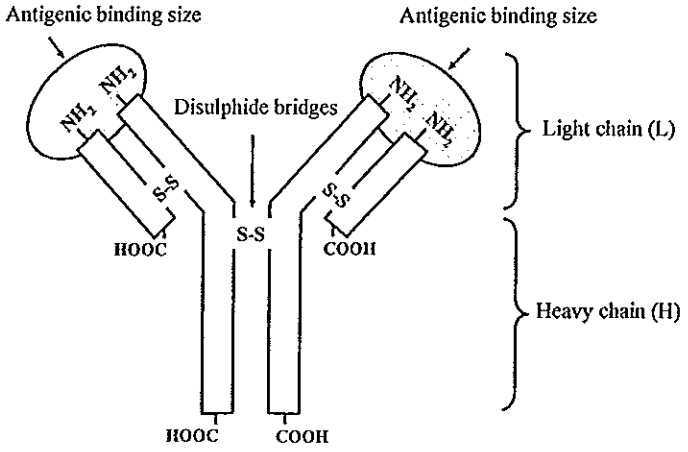

Figure 2.3 Structure of IgG antibody.

Label-free immunosensor based on direct detection of antibody–antigen interactions have also gained growing interest. The recognition element; antigen or antibody was immobilized on a transducer surface. After antigen-antibody complex was formed and the detection can be detected by the physical change of mass (Owen *et al.*, 2007; Zhang *et al.*, 2008a; Zhang *et al.*, 2008c), electrochemical property (Loyprasert *et al.*, 2008; Thavarungkul *et al.*, 2007; Zhang *et al.*, 2008b) or optical (Dudak and Boyaci, 2007; Dutra *et al.*, 2007; Gobi *et al.*, 2007). The vital advantages of these direct immunosensors are simple, rapid analysis, and low cost (Dutra *et al.*, 2007). Therefore, they have been widely applied in many fields including environmental (Gobi *et al.*, 2005; Hu *et al.*, 2003; Loyprasert *et al.*, 2008; Rahman *et al.*, 2007), clinical (Gobi *et al.*, 2007; Liang *et al.*, 2008; Michalzik *et al.*, 2005;

Okuno *et al.,* 2007), and food safety (Dudak and Boyaci, 2007; He *et al.,* 2009; Lin and Tsai, 2003; Thavarungkul *et al.,* 2007).

For labeled immunosensor, the methodology is based on the use of labels, which can amplify the primary signal of the immunosensor to enhance the sensitivity of sensor. Generally, enzymes (Ionescu *et al.,* 2007; Lu *et al.,* 2008; Wu *et al.,* 2007b; Zhao *et al.,* 2007), electroactive compounds (Polsky *et al.,* 2006; Wang *et al.,* 2003a; Wang *et al.,* 2003b), quantum dots (Jie *et al.,* 2008; Kerman *et al.,* 2007), and nanoparticles (Choi *et al.,* 2008; Kawaguchi *et al.,* 2008; Lin *et al.,* 2008; Suni, 2008; Tang *et al.,* 2004) have been widely used as labels.

Labeled immunosensors take advantage of the high selectivity provided by the molecular recognition of antigen by antibodies so, they are useful to detect analytes in several areas such as, clinical (Tang *et al.,* 2008b), environmental monitoring (Gonzalez *et al.,* 2001), and food control (Laschi *et al.,* 2003). However, one of the problems of immunosensors is the immobilization antibodies, generally through lysine residues. This is because they are several lysine residues on an antibody, the immobilization is random resulting in multiple orientations of the antibody on the surface and lead to reduce the antigen binding capacity (Bonroy *et al.,* 2006).

2.2.4 Others

2.2.4.1 Lectin-carbohydrate

Lectins are structurally diverse proteins from many sources; plant, animal, viruses, and microorganisims, which have a high degree of carbohydrate specificity and this making a useful biorecognition element (Chambers *et al.,* 2008; Safina *et al.,* 2008). Their interaction with polysaccharides is via multivalent interactions arising from the spatial organization of oligosaccharide ligands (Chambers *et al.,* 2008). Lectins constitute a large class of carbohydrate-binding proteins of which concanavalinA (Con A) is the most studied due to its excellent chemical stability at body temperature (Ballerstadt and Ehwald, 1994; Ballerstadt *et al.,* 2004). Con A is a lectin protein found in Jack bean. It contains four identical binding sites to a branched trimannoside core unit, located in *N*-glycosidic carbohydrate–peptide linkages of glycoproteins often associated to cell surfaces as shown as Figure 2.4 (Wei *et al.,*

2006). In affinity biosensor, lectin was immobilized on transducer surface via direct adsorption (Serra *et al.,* 2008), self-assemble monolayer of thiol (Safina *et al.,* 2008), and sol-gel (Oliveira *et al.,* 2008) and have been applied in both label-free and labeled assays. Label-free assay of lectin-carbohydrate interaction has been via the detection of change in optical (Duverger *et al.,* 2003; Vornholt *et al.,* 2007), mass (Pedroso *et al.,* 2008; Pei *et al.,* 2005), and electrochemical properties (La Belle *et al.,* 2007). Immobilized lectin has been applied to detect various types of cells such as *Campylobacter jejuni*, *Helicobacter pylori* (Safina *et al.,* 2008), *Escherichia coli* (Serra *et al.,* 2008), and Pleurotus *ostreatus* (Kobayashi *et al.,* 2005) since it can bind to sugar residues on their surface. Although lectin is easy to purify and low cost, it lacks specificity (Santana *et al.,* 2008) since it can bind to various carbohydrates such as starch, mannan, fucoidon, and so on (Vornholt *et al.,* 2007).

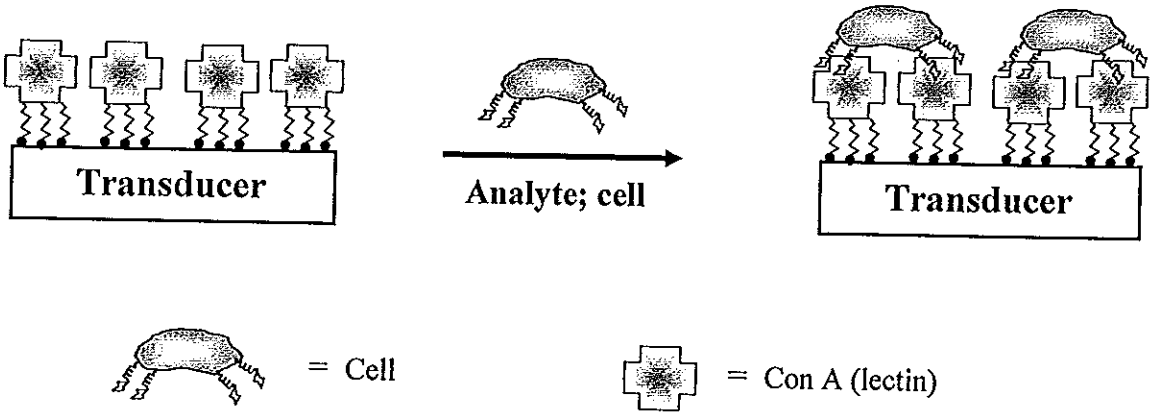

Figure 2.4 Scheme showing cells-binding Con A immobilized on the surface of a transducer.

2.2.4.2 Protein-metal

A variety of proteins, ranging from naturally occurring metal-binding proteins to various engineered proteins, have been utilized as biorecognition elements to bind

specific metal ions (Figure 2.5). There are two classes of metal-binding protein, metallothioneins and regulatory mercury protein (Bontidean *et al.,* 1998). Metallothionein is a low molecular weight, cysteine-rich protein with high selectivity capacity of binding with heavy metal ions such as zine, cadmium, copper, and mercury (Varriale *et al.,* 2007). It has the shape of a dumbbell and envelops metal in two separate domains; N-terminal-domain and C-terminal-domain (Stillman, 1995). Another class is regulatory mercury protein (MerR). It was encoded by the *mer* operon of Tn*501* in *Pseudomonas aeruginosa,* offered increased selectivity and could possibly be used in biosensors specific for mercury ion (Corbisier *et al.,* 1999). The selective mercury ion recognition occurs at both N-terninal and C-terninal domains and causes conformational change (Chen and He, 2008).

Applications of protein-metal binding were performed by immobilization of protein on transducer surface. Most of the applications were by direct detection during the binding of metal with proteins using capacitive (Bontidean *et al.,* 2003; Bontidean *et al.,* 1998; Bontidean *et al.,* 2000; Corbisier *et al.,* 1999) and surface plasmon resonance suytems (Zhang *et al.,* 2007). The main advantages of this affinity binding pair are useful storage stability (2 weeks) and could be regenerated using EDTA (Bontidean *et al.,* 2003). However, it can bind to several metal such as Hg^{2+}, Cu^{2+}, Zn^{2+}, and Cd^{2+} (Bontidean *et al.,* 2000; Verma and Singh, 2005), i.e. not specific.

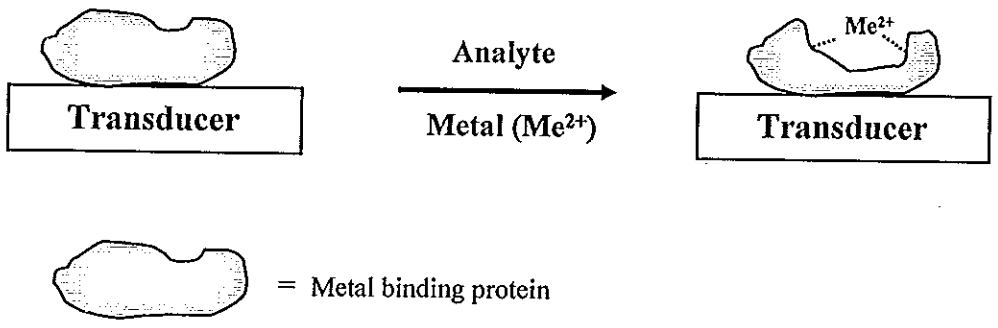

Figure 2.5 Protein-based affinity biosensor for monitoring conformational change upon binding of heavy metal ions.

2. 3 Labeled affinity biosensors

2.3.1 Type of labeled affinity biosensor

Labeled affinity biosensor involves a label to quantify the amount of analyte. Widely used labels including enzymes (Chen *et al.,* 2005), nanoparticles (Hu *et al.,* 2003), and fluorescent (Charles *et al.,* 1995) or electroactive material (Wang *et al.,* 2003b). Generally, labeled affinity biosensor can be divided into sandwich and competitive assays.

Procedures of sandwich assay consist of two recognition steps (Figure 2.6a). First, the biological recognition element is immobilized on a transducer surface, allowing it to capture analyte. Next, the labeled secondary biological recognition element is added to bind with previously captured analyte. Signal is detected via labeling compounds and related to concentration of analyte. This method can give low detection limit and have been widely applied in biosensor research (Pei *et al.,* 2002; Zhang *et al.,* 2008a), e.g., for estradiol (Liu and Wong, 2009), α-fetoprotein (Lin *et al.,* 2009a), atrazine(Valera *et al.,* 2008), and *Vibro parahaemolyticus (Zhao et al., 2007).*

Another type of labeled affinity biosensor is based on competitive assay. It is often used to enhance the sensitivity for detection of small molecule (Aizawa *et al.,* 2007; Kawaguchi *et al.,* 2007; Shankaran *et al.,* 2007). A scheme of the principle of competitive assay is given in Figure 2.6b. In this types of assay the analyte is labeled instead of the biological recognition element. Unlabeled analyte and the labeled analyte compete for the binding with the biological recognition pair and a decrease in signal indicates the presence of the analyte in the sample. Therefore, the signal is inversely proportional to analyte concentration.

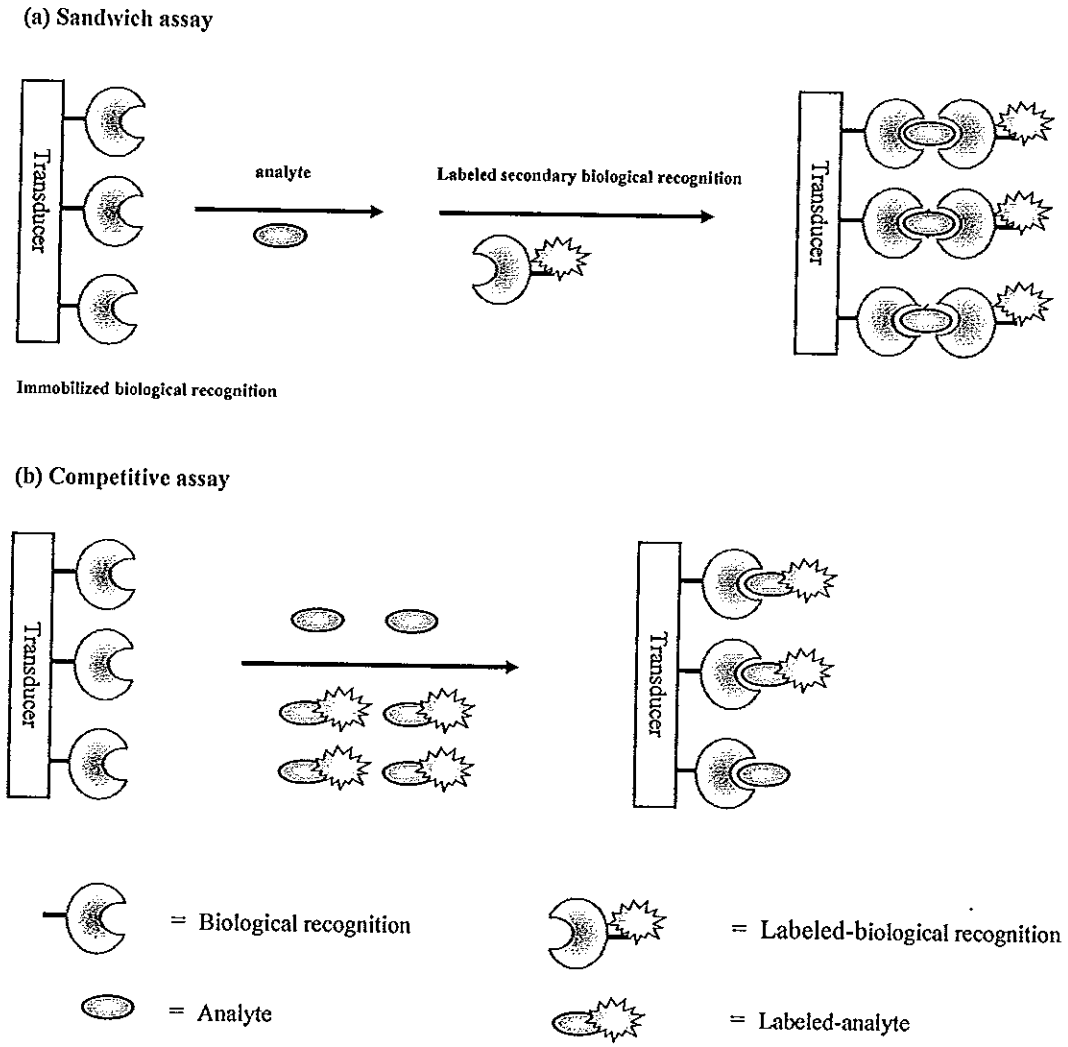

Figure 2.6 Types of labeled affinity biosensor detection (a) sandwich assay (b) competitive assay.

2.3.2 Detection principle of labeled affinity biosensor

The biological sensing element determines the degree of selectivity of the biosensor, while the sensitivity of the biosensor is greatly influenced by the transducer (Leca and Blum, 2005). Several detection principles have been applied for labeled affinity biosensors such as amperometry, stripping voltammetry, conductrimetry, and fluorescence.

2.3.2.1 Amperometric detection

This type of detector is designed to measure the current flow generated by oxidation or reduction of redox species at the electrode surface with constant voltage (Wang, 2000). Since most protein analytes are not intrinsically able to act as redox partners in an electrochemical reaction (Luppa *et al.*, 2001), labels are required. In general, enzymes such as horseradish peroxidase and alkaline phosphatase were used as labels then the substrate or the product of the enzymatic reaction can be monitored amperometrically. Amperometric affinity biosensor is attractive because it is sensitive and requires less complicated instrumentation (Yuan *et al.*, 2005). Therefore, this technique is preferred and this is the subject of a further review in the chapter 4.

2.3.2.2 Voltammetric stripping detection

Electrochemical stripping analysis is still recognized as one of the most convenient techniques for measuring trace amount of heavy metal ions. Because of its capability of pre-concentrating analytes at/in the surface of the working electrode, quantification of detection limits are lower by two to three orders of magnitude compared to solution-phase voltammetric measurements (Wang, 2006). The applications of this technique for affinity biosensor were carried out by metal nanoparticles labels and provided high sensitive detection (Wang *et al.*, 2008c) (see further review in chapter 4).

2.3.2.3 Conductricmetric detection

Conductimetric affinity biosensors measure the changes in the conductance of solution between a pair of metal electrodes which results from affinity binding of analyte (Gerard *et al.*, 2002; Valera *et al.*, 2008). The response of conductimetric in affinity biosensor can be improved by nanoparticles. Metal nanoparticles represent an excellent labeling system that can generate significant resistance changes when the binding event occurs (Ambrosi *et al.*, 2008). This transducer is further reviewed in chapter 4.

2.3.2.4 Fluorescence detection

Fluorescence detection is based on using fluorescent labeled in sandwich and competitive assay. Biological recognition element was immobilized on a transducer surface to bind with analyte. Labeled fluorescent secondary biological recognition element was added to capture with the analyte. Then fluorescent label was excited by light source and fluorescent product was detected. Several fluorescent labels have been used such as fumonisin B_1-fluorescein isothiocyanate (Klotz *et al.*, 1998), Cy 5 dye (Mosiello *et al.*, 1997), Cy 5.5 dye (Thompson and Maragos, 1996). The fluorescence detection is widely applied in labeled affinity biosensors due to its high sensitivity, good selectivity, and fast response time (Mosiello *et al.*, 1997) (see further review in the chapter 3).

Although, labeled affinity biosensor is more sensitive, it is relatively time-consuming, and real time monitoring is not possible (Jiang *et al.*, 2008).

2. 4 Label-free affinity biosensors

This procedure directly detects the binding between immobilized biological recognition element on a transducer surface and analyte without any labels (Figure 2.7) causes by the change in physical properties such as optical, mass, and electrochemical. The signal is directly proportional to the amount of analyte. The main advantages of these direct affinity biosensor include rapid detection, simplicity, and low cost (Teles and Fonseca, 2008). However, such direct affinity biosensor is often insufficient to detect analyte in low concentration or low molecular mass (Liu *et al.*, 2004).

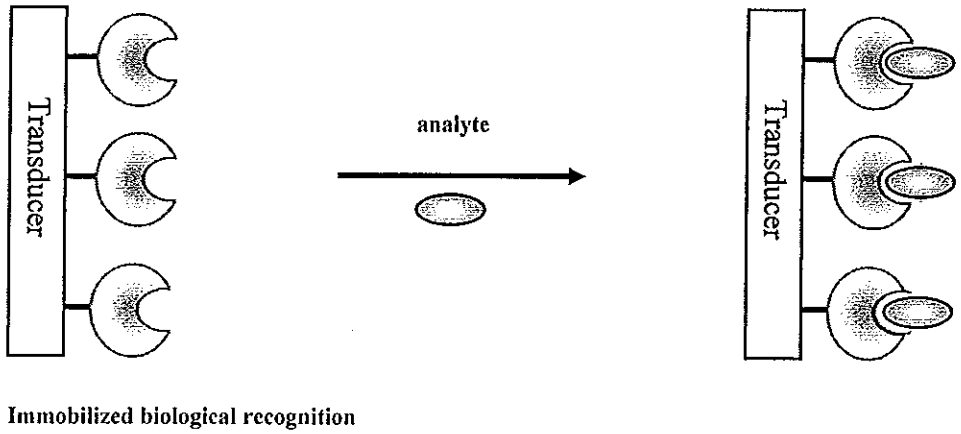

Figure 2.7 Label-free affinity biosensor detection by measuring of changes in any physical property as a result of analyte-biological recognition complex.

2. 4.1 Detection principle of label-free affinity biosensor detection

Many transducers such as quartz crystal microbalance, surface plasmon resonance, and capacitive methods have been used for label-free affinity biosensor detection.

2.4.1.1 Quartz crystal microbalance detection

Quartz crystal microbalance affinity biosensors are based on the coupling of the biological recognition element with a piezoelectric element. Piezoelectricity is the ability of some material to generate electric potential in response to applied mechanical stress. Many types of materials (quartz, tourmaline, lithium niobate or tantalate, oriented zinc oxide or aluminum nitride) exhibit the piezoelectric effect, but the properties of quartz make it the most common crystal type used in analytical applications (Kurosawa *et al.*, 2006; Luo *et al.*, 2007; Mannelli *et al.*, 2003 ; O'Sullivan and Guilbault, 1999). The measuring device, consisting of a quartz disk with thin-film electrodes plated on it, is usually denoted as quartz crystal microbalance (QCM) (Figure 2.8). An external potential is applied to a piezoelectric material produces internal mechanical stress and causes a vibration at some

frequency. The QCM then measures the frequency of oscillation in the crystal. When used as a transducer in biosensor, the QCM can detect changes in frequency of the crystal due to changes in mass on the surface of the crystal (Luo *et al.,* 2007). Biological recognition elements were immobilized on the surface of crystal to capture the target molecule. The analytes interact with biological recognition elements resulting in decreasing of frequency. The quantitative relationship between the frequency shifts and the mass changes of the crystal is given by the well known Sauerbrey equation (Sauerbrey, 1959).

$$\Delta f = -2\frac{f_0^{\,2}}{A\sqrt{\rho_q \mu_q}}.\Delta m \qquad (2.1)$$

Where Δm is the mass change on the sensor surface, f_0 the fundamental frequency, A the electrode surface area, and ρ_q and μ_q are the density and the shear modulus of the QCM sensor, respectively. Therefore, both direct and indirect quartz crystal microbalances have been developed for affinity biosensor. Because of its simplicity, convenience, low cost, and real-time response, this method has been important for detection of drugs (Ming-Chung Tseng *et al.,* 2007; Tseng *et al.,* 2007; Zhang *et al.,* 2008a), tumor makers (Ding *et al.,* 2008b), viruses (Lee and Chang, 2005; Owen *et al.,* 2007), and DNA (Duman *et al.,* 2003; Mannelli *et al.,* 2003). Since, QCM detection is via frequency change due to the change in the amount of mass coupled to the surface. Its limitation is from the interferences of water molecule when used on liquid media and highly reproducibility results should be difficult to achieve (Peh *et al.*, 2007; Laricchia-Robbio and Revoltella, 2004).

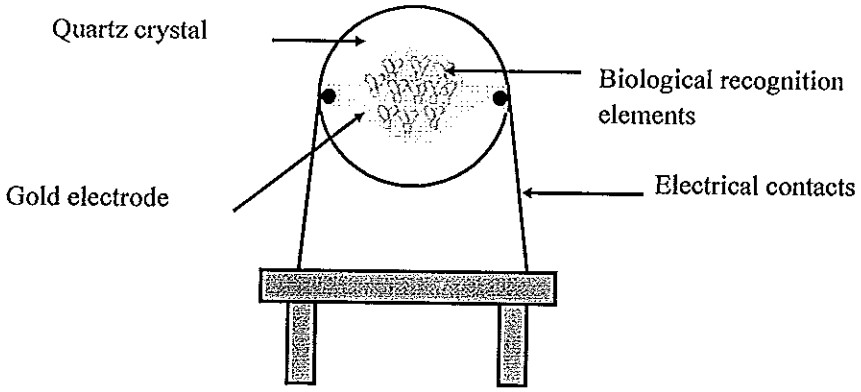

Figure 2.8 Schematic of a piezoelectric crystal.

2.4.1.2 Surface plasmon resonance

Surface plasmon resonance biosensors are a powerful detection and analysis tool for bioanalysis which have been widely applied in many fields. This is due to the advantages of real time monitoring, fast response, and kinetic measurement (Yu *et al.*, 2005). This transducer can be applied for both label-free and labeled detections. For label-free detection, target molecules are not labeled and detected in their natural forms. This type of detection is relatively easy and cheap to perform, and allows for quantitative and kinetic measurement of molecular interaction. Due to these advantages, the labeled-free optical biosensors have been popularly used for the detection of DNA (Leung *et al.*, 2008; Peeters *et al.*, 2008; Su *et al.*, 2008), pathogens (Dudak and Boyacı, 2007; Kim *et al.*, 2007a), toxins (Hong *et al.*, 2008; Jyoung *et al.*, 2006; Soykut *et al.*, 2008; Taylor *et al.*, 2008), and tumor markers (Chou *et al.*, 2004; Teramura and Iwata, 2007).

Therefore, label-free optical affinity biosensors are preferred and this is the subject of a review in the chapter 3.

2.4.1.3 Capacitive detection

Electrochemical biosensors are bioanalytical tools characterized by the simplicity of construction, the possibility to be mass-produced, the cost-effectiveness, the easiness of use, the feasible miniaturization and the subsequent portability (Chen *et al.*, 2006a; Chen *et al.*, 2008b). Among several electrochemical transducers,

capacitive detection has recently been extensively studied (Bontidean *et al.,* 2003; Li *et al.,* 2005; Limbut *et al.,* 2006a; 2006b; Loyprasert *et al.,* 2008; Yang *et al.,* 2005; Yin *et al.,* 2006). This technique is based on the change of capacitance at the electrode–electrolyte interface as a result of the affinity binding. In fact, capacitive system provides both sensitive and specific (Li *et al.,* 2005). These advantages make the capacitive affinity biosensor attractive as a transducer (Limbut *et al.,* 2006a; Loyprasert *et al.,* 2008; Yang *et al.,* 2005; Yin *et al.,* 2006). This technique was investigated and reviewed in the chapter 4.

CHAPTHER 3

Optical Detection

The interest in optical detections of biomolecular interaction is due to their nondestructive operation and rapid signal generation and reading (Luppa *et al.*, 2001a). Optical affinity biosensors function by detecting affinity binding through changes in optical characteristics such as fluorescence, chemiluminescence, and refractive index when light is reflected at sensing surface. There are applications of optical transducers for both labeled and label-free affinity biosensors.

3.1 Labeled optical affinity biosensor

3.1.1 Evanescent wave fluorescence fiber optic

Nowadays, optical fibers play an important part in sensor technology including biosensor. As a result of their properties; excellent light delivery, long interaction length, low cost and ability not only to excite the target molecules but also to capture the emitted light from the targets are the main points in favor of the use of optical fibers in biosensors (Bosch *et al.*, 2007). The fiber-optic evanescent wave biosensor is based on total internal reflection, a fundamental characteristic of an optical fiber.

Optical fibers consist of a cylindrical core surrounded by a cladding layer, both made of silica (Figure 3.1a). For application of optical fibers in affinity biosensor, a section of the cladding layer was usually removed (Figure 3.1b). In this space biological recognition element would be immobilized to bind with analyte.

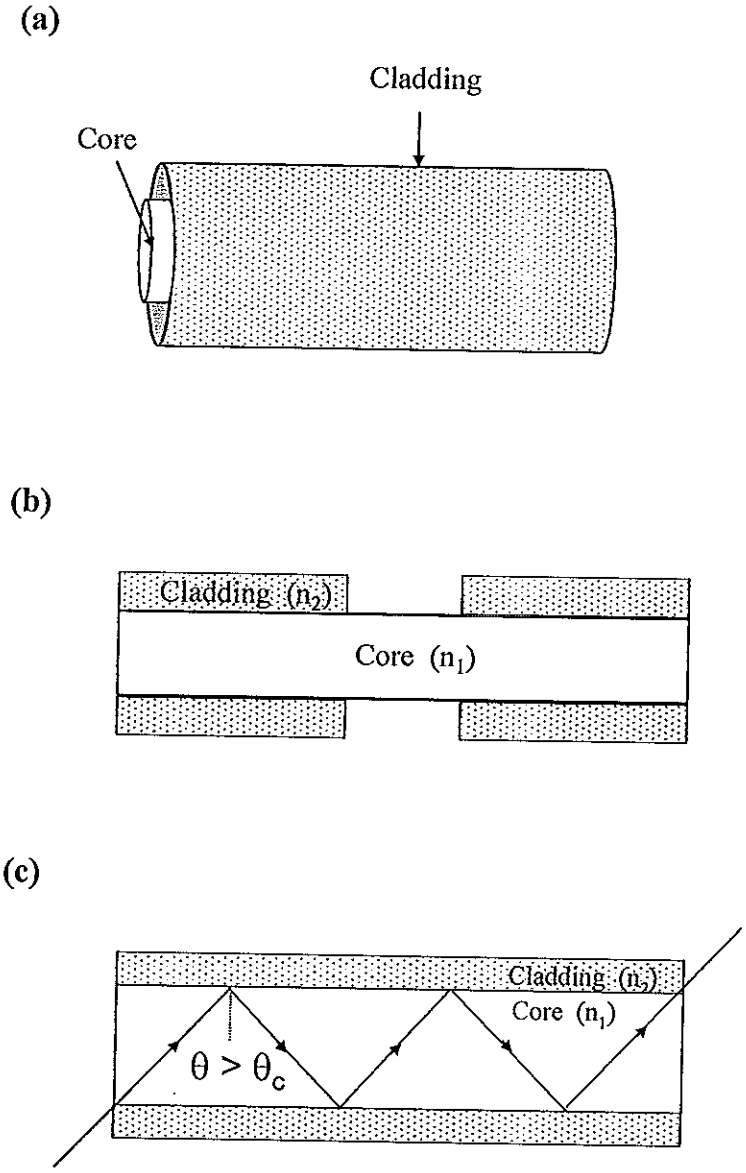

Figure 3.1 (a) Structure of an fiber optic and (b) a section of cladding was removed in this application for affinity biosensor (modified from Leung *et al.*, 2007; Epstein and Walt, 2003) (c) light propagates though optical fiber by total internal reflection when incident angle (θ) is more than critical angle (θ_c).

Commonly, the core is doped with germanium to make its refractive index (n_1) slightly higher than the cladding (n_2). Since the core has a higher refractive index than the cladding total internal reflection can occur enabling light to propagate through the optical fiber (Leung and Mutharasan, 2007). This phenomenon occurs when a ray of

light strikes a medium boundary interface between different refractive index and the angle of incidence is larger than the critical angle (θ_c), it will be totally internally reflected and propagated through the fiber followed Snell's law (Marazuela and Moreno-Bondi, 2002).

$$\theta_c = \sin^{-1} \frac{n_2}{n_1} \tag{3.1}$$

Fiber optic used as a transducer can be classified into two types, intrinsic and extrinsic. For intrinsic sensor, interaction of analyte occurs within an element of optical fibers. In extrinsic sensor, analyte binding takes place outside the fiber.

Evanescent wave fluorescence basis is widely applied for fiber optic detection (Ko and Grant 2006; Long *et al.*, 2008; Taitt *et al.*, 2005). Fluorescence detection provides sensitive detection of biomolecules since its intensity is proportional to the excitation intensity, even weak signals can be observed. Evanescent wave fluorescence fiber optic can be achieve by fluorophore labels such as fumonisin B_1-fluorescein isothiocyanate, Cy 5 dye, Cy 5.5 dye (Klotz *et al.*, 1998; Mosiello *et al.*, 1997; Thompson and Maragos, 1996). The evanescent wave excites fluorescent molecules near the optical fiber surface resulting in fluorescence signal.

In general, evanescent wave fluorescence fiber optic biosensor is based on a sandwich technique (Figure 3.2). The application of evanescent wave fluorescence fiber optic in affinity biosensor; i.e. immunosensor was performed by immobilization of primary antibody on the core surface of the uncladded fiber. On the addition of antigen and a secondary fluorescence-labeled antibody, then the sandwich fluorescence-labeled antibody/ antigen/antibody is formed near the fiber surface after that the fluorescence signal was detected (Lin *et al.*, 2009b). The maximum penetration depth of the evanescent field into the surrounding medium is of the order of some hundred nanometers that is able to only detect analyte binding. Therefore, this technique is insensitive to the influence by non interacting background molecules (Hsieh *et al.*, 2007). Evanescent wave fluorescence fiber optic have been applied for clinical diagnostics (Abel *et al.*, 1996), food control (Ko and Grant, 2006), and environmental monitoring (Ligler *et al.*, 1993). Although this assay offers many

advantages such as high sensitivity, good selectivity, and fast response time, fluorescence-based sensors require an excitation light source and the spectral separation of exciting and emitted light, which implies relatively sophisticated equipment producing high background signals (Zhang *et al.*, 1999).

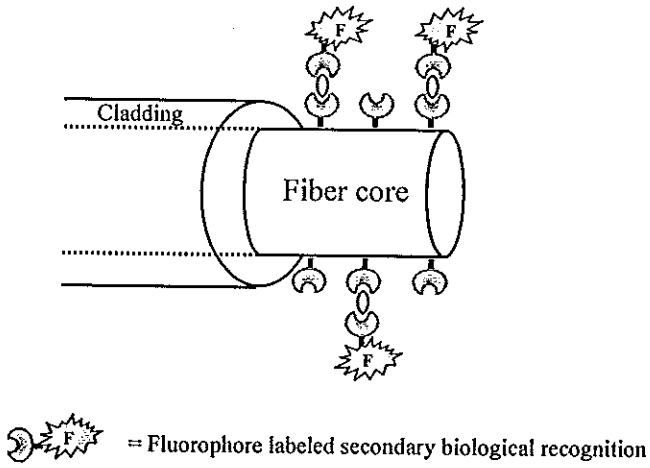

Figure 3.2 Fluorescent fiber affinity biosensor detection; the detecting of fluorescent signal after secondary biological recognition capture with analytes by optical fiber (Modified from Lin *et al.*, 2009b).

3.1.2 Chemiluminescence measurement

Chemiluminescence is the emission of light that occurs as a result of certain chemical reactions that produce high amounts of energy which is lost in the form of photons when electronically excited product molecules relax to their stable ground state. Because chemiluminescence does not involve initial absorption of light so, measurements of chemiluminescence emission are made against a lower background, thus allowing greater sensitivities of detection (Zhang *et al.*, 1999). The principle of chemiluminescence was performed for affinity biosensor through the labeled marker reaction, usually an enzymatic reaction. The most frequently used enzyme is horseradish peroxidase (Lin *et al.*, 2004) or alkaline phosphatase (Chen *et al.*, 1998) to carry out a chemiluminescence reaction in the presence of chemiluminescence reagents such as luninol and hydrogen peroxide and then produce a

chemiluminescence light signal as shown in Figure 3.3. Consequently, light intensity is directly proportional to the concentration of analyte. The chemiluminescence affinity biosensors are successful for the detection of tumor markers (Fu *et al.*, 2006), virus (Herrmann *et al.*, 2005), chloramphenicol (Park and Kim, 2006), and DNA (Chen *et al.*, 1998). Moreover, chemiluminescence biosensor has two major advantages: a very high sensitivity and a wide dynamic range (Salama *et al.*, 2007). However, the problems are the need to find many optimum conditions for both the electrochemical and chemiluminescence reactions and poor reproducibility of response because of the occurring of oxide on the electrode surface, requiring frequent refreshing of the electrode surface (Knight 1999).

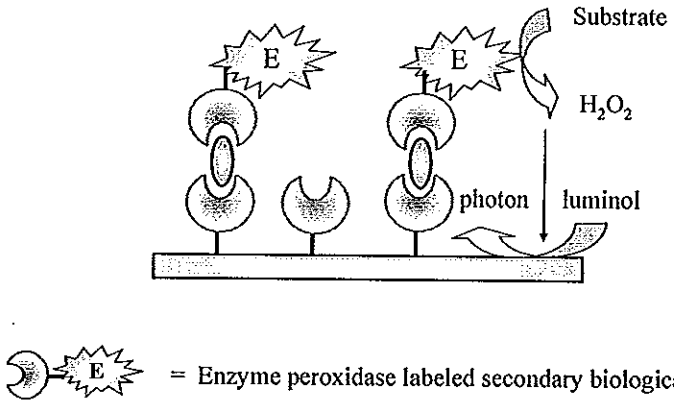

Figure 3.3 Chemiluminescence-based labeled affinity biosensor using enzyme oxidase.

3.2 Label-free optical affinity biosensor

3.2.1 Reflectometric interference spectroscopy

Reflectometric interference spectroscopy is a label-free technique for optical biosensor that is able to detect biomolecular interactions of molecules immobilized on the surface of a transducer with analytes in solution. It is based on the interference of light beams, which are reflected at interfaces with different refractive indices at the top layer of the sensor. The reflectometric interference spectroscopy transducer consists of a glass substrate (≈ 1 nm thick) coated with a sensitive layer of a material

such as Ta_2O_2, SiO_2, and polymer (Proll *et al.*, 2007). This layer was modified to immobilize biological sensing element.

Figure 3.4 shows the principle of reflectometric interference spectroscopy. A light beam passing the interface between two media of different refraction indices will be reflected in part. Reflected beams occurred when glass substrate was immobilized with biological recognition element (I_1) as shown in Figure 3.4a. Changes in the optical thickness of the layer due to the binding of analyte with immobilized biomolecules recognition elements causing a change in the interference spectrum of the reflected light from I_1 to I_2 (Figure 3.4b).

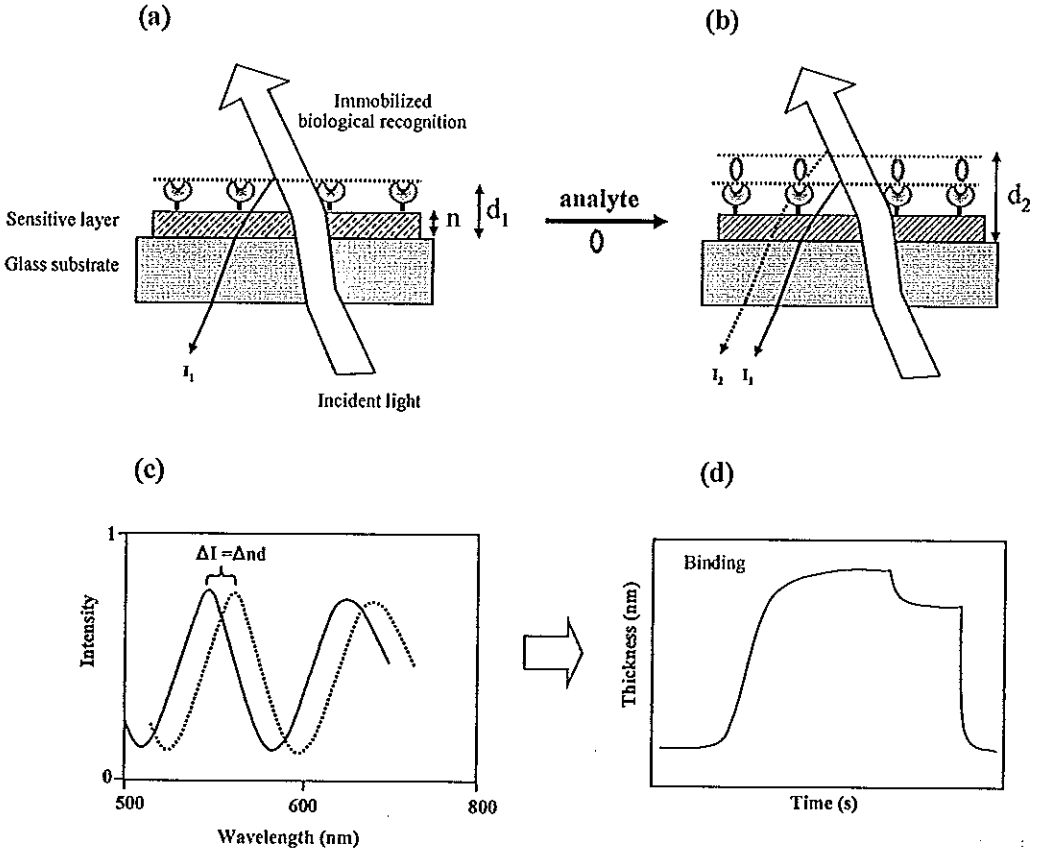

Figure 3.4 Scheme of reflectometric interference spectroscopy detection; the change of the optical thinness during a binding between antibody (a) and antigen on transducer surface. The corresponding change interference spectrum is shown in (c) and the resulting binding curve is given in (d) (Modified from Proll *et al.*, 2007).

These reflected beams depend on wavelength, thickness of the layer, which is given by the product of the refractive index of the layer (n) and its physical thickness (d). All of these conditions result in an interference spectrum (Brecht *et al.*, 1995; Gauglitz 2005).

$$\Delta I = \Delta nd \tag{3.2}$$

The binding of an analyte molecule to the sensor surface caused the change in n or d then the interference pattern shifted (Figure 3.4c). To evaluate the binding signal, the wavelength position of one extremum of the interference pattern is tracked over time and was converted to the optical thickness (nd) of the interference layer by the relation $nd = m\lambda/2$, where m denotes the order value of the extremum evaluated. The plot of nd against the time gave the binding curve of response as shown in Figure 3.4d (Länge *et al.*, 2004; Brecht *et al.*, 1995).

Reflectometric interference spectroscopy has successfully been employed for time-resolved detection of biomolecular interactions (Brecht *et al.*, 1993) with detection limits of a few picograms per square millimeter (Piehler *et al.*, 1996). This technique is simple, robust, and can be used for kinetic analysis (Belmont *et al.*, 2007; Lange *et al.*, 2002). Due to these advantages, it has been employed for several analytes, such as cytokine interferon α2 (Piehler and Schreiber, 2001), bacterial infection (Nagel *et al.*, 2008), pesticides (Brecht *et al.*, 1995), and benzo[*a*]pyrene (Lange *et al.*, 2002). However, since all molecules can easily adsorb on glass surface, non-specific binding at the transducer surface has become a problem for detection (Birkert *et al.*, 2000; Piehler *et al.*, 1996; Piehler *et al.*, 2000).

3.2.2 Interferometry

Interferometry is a well-established label-free optical technique for high precision method in many fields (Prieto *et al.*, 2003a). It has also been applied in biosensing transduction, allowing high sensitivity. It is based on the optical waveguide of total internal reflection (TIR). The TIR take place when the light passes through from high refractive index into low refractive index solution. Although, the light is confined within the core of the wavelength, there is a part of the

guided light that travels through that extends into the medium surrounding the waveguide (called the evanescent field). The interaction of the analyte within the evanescent field caused refractive index change and the phase of the guiding light is then shifted.

Mach-Zehnder interferometer is the most common configuration in biosensing devices as shown in Figure 3.5. In a typical configuration the optical waveguide is split into two beams at a Y conjunction with equal intensity (Figure 3.5a). One channel is considered as reference and the other as sensor. In the sensor channel the biorecognition sensing element was immobilized on surface to bind with analyte. The change of the refractive index due to interaction of biomolecule and analyte in the sensor channel comparing to reference channel resulting in optical phase shift ($\Delta\Phi$) (Prieto *at el.*, 2003a,b).

$$\Delta\Phi = 2\pi \frac{L}{\lambda}(n_{eff}^{S} - n_{eff}^{R}) \qquad (3.3)$$

Where L is the reference and sensor channel length, λ is the optical signal wavelength, n_{eff}^{S} is the effective refractive index of sensor channel and n_{eff}^{R} is the effective refractive index of reference channel.

The phase-difference shift of the propagation modes guided in the sensor and in the reference channels modulates the output intensity of light (I_{out}) via an interference phenomenon.

$$I_{out} = \frac{I_{in}}{2}(1 + \cos\Delta\Phi) \qquad (3.4)$$

Where I_{in} is the input intensity of light signal coupled into the interferometer. The refractive index and optical phase changed can then be converted to intensity of light. A binding curve was then obtained by plotting intensity of light *vs* time as shown in Figure 3.5b (Drapp *et al.*, 1997).

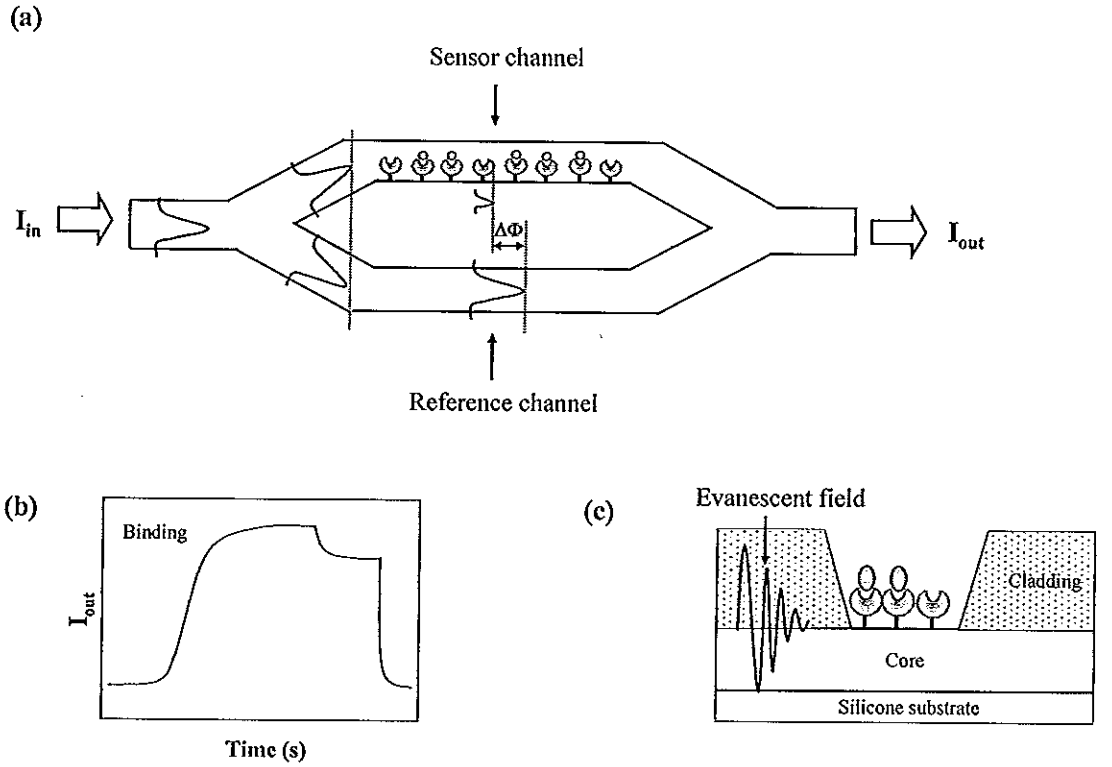

Figure 3.5 (a) Scheme of Mach-Zehnder interferometer. (b) Real-time detection of binding curve obtained from intensity of light *vs* time. (c) The cross-section of sensor channel; the cladding layer was removed to immobiliz biorecognition elements, the interaction of bimolecule take place at core-cladding interface within evanescent field region (Modified from Prieto *at el.*, 2003a; Heideman *et al.*, 1993).

Typically in an interferometer design, large refractive index differences of the core/cladding layer are required to achieve high detection sensitivity (Heideman *et al.*, 1993). High refractive index (RI) contrast between the core and the cladding can be obtain from Si_3N_4 (RI = 2.036) and SiO_2 (RI = 1.459) materials, respectively (Ymeti *et al.*, 2002). The cladding was removed to immobilize biological recognition element on the core (Figure 3.5c). In general, the core was made of silicon materials, so the surface was modified via the method of plasma induce graft copolymer (Shew *et al.*, 2008) or silanization with 3-aminopropyltriethoxysilane (Brosinger *et al.*, 1997) in order to immobilize biological recognition elements on sensor channel

surface. Interferometry has been applied for environmental monitoring (Lechuga *et al.*, 1995), clinical diagnostic (Brynda *et al.*, 2002) with label-free affinity biosensor. Although, interferometer provided extremely high sensitivity, it required a complex experimental set-up (Brosinger *et al.*, 1997).

3.2.3 Surface plasmon resonance

3.2.3.1 Principle of surface plasmon resonance

Surface plasmon resonance (SPR) is a surface sensitive analytical method for chemical and biological detection that is based on detecting changes in refractive index (RI) on the metal surface. SPR was first developed for biosensor in 1983 (Liedberg *et al.*, 1983). A surface plasmon is a charge density wave occurring at the interface between a metal and a dielectric. A surface plasmon can be excited by evanescent wave at the incoming light as demonstrated in Figure 3.6 (Green *et al.*, 2000; Liedberg *et al.*, 1995).

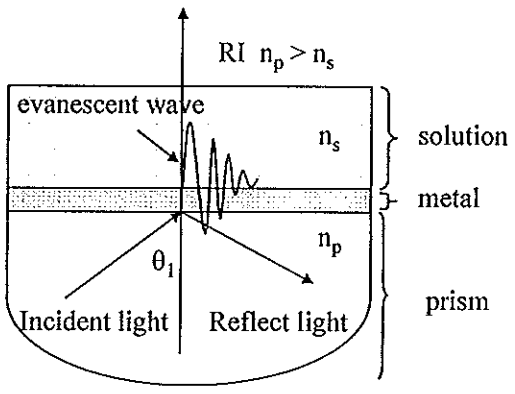

Figure 3.6 Total internal reflection phenomenon.

There are four basic methods to excite the SPR; waveguide coupling, fiber optic coupling, grating coupling, and prism coupling as shown in Figure 3.7. SPR using optical waveguide configuration (Figure 3.7a) consists of a thin film planar waveguide with a thin metal over layer. A light wave is guided by the waveguide and entered in thin metal over layer, it evanescently penetrates through the metal layer (Levy and Ruschin, 2007). The second type is based on fiber optic (Figure 3.7b). SPR

sensing is made of optical fiber with removed cladding and a thin metal film deposited around the exposed section of fiber core. The light is used as source of a range of optical wavelengths guided into the optical fiber (Slavik et al., 1999). The third type is based on grating coupling (Figure 3.7c). The grating SPR sensor was covered by a thin metal film. The grating was designed to couple light to the surface plasmon wave guided along an interface between the SPR-active metal and aqueous medium (Dostalek et al., 2005). The last and mostly used is based an prism coupling (Figure 3.7d). Nowadays, commercial systems SPR biosensors are generally based on this configuration. The approach is simple, sensitive and robust (Hoa *et al.*, 2007).

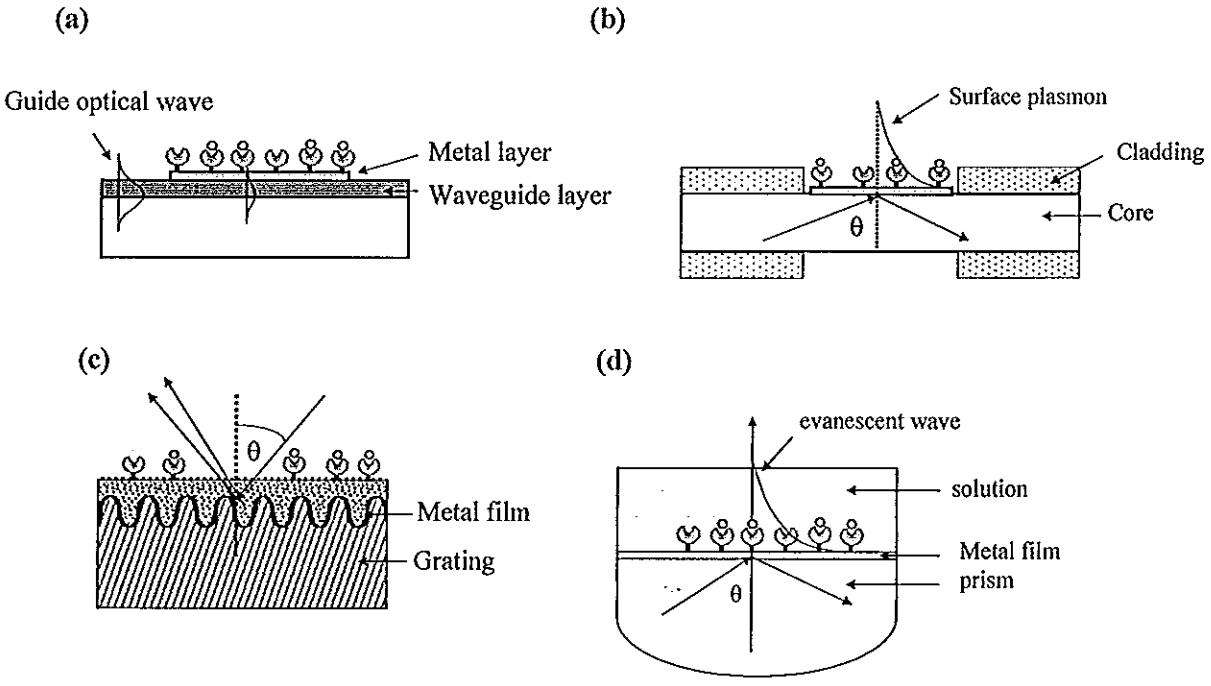

Figure 3.7 Configurations of SPR sensors (a) optical waveguide, (b) fiber optic, (c) grating prism and (d) prism coupling (Modified Hoa *et al.*, 2007; from Homola *et al.*, 1999).

In the prism coupling when monochromatic and plain polarized light strikes a prism, the light is bend toward the plane of interface. When it is passing from a more dense to a less dense medium with angle of incidence greater than the critical angle total internal reflection occurs. An important side effect of total internal reflection is

the propagation of an evanescent wave across the boundary surface (Luppa *et al.*, 2001b).

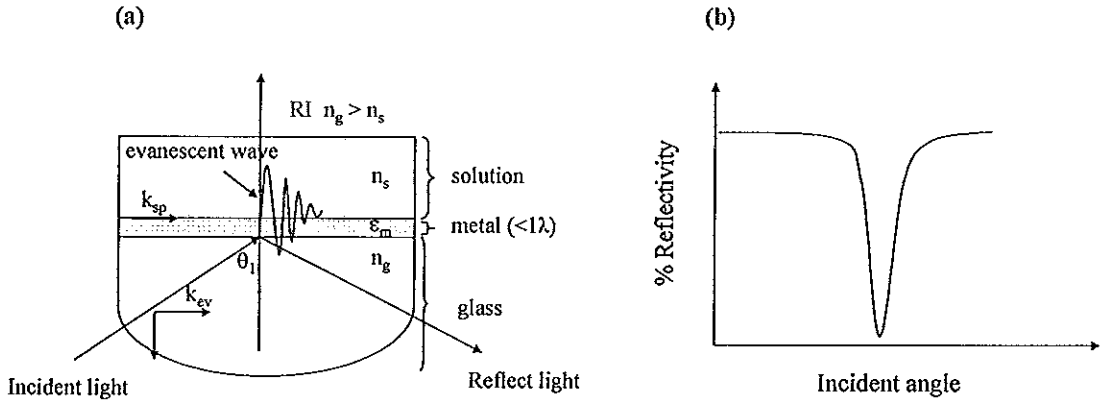

Figure 3.8 (a) principle of surface plasmon resonance based on glass coupling and (b) a shape of reflectance minimum is produced at resonance angle (modified form Gupta and Kondoh, 2007; Green *et al.*, 2000).

Figure 3.8a showed the configuration of the SPR, a monochromatic; *p*-polarized light source is used and the interface between the two optically dense media is coated with a thin metal film, commonly is gold, (of thickness less than one wavelength of light). The wave vector of the evanescent field (k_{ev}) is given by

$$k_{ev} = \frac{w_0}{c} n_g \sin\theta_1 \qquad (3.5)$$

Where w_0 is the frequency of incident light, n_g the refractive index of the dense medium (glass), θ_1 is the angle of incidence of the light and c the speed of light in a vacuum. The wave vector of a surface plasmon (k_{sp}) can be approximated to

$$k_{sp} = \frac{w_0}{c} \sqrt{\frac{\varepsilon_m n_s^2}{\varepsilon_m + n_s^2}} \qquad (3.6)$$

Where ε_m is the dielectric constant of the metal film and n_s is the refractive index of the dielectric medium (Matsubara *et al.*, 1988).

The evanescent wave of the incoming light is able to couple with the free oscillating electrons (plasmons) in the metal fillm at a special angle of incidence corresponding to when $k_{sp} = k_{ev}$, and thus the surface plasmon is resonantly excited. This caused energy from the incident light to be lost to the metal film resulting in a decrease of reflected light intensity (Green *et al.*, 2000) (Figure 3.8b). This reflectance minimum occurs in the reflected light at an acutely defined incident angle, called resonance angle (θ_{SPR}).

There are two basic modes of detection as shown in Figure 3.9 (Homola *et al.*, 1999; Ince and Narayanaswamy, 2006). In the first mode (Figure 3.9a), the wavelength is fixed and the incident angle is swept until resonance is observed as a dip in the reflectivity curve. This is called resonant angle SPR, and the shift in the resonance angle is measured (Kawaguchi *et al.*, 2008; Li *et al.*, 2008d). In the other mode (Figure 3.9b), the incident angle is fixed near resonance and the wavelength swept until resonance is observed as a dip in the reflectivity curve. This is called resonant wavelength SPR, and the shift in resonance wavelength is measured (Liu *et al.*, 2004; Wei *et al.*, 2003). The resonance condition is dependent on the metal, the structure of the metal's surface, and the nature of the medium in contact with the metal's surface.

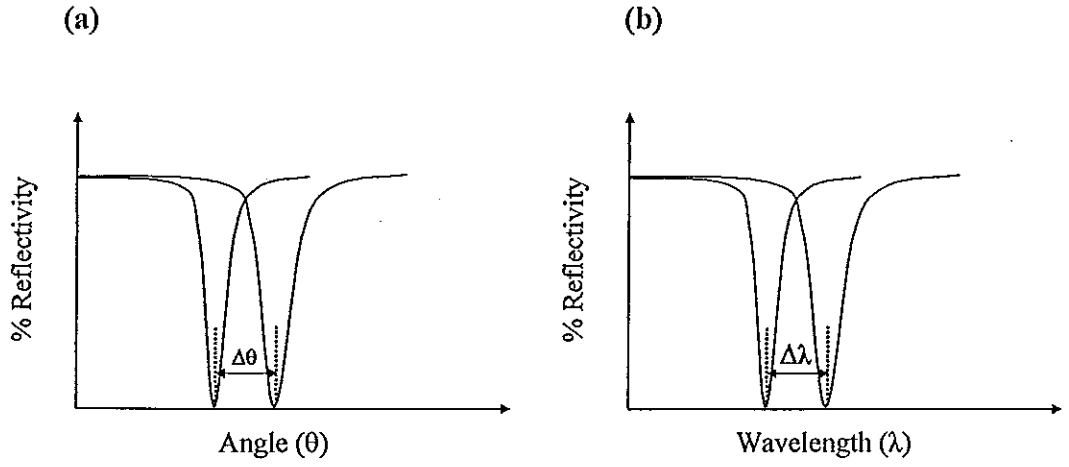

Figure 3.9 Two basic SPR detection (a) angle measurement for a fixed wavelength (b) wavelength measurement for a fixed angle.

3.2.3.2 Application of SPR for affinity biosensor

Many configurations of SPR biosensor have been developed, depended on elements used for excitation surface plasmon wave. Such elements include prism, grating (Gupta *et al.*, 2008), waveguide (Levy and Ruschin, 2007), and fiber optic (Iga *et al.*, 2004). The most commonly used is the prism because the incident light comes from the high refractive index medium (prism) and reflects at the gold surface without traveling through the liquid (Beusink *et al.*, 2008). The layer above the prism is a metal film. To be useful for SPR, a metal must have conduction band electrons capable of resonating with light at a suitable wavelength. A variety of metallic elements included gold, silver, copper, and aluminum. Of the candidate metals, gold is the most used due to its stability, antioxidation, and compatible with biological molecules (Yingying *et al.*, 2008). The SPR generating surface is usually composed of 50 nm thick layer of gold covered on a prism. For the application of SPR in biosensor, biological recognitions were immobilized on gold surface. When the sensor is exposed to a sample that contained analyte molecules, they bind to the sensor surface via their specific interaction. This causes the change of refractive index of the medium and produces the shift in resonance angle of SPR (or wavelength) as shown in Figure 3.10. The magnitude of the shift is proportional to the amount of binding take place. The effective penetration depth of the evanescent field which arises under conditions of total internal reflection is approximately 300 nm. Therefore, only refractive index changes occurring within this distance from the surface will cause a change in the generated SPR signal (Leonard *et al.*, 2004).

(a) (b)

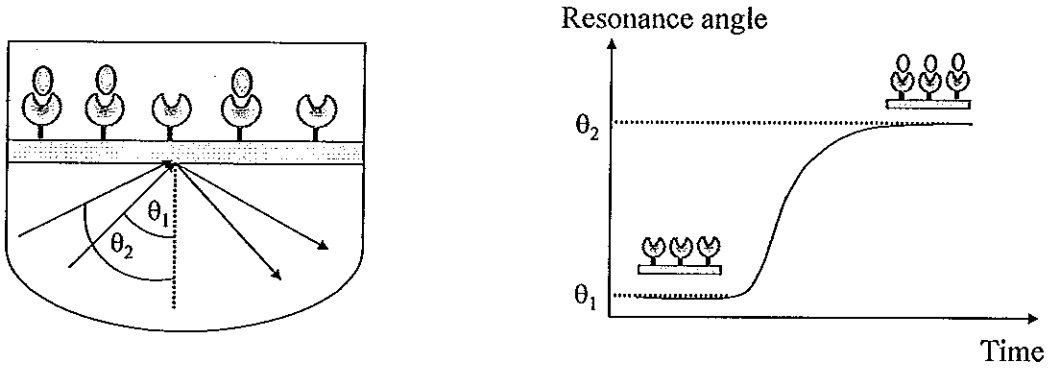

Figure 3.10 (a) Surface plasmon resonance application for affinity biosensor; interaction between immobilized biological recognition element on gold substrate surface and analytes caused an increase in resonance angle (b).

SPR technique provides many advantages such as, fast analysis, real-time detection, and simple to use (Toyama *et al.*, 1998; Yu *et al.*, 2005). Therefore, it has been applied in medical diagnostics (Chung *et al.*, 2006; Dutra and Kubota, 2007; Yuk *et al.*, 2007), food safety (Indyk 2009; Mazumdar *et al.*, 2008; Rebe Raz *et al.*, 2008), environmental (Hong *et al.*, 2008; Mauriz *et al.*, 2007; Rajan *et al.*, 2007), and forensic (Manera *et al.*, 2008; Mizuta *et al.*, 2008; Uzawa *et al.*, 2008). However, the SPR sensor is only successfully applied for the detection of large molecule (MW> 100,000). It does not have a high enough sensitivity to detect a small molecule (Kawaguchi *et al.*, 2008).

CHAPTER 4

Electrochemical Detection

Electrochemical detections have played a major role in the move of affinity biosensor towards simplified method. The rapid development is due to their significant advantages; high sensitivity, selectivity, low cost, easy fabrication, miniaturization, and use (Chen *et al.*, 2006b; Tang *et al.*, 2004). Most electrochemical transducers for affinity biosensor are based on the immobilization of biological recognition on the electrode surface and the detection of analytes though changes of potential, impedance, current, and capacitance owing to affinity binding. Depending on the electrochemical property to be measured electrochemical detections can be divided into potentiometric, impedimetric, amperometric, and capacitive.

4.1 Labeled electrochemical affinity biosensor

4.1.1 Potentiometric transducer

Potentiometric measurement is base on the determination of the potential difference between a working and a reference electrode. The system functions under equilibrium conditions and monitors the accumulation of charge, at zero current, created by selective binding at the electrode surface. The potential difference (E) is measured between a working electrode and a reference electrode (Figure 4.1) and is proportional to logarithm of ion activity (concentration of analyte) as described by the Nernst equation (Wang, 2000).

$$E = E^0 + \frac{2.3RT}{nF}\log\frac{a_{ox}}{a_R} \qquad (4.1)$$

Where E^0 is the standard potential for redox reaction, R is the universal gas constant (8.314 K^{-1} mol^{-1}), T is the Kelvin temperature, n is the number of electrons transferred

in the reaction, F is the Faraday constant (96,487 coulombs), and a_{ox} and a_R are activities of oxidation and reduction species, respectively.

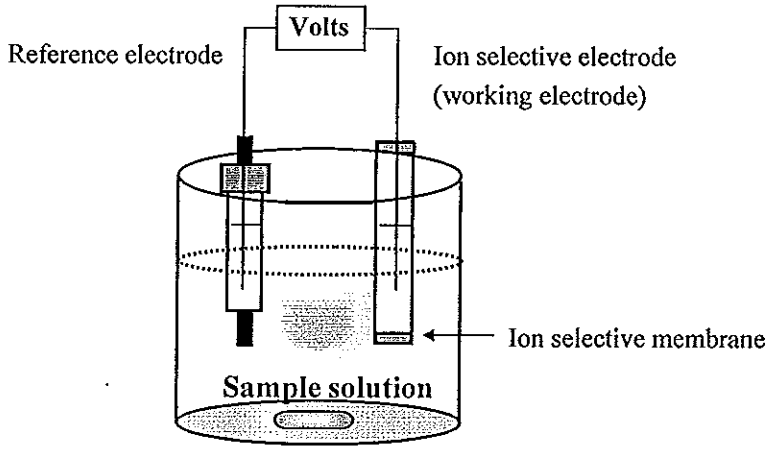

Figure 4.1 Schematic diagram of an electrochemical cell for potentiometric measurement (Modified from Wang, 2000).

Ion selective electrodes, in particular, have expanded the range of applications of potentiometry for affinity biosensor areas. The ion selective electrode is a working electrode capable of selectively measuring the activity of a particular ionic species. Ion selective electrodes are mainly membrane-based devices, with the membrane placed at the tip of electrode. The composition of membrane is chosen in order to yield a potential that is primarily associated with the ion of interest via a selective binding process (i.e., ion exchange) at the membrane–electrolyte interface (Wang, 2000). Recently, there has been development of polymeric ionophore-based membrane to improve the electrode sensitivity, selectivity and detection limit by minimizing passive zero current ion fluxes from the membrane into the sample solution (Chumbimuni-Torres *et al.*, 2006; Numnuam *et al.*, 2008b). Application of potentiometric transducer for affinity biosensor is usually carried out by labeling method. For example, potentiometry affinity biosensor based on a sandwich method where the target analyte is captured by the primary biological recognition element modified gold substrate, followed by the addition of a secondary biological

recognition element conjugated to quantum dots such as CdSe tags (Figure 4.2). The CdSe quantum dots are later dissolved/oxidized with hydrogen peroxide and are detected by Cd^{2+}- selective electrode. The potentiometric response is related to concentration of analytes (Thurer *et al.*, 2007).

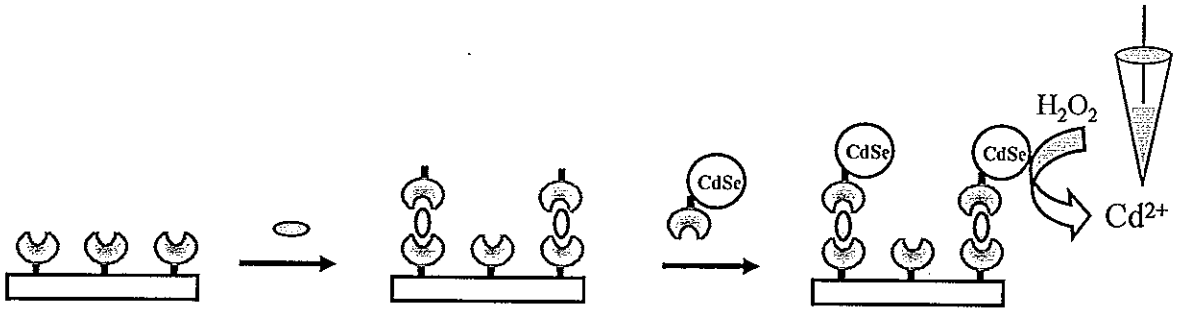

Figure 4.2 Potentiometric affinity biosensor detection based on sandwich assay labeled with quantum dot (Modified from Thurer *et al.*, 2007).

Using this procedure, affinity biosensors are applied to detect DNA (Numnuam *et al.*, 2008b), thrombin (Numnuam *et al.*, 2008a), and human IgG (Thurer *et al.*, 2007). This technique offers several advantages such as simple to use and inexpensive analytical tools, wide range of applications (Rao and Kala, 2008). However, many steps are required (Thurer *et al.*, 2007).

4.1.2 Amperometric transducer

Amperometric measurements are made by recording the current flow in the cell at a single applied potential (Scholz, 2002). The basic instrumentation requires controlled-potential equipment and an electrochemical cell consists of three electrodes, a working electrode, a reference electrode, and an auxiliary electrode, immersed in a suitable electrolyte (Wang, 2000). Since most protein analytes are not intrinsically able to act as redox partners in an electrochemical reaction most applications were achieved by either sandwich (Campas and Marty, 2007) or competitive assays (Wang *et al.*, 2008b). The principle of operation of amperometric labeled affinity biosensor is either by determining the concentration gradient of an

electroactive product of an enzyme reaction or a change in the concentration of an electrochemically active label. The combination of enzyme reaction with amperometric detection is widely employed by measuring of the current generated by oxidation/reduction of enzyme reaction products in the present of mediator (Figure 4.3). The amperometric labeled enzyme affinity biosensor gain much attention because they can achieve a relatively low detection limit and high sensitivity (Song *et al.*, 2006; Wu *et al.*, 2007b). A number of enzymes have been applied as labels such as alkaline phosphatase (Preechaworapun *et al.*, 2008), horseradish peroxidase (Kurtinaitiene *et al.*, 2008), and glucose oxidase (Mackey *et al.*, 2007).

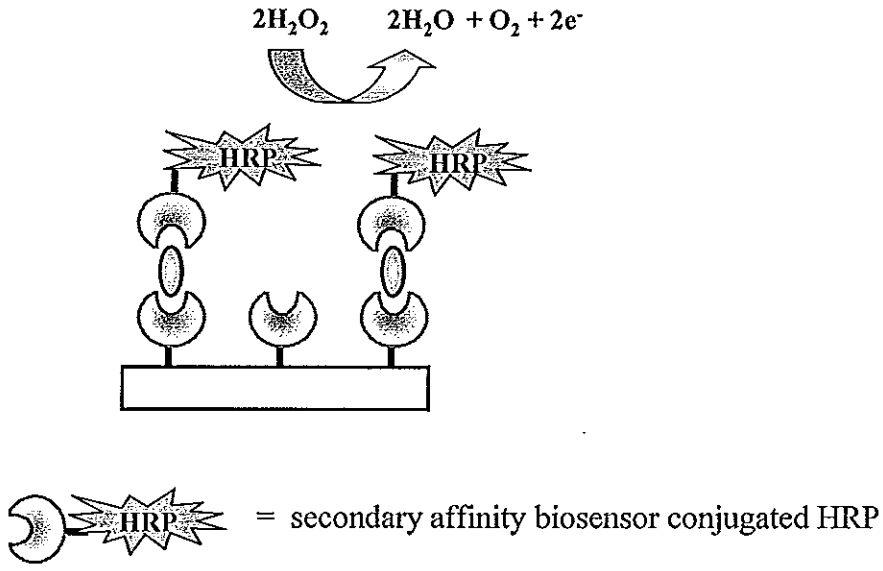

Figure 4.3 Principle of enzyme affinity biosensor by using amperometric measurement.

However, some enzyme labels are expensive, not readily available on the market and have short-term stability (Huang *et al.*, 2006; Karyakin *et al.*, 2000). In some case addition of mediator in the analyte solution is necessary and this leads to a more complicated system, increases analytical time and expense (Huang *et al.*, 2006). Therefore, electrochemical active reagents have now also been widely used in amperometric biosensor (Chen *et al.*, 2008c; Ou *et al.*, 2008; Shen *et al.*, 2008; Yuan *et al.*, 2005).

Electroactive reagents such as platinum nanoparticle or Prussian blue which is able to catalyze the electrochemical reduction of hydrogen peroxide have been extensively used in the construction of amperometric biosensor without using any mediator (Ricci *et al.*, 2007). The main advantages of using electroactive reagents are low cost, high stability at certain conditions, and easy to synthesized (Polsky *et al.*, 2006; Karyakin, 2001). According to these advantages, one part of the present work was carried out by using Prussian blue as label in the investigation of affinity biosensor based on amperometric detection. It is expected that the use of Prussian blue can help to detect analyte at low concentration.

4.1.3 Voltammetric stripping transducer

Stripping analysis is a powerful electroanalytical technique for trace metal measurements (Wang, 2000). Therefore, stripping technique is one of the methods which is widely applied for labeled affinity biosensor (Moa *et al.*, 2007; Liu *et al.*, 2007; Chu *et al.*, 2005a; Cai *et al.*, 2002a). First, the analyte species in the sample solution is concentrated onto or into a working electrode. It is this crucial preconcentration step that results in the exceptional sensitivity that can be achieved. During the second step, the preconcentrated analyte is measured or stripped from the electrode by the application of a potential scan (Wang, 2002; Scholz, 2002). The three most commonly used variations are anodic stripping voltammetry, cathodic stripping voltammetry, and adsorptive stripping voltammetry for affinity biosesnors (Wang, 2000). Among these, anodic stripping voltammetry (ASV) is the most used for labeled affinity biosensor because it has a practical detection limit in low concentration (Chen *et al.*, 2008b; Dungchai *et al.*, 2008; Hason *et al.*, 2008; Lin *et al.*, 2008; Wang *et al.*, 2008b). In this analytical technique, the metal is cathodically electrodeposited onto the surface of an electrode during a preconcentration period, and it is then stripped from the electrode by anodic oxidation (Figure 4.4).

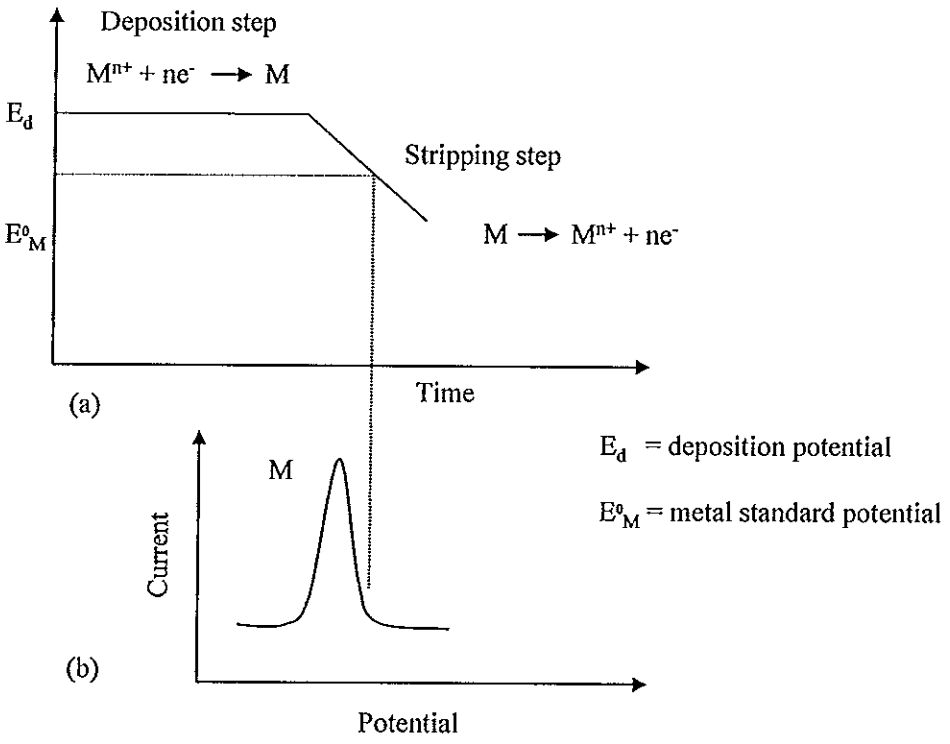

Figure 4.4 Anodic stripping voltammetry (a) the potential-time waveform, (b) along with the resulting voltammogram (Modified from Wang, 2000; Scholz, 2002).

Application of stripping voltammetry in affinity biosensor is based on sandwich assay through labeling agents. Many materials were used as labels including gold nanoparticles, silver nanoparticles and quantum dot. Figure 4.5 shows application of stripping voltammetric detection for labeled affinity biosensor. First, biological recognition element was immobilized on gold electrode. The analyte was first captured by the primary biological recognition element and then sandwiched by secondary biological recognition element labeled with metal nanoparticles. Then these metal nanoparticles were dissolved by chemical reagent which depends on metal nanoparticles used. For example, nitric acid is required for the efficient dissolution of silver. Metal nanoparticles-labeled based stripping volttametry provided main advantage in term of high sensitive detection (Wang *et al.,* 2008b). However, the procedure of this technique has many steps making it rather time-consuming (Du *et al.,* 2008) and sometime the sensitivity is lost when metal

nanoparticles were not completely dissolved or/and sometime metal nanoparticles adsorbed on container surface so, dissolution and washing steps are an important (Chu *et al.*, 2005a).

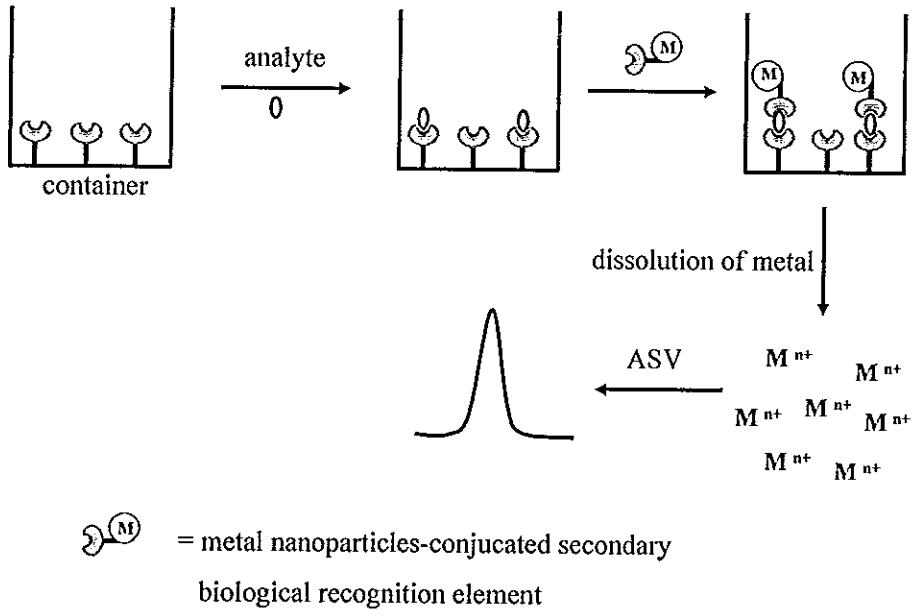

Figure 4.5 Volttametric stripping detection of affinity biosensor based on metal nanoparticle label (Modified from Chu *et al.*, 2005a).

4.1.4 Conductimetric transducer

The conductimetric transducer is a miniature two-electrode device designed to measure the conductivity of the thin electrolyte layer adjacent to the electrode surface. Generally, conductimetric affinity biosensor measurement can be achieved by labeled agent such as nanopaticles. Figure 4.6 shows schematic diagram of a conductivity affinity biosensor assay, labeled with nanoparticles. Biological recognition element was immobilized on the surface between electrodes and allowed to bind with analyte. When secondary biological recognition element labeled with nanopartice was added it binds to the analyte and caused conductivity to change. The change of conductivity in solution was monitored with a conductivity meter.

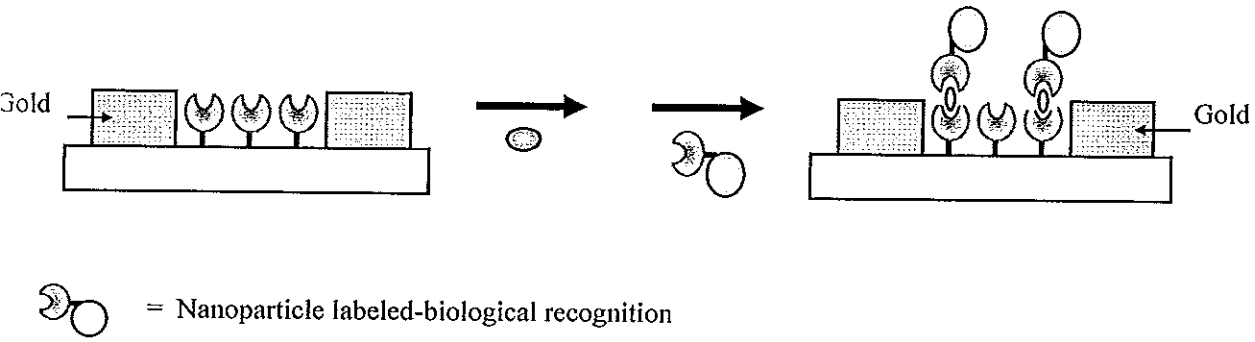

Figure 4.6 Schematic diagram of labeled nanoparticles conductrimetric affinity biosensor assay (Modified from Valera *et al.*, 2008).

There are some very practical considerations that make conductimetric methods attractive, such as low cost and simplicity, since no reference electrodes are needed (Stradiotto *et al.*, 2003). However, this technique provided a drawback of non-specificity measurement. Since conductance of solution was also measured in a complex matrix (e.g., a biological sample) the high ionic strength of the medium may mask the comparatively small net conductivity change caused by the biointeraction (Ambrosi *et al.*, 2008).

4.2 Label-free electrochemical affinity biosensor

4.2.1 Impedance detection

Impedance spectroscopy is a powerful method of analyzing the complex electrical resistance of a system and is sensitive to surface phenomena and changes of bulk properties (Lisdat and Schäfer, 2008). So it was useful to study electrical behavior of several surface-modified electrodes and was also able to detect specific binding of biomolecules (Silva *et al.*, 2008; Yang *et al.*, 2008; Yang and Li, 2005). The principle of impedance is a totally complex resistance encountered when a current flows through a circuit made of resistors, capacitors, or inductors, or any combination of these (Fernández-Sánchez, 2005). Depending on how the electronic components are configured, both the magnitude and the phase shift of an AC signal

can be determined. Because an inductive effect is not usually encountered in electrochemistry, a simple equivalent circuit can be applied as shown in Figure 4.7.

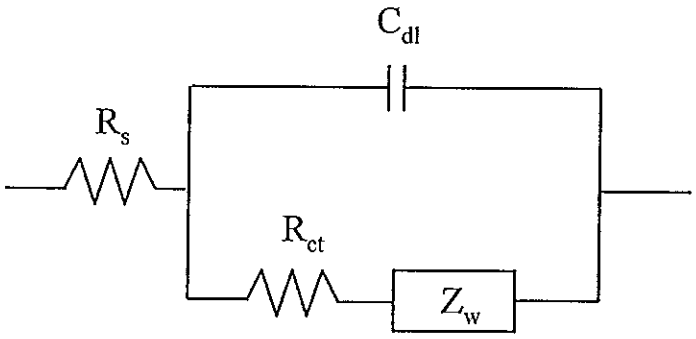

Figure 4.7 Randles' equivalent circuit of electrode in electrolyte (modified from Fernández-Sánchez, 2005).

The impedance results are usually fitted to equivalent circuits of resistors and capacitors. It consist of charge transfer resistance (R_{ct}), double layer capacitance (C_{dl}), solution phase resistance (R_s), and Warburg impedance (Z_w) which results from the diffusion of the ion from the bulk electrode interface. Ideally, Z_w and R_s represent the properties of the electrolyte solution and diffusion of the redox probe, thus they are not affected by modifications occurring at the electrode surface so, and it resulted in constants. The other two components in the circuit, C_{dl} and R_{ct} depend on the dielectric and insulating features at the electrode/electrolyte interface, hence they are affected by the changes at the electrode surface (Yang and Li., 2005). These parameters can be used to indicate the binding between biological recognition element and analyte at electrode surface. The binding of analyte with immobilized biological recognition element on electrode surface led to increase in charge transfer resistance and decrease in double layer capacitance (Shen *et al.*, 2008; Yang and Li., 2005).

Two convenient ways of treating the impedance data are the Nyquist plot and the Bode plot (Kim *et al.*, 2007b).

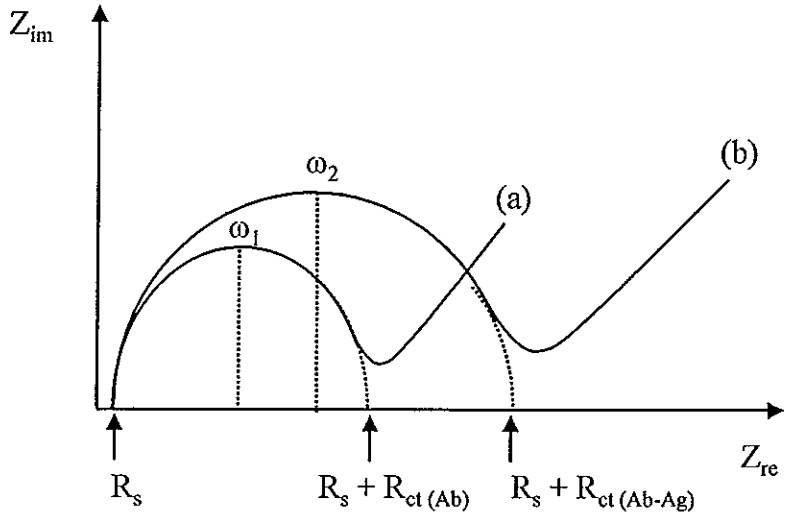

Figure 4.8 Nyquist plot of immobilized antibody (Ab) on the surface of the electrode (a) and antibody-antigen (Ab-Ag) complex on the surface of the electrode (modified from Fernández-Sánchez 2005).

In Nyquist plot, imaginary part of the impedance (Z_{im}) is plotted against the real part (Z_{re}) as shown in Figure 4.8. In an affinity biosensor system biological recognition element such as antibody (Ab) was immobilized on electrode surface and the value of R_s and $R_{ct\ (Ab)}$ before the binding can be easily determined from intercept of real part axis (Figure 4.5 curve a). When immobilized antibody bound to antigen (analyte) this caused charge transfer resistance to increase (curve b). The capacitance, C_{dl}, can also be calculated from this Nyquist plot from the frequency at the maximum of the semicircle.

$$\omega = 2\pi f = \frac{1}{R_{ct} C_{dl}} \qquad (4.2)$$

Where ω is the radial frequency, π is constant value (3.14), f is frequency (Hz), R_{ct} is charge transfer resistance and C_{dl} is double layer capacitance. When antigen-antibody complex was formed C_{dl} value decreased.

In Bode plot, log of impedance (Z) and phase angle (ϕ) were plotted as a function of log of frequency (f) as presented in Figure 4.9. Unlike the Nyquist plot, these data presentations give direct information about frequency and phase angle that

help ascertain the different constituent phases of the system more easily. Thus, in those frequency regions where a resistive behavior is dominant, a horizontal line is observed for the log Z *vs* log f representation and a phase angle close to 0° is measured. Also, capacitive behavior within a frequency region is described by a straight line with a slope of -1 in the log Z *vs* log f plots and a phase angle get closer to 90° (Fernández-Sánchez, 2005). Therefore, either measurement of resistance or capacitance was selected for impedance detection at certain frequency.

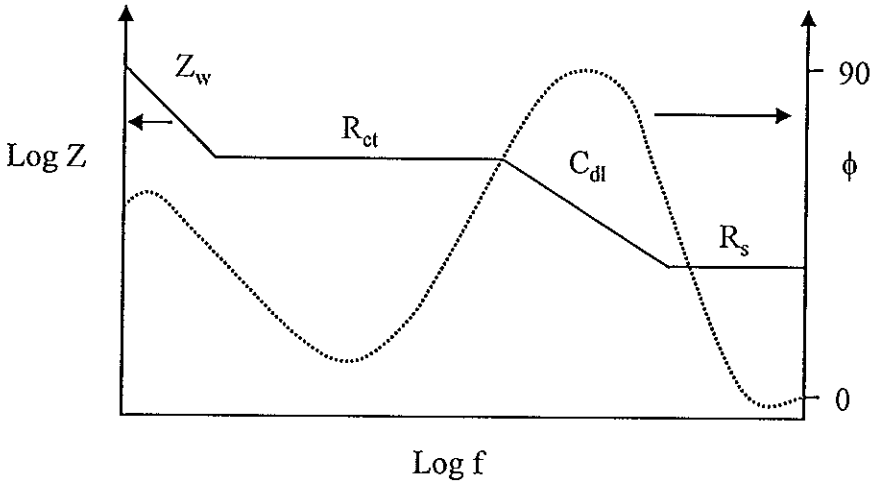

Figure 4.9 Bode Plot that describes impedance behaviour of a simple electrochemical cell (modified from Fernández-Sánchez, 2005).

Impedance spectroscopy is used in clinical diagnostics, food quality control, and environmental analysis, for the detection of tumor markers (Fernández-Sánchez, 2004; Tang *et al.*, 2007b), antibiotic (Thavarungkul *et al.*, 2007), and pesticides (Rodŕguez *et al.*, 2008), respectively.

Although impedance detection have a number of advantages such as sensitive, rapid, and can detect at very low concentration, instrument is expensive (Bart *et al.*, 2005).

4.2.2 Capacitance detection

Capacitive affinity biosensor is based on the determining of dielectric properties change because of the interaction between immobilized recognition

element and analyte. The capacitance change can be measured between two phases, one consists of a metal surface and the other of an electrolyte solution. The surface of metal electrode was immobilized with recognition element, which was immersed in electrolyte solution. The change in capacitance is expected when analyte binds to the recognition element on electrode surface, the increased thickness of the layer would decrease the capacitance (Berggren *et al.*, 2001). Capacitance measurements can be made in two principally different ways as shown in Figure 4.10.

(a) Parallel metal plates

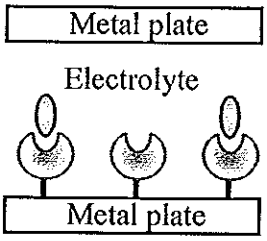

(b) Interdigitated electrode

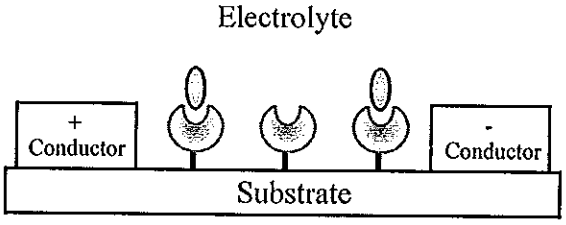

Figure 4.10 Schematic diagram of capacitive affinity arrangements to measure the capacitance change due to (a) the change in distance between two plates and/or the change in dielectric constant or (b) due to change in the dielectric constant using interdigitated electrode (Modified from Gebbert *et al.*,1992; Berggren *et al.*, 2001).

In the first set up the biorecognition element was immobilized in between two parallel metal plates (Figure 4.10a). The capacitance of the medium between the two

plates can be measured with a high precision capacitance bridge. The capacitance (C) is described by the following equation:

$$C = \frac{\varepsilon_0 \varepsilon A}{d} \tag{4.3}$$

Where ε_0 is the dielectric constant of the material between the plates, ε is the permittivity of free space, A is the surface area of the plates, and d the distance between them (Bontidean *et al.*, 1998; Gebbert *et al.*,1992). Biological recognition element was immobilized on the metal surface, and binding of the corresponding analyte resulted in the change in dielectric properties in the material between the plates, so a change in capacitance will occur (Gebbert *et al.*, 1992).

Another is interdigitated electrode, biological recognition element was immobilized between them. When the biological recognition element interact with analyte resulting in dielectric properties change between the electrodes causing the capacitance to change (Figure 4.10b). However, the limitations of this approach are difficulties in producing a short and reproducible distance between the two conductors and the method is very sensitive to changes in the bulk solution (Bontidean *et al.*, 1998).

Alternatively, capacitance change can be measured between two phases, one consists of a metal surface and the other of an electrolyte solution in a potentiostatically controlled three-electrode system; working electrode, reference electrode and auxiliary electrode, by applying an electrical perturbation signal to the electrode. A number of works utilized capacitance measurements based on this principle detection (Loyprasert *et al.*, 2008; Limbut *et al.*, 2006a,b; Yin *et al.*, 2006; Hu *et al.*, 2002). The biological recognition element was immobilized on working electrode surface. The interaction between the immobilized biological recognition element and the analyte results in a capacitance change at the metal surface–solution interface due to alterations of the electric double layer created in close to the transducer during the applied potential pulses as shown in Figure 4.11 (HedstrÖm *et al.*, 2005).

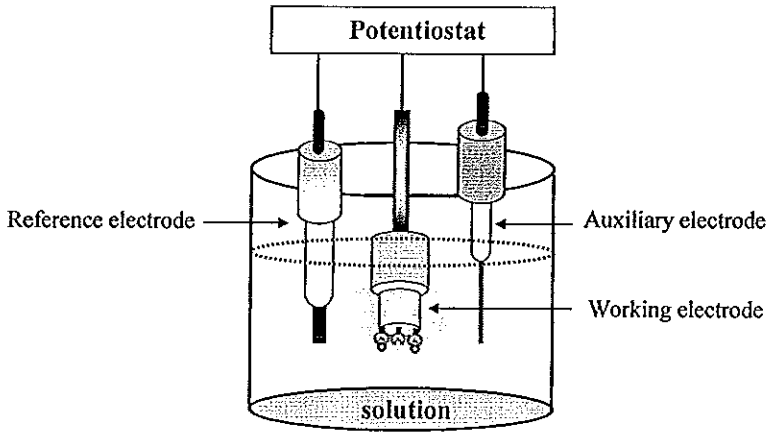

Figure 4.11 Schematic diagram of capacitive affinity biosensor measures the change in the capacitance at the electrode/solution interface.

At metal electrode immersed in an electrolyte solution, a specific interfacial region is formed. This region is called the double layer. In an electrical circuit used to the measure the current flow at working electrode, the double layer can be resembled as a capacitor in its ability to store charge (Scholz, 2002). An imposition of a potential from an external source such as potentiostat to a metal electrode caused the generation of charge (q_m) on the metal and a charge q_s in the solution, where q_m will be equal to $-q_s$. Charged species and dipoles will be oriented at the metal/solution interface, hence making up the electrical double-layer (Bard and Faulkner, 2001). Figure 4.12a showed electrical double layer which consists of several regions. First the inner layer, it is closest to the electrode surface (at distance X_1), solvent and specifically adsorbed species constitute the compact Helmholtz plane or the Stern layer and solvated ions, i.e. water, can only approach the electrode surface to a distance of a monolayer of oriented solvent molecules. The second layer is called the outer Helmholtz plane (OHP) (at distance X_2) and passed through the centers of the solvated ions which can approach the metal surface. The solvated ions are nonspecifically adsorbed and are attracted to the surface by long-range electrostatic forces; in fact they are said to be non-specifically adsorbed ions since their interaction is independent of the chemical properties. The next layer is the diffuse layer (or Gouy layer), which developed outside the OHP. The thickness of this layer depends on the total ionic concentration of the solution. The total charge of the compact and diffuse

layers equals (and is opposite in sign to) the net charge on the electrode side. The potential distance profile across the double-layer region involves two segments, with a linear decrease up to the OHP and an exponential decrease within the diffuse layer. The change in the electric potential within the double layer is displayed in Figure 4.12b (Bard and Faulkner, 2001; Wang, 2000). The potential (φ) profile in the double layer formed at a metal electrode and solution interface across the double layer. The electric potential of metal (φ_M) is virtually constant throughout the metallic phase except for the layer of metal atoms located next to the solution (φ_S) (Scholz, 2002, Wang, 2000).

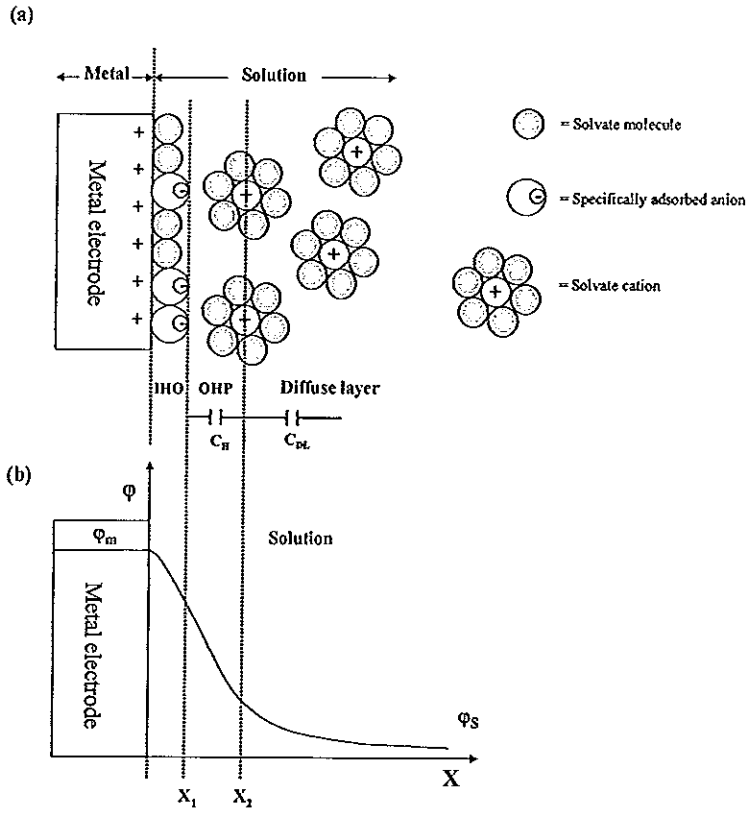

Figure 4.12 Schematic representation of (a) model of the double layer region consists of an Inner Holmholtz plane (IHP), an Outer Holmholtz plane (OHP) and a diffusion layer, C_H is the capacitance due to Holmholtz layer and C_{DL} is capacitance due to the diffusion layer; (b) potential (φ) profile in the double layer formed at a metal electrode and solution interface across the double layer; φ_m is electric potential of metal and φ_s is electric potential of solution (Modified from Scholz, 2002, Wang, 2000).

When a metal electrode surface is immersed in solution, any charged molecule captured at the interface with the electrolyte produces a change both in the capacitance structure and its electrical behaviour. Consequently, the presence of molecules bound to the surface transducers leads to a change in capacitance (Berggren *et al.*, 2001). The total capacitance (C_{tot}) is given by

$$\frac{1}{C_{tot}} = \frac{1}{C_H} + \frac{1}{C_{DL}} \qquad (4.4)$$

Where C_H is the capacitance due to the Helmholtz layer and C_{DL} is the capacitance due to the diffuse layer.

In biosensor, a metal electrode surface modified with biological recognition element can be considered as a capacitor when placed in an electrolyte solution. The total capacitance is built up from several capacitors in series, as shown in Figure 4.13 (Berggren *et al.*, 2001).

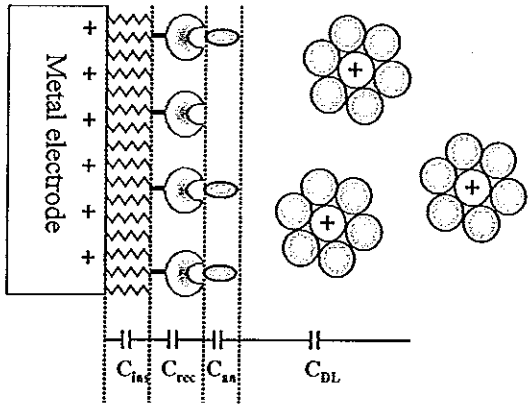

Figure 4.13 Affinity biosensor based electrical double layer organized on the metal electrode solution interface (Modified from Berggren *et al.*, 2001).

The first is the capacitance of insulating layer on the surface (C_{ins}), followed by the capacitance of immobilized biological recognition element layer (C_{rec}). The third is the capacitance of the binding analyte to the immobilized biological recognition element layer (C_{an}). The last is the capacitance of the concentration

dependent diffusion layer extending out into the bulk of the solution (C_{DL}) (Berggren *et al.*, 1998, 2001). The total value of the capacitance can be described by

$$\frac{1}{C_{tot}} = \frac{1}{C_{ins}} + \frac{1}{C_{rec}} + \frac{1}{C_{an}} + \frac{1}{C_{DL}} \qquad (4.5)$$

In affinity biosensor, this capacitance is measured though electrochemical method such as impedimetric or potential step.

4.2.2.1.1 Impedimetric

The imaginary part of the impedance (Z_{im}) can be used to calculate a value for the capacitance (Berggren *et al.*, 2001) The fundamental principles of impedimetric method have been discussed in Nyquist plot (Figure 4.5) where the capacitance can be obtained at the frequency (ω_1 and ω_2) which observed at the maximum value of Z_{im}. The relationship between capacitance and impedance can be given by the equation.

$$C_{dl} = \frac{1}{2\pi f R_{et}} \qquad (4.6)$$

R_{et} is known from the intercept on the Z_{re} so, the capacitance values can be calculated according to this equation. The measurement of capacitance via impedance has been applied for several analytes such as human serum albumin (Li *et al.*, 2005), transferrin (Yin *et al.*, 2006), glutathione (Yang and Li, 2005), and human IgG (Ren *et al.*, 2005). However, the obtained data form this detection is difficult to interpret and the instrumentation is also expensive (Bontidean *et al.*, 1998).

4.2.2.1.2 Potential step

For this method the measurement of capacitance is performed by applying a potential pulse for a defined period to a working electrode, resulting in current decay response (Figure 4.14) (Bontidean *et al.*, 1998), which can be described by

$$i(t) = \frac{u}{R_s}\exp(-\frac{t}{R_s C_{tot}}) \qquad (4.7)$$

Where $i(t)$ is the current response as a function of time, u is the applied pulse potential, R_s is the resistance of the solution, and C_{tot} is the total capacitance at the electrode/solution interface. By taking the natural logarithm of equation 4.6, a linear relationship will exist between ln(i) and t, C_{tot}, and R_s can then calculated from a linear least-squares fitting.

$$\ln i(t) = In\frac{u}{R_s} - \frac{t}{R_s C_{tot}} \qquad (4.8)$$

Then, C_{tot} and R_s were obtained from the slope and intercept of the linear least-square fitting of ln $i(t)$ versus t as shown in Figure 4.15 (Bontidean *et al.*, 1998).

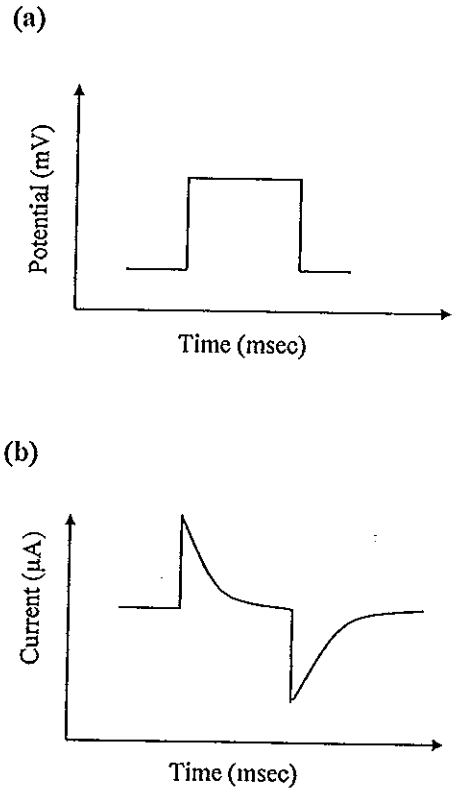

Figure 4.14 Potential step technique principle (a) applied potential pulse and (b) resulting current decay.

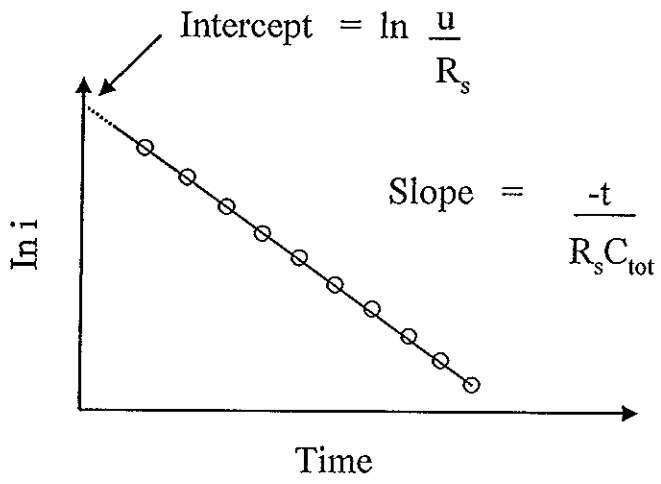

Figure 4.15 Logarithm of current *vs* time.

CHAPTER 5

Sensitivity Enhancement of Affinity Biosensor

Achieving high sensitivity is a major goal of affinity biosensor to approach low concentration detection. Recently a number of methods have been investigated to enhance sensitivity for both labeled and label-free affinity biosensors.

5.1 Labeled competitive biosensor

Labeled affinity biosensors are generally based on sandwich and competitive assays. Sensitivity enhancement is more commonly used with sandwich type assay. For competitive assay there are only a few applications. In general sensitivity enhancement was carried out by amplification of signal after competitive step. For example, in the work of Vig *et al.* (2009) analyte (antigen)-carrier bovine serum albumin (BSA) conjugate is firstly immobilized on the electrode surface. The analyte is then mixed with antibody labeled with AuNPs. When an equilibrium mixture of antibody and analyte is introduced over the analyte immobilized surface, only the unbound antibody labeled with AuNPs is available for binding (Figure 5.1). The measured binding response is, therefore, inversely proportional to the concentration of analyte in solution. The AuNPs labeled were further amplified by electrodeposition of silver on AuNPs at a fixed applied potential and the signal was detected with impedimetric technique. This system can detect analyte in the ppt range.

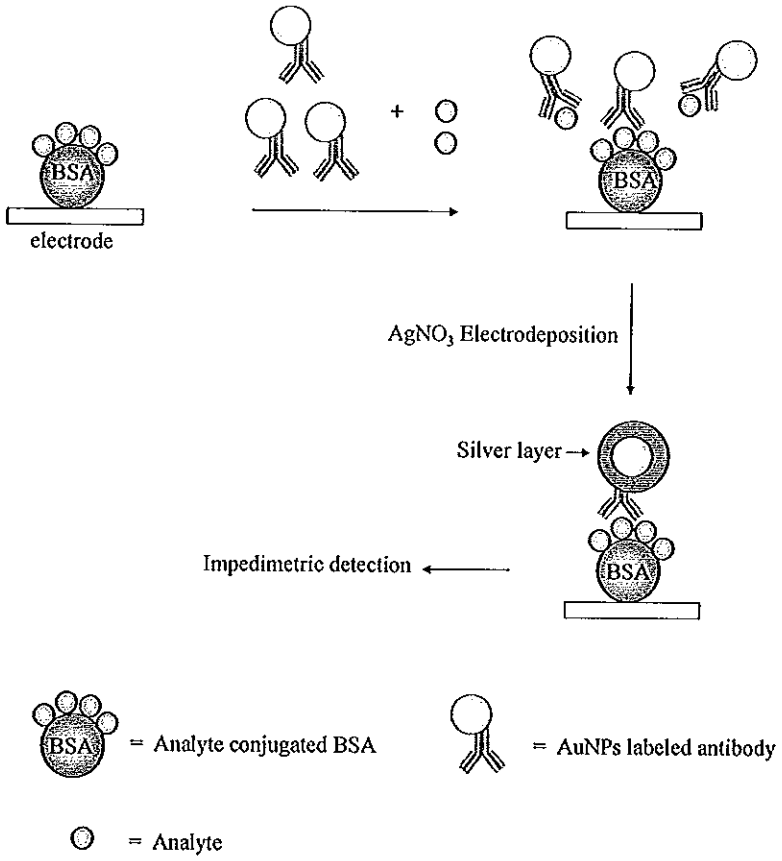

Figure 5.1 The analyte-BSA conjugate was adsorbed on the working electrode surface. Analyte in the sample competes with the immobilized one to bind to AuNPs labelled antibody. Signal was amplified by electrodeposition of silver at a fixed applied potential on gold (Modified from Vig *et al.*, 2009).

Another work is based on enzymatic silver deposition amplification in electrochemical detection as shown in Figure 5.2 (Tan *et al.*, 2009). The immunosensor was based on an indirect competitive format between free analyte in the solution and analyte-bovine serum albumin (analyte-BSA) conjugate immobilized on the electrode surface to bind to a fixed amount of antibody. Then alkaline phosphatase (ALP)-labeled anti-mouse immunoglobulin G (IgG) secondary antibody was bound through reaction with primary antibody. Finally, ALP catalyzed the substrate, ascorbic acid 2-phosphate, into ascorbic acid that reduced silver ions in the

solution to metal silver deposited onto the electrode surface. Linear sweep voltammetry was carried out to quantify the deposited metal silver.

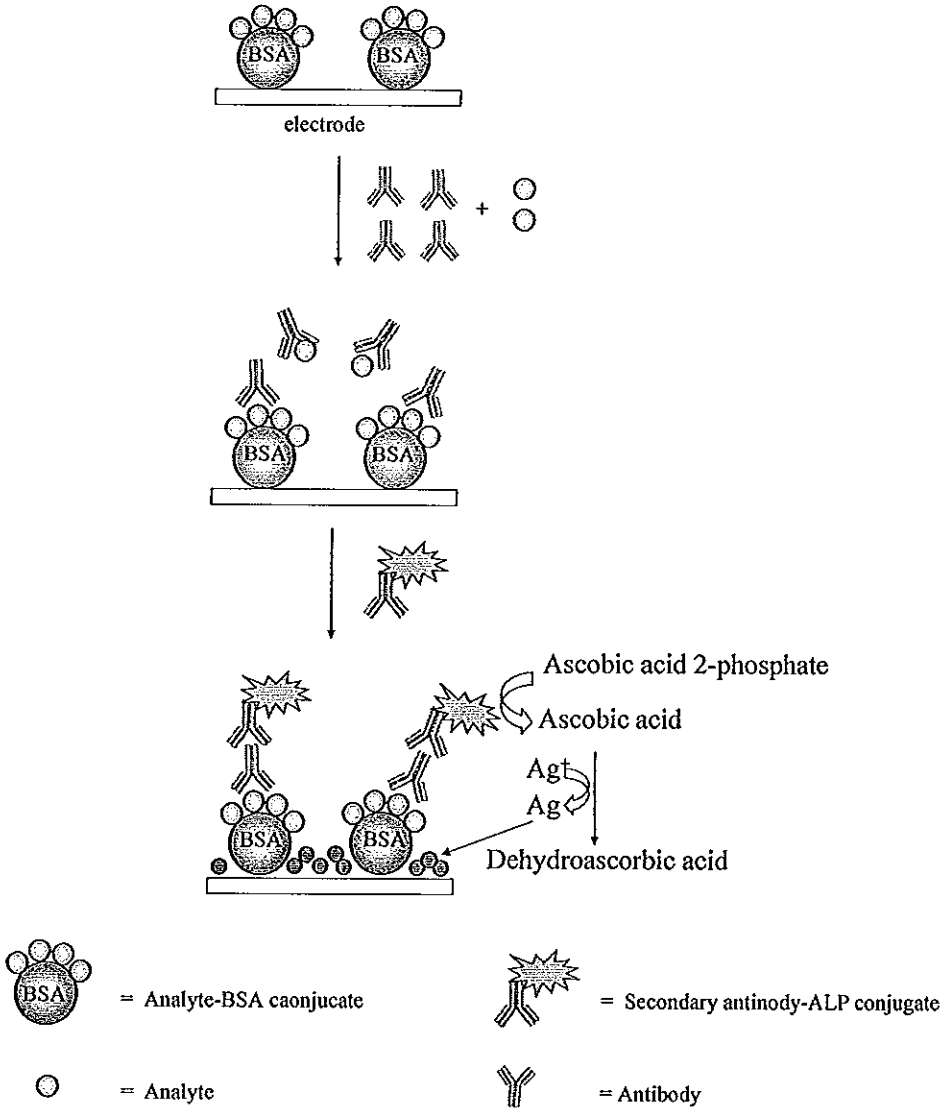

Figure 5.2 Schematic diagram of an electrochemical competitive biosensor. Immobilized analyte–BSA conjugate on the gold electrode surface competes with free analyte in the solution to bind to a fixed amount of antibody. Secondary antibody–ALP conjugate was added followed by enzymatic silver deposition (Modified from Tan *et al.*, 2009).

5.2 Labeled sandwich biosensor

For sensitivity enhancement of sandwich assay, the label materials were conjugated with secondary biological sensing element to capture target analyte. Many labeled materials have been utilized, such as enzymes, nanoparticles, and others to amplify the original signal.

5.2.1 Enzyme

Enzymatically catalyzed amplification is very effective for sensitivity enhancement in various affinity biosensing methods such as electrochemical, SPR, and QCM detection. For electrochemical detection, the approach is to monitor electron transfer in the solution. Many enzymes including horseradish peroxidase (HRP) (Campas and Marty 2007; Du *et al.*, 2007; Wu *et al.*, 2007c; Yu *et al.*, 2004), choline esterase (Babkina *et al.*, 1996), and alkaline phosphatase (Lin *et al.*, 2009; Huang *et al.*, 2008) are used extensively to conjugate with the biomolecules. Among these, HRP is widely used because high turnover rate of the enzymatic reaction, commercial availability, low cost, high stability and easy coupling with many biomacromolecules without significant loss of its catalytic activity (Li *et al.*, 2008b; Zhuo *et al.*, 2005).

5.2.1.1 Electrochemical detection

Electrochemical detections based on enzyme label have been investigated via electrocatalytic current generated by the enzyme. Electrochemical response from HRP activity can result either from the catalytic conversion of an electron donor cosubstrate into an electroactive product (Azek *et al.*, 2000) or a redox-mediated electrocatalytic reduction of hydrogen peroxide (Jia *et al.*, 2002). This latter approach offers the advantages of being volume and reaction time independent (Lumley-Woodyear *et al.*, 1996). For example, in HRP labeled amplification of electrochemical detection sandwich assay (Campas and Marty, 2007), HRP is conjugated to the secondary biomolecule that binds to the analyte. Substrate (H_2O_2) is

added to the detection solution as mediator transfers electron between H_2O_2 and the enzyme. Electrochemical signal was detected during the enzymatic reation (Figure 5.3).

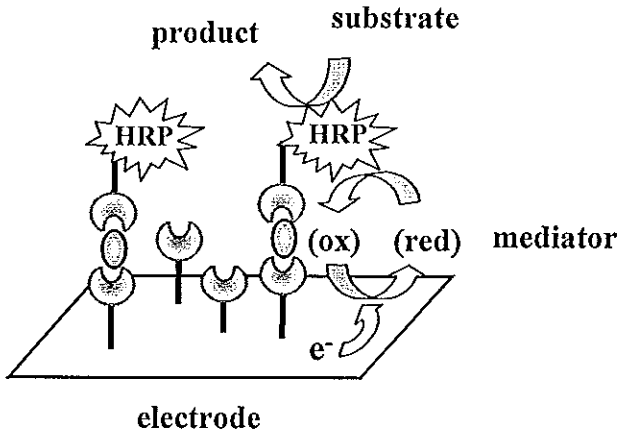

Figure 5.3 Schematic representation of sandwich type affinity biosensor labeled with horseradish peroxidase (HRP). Analyte binds to immobilized primary biological recognition element. Addition of secondary biological recognition element conjugated with HRP followed by substrate in the present of mediator helps the transferring of electron between solution and electrode (Modified from Campas and Marty, 2007).

Electrochemical enzyme labeled is useful for sensitivity enhancement of various analytes such as DNA (Song *et al.*, 2006), microcystin (Campas and Marty, 2007), tumor markers (Wilson and Nie, 2006) and human serum IgG (Zhong, *et al.*, 2009).

5.2.1.2 SPR detection

In SPR detection, enzyme label was usually employed to amplify original signal by increasing the mass deposition via the precipitation of enzymatic reaction products. For example, HRP was used as label in the presence of H_2O_2. HRP catalyzed the oxidation of some compounds such as 4-chloro-1-naphthol (Kim *et al.*,

2005) and 3,3' diaminobenzidine tetrahydrochloride (Cao and Sim, 2007) to yield insoluble products as shown in Figure 5.4. This precipitation reaction increased the refractive index near the sensor surface and thus results in a shift of the SPR angle. This method has been applied to enhance SPR signal for the biosensing of anti-glutamic acid decarboxylase antibody (Cao and Sim, 2007), human interferon (Kim *et al.*, 2005), mouse immunoglobulin G (Tang *et al.*, 2007a) and DNA (Zeng *et al.*, 2007).

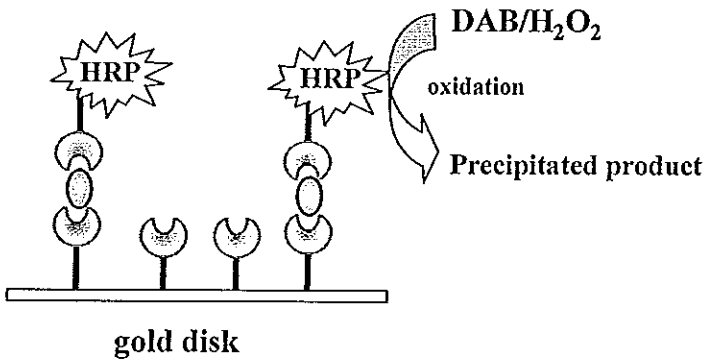

Figure 5.4 Diagram of a method to enhance the sensitivity of SPR response based on enzyme labeled sandwich assay. HRP will catalyze the oxidation of 3,3' diaminobenzidine (DAB) in the presence of H_2O_2 to generate precipitation insoluble product to enhance the SPR signal (Modified from Cao and Sim, 2007).

5.2.1.3 Mass detection

Enzyme precipitation mechanism has also be applied to enhance the signals of QCM biosensor based on sandwich assay. When enzyme conjugated secondary biolomolecules are used, the sandwiched complex can be exposed to related substrates. The deposition of enzymatically generated products caused further decrease in frequency signal as shown in Figure 5.5 (Su and Li, 2001). This enhancement principle has been applied for detection of *Helicobacter pylori* antibody (Su and Li, 2001), *Toxoplasma gondii* -specific IgG (Ding *et al.*, 2005), DNA (Feng *et al.*, 2007b) and anti-dinitrophenyl (Alfonta *et al.*, 2001).

Athough the assay sensitivity could be improved by using enzyme as enhancer there are some limitations of stability and high cost (Tang *et al.*, 2008b).

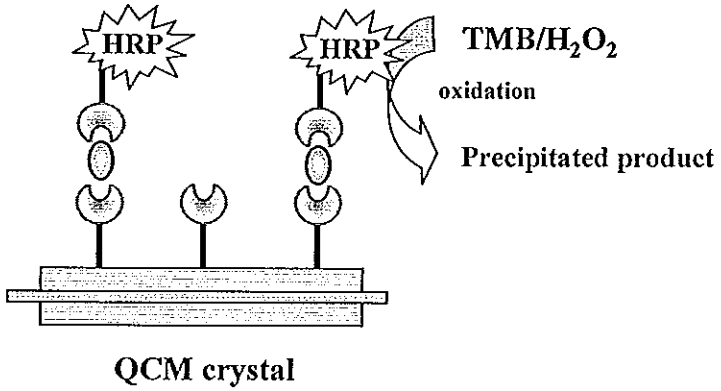

Figure 5.5 Enzymatic reaction schemes. HRP catalyzes H_2O_2 oxidation of 3,3',5,5'-tetramethylbenzidine (TMB) to form precipitation product and causes change in QCM signal (Modified from Su and Li, 2001).

5.2.2 Nanoparticle

Recently, inorganic nanoparticles (NPs) with specific size have attracted increasing interest due to the influence of their size on their electronic, optical, magnetic and catalytic properties. They were widely employed in various fields such as electronics (Nguyen *et al.*, 2007), optics (Sharma and Gupta, 2005), biomedicine (Sharma *et al.*, 2009) and especially in biosensors (Guo and Dong, 2009; Kong *et al.*, 2008; Lin *et al.*, 2009; Tang *et al.*, 2008b).

Many inorganic materials such as gold (Wang and Zhou, 2008), silver (Cai *et al.*, 2002a), platinum (Polsky *et al.*, 2006), and magnetic nanoparticles (Wang *et al.*, 2003c) have been used as labels in affinity biosensors. Among these, gold nanoparticles (AuNPs) are the most widely used. AuNPs have been recognized as a versatile and efficient label for the conjugation of biomolecules due to their rapid and simple chemical synthesis, a narrow size distribution, and efficient coating by thiols or other bioligands (Guo and Dong, 2009; Erdem, 2007; Seydack, 2005). Their excellent biocompatibility and unique structural, electronic, magnetic, optical and

catalytic properties have also made them a very attractive nanomaterial to enhance the sensitivity in biosensor techniques (Chen *et al.*, 2006b; Choi *et al.*, 2008; Guo and Dong, 2009; Lai *et al.*, 2009; Ren *et al.*, 2005; Suni, 2008). AuNPs have successful been used to increase signal in SPR, electrochemical, QCM and fluorescence detections.

5.2.2.1 SPR detection

SPR is suitable for detecting large molecules (Kawaguchi *et al.*, 2008). However, it is generally difficult to detect small molecule due to the low response of analytes with a limited mass. Signal amplification can be achieved by using AuNPs labels (Wang *et al.*, 2008a; Takae *et al.*, 2007; Mitchell *et al.*, 2005; Lyon *et al.*, 1998). In general, primary biological recognition element is firstly immobilized on a gold disk usually via thiol group (Liu *et al.*, 2004; Mitchell *et al.*, 2005; Lyon *et al.*, 1998; Wang *et al.*, 2008a). After the binding with analyte, AuNPs-conjugated secondary biological recognition element was added. The coupling of AuNPs to biomolecules can in turn cause refractive index shifts during the biomolecular recognition event (Figure 5.6). Signal enhancement by AuNPs labels for the detection of small molecules have been achieved for adenosine (Wang *et al.*, 2008a), chloramphenicol (Yuan *et al.*, 2008), D-galactose (Takae *et al.*, 2007) and progesterone (Mitchell *et al.*, 2005). Such AuNPs enhance the signal not only through their high mass but also by virtue of their ability to undergo SPR themselves and so reinforce the SPR signal (Lyon *et al.*, 1999).

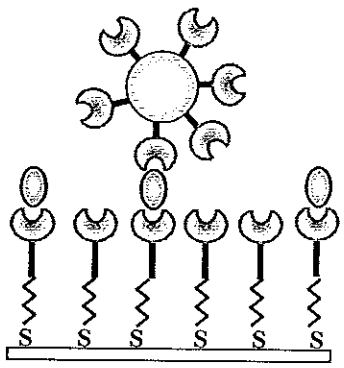

= primary biological recognition element

= AuNPs-conjucated secondary biological recognition element

= analyte

Figure 5.6 Schematic presentation of immunoassay configuration for signal enhancement based on the conjugation of AuNPs and secondary biological recognition element (Modified from Choi *et al.*, 2008).

5.2.2.2 Electrochemical detection

In electrochemical detection based on sandwich assay, analyte concentration can be achieved by measuring the specific properties of AuNPs label after a releasing step by dissolution of the AuNPs labels and measuring the dissolved ions. Anodic stripping voltammetry has been used for trace metal ion measurement with high sensitivity (Chu *et al.*, 2005a; Wang *et al.*, 2001; Dequaire *et al.*, 2000). For example, in the work of Dequaire *et al.* (2000), primary biological recognition element specific for analyte is adsorbed on the solid support. The analyte is first captured by the primary antibody and then sandwiched by a secondary AuNPs-labeled biological recognition element. Then AuNPs are dissolved in an acidic oxidative solution such as HBr and the gold ions (Au^{3+}) thus released into the solution are quantitatively determined by anodic stripping voltammetry as shown in Figure 5.7.

Figure 5.7 AuNPs labeled enhance signal of electrochemical detection via sandwich assay. After secondary biological recognition binds with target analyte, the labeled AuNPs are dissolved with HBr solution to release gold (III) ions and detected with anodic stripping voltammetry (ASV) (Modified from Dequaire *et al.*, 2000).

Many applications based on nanoparticles labeling have been developed using electrochemical measurement. These include detection of human IgM (Mao *et al.*, 2008a) and *Escherichia coli* by square wave stripping voltammetry (Kerman *et al.*, 2004), papillary thyroid carcinoma (Liao *et al.*, 2009) and prostate-specific antigen by stripping voltammetry measurement (Lin *et al.*, 2008), human hepatitis B virus by square wave stripping chronopotentiometry measurement (Hanee *et al.*, 2007).

Recently, the dissolution of the nanoparticles labels has also been detected by ion-elective electrodes for DNA and thrombin detections (Numnuam *et al.*, 2008a,b). Further enhancement of sensitivity has also been investigated by deposition of silver on AuNPs labeled. The deposited silver was dissolved into silver ions and detected with ion selective electrode (Chumbimuni-Turres *et al.*, 2006). For example using ion selective electrode, in the work of Chumbimuni-Turres and coworkers (2006) (Figure 5.8), antigen (analyte) is captured by immobilized primary antibody on gold substrate, followed by addition of AuNPs-labeled secondary antibody and by catalytic silver enlargement onto the AuNPs. The silver deposition was dissolved by hydrogen peroxide and the silver ions are detected by ion-selective electrode.

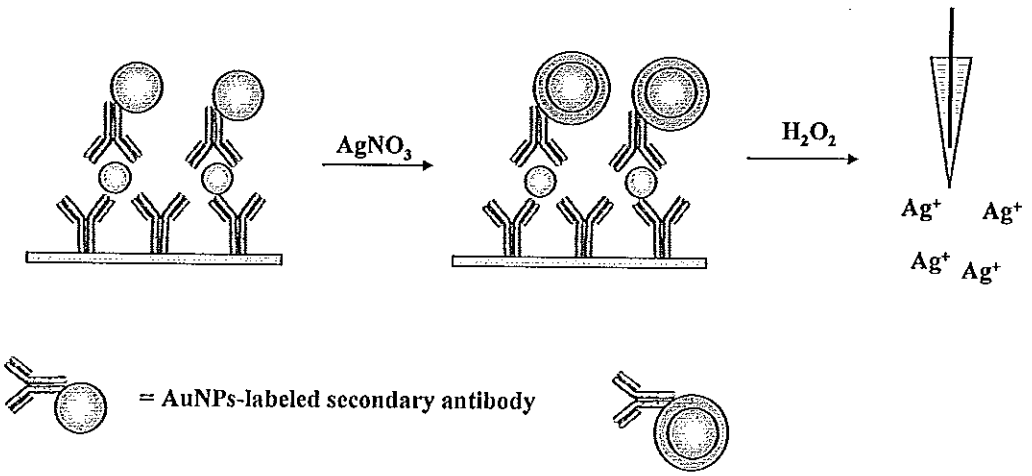

Figure 5.8 Sensitivity enhancement based on silver-enhanced AuNPs labels, precipitation of silver on AuNPs was dissolved in H_2O_2 and detected by ion-selective electrode (Modified from Chumbimuni-Turres *et al.*, 2006).

5.2.2.3 Mass detection

Nanoparticles, especially gold, are utilized as the amplifiers in QCM detection via sandwich assay (Mo *et al.*, 2005; Chu *et al.*, 2006; Xia *et al.*, 2008). AuNPs are used as mass enhancer to amplify the frequency change depending on its relatively large mass compared to target analyte. For example, AuNPs has been used to enhance the signal via sandwich detection of DNA sequence as shown in Figure 5.9. First, primary thiolated DNA (probe 1) is immobilized on QCM gold surface. Then target DNA is added to bind with probe 1. To enhance the signal, AuNPs conjugated thiolated DNA (probe 2) is injected to capture the target DNA through hybridization event. Deposition of the AuNPs-bioconjugate on a gold surface by thiol–gold reaction is monitored by QCM. This system can enhance the detection limit down to atto molar level (Mo *et al.*, 2005).

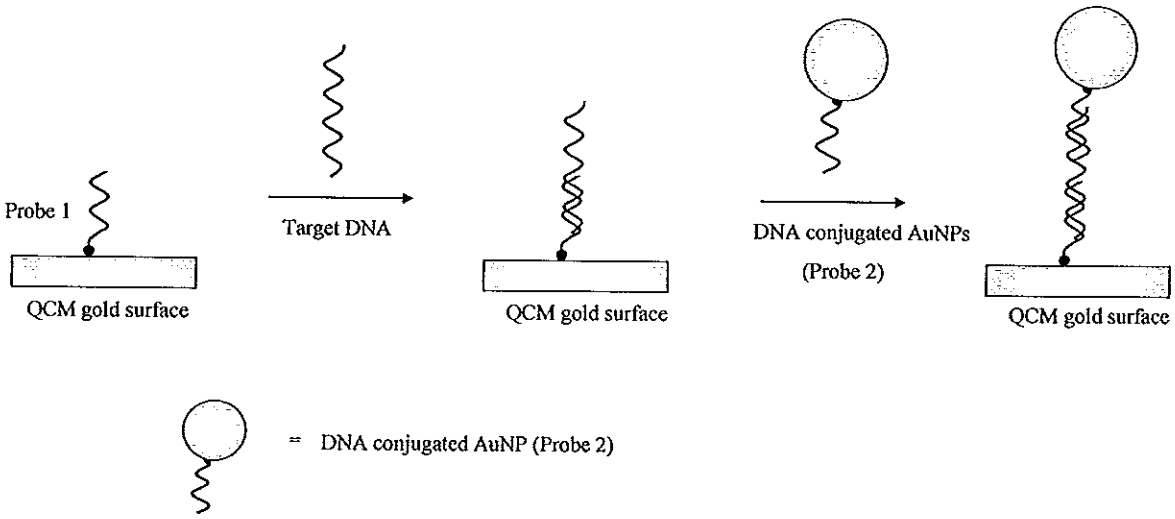

Figure 5.9 Hybridization assay of target DNA with amplified QCM detection with labeled AuNPs. Primary DNA (probe 1) was immobilized on QCM gold disk surface after the binding with target DNA, secondary DNA tagged with AuNPs was then added (Modified from Mo *et al.*, 2005).

AuNPs have promising applications to effectively improve the detection limit and sensitivity in the QCM detection for various analytes such as *Staphylococcus* (Xia *et al.*, 2008), *Escherichia coli* (Mao *et al.*, 2006), DNA (Mo *et al.*, 2005) and human IgG (Chu *et al.*, 2006).

5.2.2.4 Fluorescence detection

For fluorescence detection, AuNPs were applied to enhance sensitivity by carrying fluorophores. Many fluorophores on AuNPs are excited and fluorescence signal is then detected causing increased of sensitive detection especially using fiber optic based on surface plasmon coupled fluorescence system. The integration of fiber optic probe with AuNPs labeling the generation of localized surface plasma waves on the AuNPs surface and thus excite fluorescence efficiently (Chang *et al.*, 2008; Hsieh *et al.*, 2007; Honh and Kang, 2006). For example, Chang and coworkers (2008) investigated a fiber biosensor based on sandwich assay as shown in Figure 5.10. Primary antibody was immobilized on the surface of fiber through preceding chemical adsorption. Then AuNPs conjugated fluorophores and secondary antibody

are added. The fluorophores are excited by using laser beam (658 nm) from laser diode and then fluorescence signal is detected. The signal is amplified because each fluorescence probe contained 40 fluorophores which are excited simultaneously. This set up helps to detect anayte at down to pico molar level.

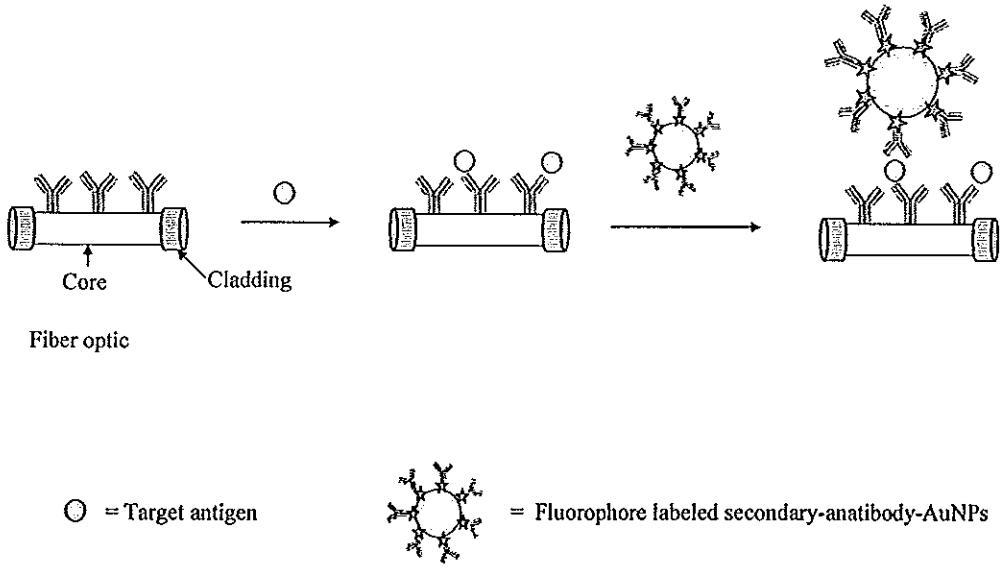

Figure 5.10 Scheme of fiber optic signal enhancement by AuNPs incorporation fluorophore. (Modified from Chang *et al.*, 2008).

Sensitivity enhancement based on labeled AuNPs for fluorescence detection have also been investigated for detection of alpha-fetoprotein (Chen *et al.*, 2008d), prion proteins (Henry *et al.*, 2004), staphylococcal enterotoxin C1 (Hun and Zhang, 2007), *Escherichia coli* (Huang *et al.*, 2009), mouse immunoglobulin G (Hsieh *et al.*, 2007) and human B-type natriuretic peptide (Hong and Kang, 2007).

5.2.3 Others

Liposome can also be applied for amplification of labeled affinity biosensor. Liposomes are large spherical membrane structures (about 100-1000 nm), therefore, they can cause large signal change. For instance, liposome sandwich surface plasmon resonance immunoassay was developed for interferon-γ detection. The results showed that, when liposomes were used, a substantial enhancement of the detection limit was

achieved. The liposome strategy improves the sensitivity for the interferon-γ assay 10,000 times with low detection limit of picomolar (Wink *et al.*, 1998).

Another method for sensitivity enhancement is using bead tags. For example, polystyrene microbeads carrying many AuNPs tags were employed for DNA measurement. The AuNPs-tagged beads were prepared by binding biotinylated metal nanoparticles to streptavidin-coated polystyrene spheres. Chronopotentiometric stripping analysis was used to dissolve gold tags (Figure 5.11). This allows detection of target DNA down to 300 amol level (Kawde and Wang, 2004).

A part of this thesis investigated the enhancement of sensitivity of electrochemical detection based on the tag with microbead.

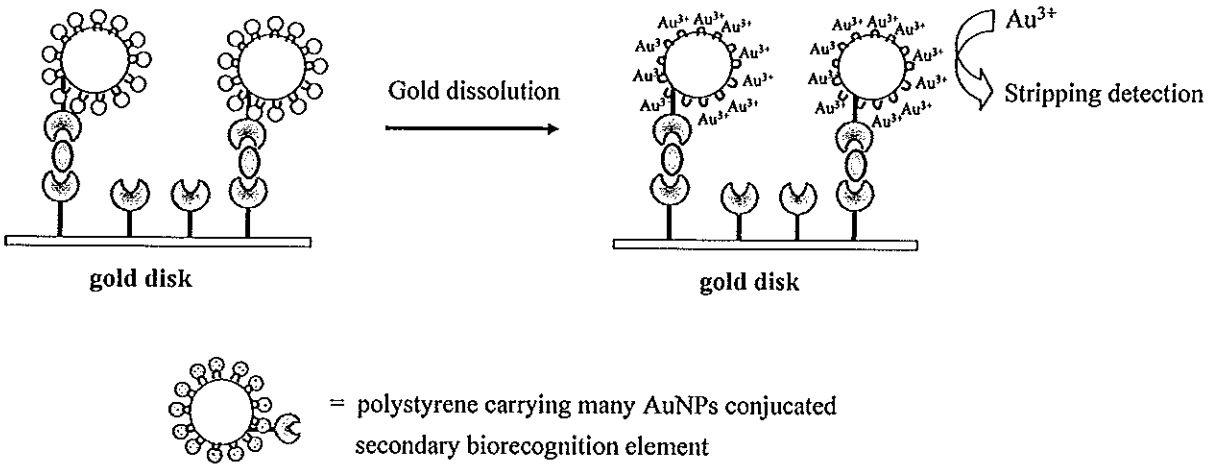

Figure 5.11 Amplification of signal via polystyrene microbeads carrier many AuNPs as labeling (Modified from Kawde and Wang, 2004).

5.3 Label-free affinity biosensor

Direct or label-free detection was performed by monitoring physical properties change due to the binding of biomolecules. Therefore, sensitivity enhancement can be achieved by increasing the amount of immobilized biological

recognition elements on a transducer surface through a layer of dendrimer or nanoparticle.

5.3.1 Dendrimer

Recently, a new class of macromolecules, dendrimers, have been synthesized and applied in biosensors. The dendrimers have a highly branched structure, and possess some excellent characteristics including a high density of active groups and three-dimensional structure as shown in Figure 5.12. The large surface area of dendrimers can increase the number of immobilized biological recognition elements on a transducer, and thus increase the sensor sensitivity. Many types of dendrimers have been employed in biosensor research such as poly(methylferrocenyl) (Armada *et al.*, 2006), poly(propyleneimine) (Dutta *et al.*, 2008), and poly(amidomine) (Wei-Jie *et al.*, 2008) which have different functional active groups. The fourth generation poly(amidoamine) dendrimer has also been widely utilized since it has 64 primary amine of functional end groups and this will increase the amount of immobilized biomolecules (Li *et al.*, 2007; Lojou and Bianco, 2006; Mark *et al.*, 2004; Shen *et al.*, 2008; Tomalia *et al.*, 1990; Tsukruk *et al.*, 1997).

An example of sensitivity enhancement by poly(amidoamine) dendrimer is shown in Figure 5.13. Poly(amidoamine) dendrimers were immobilized on the sensing surface through primary cystamine monolayer assembled onto gold electrodes associated with the piezoelectric quartz crystal. Dendrimers on the modified electrode greatly increased the sensitivity of the whole sensor due to high loading of biological recognition elements (Shen ., 2008).

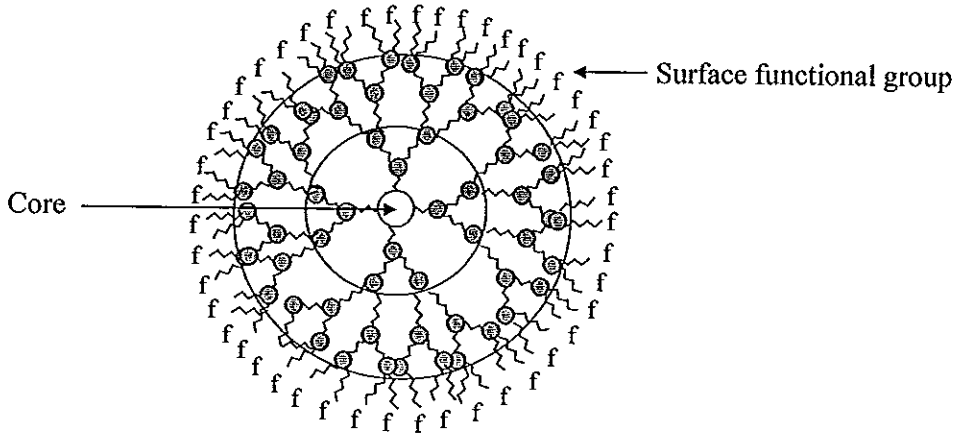

Figure 5.12 Structure of the fourth generation dendrimer (Modified from Lojou and Bianco, 2006).

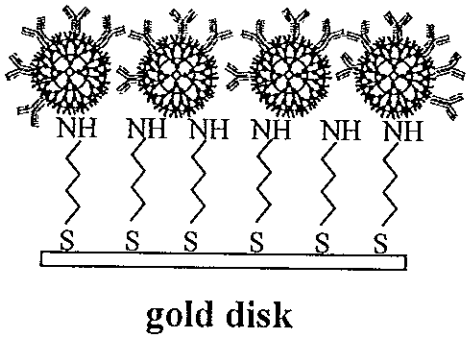

Figure 5.13 Schematic illustration of immobilized polyamidoamine dendrimer on amine monolayer (Modified from Shen *et al.*, 2008).

Various works based on dendrimer sensitivity enhancement have been developed for detection of drug (Svenson, 2008), DNA (Li *et al.*, 2007), α-fetoprotein (Shen *et al.*, 2008) and human IgG (Tang *et al.*, 2008a).

Although dendrimers can successfully enhance detection performance, they are expensive and difficult to synthesize (Okugaichi *et al.*, 2006).

5.3.2 Nanoparticles

The expanding availability of a variety of materials with unique properties at nanoscale dimension, such as nanoparticles, has attracted widespread attention in their utilization for the sensitivity enhancement in label-free affinity biosensor. Applications of nanoparticles for direct affinity biosensor were immobilized via thiol group of sol-gel (Zhange *et al.*, 2005; Jia *et al.*, 2002), amine groups of polymer layer (Hu et al., 2005) and amine groups of self-assemble monolayer (Liu *et al.*, 2008a; Loyprasert, *et al.*, 2008; Wang *et al.*, 2004) as shown in Figure 5.14.

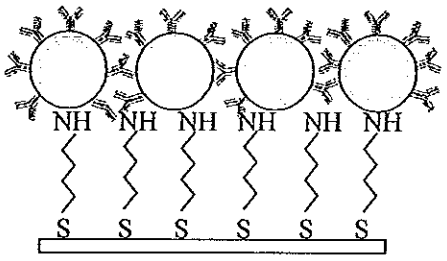

Figure 5.14 Sensitivity enhancement is based on immobilizing AuNPs on amine groups of self-assemble monolayer. Antibody was then immobilized on AuNPs surface by adsorption technique to enhance amount of antibody for interested analyze detection (Modified from Huang *et al.*, 2006).

Metal nanoparticles have many unique properties such as large surface-to-volume ratio, high catalytic efficiency and excellent optical property.

5.3.2.1 Large surface area

Advantages of nanoparticles are high surface area to volume ratio which can enhance amount of biomolecule immobilization (Zhang *et al.*, 2002). Most of the nanoparticles carry charges, they can electrostatically adsorb biomolecules. Besides this interaction, some nanoparticles can also immobilize biomolecules by other interactions. For example, AuNPs can immobilize proteins through the covalent bonds formed between the gold atoms and the amine groups such as glycine, praline,

cysteine, through their NH_2, NH^-, COO^- and S^- groups (Suh *et al.*, 1986; Gole *et al.*, 2001). Moreover, the adsorption of biomolecules onto the surfaces of AuNPs can retain their bioactivity because of the biocompatibility of nanoparticles (Zhang *et al.*, 2002). According to large specific surface area and biocompatibility of nanoparticles, it helps to increase the amount of immobilized biomelecules and retaining their activity on transducer surface resulting in increased sensitivity detection (Huang *et al.*, 2006). Signal enhancement using nanoparticle to increase surface area has been used for detection of murine antibody using AuNPs by impedance measurement (Huang *et al.*, 2006), microcystin-LR using silver nanoparticles by capacitance measurement, (Loyprasert *et al.*, 2008) and Hepatitis B virus surface antigen using AuNPs by impedance measurement (Wang *et al.*, 2004).

5.3.2.2 Catalysis electrochemical reactions

Nanoparticles not only provided large surface area but they can also help to increase catalytic efficiency of an electrochemical reaction (He *et al.*, 2007). Metal nanoparticles have excellent catalytic properties due to their superior stability and complete recovery in biochemical redox processes (Kerman *et al.*, 2008). For example, platinum and Prussian blue nanoparticles exhibited good catalytic properties for H_2O_2. The combination of the catalytic properties of nanoparticles with biosensors can result in the construction of highly sensitive sensor systems for detection of DNA using platinum nanoparticles by amperometric measurement (Zhu *et al.*, 2005) and detection of hepatitis B surface antigen (He *et al.*, 2007), carcinoembryonic antigen (Zhuo *et al.*, 2009) and carcinoma antigen 125 (Chen *et al.*, 2008e) using Prussian Blue nanoparticles by amperometric measurement.

5.3.2.3 Increase optical property

Metal nanoparticles characteristically exhibit a strong absorption band (Xu and Kall, 2002). This absorption band results when the incident photon frequency is resonant with the collective oscillation of the conduction electrons and is known as the localized surface plasmon resonance (LSPR) (Xu and Kall, 2002). The resonance

frequency of the LSPR is highly dependent upon the local environment of the nanoparticle (Khlebtsov, 2004). As such, the optical properties (e.g., absorbance and peak wavelength) of metal nanoparticles are sensitive to the refractive index of the surrounding solvent. Therefore, nanoparticles can helps to increase sensitivity for SPR transducer. The electronic coupling between the localized surface plasmon of the gold nanoparticals and the plasmon wave associated with the surface leads to enhanced shifts of the resonance angles (Chah *et al.*, 2001). Signal enhancement using AuNPs have been developed for detection of transferrin (Liu *et al.*, 2006), *Salmonella typhimurium* (Ko *et al.*, 2009) and trinitrotoluene (Kawaguchi *et al.*, 2008) by SPR measurement.

CHAPTER 6

Performance Criteria

Method validation is the process of proving that an analytical method is suitable for its intended purpose (Mark Green, 1996). Therefore, it is an important requirement for biosensor technique. Typical validation characteristics which should be considered are linear range, sensitivity, limit of detection, selectivity, and reproducibility. The performances criteria need to be evaluated are based on the followings criteria.

6.1 Linear range, sensitivity and limit of detection

For quantitative method, it is necessary to determine the range of analyte concentrations or property values over which the method may be applied. It was performed by plotting between response *vs* concentrations of standard or response *vs* the logarithm of standard concentrations (Thévenot *et al.*, 2001). At the lower end of the concentration range the limiting factor is the value of the limit of detection. At the upper end of the concentration range limitations will be imposed by various effects depending on the instrument response system. Within the working range there may exist a linear response range. Within this the linear range signal response will show a linear relationship to analyte concentration (Eurachem, 1998). Therefore, the linear range of a good calibration curve should be covering the unknown concentration.

The sensitivity is also an important parameter for an analytical method. It is effectively the gradient of the linear concentration range of a calibration curve which determined by the ratio of the response change vs analyte concentration ($\Delta R/\Delta C$) or response response change *vs* logarithm of analyte concentration ($\Delta R/\log C$) (Thévenot *et al.*, 2001). When the response has been established as linear with respect to concentration or log of concentration and the intercept of the response curve has been determined, sensitivity is a useful parameter to calculate and use in formulae for quantitation of unknown concentration. Therefore, a sensitive method is called if a

small change in concentration or amount of analyte causes a large change in the measured signal (Eurachem 1998).

Another important parameter for analytical method is limit of detection (LOD) which is the lowest amount of an analyte that can be confidently detected (Thévenot *et al.*, 2001). There are several methods to determine LOD. The LOD employed in this thesis follows either the IUPAC recommendation in 1994 (Buck and Lindneri, 1994) or the signal-to-noise ratio method (Miller and Miller, 1993). If the calibration curve has the shape as shown in Figure 6.1 LOD was determined by following IUPAC recommendation 1994 (Buck and Lindneri, 1994). In this case LOD is the concentration of the analyte at which the extrapolated linear portion of the calibration curve intersects the baseline-a horizontal line corresponding to zero change in response over several decades of concentration change. For the calibration curve that has the shape as shown in Figure 6.2 the LOD was determined by signal-to-noise ratio method. This was determined by comparing the measured signals from samples and establishing the minimum concentration at which the analyte can be reliably detected (S_{min}), by exceeding three times the standard deviation of blank signal (*SD*).

$$S_{\min} = 3SD \tag{6.1}$$

The lowest concentration of detection (C_L) was then calculated from a function of S_{min} as follows where m is the analytical sensitivity and S_{blank} is the value of blank response.

$$C_L = \frac{S_{blank} + S_{\min}}{m} \tag{6.2}$$

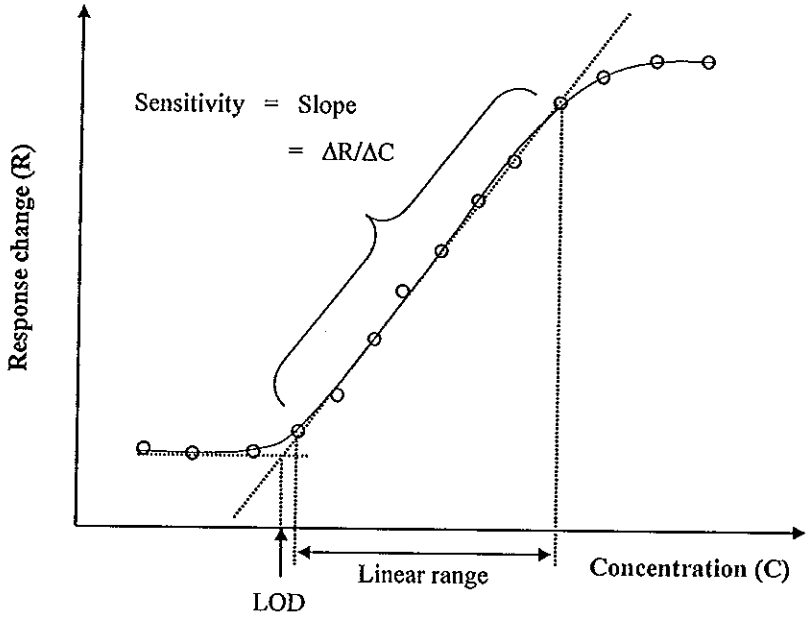

Figure 6.1 Schematic of a calibration curve showing relationships for determining linear range, sensitivity and limit of detection (Buck and Lindner, 1994; Eggins, 1996; Thevenot *et al.*, 1999; Wang, 2000).

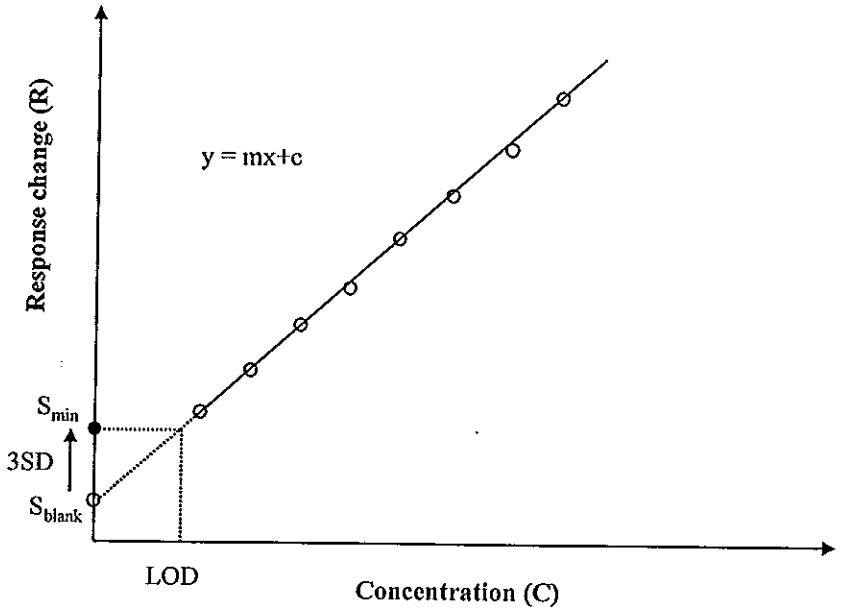

Figure 6.2 Calibration graph for LOD detection based on the signal-to-noise ratio method (modified from Miller and Miller, 1993).

6.2 Selectivity

Selectivity of a method refers to the extent to which it can determine particular analyte in a complex mixture without interference from the other components in the mixture. In biosensor, selectivity of a system depends on the nature of the biological sensing element (*i.e.*, enzyme, antibody, and nucleic acid) and its selectivity for the substrate, as well as on the operational parameters (Eggins, 1996). The method for biosensor selectivity determination can be performed by measuring the biosensor response to interfering compounds, a calibration curve for each interfering compound is plotted and compared to the analyte calibration curve, under identical operating conditions (Thévenot *et al.*, 1999; 2001). The selectivity of the work in this thesis was tested by using different substances that have physical or chemical characteristics similar to the target analytes or other substances that will be presented in real sample.

6.3 Regeneration, stability and reproducibility

A successful surface regeneration allows the same surface to be reused several times. The analyte should be totally removed, and the immobilized biological recognition element should retain its full binding capacity (Thévenot *et al.*, 1999; 2001). The interaction between target analyte and the immobilized biorecognition element used in this work is via non-covalently binding (*i.e.*, electrostatic interactions, hydrogen bonding, hydrophobic interactions and Van der Waals interactions) (Byfield and Abuknesha, 1994; Rabbany *et al.*, 1994). Thus, the dissociation of the target analyte-biorecognition element complex is possible by using suitable regeneration solution. The regeneration of the biosensor system presented in this thesis was evaluated by considering the residual activity of the biorecognition electrode after regeneration. Although affinity biosensor provides advantage in term of reusable, the biological materials have limited lifetimes when expose to violent environment. To study the stability of the new developments of biosensor, the change of biosensor signal obtained from the same concentration of standard analyte over a period of time was investigated (Eggins, 1996; Thévenot *et al.*, 1999; 2001).

Another important factor for analytical method is reproducibility. Reproducibility is a measure of the scatter or the drift in a series of observations or results performed over a period of time (Thévenot *et al.*, 1999; 2001). The degree of reproducibility of the results is expressed as % RSD which depended on concentration of analyte (Taverniers *et al.*, 2004).

CHAPTER 7

Comparison of Surface Plasmon Resonance and Capacitive Immunosensors for Cancer Antigen 125 Detection in Human Serum Samples

7.1 Introduction

Cancer antigen 125 (CA 125) is a tumor marker for ovarian cancer. It is present in 80 % of nonmucinous for ovarian cancer and circulates in the serum of patients (Endo *et al.*, 1988). For healthy human, the concentration levels of CA 125 are lower than 35 U ml^{-1} (Wilder *et al.*, 2003). The determination of CA-125 level in human serum is very useful to clinical diagnoses since it can give information of the disease stage, monitoring the progress of ovarian cancer patients following cytoreductive surgery and chemotherapy.

For clinical laboratory, CA 125 levels are often measured by radiometric (Marguerite *et al.*, 1987; Mcquarrie *et al.*, 1997) and enzyme immunoassay (Dai *et al.*, 2003; Wu *et al.*, 2007a; Yan *et al.*, 1999; VIDAS® CA 125 II ™). These conventional immunoassays have some shortcoming, they are time consuming, required several separation steps and special equipped laboratories and/or skilful personnel (He *et al.*, 2003; Lin and Ju, 2005). In view of these development of an alternative specific method for the determination of CA 125 which is relatively easy to operate is interesting. One approach is immunosensor.

Immunosensors belong to a class of affinity biosensors which combine the natural specificity of antibody and antigen reaction with high sensitivity of various physical transducers. They can be divided into labeled and label-free techniques. Most immunosensors for CA 125 are labeled with enzyme (Dai *et al.*, 2003; Fu *et al.*, 2008; Wu *et al.*, 2007a) and the analysis procedure requires several steps (Bange *et al.*, 2005). Label-free immunosensor is more attractive since it detects affinity binding directly by monitoring changes in physical properties owing to the antibody-antigen binding on the transducer surface. It has many advantages such as rapid, low cost, and simplicity. For label-free, there was only one report on the analysis of CA 125 by

using differential pulse voltammetry, provided a detection limit of 1.8 U ml^{-1} and a linear range of 10-30 U ml^{-1} (Tang *et al.*, 2006a). Therefore, it would be interesting to investigate this label-free technique with other detection method to see whether it can improve the performance.

Several transducers have been developed for label-free immunosensors. These include, for examples, quartz crystals microbalance or surface acoustic wave oscillators to monitor physical changes in mass (Corso *et al.*, 2006; Deobagkar *et al.*, 2005; Zeng *et al.*, 2006), potentiometric, amperometric, impedimetric and capacitive for electrochemical property (Li *et al.*, 2008a; Limbut *et al.*, 2006b; Qiang *et al.*, 2006; Thavarungkul *et al.*, 2007), and surface plasmon resonance (SPR) for optical change (Chung *et al.*, 2005; Dudak and Boyaci, 2007; Dutra *et al.*, 2007). Capacitive and surface plasmon resonance transducers have recently attracted a lot of interest especially for direct detection of biomolecular interactions (Berggren and Johansson, 1997; Dudak and Boyaci, 2007; Limbut *et al.*, 2006b; Loyprasert *et al.*, 2008; Mazumdar *et al.*, 2008; Teramura and Iwata, 2007; Yin *et al.*, 2006). SPR biosensor has become particularly powerful because of its high surface sensitivity, real-time monitoring, and kinetic analysis (Campagnolo *et al.*, 2004 Toyama *et al.*, 1998) while the main advantages of capacitive biosensor are its high sensitivity, simple to operate, and relatively inexpensive.

Therefore, in the present work, we employed both surface plasmon resonance and capacitive transducers for the direct detection of CA 125 using anti-CA 125 immobilized on a gold surface by self-assembled monolayer. Parameters affecting the response of both transducers were optimized then their performances were compared. To show real application, human serum samples were tested by both systems under optimum conditions. The results were then compared to a commercial method, enzyme linked fluorescent assay (ELFA). To the best of our knowledge this is the first time SPR and capacitive systems are investigated for direct detection of CA 125. This is also the first time that the performances of these two systems were compared under optimum conditions and applied to detect analyte concentration in real samples.

7.2 Experimental

7.2.1 Materials

Monoclonal anti-cancer antigen 125 (anti-CA 125) and cancer antigen (CA 125) from human were obtained from US biological (USA), anti-alpha-fetoprotein antibody (anti-AFP) and alpha-fetoprotein (AFP) were obtained from Dako (Denmark) and anti-human carcinoembryonic antigen (anti-CEA), carcinoembryonic antigen (CEA) obtained from Sigma (St. Louis, USA), 11- mercaptoundecanoic acid from Aldrich (MO, USA), N-(3-Dimethylaminopropyl)-N-ethylcarbodiimide hydrochloride (EDC), N-Hydroxysuccinimide (NHS) from Aldrich (Steinheim, Germany), 1-dodeccanethiol ethanolic acid from Aldrich (Milwaukee, USA), ethanolamine from Merck (Darmstadt, Germany), bovine serum albumin (BSA) from Fluka (Steinheim, Germany). All other chemicals used were of analytical grade. All buffers were prepared with distilled water treated with a reverse osmosis-deionized system. Before used, the buffers were filtered through an Albet® nylon membrane filter (Albet, Spain), pore size 0.20 μm, with subsequent degassing.

7.3 Experimental

7.3.1 SPR immunosensor

7.3.1.1 Anti- CA 125 immobilization

A gold disk (ϕ = 2.5 cm.; 50 nm thick gold-coated BK-7 glass plate, Eco Chemie B.V., Netherlands) was cleaned with piranha solution (3:1 mixture of H_2SO_4 and H_2O_2). Then it was thoroughly rinsed with water and ethanol, dried in a stream of nitrogen gas, after that the glass side of this gold disk was adhered to the prism via a matching oil with the same refractive index (n = 1.518) and placed inside the holding block of the SPR equipment (AutoLab Spirit®, Eco Chemie B.V., Netherlands) with the gold surface facing upward. A custom built flow cell was screwed into place, on top of the gold disk, leaving a space of 10 μl (ϕ = 3 mm) where solution can pass through the gold surface. Immobilization steps were monitored by SPR detection, controlled by Autolab SPR version 4.2.1 software.

The freshly cleaned disk was incubated in 150 mM 250 µl of 11-mercaptoundecanoic acid solution for 5 h. During this time self-assembled monolayer was formed on the gold surface. These optimum values of concentration and incubation time were obtained from prior tests when the angle shift of the self assembled layer of 11- mercaptoundecanoic acid on gold disk surface reach a steady value. Then this surface was washed with 1,000 µl of ethanol following 1,000 µl of distilled water. For the coupling of anti-CA 125, the surface was activated with 500 µl of 0.2 M EDC/ 0.05 M NHS for 50 min followed with 10 ml of distilled water, the optimum activation time. Then, 30 µg $ml^{-1}$of 100 µl anti-CA 125 in 10 mM Tris-HCl pH 7.50 was incubated on this surface, washed with 1,000 µl of 10 mM phosphate buffer containing 150 mM NaCl pH 7.2. Next, this surface was incubated with 500 µl of ethanolamine pH 8.50 for 7 min to block the remaining reactive sites and then washed with 1,000 µl of 10 mM phosphate buffer containing 150 mM NaCl pH 7.2. Finally any pinholes on the surface were blocked with 500 µl of 1%(w/v) BSA for 1 h and followed with 1,000 µl of 10 mM phosphate buffer containing 150 mM NaCl pH 7.2.

7.3.1.2 SPR system

All SPR experiments were performed using SPR AutoLab. Solution was delivered using a syringe pump (Kd Scientific, USA) into the SPR flow injection system, equipped with a custom build flow cell as shown in Figure 7.1. Standard CA 125, serum sample, and regeneration solution were loaded with a sample injector (Valco, USA). The flow cell was maintained at 25°C for all measurements by a circulating water bath (Grant Instrument, UK). A monochromatic p-polarized laser (λ = 670 nm) was directed through prism onto the gold disk. The interaction between immobilized anti-CA 125 on the gold disk and CA 125 antigen was measured as the SPR angle shift by a photodiode detector among a dynamic range of 4,000 millidegree.

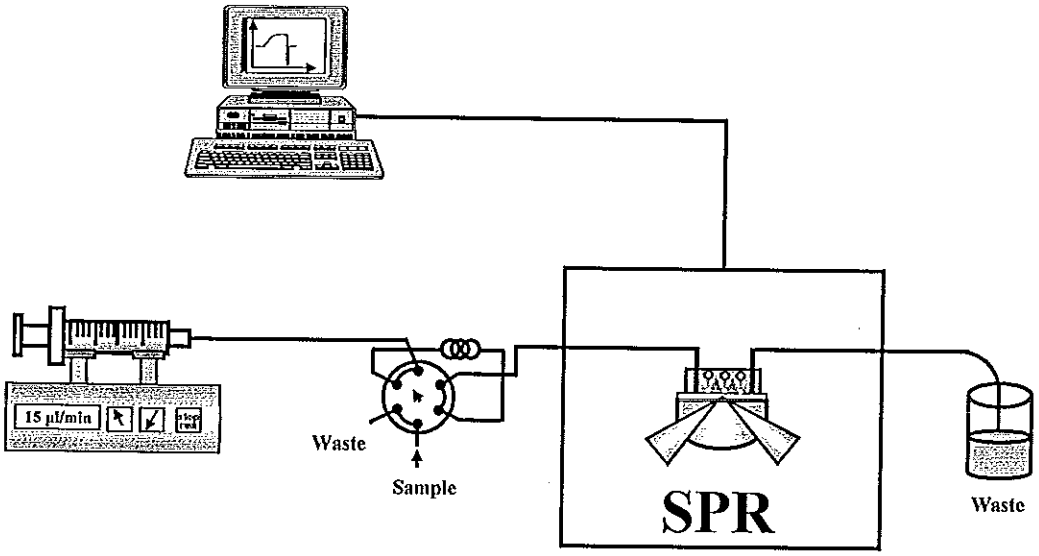

Figure 7.1 Schematic diagram shows the flow injection SPR immunosensor system.

7.3.2 Capacitive immunosensor

7.3.2.1 Anti- CA 125 immobilization

Gold rod electrodes (ϕ=3 mm, 99.99 % purity) were used as immobilized substrate for a capacitive immunosensor. Before used the gold rod electrodes were polished (Gripo® 2V polishing machine, Metkon Instruments Ltd., Turkey) with slurries of alumina oxide powder (particle diameters 5, 1, and 0.30 µm) and then cleaned through sonication subsequentially in distilled water for 15 min. They were then washed in distilled water and dried followed by electrochemical etching in 0.5 M H_2SO_4 solution by cycling potential from 0 to +1.5 V *vs.* Ag/AgCl reference electrode with a scan rate of 0.1 V s^{-1} for 25 scans. Finally they were dried with pure nitrogen gas. The immobilization of anti-CA 125 followed the same steps as the immobilization of SPR immunosensor except the time allowed for self-assemble monolayer and the chemical used in the blocking step. The gold rod electrode was immersed in 500 µl of 150 mM 11- mercaptoundecanoic acid solution for 15 min to form monolayer then was washed with 10 ml of distilled water. This optimum value was obtained by determining percentage of surface coverage of 11-mercaptoundecanoic acid formation on electrode surface (Limbut *et al.*, 2006a). For the blocking step, gold rod surface was blocked with 500 µl of 10 mM 1-dodeccanethiol ethanolic acid for 20 min then was washed with 10 mM Tris-HCl pH

7.20. The electrochemical behavior of each immobilization step was studied by cyclic voltammetry (Eco Chemie μ-autolab B.V., Netherland, and software package GPES 4.7) in 5 mM $K_3[Fe(CN)_6]$ and 0.1 M KCl, at scan rate of 0.1 V s^{-1}.

7.3.2.2 Capacitive system

Figure 7.2 showed the flow injection capacitive system. The reaction cell (10 μl) of the capacitive flow system consisted of a three electrodes system, i.e. an anti-CA 125 modified gold working electrode, a custom made Ag/AgCl reference electrode and a stainless steel tube auxiliary electrode. They were connected to a potentiostat (ML 160, AD Instruments, Australia). Carrier buffer was flowed through the system using a peristaltic pump (Gilson, France). Standard CA 125, serum sample, and regeneration solution were injected into the flow cell by a sample injector (Valco, USA). The capacitance was measured using a potentiostatic step method (Berggren et al., 1998). The current responses obtained from the application of 50 mV potential pulses were used to calculate the capacitance followed the procedures described in chapter 4.

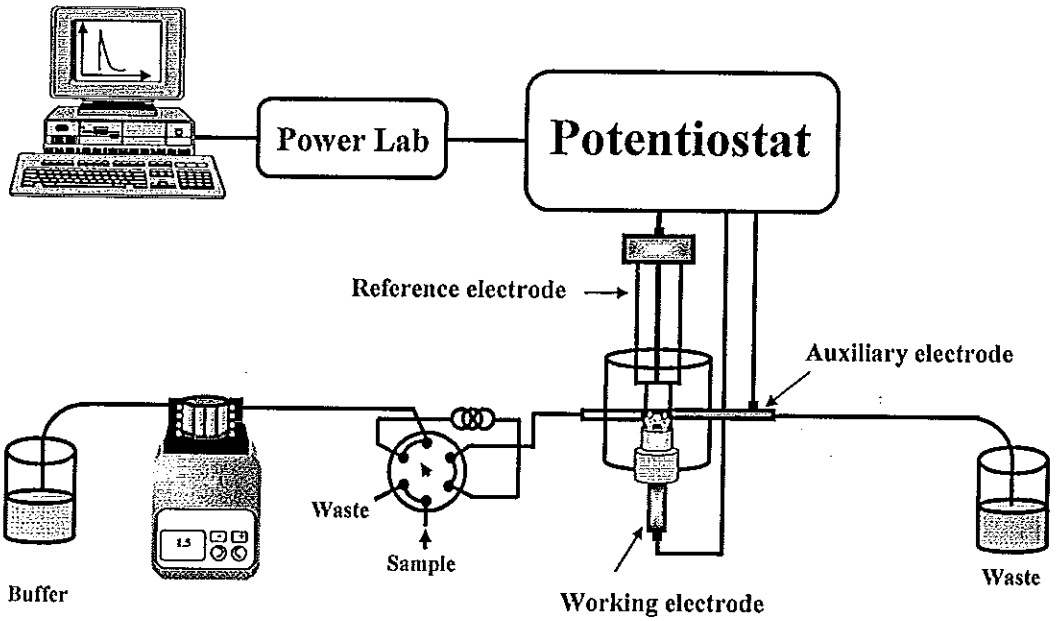

Figure 7.2 Schematic diagram shows the flow injection capacitive immunosensor system.

7.3.3 Optimization of the flow injection SPR and capacitive immunosensors

Parameters affecting the performances of both SPR and capacitive immunosensors such as type and pH regeneration solution, type, pH and concentration of buffer, flow rate and sample volume were optimized. Initial conditions were 300 µl of 10 U ml^{-1} of CA 125 with 10 mM phosphate buffer pH 7.20 at a flow rate of 10 µl min^{-1} for SPR and 200 µl of 5 U ml^{-1} of CA 125 with 10 mM Tris-HCl pH 7.20 at a flow rate of 100 µl min^{-1} for the capacitive system (Wu *et al.*, 2006a). The response was the average of three injections. The optimization was performed by changing a single parameter while keeping other parameters constant. The optimum operating condition was considered by balancing between the signal and analysis time for one analysis. When an operating condition was obtained it was used for the optimization of the next parameter.

7.3.4 Selectivity

To investigate the selectivity of the immunosensor, carcinoembryonic antigen (CEA) and α-1-fetoprotein (AFP), two other tumor markers indicating ovarian cancer (Wu *et al.*, 2007a), were tested. This experiment was carried out by immobilization of anti-CA 125 on gold substrate to detect CA 125, CEA and AFP. The calibration curves were studied between 0.15 and 0.3 µg ml^{-1}. Then the sensitivity (slope of calibration curve) obtained from CEA and AFP were compared with CA 125.

7.3.5 Determination of CA 125 in real samples

Human serum samples were obtained from Hat Yai Hospital, Songkhla, Thailand. The efficiency of the two immunosensor systems were tested by detecting CA 125 in these samples and compared with ELFA technique (obtained from the Hospital).

7.4 Results and discussion

7.4.1 Immobilization of anti-CA 125

7.4.1.1 SPR immunosensor

The steps of immobilization of anti-CA 125 on gold disk were continuously monitored in a batch system by the SPR angle change as shown in Figure 7.3. The first step was to directly inject 250 μl of 150 mM 11- mercaptoundecanoic acid into the flow cell (a in Figure 7.3). After 5 h this surface was rinsed with ethanol until the signal returned to a steady base-line (θ_1). It can be seen that SPR angle increased from the original θ_0 to θ_1. This was due to the formation of SAM on gold disk surface. The surface was then washed with distilled water and the SPR angle decreased from θ_1 to θ_2 because refractive index of water (1.33) is lower than ethanol (1.36) (Weast, 1974). The carboxyl groups of the monolayer were then activated by adding EDC/ NHS (point b). After 50 min of incubation, distilled water was added to remove unbounded material resulting in the decrease of SPR angle to a new base-line (θ_3). The increase of SPR angle from θ_2 to θ_3 was due to the forming of active esters after the activation. Next, anti-CA 125 was injected and incubated for 2 h (point c) before washing with washed with 10 mM phosphate buffer containing 150 mM NaCl pH 7.20 to remove any weakly adsorbed antibody. The SPR angle then increased to θ_4 due to the binding of antibody to ester groups on the immobilized self-assemble monolayer via covalent bond. The remaining ester groups were deactivated by ethanolamine hydrochloride (point d) for 7 min. The surface was washed with buffer until a stable base-line was attained. The SPR angle decreased from θ_4 to θ_5 when excess activated ester groups bound to ethanolamine. Finally, any pinholes of this surface were blocked with 1% (w/v) BSA for 1 h (point e) to reduce non-specific binding and washed with buffer until the SPR signal returned to a new base-line (θ_6).

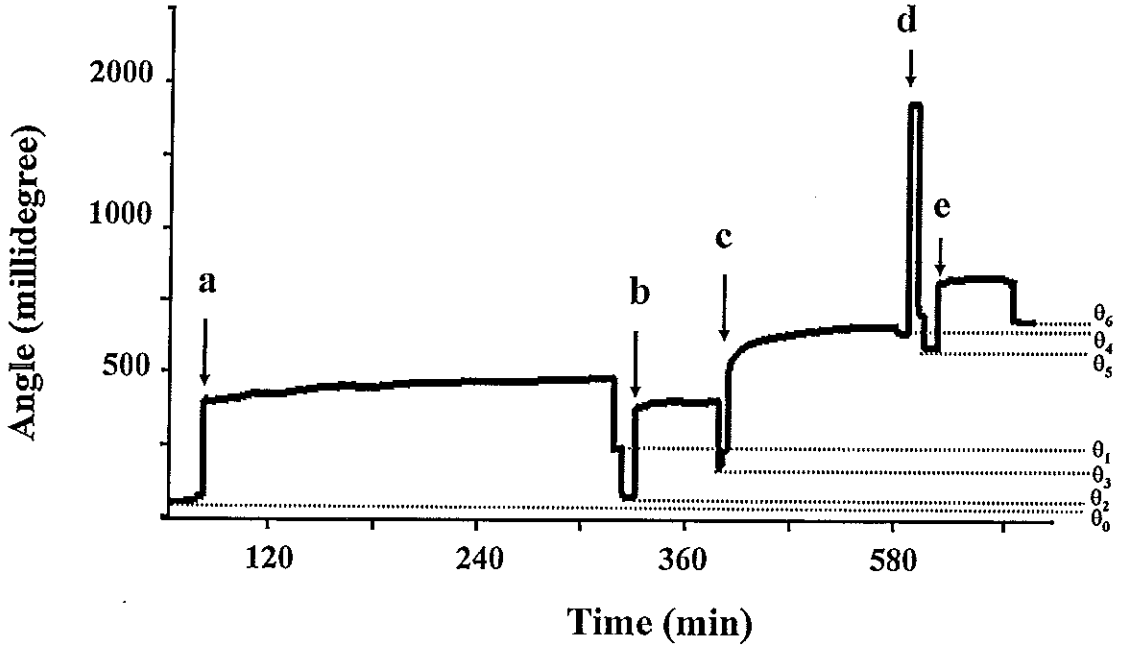

Figure 7.3 SPR sensorgram showed the change in SPR signal during anti-CA 125 immobilization steps. Arrows indicate injection of (a) 11-mercaptoundecanoic acid on cleaned gold disk, (b) NHS/EDC, (c) anti-CA 125, (d) ethanolamine hydrochloride and (e) BSA.

7.4.1.2 Capacitive immunosensor

The immobilization steps were monitored by cyclic voltammetry (Figure 7.4). At the clean gold surface, the reversible oxidation and reduction peaks of the redox species were observed (Figure 7.4 curve a). When the self-assembled monolayer of 11 - mercaptoundecanoic acid covered the gold surface, the redox peaks were reduced because the electrode surface became less accessible for the redox species (curve b). Following the procedures the rodox peaks decreased more and more when anti- CA 125 was immobilized on the electrode surface (curve c), the surface was treated with ethanolamine hydrochloride (curve d), and finally after the electrode was blocked with 1-dodecanethiol, the redox peak disappeared (curve e). (After each step, the surface was washed distilled water to remove excess unbound substance.)

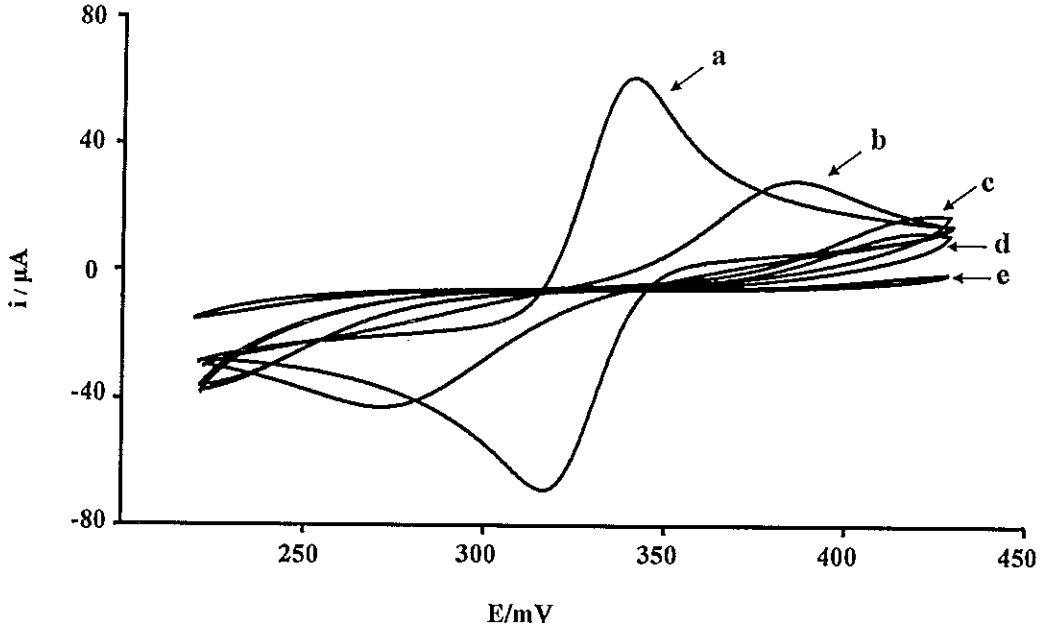

Figure 7.4 Cyclic voltamograms of a gold electrode obtained with 5 mM $K_3[Fe(CN)_6]$ in 0.1 M KCl solution at a scan rate of 0.1 Vs^{-1} vs. Ag/AgCl reference electrode. The voltage range was −0.3 to 0.8 V. (a) Clean gold electrode, (b) self-assembled 11-mercaptoundecanoic acid layer, (c) anti-CA 125, (d) ethanolamine hydrochloride, and (e) 1-dodecanethiol treatment.

7.4.2 Immunosensor responses

7.4.2.1 SPR response

Figure 7.5 shows the SPR response caused by the interaction between anti-CA 125 and CA 125. When CA 125 was injected into the flow system it bound to anti-CA 125 on the surface of modified gold disk and the refractive index increased resulting in the increase of SPR. When the signal reached a steady state (after 5 min) 300 μl of regeneration solution was injected with a flow rate of 100 μl min^{-1} to dissociate the binding between antibody and antigen. This caused the reduction of SPR angle due to the lower refractive index of regeneration solution compared to the running buffer (Weast, 1974; Yu *et al.*, 2005). When the running buffer was flowed again the signal returned to a steady base-line, then a new CA 125 was injected. The response was detected by measurement of SPR angle change ($\Delta\theta$).

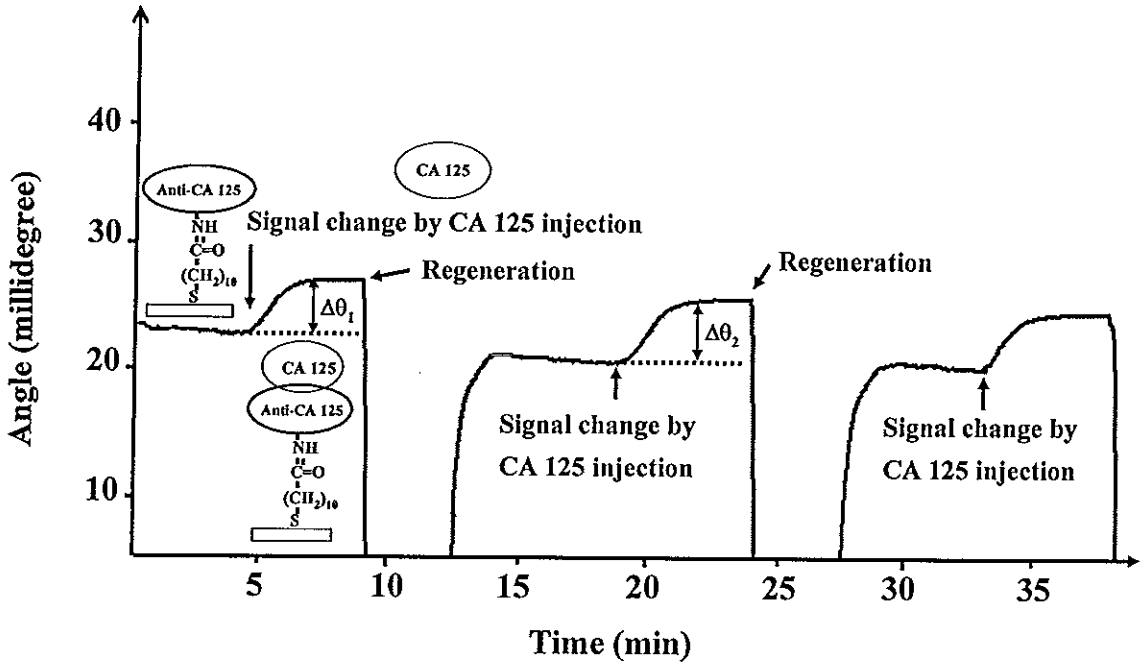

Figure 7.5 SPR sensorgram obtained from the injections of 10 U ml^{-1} CA 125 over the anti-CA 125 immobilized SAM resulting in the increase of SPR angle.

7.4.2.2 Capacitive response

The capacitance obtained from a current response was plotted as a function of time as shown in Figure 7.6. When CA 125 was injected into the system, it bound to the immobilized anti-CA 125 on the electrode surface causing the increase of dielectric layer thickness and/or the change of dielectric behavior resulting in the decrease of total capacitance. The time allowed for the steady state signal was 15 min. The capacitance response was measured by detecting the change in capacitance before and after antigen-antibody interaction (ΔC). The surface was then regenerated with regeneration solution to remove CA 125 binding. The increase of signal after regeneration solution injection was because the regeneration solution has higher ionic strength than the running buffer (Limbut *et al.*, 2006b; Jiang, *et al.*, 2003; Berggren *et al.*, 1998).

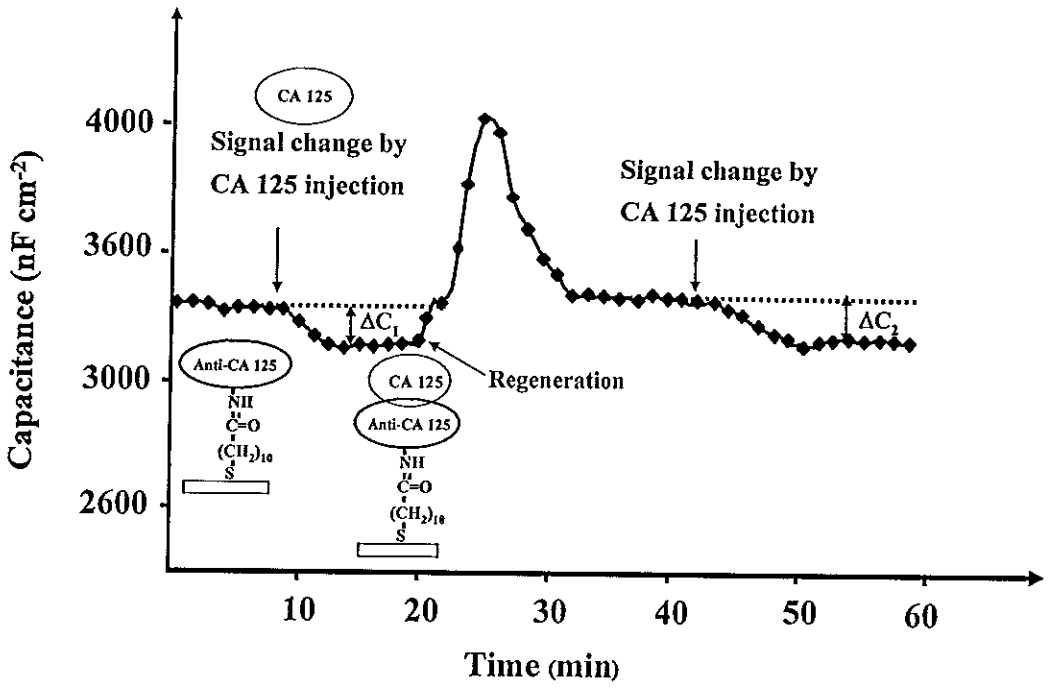

Figure 7.6 Capacitive signal obtained from the injections of 5 U ml^{-1} CA 125 causing the capacitance to decrease. The binding between anti-CA 125 and CA 125 was dissociated with HCl pH 2.6 before injection of a new CA 125.

7.4.3 Optimization of the flow injection SPR and capacitive immunosensor systems

7.4.3.1 Regeneration solution

The reusability of the sensor surface is the main advantage of immunosensors over other immunological methods, e.g. ELISA. The breaking of the non-covalent binding between anti-CA 125 and CA 125 using regeneration solution is essential for the repeated use of the sensor. Several types of regeneration solutions were tested; i.e., acidic (glycine-HCl buffer and HCl) (Loyprasert *et al.*, 2008; Thavarungkul *et al.*, 2007), basic (NaOH) (Li *et al.*, 2006) and salt ($MgCl_2$) (Andersson *et al.*, 1999). For SPR systems the experiments were done by using 300 µl of regeneration solution with a 100 µl min^{-1} flow rate and 300 µl of sample solution with a 10 µl min^{-1} flow rate. While for capacitive system 200 µl with a 100 µl min^{-1} flow rate were applied

for both regeneration and sample solution. These are optimum values obtained from the other study in our laboratory based on the binding between human serum albumin and anti human serum albumin (unpublished data). These parameters were later optimized for the present systems (see 3.4.3 and 3.4.4).

The efficiency of regeneration solution was determined by residual activity of the immobilized anti-CA 125 monitored from the change in response ($\Delta\theta$ or ΔC) due to the binding between CA 125 before ($\Delta\theta_1$ or ΔC_1) and after regeneration ($\Delta\theta_2$ or ΔC_2) (Figures 7.5 and 7.6) as follows:

$$\% \text{ Residual activity} = \frac{\Delta\theta_2 (or \Delta C_2) \times 100}{\Delta\theta_1 (or \Delta C_1)} \quad (7.1)$$

Tables 7.1 and 7.2 showed the results of regeneration solution for SPR and capacitive system, respectively. The highest residual activity of both transducers was from HCl pH 2.50 (SPR = 93±3 %, capacitive = 94±2 %). The influence of different pH of HCl solution was then studied. Residual activity increased from pH 2.80 to 2.60 then decreased. This may be because low pH can destroy the SAM layer (Jiang *et al.*, 2003). Therefore, pH 2.60 was selected (SPR = 96±2 %, capacitive = 98±3 %).

Table 7.1 Tested and optimum conditions of the type, pH and concentration of regeneration solution of SPR immunosensor.

Parameters	Investigation condition	Efficiency of CA 125 removal (% average of residual activity ± SD)	Regeneration time* (min)
Type	50 mM glycine-HCl pH 2.50	78 ± 3	9
	HCl pH 2.50	93 ± 3	8
	NaOH pH 10.00	72 ± 3	28
	25 mM $MgCl_2$	51 ± 4	50
pH	2.20	74 ± 3	5
	2.40	87 ± 4	7
	2.50	93 ± 2	8
	2.60	96 ± 2	8
	2.70	92 ± 2	9
	2.80	91 ± 5	9

*Regeneration time was obtained from the time that required for the signal start changing after injection of regeneration solution to reach a steady state.

Table 7.2 Tested and optimum conditions of the type, pH and concentration of regeneration solution of capacitive immunosensor.

Parameters	Investigation condition	Efficiency of CA 125 removal (% average of residual activity ± SD)	Regeneration time (min)
Type	50 mM glycine-HCl pH 2.50	88 ± 2	17
	HCl pH 2.50	94 ± 2	15
	NaOH pH 10.00	73 ± 3	28
	25 mM $MgCl_2$	46 ± 4	39
pH	2.20	73 ± 1	12
	2.40	76 ± 2	13
	2.50	93 ± 4	14
	2.60	98 ± 3	15
	2.70	94 ± 1	17
	2.80	92 ± 3	22

7.4.3.2 Running buffer solution

Investigations of running buffer were carried out using the same sample volume and flow rate as in 7.3.3.1. The influence of three types of buffer commonly used in immunosensor system was first studied (Figure 7.7). For SPR system, calibration curve of standard CA 125 at 10, 15, 20, and 25 U ml^{-1} (preliminary study indicated linear range at these concentrations) was performed. While for capacitive system, standards CA 125 from 5 to 20 U ml^{-1} were studied. Sensitivity (slope of calibration curve) obtained from the plot between SPR angle shift or capacitance change and concentrations of CA 125 for the three running buffer were compared.

Sodium phosphate saline buffer and Tris-HCl buffer provided the lowest base-line for SPR and capacitive immunosensor systems, respectively. Hence, they gave the highest sensitivity (SPR = 0.042±0.001 millidegree/U ml^{-1}, capacitive = 4.1±0.1 –nF cm^{-2}/U ml^{-1}).

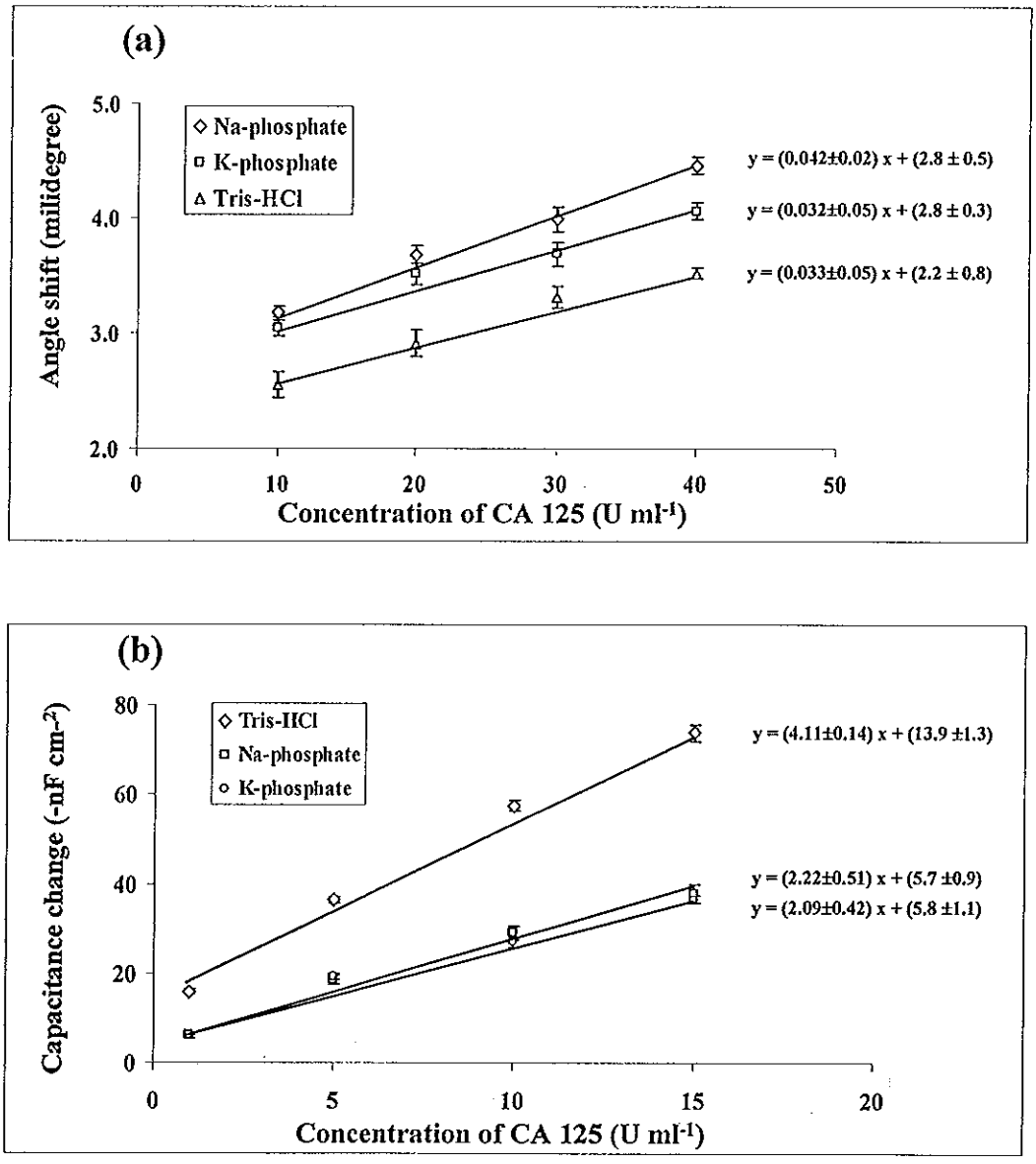

Figure 7.7 Response of (a) SPR immunosensor, (b) capacitive immunosensor to CA 125 using different types of buffer.

The influence of pH of running buffer was then investigated from 6.80 to 7.60 by using 10 U ml^{-1} of CA 125 in 10 mM of sodium phosphate saline for SPR and 5 U

ml^{-1} of CA 125 in 10 mM of Tris-HCl for capacitive system. These concentrations were selected since they can give relatively high signal. Other parameters were the same as for the study of types of buffer. The highest response was at pH 7.20 for both systems.

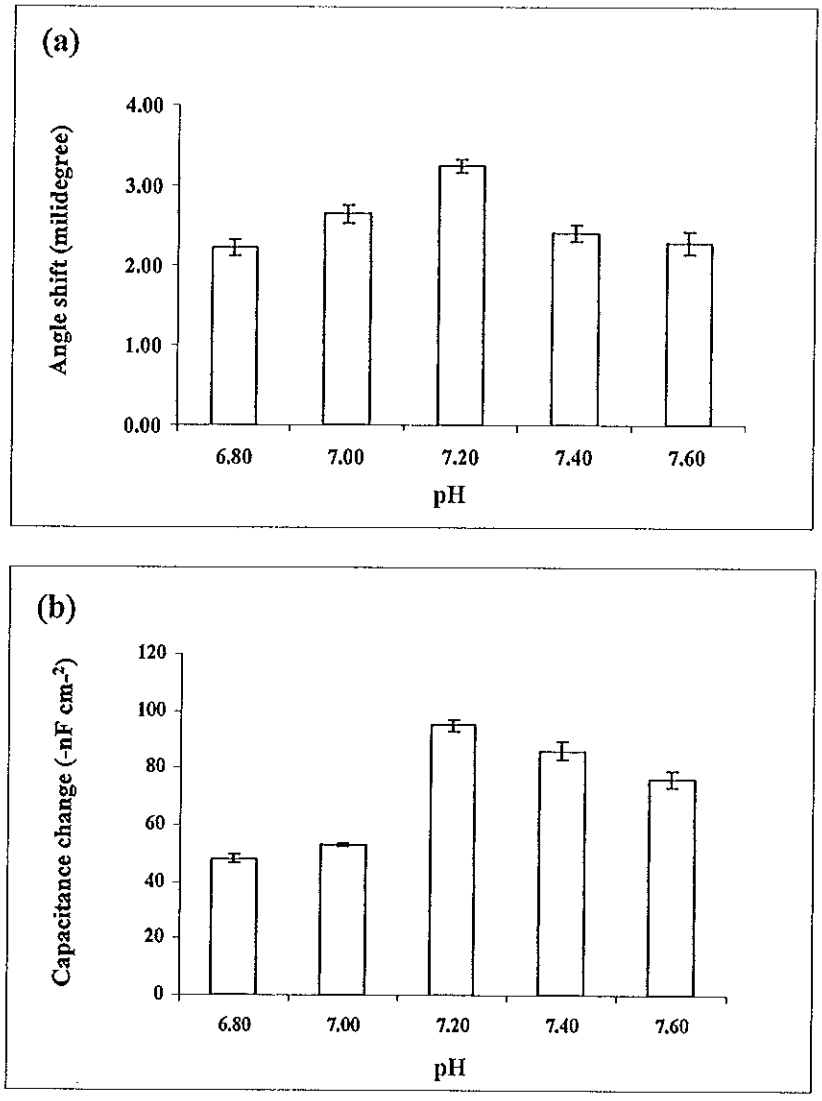

Figure 7.8 Response of (a) SPR immunosensor, (b) capacitive immunosensor to CA 125 using different pH of buffer.

Buffer concentrations were also studied since ionic strength of solution is also a factor that affect the association and dissociation affinity binding (Shankaran *et al.*, 2007). Different concentrations of sodium phosphate pH 7.20 and Tris-HCl pH 7.20

were studied for SPR and capacitive systems, respectively. The maximum responses were obtained at 15 mM for both immunosensor systems as shown in Figure 7.9.

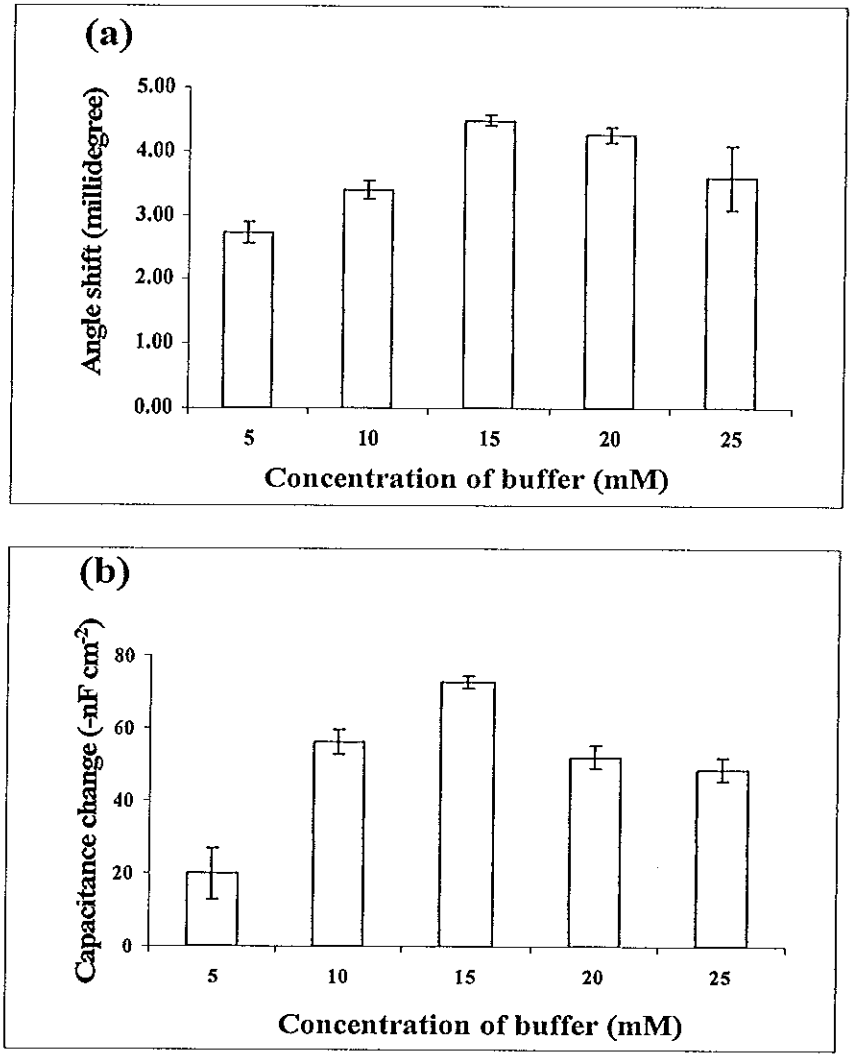

Figure 7.9 Response of (a) SPR immunosensor, (b) capacitive immunosensor to CA 125 using difference concentrations of buffer.

7.4.3.3 Flow rate

The influence of the flow rate was investigated. The responses for both systems increased when the flow rate decreased because slower flow rate allowed CA 125 to retain longer in the flow cell to bind with anti-CA 125. However, for SPR the

response between 10 µl min^{-1} (5.3±0.2 millidegree) and 15 µl min^{-1} (4.8±0.2 millidegree), were not much different (9 %) but the time required to reach a steady state of 15 µl min^{-1} was much shorter, 5 min compared to 8 min. Therefore, 15 µl min^{-1} was selected. Similarly, 100 µl min^{-1} (66±1 –nF cm^{-2}) was chosen for capacitive immunosensor because the response was only 3 % lower than 50 µl min^{-1} (68±3 –nF cm^{-2}), but the time was much shorter, 15 compared to 25 min.

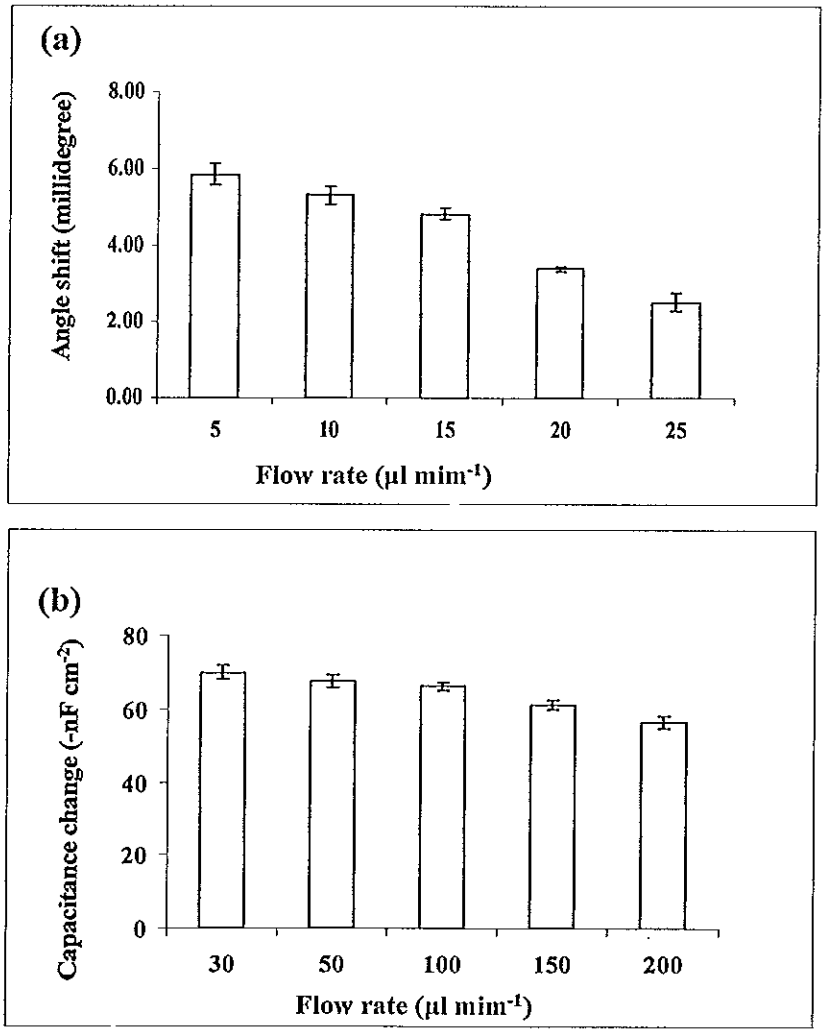

Figure 7.10 Response of (a) SPR immunosensor, (b) capacitive immunosensor to CA 125 using different flow rate of buffer.

7.4.3.4 Sample volume

The variation of response with the injected sample volume was studied (Figure 7.11). Initially the response increased with the volume. However, antigen-antibody binding also depends on the amount of anti-CA 125 immobilized on the surface. So, too much CA 125 for the same amount of anti-CA 125 cannot increase the response. The response reached a plateau at 300 µl for SPR (5.1±0.5 millidegree) and 250 µl for capacitive system (74±1 –nF cm^{-2}). These values were then chosen for further experiments.

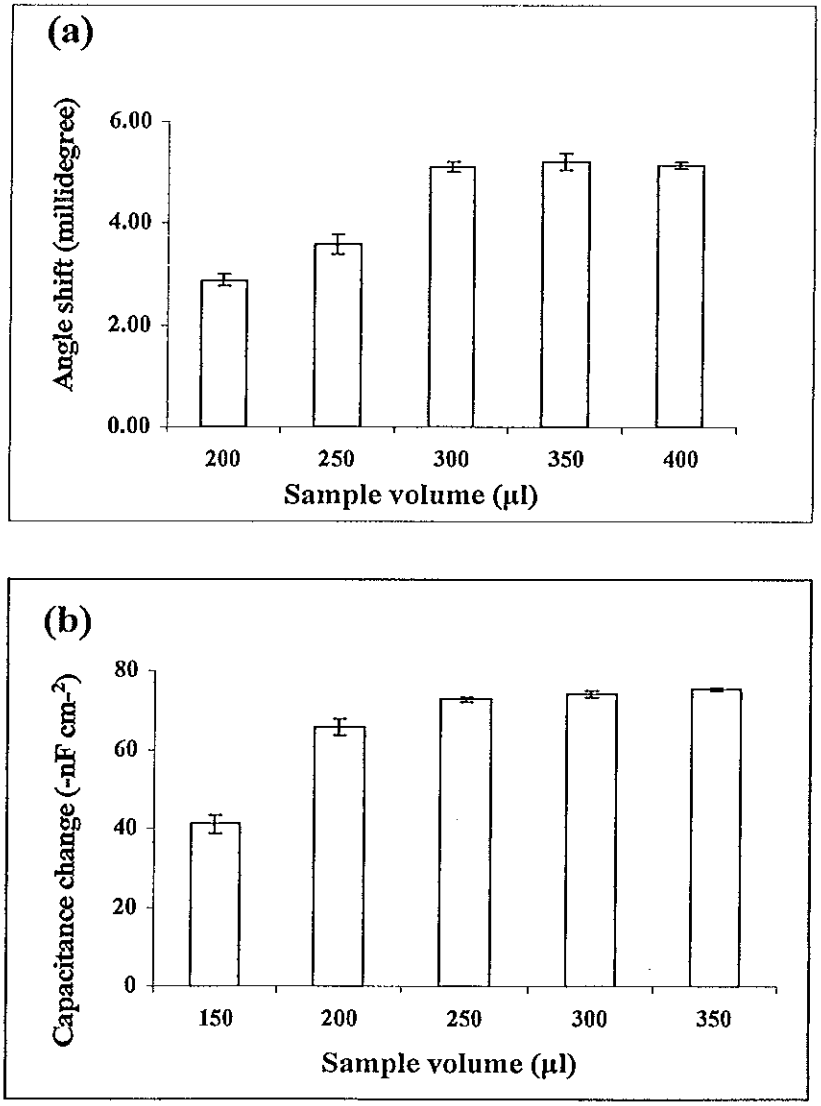

Figure 7.11 Response of (a) SPR immunosensor, (b) capacitive immunosensor to CA 125 using different sample volume of buffer.

7.4.3.5 Linear range and detection limit

Different concentrations of CA 125 were tested by the SPR and capacitive systems under their optimum conditions, each concentration was injected 3 times. Since the calibration curve (Figure 7.12) has similar shape to the calibration plot of ion selective electrode the limit of detection was determined followed IUPAC Recommendation 1994 (Buck and Lindneri, 1994). For surface plasmon resonance the linear range was between 0.1 and 40 U ml^{-1} (Figure 7.12 (a)) with a detection limit of 0.1 U ml^{-1} (Figure 7.12(a) inset). Slightly wider linear range, 0.05-40 U ml^{-1} and a lower detection limit, 0.05 U ml^{-1} were obtained for capacitive system (Figure 7.12 b). Both immunosensors provided detection limits much lower than the 35 U ml^{-1} which is the concentration of CA 125 in normal human blood. The detection limits of present work are much lower than enzyme-labeled immunosensors; 1.29, 1.73, and 4 U ml^{-1} (Dai *et al.*, 2003, Wu *et al.*, 2006a, VIDAS ® CA 125 II ™).

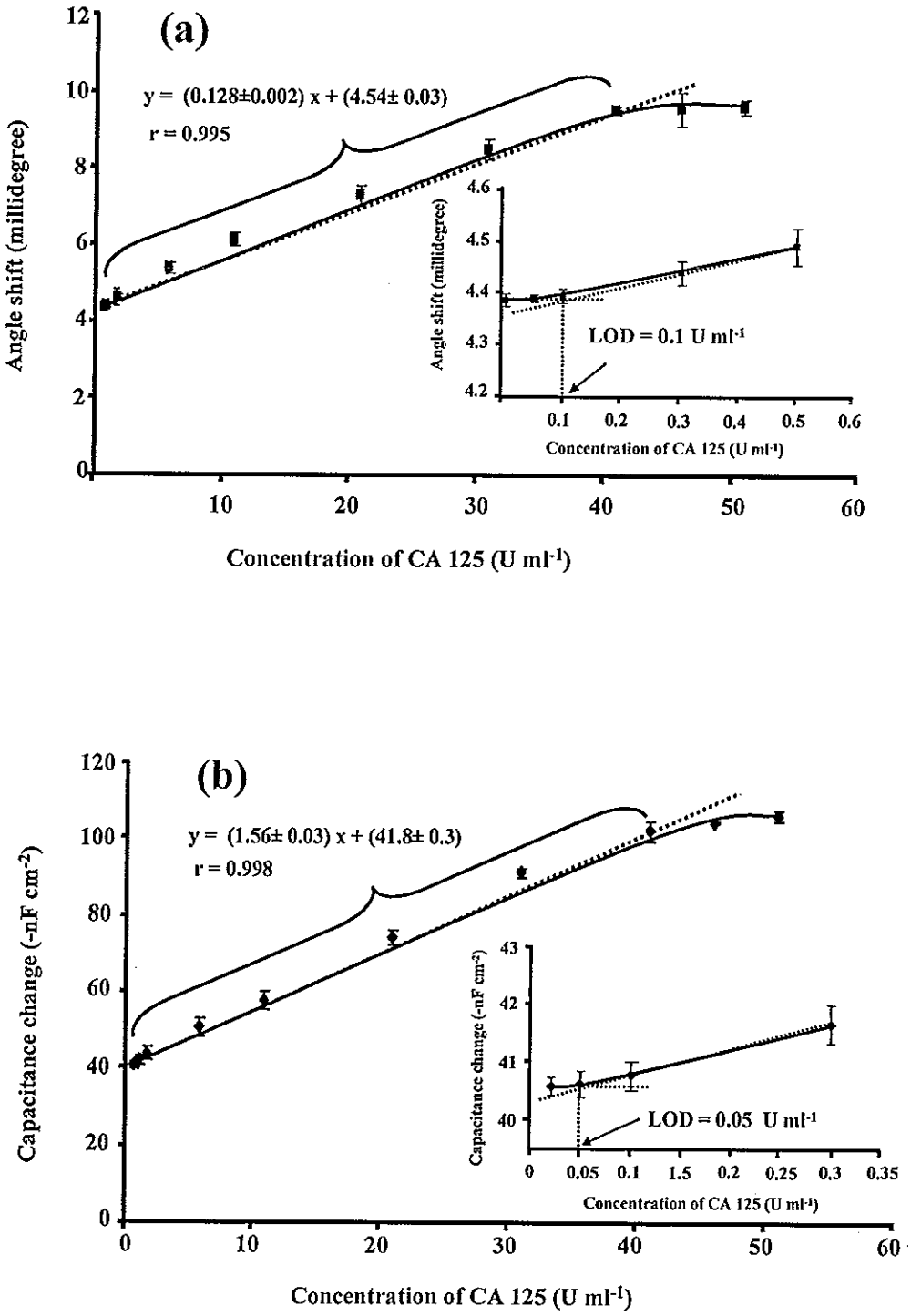

Figure 7.12. Calibration curve for CA (a) SPR immunosensor and (b) capacitive immunosensor. The insets show the detection limit of each system.

7.4.3.6 Selectivity

One of the potential advantages of using biological molecules as recognition elements in biosensors is its selectivity towards the analyte. CEA and AFP were used to evaluate the selectivity of both immunosensors because they are important tumor markers responsible for clinical diagnosis such as lung, pancreas, ovaries, and other types of tumor (Wu *et al.*, 2007a). The results in Figure 7.13 indicated that for both immunosensors CEA and AFP gave much lower responses than CA 125, the same response as blank (running buffer; 0.7 millidegree and 17 -nF cm^2 for SPR and capacitive system) and lower than the response at the detection limit of CA 125 (4.3 ± 0.1 millidegree and 40.7± 0.9 -nF cm^{-2} for SPR and capacitive system, respectively) so their presence would not interfere with these systems. Thus, both immunosensors have good selectivity to CA 125 analysis.

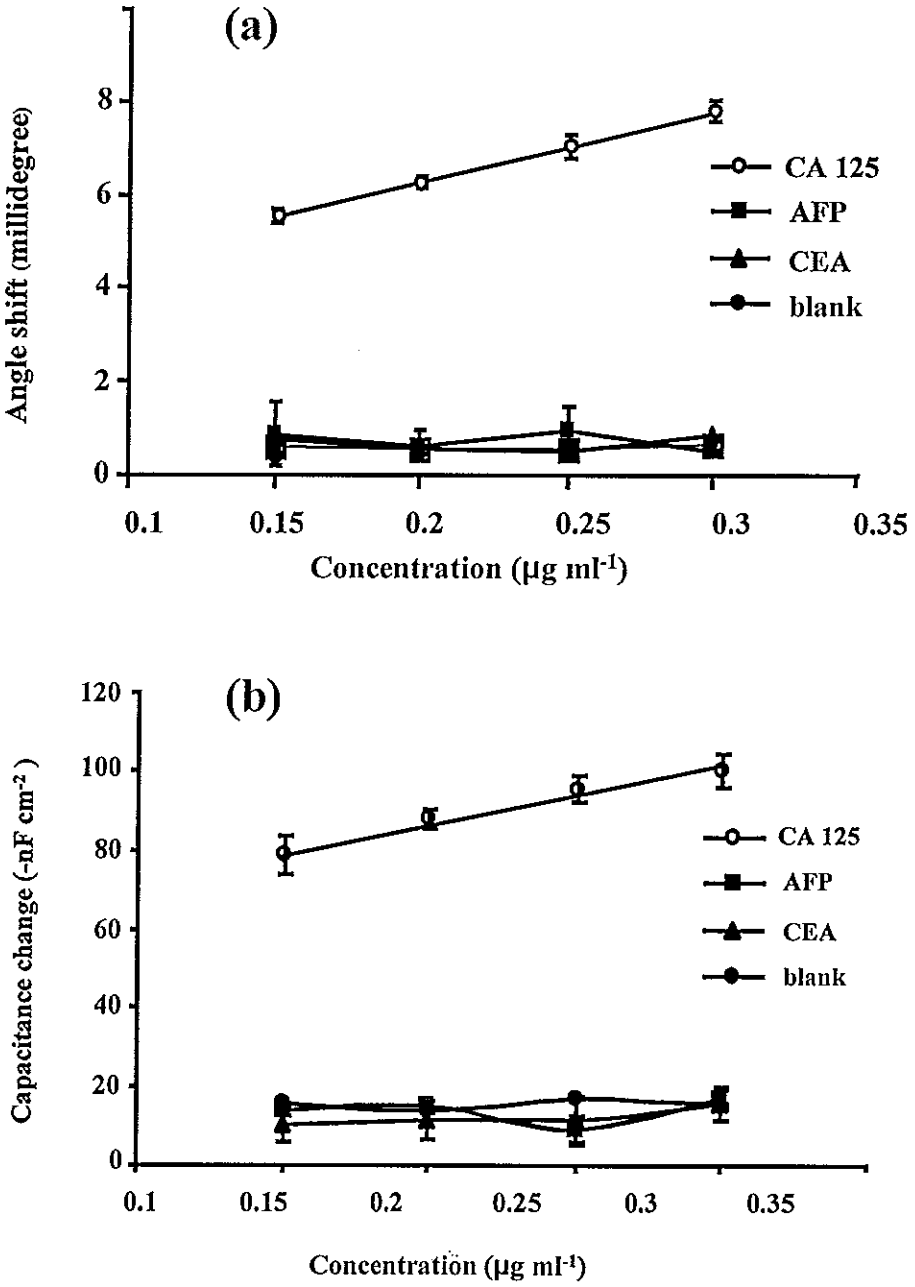

Figure 7.13 Response change *vs* the concentration of CA 125, CEA, AFP, and blank (running buffer) in SPR (a) and capacitive (b) immunosensors.

7.4.3.7 Reproducibility

The reproducibility was tested by continuously injecting the same concentration of standard CA 125 (10 U ml^{-1} for SPR and 5 U ml^{-1} for capacitive system) with subsequent regeneration to remove CA 125 from the anti-CA 125 immobilized on surface of gold substrate. Then percentage of residual activity was calculated. The result found that for SPR immunosensor after 32 times of regeneration (2 days) the percentage of residual activity maintained an average of 96 ± 4 (4 % RSD) after which the response decrease rapidly. For capacitive immunosensor the percentage of residual activity gave an average of 97 ± 3 (3 % RSD) after 48 times of regeneration cycle (3 days). Both immunosensors provided good reproducibility with RSD lower than 4% for sensing surface detection of CA 125.

In the capacitive system cyclic voltamogram of the modified electrode after the decrease of activity was tested and found to be similar to the one before the electrode was used. For SPR system, the base-line of the system when the response decreased was similar to the one before the modified electrode was first used. These indicated that the SAM layer remained intact. Therefore, the decreasing of response is probably caused by the loss of activity of anti-CA 125 because the self-assemble monolayer was not destroyed by regeneration solution.

The lesser number of reuse for SPR sensor (32 times) when compared to the capacitive system (48 times) may be because in the SPR system the immobilized antibody was exposed to the regeneration solution slightly longer than in the capacitive system. For each regeneration cycle the volume of regeneration solution and flow rate of SPR were 300 µl and 100 µl min^{-1}, respectively resulting in an exposure time of 3 min. While 250 µl of regeneration volume and 100 µl min^{-1} of flow rate were used for the capacitive system, i.e. 2.5 min exposure time.

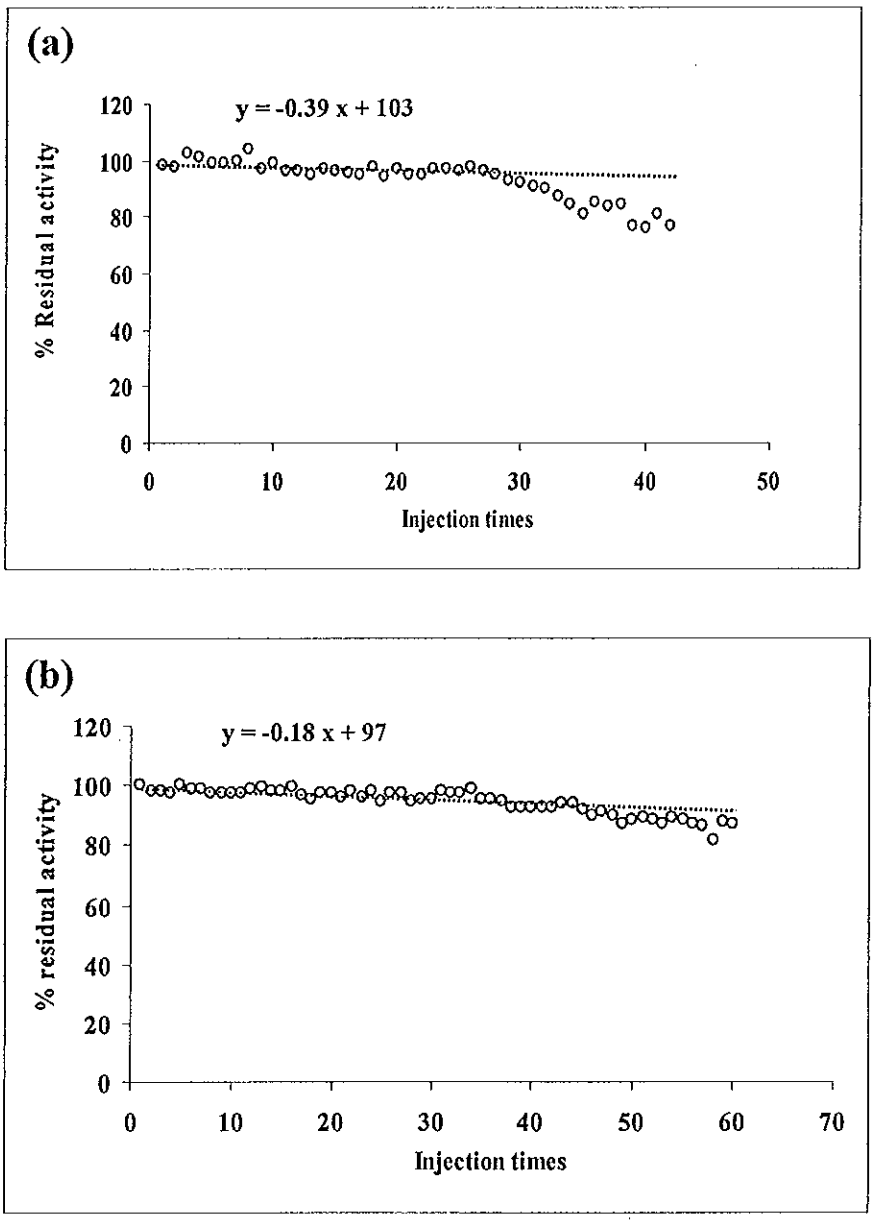

Figure 7.14 Reproducibility of response of CA 125 to injection of CA 125 for SPR (a) and capacitive (b) immunosensors with regeneration steps between each individual assay.

7.4.3.8 Matrix effect

Ten human serum samples were obtained from Hat Yai Hospital, Thailand. For SPR, the linear range was 0.1 – 40 U ml^{-1} and 0.05 - 40 U ml^{-1} for capacitive system. Since the concentration of CA 125 in blood of healthy human is lower than 35 U ml^{-1}, analysis of the human serum sample can be diluted at least 100 times. To study the matrix effect, the calibration curves of spiked (obtained from spiking CA 125 into real sample) and standard (obtained from spiking CA 125 into running buffer) were done for every samples. Different concentration of standard CA 125 were spiked into serum samples and then diluted with running buffer at 100 and 1000 times. The slope of standard solution curve and the spiked curve were compared by using two-way ANOVA (analysis of variance), calculated by R software (R development Core Team, 2006). If there is no significant difference (P<0.05), it indicates that the matrix has no effect on response of the immunosensors. Figure 7.15 shows the standard curve and spiked curve for the study of matrices interference of human sample. The response of the spiked curve is higher than the one obtained from standard curve. This may be because of the CA 125 in human serum samples, therefore, for spiked samples, the concentration of CA 125 is higher than standard. For all ten samples, 100 times dilution the matrix has no effect. Therefore, all samples, after 100 times dilution, can be directly analyzed by using standard calibration curve.

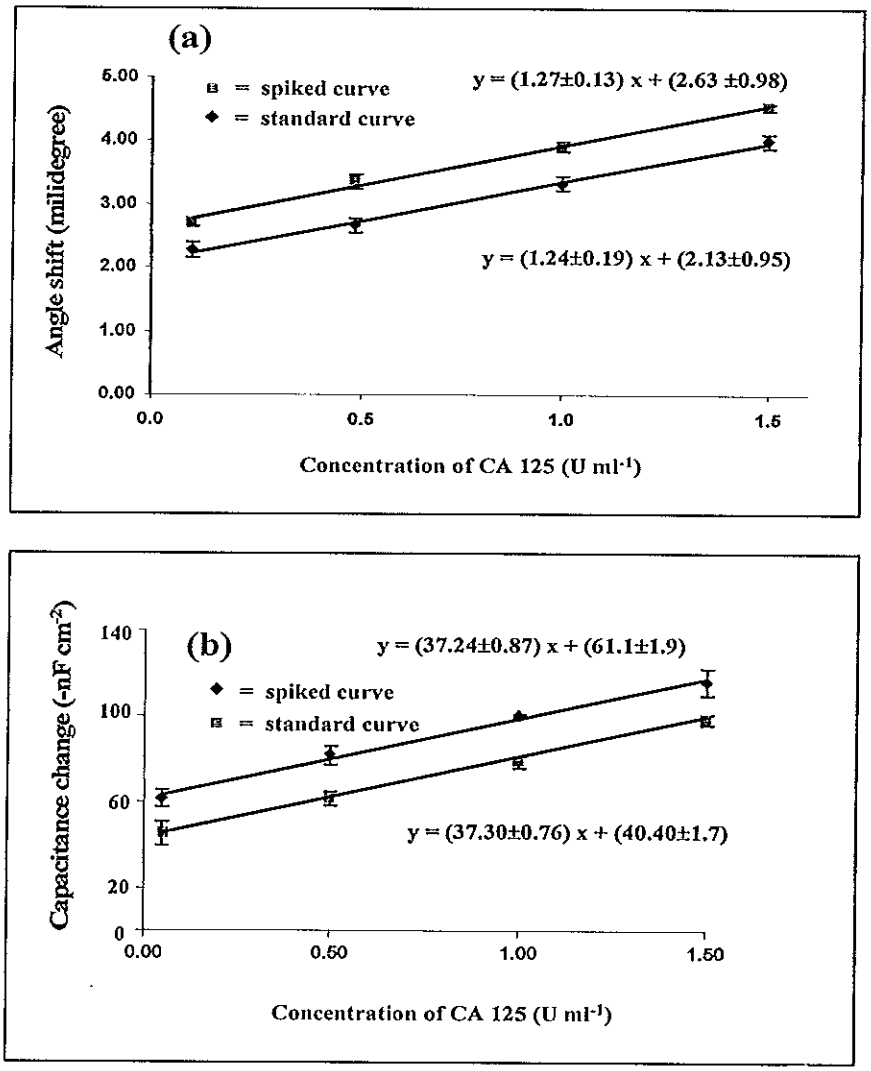

Figure 7.15 The standard curve and spiked curve for the study of matrices interference of human sample at dilution factor of 100 times.

7.4.3.9 Real samples

Ten serum samples were analyzed by using SPR and capacitive immunosensors and the results were compared with an enzyme linked fluorescent assay (VIDAS® CA 125 II™), a conventional method in clinical laboratory used by Hat Yai Hospital. In brief, this method is based on a sandwich enzyme immunoassay. Secondary antibodies were labeled with alkaline phosphate to catalyze the hydrolysis of 4-methyl umbelliferyl phosphate substrate into a fluorescent product (4-methyl umbelliferone) the fluorescent of which is measured at 450 nm.

Calibration curves of the immunosensors were first constructed using standard solution between 0.1 and 1.5 U ml^{-1} for SPR and between 0.05 and 1.5 Uml^{-1} for capacitive immunosensors. Samples were diluted with running buffer at 100 and 1000 times. The immunosensors responses of each sample were used to determine CA 125 concentration from the calibration curve of CA 125 standard and multiplied by the dilution factor. The two immunosensors results were compared to ELFA method by Wilcoxon singned rank test as shown in Table 7.3 (Triola, 1998). In this test, the null hypothesis (there is no difference between the two methods) is rejected at a significance level ($P = 0.05$) if the experimental value is less than or equal to the critical values. The results in Table 7.4 and Table 7.5 for SPR and capacitive systems, respectively showed that the null hypothesis is retained. There is no evidence for systematic differences between the results obtained from both immunosensors and the enzyme linked fluorescent method ($P = 0.05$). That is, the concentration determined by both immunosensors and enzyme linked fluorescent are in good agreement.

Table 7.3 Comparison of CA 125 concentrations in human resume samples were obtained from SPR, capacitive immunosensors with conventional method in hospitals. (mean ± SD, n=3)

Sample	CA 125 concentration (U ml^{-1}) (RSD)		
	ELFA	SPR	Capacitive
1	31	28 ± 1 (4%)	29.5 ± 0.3 (1%)
2	32	33 ± 1 (3%)	30 ± 1 (3%)
3	33	30 ± 1 (3%)	33 ± 1 (3%)
4	85	83 ± 1 (1%)	82 ±2 (2%)
5	99	98 ± 2 (2%)	101 ± 4 (4%)
6	106	109.2 ± 0.4 (0.4%)	108 ± 3 (3%)
7	113	115 ± 2 (2%)	110 ± 2 (2%)
8	114	115 ± 1 (1%)	118 ± 2 (2%)
9	177	175 ± 4 (2%)	177 ±5 (3%)
10	662	658 ± 26 (4%)	663 ± 30 (5%)

Table 7.4 The Wilcoxon sign rank test for the comparison of the concentration of CA 125 in sample from the SPR immunosensor system and ELFA technique.

Sample	CA 125 concentration (U ml^{-1})			Rank
	ELFA technique	SPR immunosensor	Difference of two methods (U ml^{-1})	
1	114	115	-1	-2
2	85	83	2	5
3	106	109	-3	-8
4	177	175	2	5
5	33	30	3	8
6	113	115	-2	-5
7	99	98	1	-2
8	32	33	1	-2
9	662	658	4	10
10	31	28	3	8
n				10
Sum of positive ranks				36
Sum of negative ranks				**19**
Test statistic at p value = 0.05, n = 10, tabulate value				**8**

n is the number in the sample having ignored the zeros which obtained from difference of two methods.

Table 7.5 The Wilcoxon sign rank test for the comparison of the concentration of CA 125 in sample from the capacitive immunosensor system and ELFA technique.

Sample	CA 125 concentration (U ml^{-1})			Rank
	ELFA technique	Capacitive immunosensor	Difference of two methods (U ml^{-1})	
1	114	118	-4	-8
2	85	82	3	6
3	106	108	-2	-3
4	177	177	0	0
5	33	33	0	0
6	113	110	3	6
7	99	101	-2	-3
8	32	30	3	6
9	662	663	-1	-1
10	31	29	2	3
n				8
Sum of positive ranks				21
Sum of negative ranks				**15**
Test statistic at p value = 0.05, n = 8, tabulate value				**4**

n is the number in the sample having ignored the zeros which obtained from difference of two method.

7.4.3.10 Recovery

To further validate the systems, the recovery was studied by spiking all serum samples with different concentration of CA 125. Percentage of recovery was calculated by the following equation

$$\text{Recovery (\%)} = \frac{C_1 - C_2}{C_3} \times 100 \qquad (7.2)$$

Where, C_1 = concentration determined in fortified (or spiked) sample, C_2 = concentration determined in unfortified sample and C_3 = concentration of fortification (Eurachem Working group, 1998).

C_2 was calculated based on standard calibration curve. For example, standard calibration equation of one sample for SPR system was y = (1.40±0.08)x + (2.13±0.09). The signal obtained from real sample after diluted 100 times was 3.29±0.02 millidegree the concentration of CA 125 was then calculated based on this equation and result found that the concentration of CA 125 was 0.83±0.01 U ml^{-1}. After that this concentration was multiplied by 100. Therefore, concentration of CA 125 in real sample was 83±1 U ml^{-1} (C_2).

Average recoveries were between 81 and 110 % with R.S.D. between 2 and 12 % as shown in Table 7.6. These are acceptable since the lowest concentration tested was 5 U ml^{-1} or 33 ppb (1 mg = 150 kU) and the acceptable recovery of 100 ppb level is 80-110 % and RSD is 15-22.6 % (Taverniers *et al.*, 2004). Thus, the present methods could satisfy the requirements for determining CA 125 in human serum in clinical diagnosis.

Table 7.6a Recoveries in spiked serum samples with 100 times of dilution factor (mean ± SD, n=3).

Sample	System	Parameter	Spiked concentration (U ml^{-1})				
			5	10	50	100	150
1	SPR C_2= 30 (U ml^{-1})	Detected (C_1) (U ml^{-1})	-	41±2	84±1	129±5	175±9
		Recovery (%)	-	105±8	108±6	99±3	97±5
	Capacitive C_2=33 (U ml^{-1})	Detected (C_1) (U ml^{-1})	38±2	-	78±4	135±3	175±8
		Recovery (%)	104±6	-	91±9	103±4	95±2
2	SPR C_2= 29 (U ml^{-1})	Detected (C_1) (U ml^{-1})	-	39±3	77±8	125±6	183±3
		Recovery (%)	-	109±10	98±10	97±9	103±3
	Capacitive C_2=30 (U ml^{-1})	Detected (C_1) (U ml^{-1})	34±2	-	77±4	132±4	182±7
		Recovery (%)	96±8	-	94±9	103±8	102±5
3	SPR C_2= 33 (U ml^{-1})	Detected (C_1) (U ml^{-1})	-	41±2	79±3	112±2	165±4
		Recovery (%)	-	87±6	93±7	80±5	89±7
	Capacitive C_2=30 (U ml^{-1})	Detected (C_1) (U ml^{-1})	35±6	-	85±4	118±3	189±2
		Recovery (%)	94±8	-	109±5	88±3	106±3
4	SPR C_2= 83 (U ml^{-1})	Detected (C_1) (U ml^{-1})	-	93±1	132±8	187±2	218±5
		Recovery (%)	-	99±6	99±9	104±2	90±5
	Capacitive C_2=82 (U ml^{-1})	Detected (C_1) (U ml^{-1})	86±4	-	133±7	164±3	209±3
		Recovery (%)	86±9	-	102±10	82±4	85±3
5	SPR C_2= 98 (U ml^{-1})	Detected (C_1) (U ml^{-1})	-	107±5	138±3	203±4	239±10
		Recovery (%)	-	94±8	81±6	105±4	94±5
	Capacitive C_2=101 (U ml^{-1})	Detected (C_1) (U ml^{-1})	106±4	-	149±3	181±2	236±3
		Recovery (%)	94±8	-	97±6	80±4	90±5

Table 7.6b Recoveries in spiked serum samples with 1000 times of dilution factor (mean ± SD, n=3).

Sample	System	Parameter	Spiked concentration (U ml^{-1})				
			50	100	500	1000	1500
6	SPR C_2= 106 (U ml^{-1})	Detected (C_1) (U ml^{-1})	-	210±11	534±10	1049±11	1684±16
		Recovery (%)	-	97±10	85±3	94±3	105±4
	Capacitive C_2=108 (U ml^{-1})	Detected (C_1) (U ml^{-1})	151±5	-	623±11	1038±16	1683±20
		Recovery (%)	87±6	-	103±3	93±8	105±9
7	SPR C_2= 113 (U ml^{-1})	Detected (C_1) (U ml^{-1})	-	213±11	545±17	995±16	1630±19
		Recovery (%)	-	98±6	86±3	88±8	101±9
	Capacitive C_2=110 (U ml^{-1})	Detected (C_1) (U ml^{-1})	150±9	-	540	990	1625
		Recovery (%)	81±5	-	86±3	88±8	101±8
8	SPR C_2= 115 (U ml^{-1})	Detected (C_1) (U ml^{-1})	-	210±11	550±15	1095±10	1555±19
		Recovery (%)	-	95±10	87±9	98±9	96±4
	Capacitive C_2=118 (U ml^{-1})	Detected (C_1) (U ml^{-1})	161±7	-	583±11	1028±11	1498±10
		Recovery (%)	85±10	-	93±7	91±4	92±3
9	SPR C_2= 175 (U ml^{-1})	Detected (C_1) (U ml^{-1})	-	266±10	630±12	1155±13	1615±15
		Recovery (%)	-	91±6	91±6	98±9	95±4
	Capacitive C_2=177 (U ml^{-1})	Detected (C_1) (U ml^{-1})	232±9	-	617±15	1157±18	1692±18
		Recovery (%)	110±5	-	88±6	98±9	101±4
10	SPR C_2= 658 (U ml^{-1})	Detected (C_1) (U ml^{-1})	-	743±11	1073±18	1518±10	2068±21
		Recovery (%)	-	85±5	83±5	86±4	94±2
	Capacitive C_2=663 (U ml^{-1})	Detected (C_1) (U ml^{-1})	713±19	-	1098±10	1643±11	2103±19
		Recovery (%)	101±5	-	87±5	98±5	96±6

7.4.2.11 Limit of quantification

Limit of quantification (LOQ) was determined by considering the lowest concentration of analyte with acceptable accuracy and precision (Taverniers *et al.*, 2004). For SPR it was studied by spiking 10 U ml^{-1} into 5 real samples (1 sample was repeated 3 times), diluted 100 times to 0.1 U ml^{-1} (LOD) or 0.7 ppb and determined the recovery and precision. Acceptable recovery and precision at 1 ppb were 40-120 % and % RSD $\leq$ 30 (Taverniers *et al.*, 2004). The recovery of SPR at 0.1 U ml^{-1} was 97±9 % (% RSD = 10) which are very well within the acceptable range (Table 7.7). Therefore, LOQ of SPR could be said to be 0.1 U ml^{-1}. Similar test was carried out with the capacitive system and found the LOQ to be 0.05 U ml^{-1} or 0.3 ppb (recovery = 95±9 %, % RSD = 10) as shown in Table 7.8. Thus, the present methods could satisfy the requirements for determining CA 125 in human serum in clinical diagnosis.

Table 7.7 Recoveries of SPR system from real samples spiked with 10 U ml^{-1} CA 125 calculated from the detected concentration (C_1) and the original concentration in the real samples (C_2).

Sample	Repeat	Detected concentration (C_1) (U ml^{-1})	% recovery
1 (C_2=30 U ml^{-1})	1	39.6	96
	2	39.9	99
	3	40.9	109
2 (C_2=28 U ml^{-1})	1	37.2	92
	2	38.0	100
	3	38.1	101
3 (C_2=33 U ml^{-1})	1	41.6	86
	2	42.3	93
	3	43.6	106
4 (C_2=83 U ml^{-1})	1	92.9	99
	2	92.3	93
	3	93.5	105
5 (C_2=98 U ml^{-1})	1	106.0	80
	2	106.5	85
	3	108.6	106
Average			97±9

Table 7.8 Recoveries of capacitive system from real samples spiked with 5 U ml^{-1} CA 125 calculated from the detected concentration (C_1) and the original concentration in the real samples (C_2).

Sample	Repeat	Detected concentration (C_1) (U ml^{-1})	% recovery
1 (C_2=33 U ml^{-1})	1	37.1	82
	2	37.8	95
	3	37.2	83
2 (C_2=30 U ml^{-1})	1	34.4	87
	2	34.0	80
	3	34.3	86
3 (C_2=30 U ml^{-1})	1	34.5	90
	2	34.7	94
	3	34.7	94
4 (C_2=82 U ml^{-1})	1	87.4	109
	2	88.2	109
	3	89.1	110
5 (C_2=101 U ml^{-1})	1	106.3	106
	2	105.9	98
	3	106.0	99
Average			95±9

7.5 Conclusions

In this chapter we presented two sensitive and accurate immunosensors for measuring CA 125 in human serum samples with no requirement of labeling. The comparison between surface plasmon resonance and capacitive immunosensors were carried out with the same immobilization technique. The analytical performances of

both techniques were evaluated at their optimum conditions. The SPR method was superior in terms of real-time monitoring making it easy to follow and monitor the immobilization and optimization steps. It also required less time for the steady response (5 min for SPR and 15 min for capacitive) and regeneration (5 min for SPR and 12 min for capacitive). Whereas, the capacitive system showed a slightly lower limit of detection (0.05 U ml^{-1}) than SPR (0.1 U ml^{-1}). The instrument is also less complicated with lower cost and the gold rod electrode can be reuse. However, our system cannot provide real-time response, the capacitance have to be calculated afterwards. Therefore, future development of a real-time capacitive system may help to improve certain aspect of this system such as real-time detection, easy to follow optimization steps and easy data interpretation.

Both immunosensors allow sensitive and accurate CA 125 determinations compared with the current clinical method. These two immunosensors have the advantages of very low detection limit and permitting a label-free analysis of CA 125 with low cost 30 bath/analysis (including antigen, antibody, reagents and gold disk) compared with ELFA 1,000 bath/analysis. Similar performances were obtained from both SPR and capacitive techniques. This is different from the findings of Labib *et al.* (2009). In their work SPR system provided higher detection limit than the capacitive system by three orders of magnitude. This may be because SPR parameters were not optimized and/or their analyte has a relatively low molecular weigh (cholera toxin; M.W. = 85 kDa). SPR detection is usually utilized for the detection of large molecule (> 100 kDa) (Kawaguchi et al., 2008). The good performance of SPR in our work may due to the large molecule of CA 125 (200 kDa). However, for label-free detection of small molecules (MW < 1000) capacitive system may be more useful (Cheng *et al.*, 2001; Loyprasert *et al.*, 2008). Further comparison between the two systems for the detection of small molecules would be an interesting study. In conclusion, these SPR and capacitive-based immunosensors were highly efficient for the clinical determination of CA 125 levels in human serum samples.

CHAPTER 8

Determination of Melioidosis using Capacitive Immunosensor

8.1 Introduction

Melioidosis is a tropical infectious disease caused by the Gram-negative bacterium *Burkholderia pseudomallei* (Cheng *et al.*, 2005). It is endemic in northern Australia and Southeast Asia and is associated with a significant mortality rate (Cheng *et al.*, 2008). *B. pseudomallei* is found in environmental saprophyte such as in wet soil. Infections may be protean; they may affect any organ in the body, but primarily the lungs and the intra-abdominal organs. Although incubation periods as long as 62 years have been described (Ngauy *et al.*, 2005), it is believed that most cases occur within 1 day to 2-3 weeks after exposure (Currie *et al.*, 2000), with a spectrum of severity ranging from overwhelming sepsis to skin lesions or more chronic disease. Laboratory diagnosis is crucial for successful patient management. Therefore, analytical method for detection of *B. pseudomallei* antibody is very important.

Conventional analyses are bacterial culture and immunological methods. For bacterial culture, its main drawback is that it takes at least 3–4 days to obtain the results and by that time it may be too late for successful management, as a high percentage of patients admitted for acute septicemia die within 24–48 h of admission (Sirisinha *et al.*, 2000). Another method is based on immunological assays such as indirect hemagglutination (IHA). Although, the results can be obtained more rapidly than the bacterial culture, it provided poor sensitivity and specificity (Gilmore *et al.*, 2007; Sirisinha *et al.*, 2000). Thus, a method that can provide high sensitivity, high selectivity and rapid analysis is required for *B. pseudomallei* antibody detection. One approach is capacitive immunosensor.

Bip D is a protein encoded by the Bip D gene of *B. pseudomallei* (Erskine *et al.*, 2006). It is a member of a Type III secretion system (TTSS) in *B. pseudomallei* which specifically reacted with melioidosis serum (Visutthi *et al.*, 2008; Erskine *et al.*, 2006), contains antibodies to Bip D. In this work Bip D protein, isolated from *B. pseudomallei* DNA (Visutthi *et al.*, 2008), was used as biological recognition element

to detect the presence of *B. pseudomallei* antibodies in serum obtained from melioidosis patients in a flow-injection capacitive immunosensor. Capacitance measurement was employed for the analysis of *B. pseudomallei* antibodies in both melioidosis (positive sample) and non-melioidosis patient's serums (negative sample).

8.2 Experimental

8.2.1 Materials

Bip D protein was provided by Dr. Wiliwan Chotigeat from Center for Genomics and Bioinformatics Research, Faculty of Science, Prince of Songkla University, Hat Yai, Songkhla, Thailand. 11- mercaptoundecanoic acid were obtained from Aldrich (MO, USA), N-(3-Dimethylaminopropyl)-N-ethylcarbodiimide hydrochloride (EDC), N-Hydroxysuccinimide (NHS) from Aldrich (Steinheim, Germany) and 1-dodeccanethiol ethanolic acid from Aldrich (Milwaukee, USA). All other chemicals used were of analytical grade. All buffers were prepared with distilled water treated with a reverse osmosis-deionized system. Before used, the buffers were filtered through an Albet® nylon membrane filter (Albet, Spain), pore size 0.20 μm, with subsequent degassing.

8.2.2 Serum samples

Serum samples were obtained from Songklanakarind Hospital. Melioidosis serum samples were obtained from patients who had been confirmed positive for *B. pseudomallei* by culture method. Pooled positive serum sample was the mixture of twenty serum samples of melioidosis patients. It was used to study optimization and performance of capacitive system. Pooled negative serum sample was the mixture of twenty healthy blood donors serum. It was used for control experiment. Positive serum sample is melioidosis patient's serum sample. Negative serum sample is healthy blood donor serum. Control serum sample is serum from hospitalized patient's with other bacterial infections. The positive, negative and control serum samples were used to evaluate performance of capacitive system.

8.3 Method

8.3.1 Immobilization of Bip D protein

The steps for cleaning gold rod electrode surface and the condition used for immobilization of Bip D protein on electrode surface followed the process as described in chapter 7. Cleaned electrode surface was incubated in 250 µl of 150 mM 11- mercaptoundecanoic acid solution for 15 min. Then this surface was activated with 400 µl 0.2 M EDC/ 0.05 M NHS for 50 min to introduce ester groups that can covalently bind to Bip D protein. Next, 20 µl of 150 µg ml^{-1} Bip D protein was placed on the modified electrode and reaction took place at 4° C for 24 h. Finally, the surface was blocked with 1,000 µl of 10 mM of 1-dodeccanethiol ethanolic acid for 20 min. The electrochemical behavior of each immobilization step was studied by cyclic voltammetry (Eco Chemie µ-autolab B.V., Netherland, and software package GPES 4.7) in 5 mM $K_3[Fe(CN)_6]$ and 0.1 M KCl, at scan rate of 0.1 V s^{-1}. The modified electrode was used as working electrode in a capacitive system.

8.3.2 Capacitance measurement

The experimental set-up of a flow injection capacitive immunosensor is described in section 7.3.3.2 (Figure 7.2). When *B. pseudomallei* antibody was injected into the flow cell it bound to Bip D causing the increase of dielectric layer thickness and/or the change of dielectric behavior resulting in the decrease of total capacitance.

8.3.3 Optimization of capacitive immunosensor

Parameters affecting the capacitive response were studied including regeneration solution (type, pH and concentration) and running buffer (pH and concentration). The parameters were optimized one by one comparing response obtained after injection of pooled positive serum sample, three replications for each test value at a flow rate of 50 µl min^{-1}, 10 mM of Tris-HCl buffer solution, pH 7.20 and a sample volume of 200 µl (Limbut *et al.*, 2006a,b). Pooled positive serum

sample was diluted 10,000 times with 10 mM of Tris-HCl buffer pH 7.20. This dilution factor was obtained from preliminary experiment by injection pooled positive serum and pooled negative serum sample at different dilutions factor. At 10,000 times of dilution factor the signal of pooled positive serum and pooled negative sample can still be separated. Therefore, this dilution factor was preliminary used to study optimization of system. After optimum conditions were obtained the dilution factor was studied again (section 8.3.6). The optimum of each parameter was evaluated by balancing between the capacitance change and analysis time.

8.3.4 Reuse of modified electrode

The reuse of modified electrode experiment was evaluated from the response to pooled positive serum sample at a flow rate of 50 µl min^{-1}, 15 mM of Tris-HCl buffer solution, pH 7.40 and a sample volume of 200 µl. The experiment was done by injection of pooled positive serum sample with subsequent regeneration solution (25 mM NaOH) to remove the binding of *B. pseudomallei* antibody form Bip D immobilized on surface of gold electrode.

8.3.5 Dilution factor

Serum dilution is an important factor affecting the screening results in immunoassay. Since serum samples have shown very strong non-specific binding due to the interfering serum components, diluting serum samples can reduce the background, but also cause a decrease in the sensitivity due to the lower *B. pseudomallei* antibodies concentration. Therefore, the effect of dilution factor of pooled positive serum sample and pooled negative serum sample was studied from 10,000 to 13,000 times under optimum conditions.

8.3.6 Individual serum sample analysis

Individual serum sample including 15 of positive samples, 15 of negative serum samples and 15 of control serum samples were investigated to evaluate the performance of capacitive immunosensor.

8.4 Results and discussion

8.4.1 Immobilization of Bip D protein

The immobilization of Bip D protein process were monitored with cyclic voltammetry using a permeable redox couple (*i.e.* $K_3[Fe(CN)_6]$) in the electrolyte solution as shown in Figure 8.1. At the clean gold surface the redox couple was oxidized and reduced in curve a. The redox peaks decreased when the surface of electrode was self-assemble of 11- mercaptoundecanoic acid in curve b. Then redox peaks further decreased due to Bip D protein was immobilized covalently on monolayer electrode in curve c. Next, the surface was then treated with ethanolamine hydrochloride then redox peak decreased in curve d. A final capping of the electrode surface was achieved by the treatment with 1-dodecanethiol, as can be seen from the disappearance of the redox peaks in curve e.

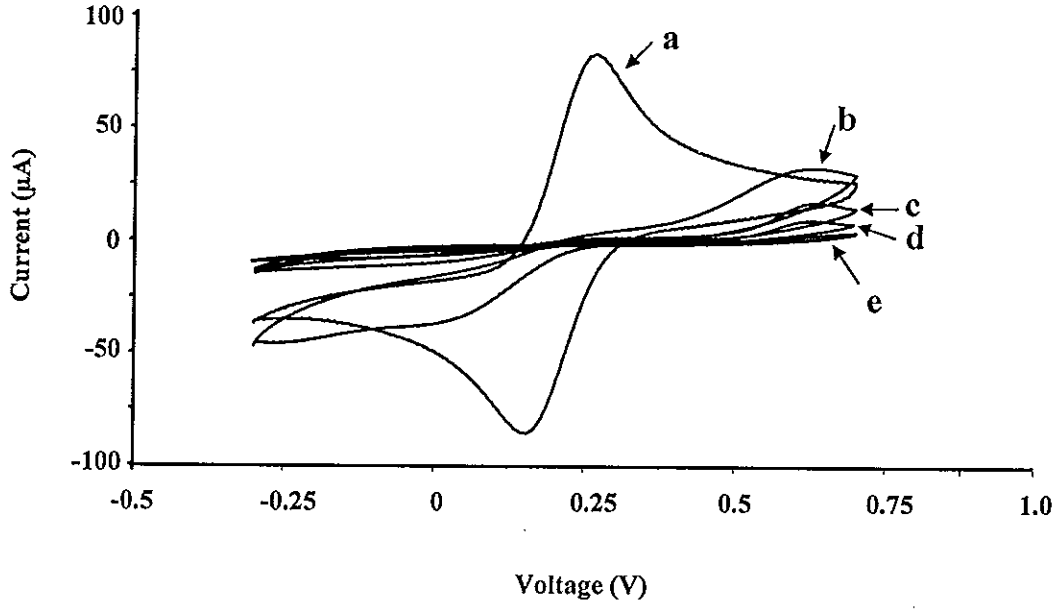

Figure 8.1 Cyclic voltammograms of a gold electrode obtained in a 5 mM $K_3[Fe(CN)_6]$ containing 0.1 M KCl solution at scan rate of 0.1 V s^{-1}. All potentials are given *vs* Ag/AgCl reference electrode. (a) bare gold electrode, (b) self-assembled of 11- mercaptoundecanoic acid monolayer covered electrode surface, (c) Bip D protein immobilized via activated monolayer electrode, (d) ethanolamine hydrochloride, and (e) 1-dodecanethiol treatment.

8.4.2 Capacitance measurement

When *B. pseudomallei* antibody was injected into the system, it bound to the immobilized Bip D protein on the electrode surface caused the increase of dielectric layer thickness and/or the change of dielectric behavior resulting in the decrease of total capacitance. The total capacitance was calculated followed the procedures described in chapter 4 (section 4.2.2.1.2). The capacitance obtained from a current response was plotted as a function of time as shown in Figure 8.2. The time required for the signal to reach a steady state was 20 min. The capacitance response was measured by detecting the change in capacitance before and after Bip D protein - *B. pseudomallei* antibody interaction (ΔC).

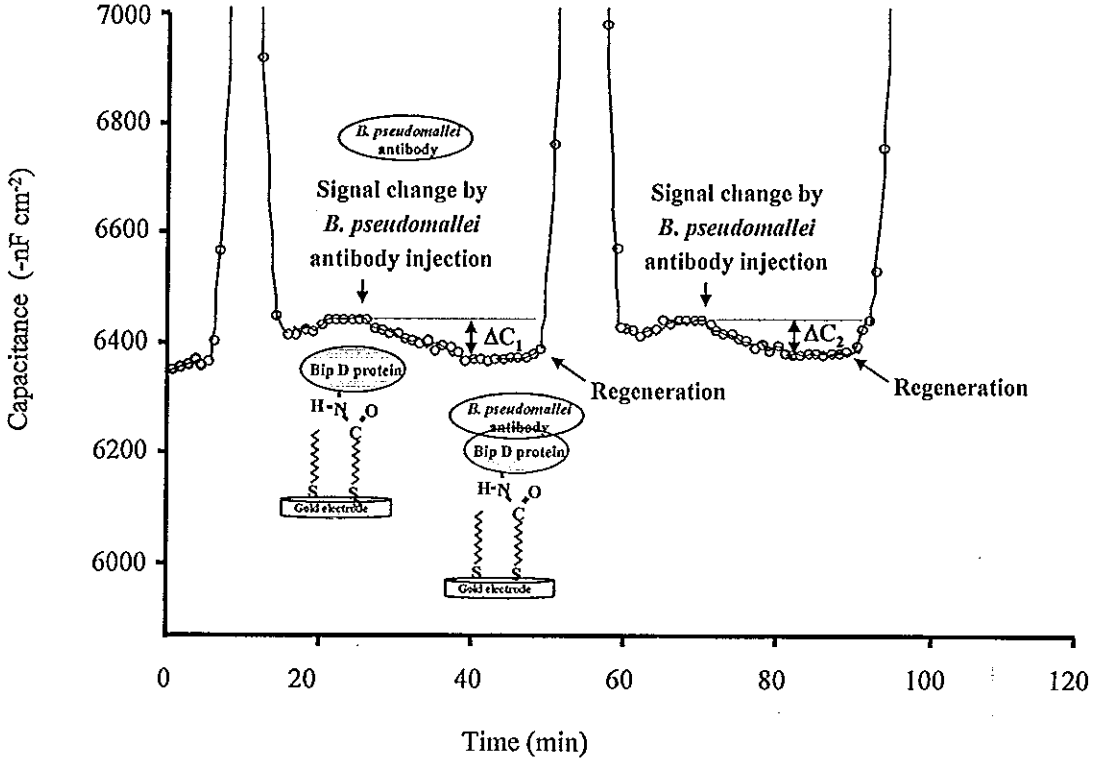

Figure 8.2 The decrease in capacitance (ΔC) resulting from the binding between Bip D protein - *B. pseudomallei* antibody with subsequent signal increase due to dissociation under regeneration conditions.

8.4.3 Optimization of capacitive immunosensor

8.4.3.1 Regeneration solution

Regeneration solution is a key factor for immunosensor response which to break the bounding between Bip D protein and *B. pseudomallei* antibody. The dissociating agent must be make for efficiently dissociating the Bip D protein - *B. pseudomallei* antibody complex without affecting activity of immobilized *B. pseudomallei* antibody on electrode surface. Thus, type and concentration of regeneration solution were optimized. The efficiency of regeneration solution was determined by residual activity, as described in chapter 7 (section 7.4.3.1), from the change in capacitance by the binding between pooled positive serum sample (*B. pseudomallei* antibody) and Bip D protein before (ΔC_1) and after regeneration (ΔC_2) by injection 200 µl of regeneration solution with flow rate of 50 µl min^{-1} (Figure 8.2).

Different types of regeneration solution were studied, i.e. acidic (glycine-HCl buffer, HCl), basic (NaOH) and salt ($MgCl_2$). The results are shown in Table 8.1, 25 mM NaOH provided the highest percentage of residual activity more than 90 %, so NaOH was further optimized to find the optimum concentration. The result showed that 25 mM provided the highest percentage of residual activity. Therefore, 25 mM NaOH was used as regeneration solution.

Table 8.1 Tested and optimum conditions of type and concentration of regeneration solution.

Parameter of regeneration solution	Tested	% Average residual activity	Regeneration time (min)
Type	50 mM glycine-HCl pH2.50	70 ± 7	15
	HCl pH 2.50	85 ± 4	17
	50 mM NaOH	91 ± 2	16
	1 M NaCl	89 ± 4	40
Concentration of NaOH	10 mM	59 ± 10	12
	25 mM	95 ± 4	15
	50 mM	90 ± 6	16
	75 mM	86 ± 2	20

*Regeneration time obtained from the time that required for the signal start changing after injection of regeneration solution to reach a steady state.

8.4.3.2 Buffer solution

8.4.3.2.1 Concentration

Buffer concentrations from 5 to 25 mM of Tris-HCl pH 7.00 were studied by injection of pool positive sample at 10,000 dilution factor. The maximum capacitance change obtained from 15 mM buffer concentration (Figure 8.3). Therefore, concentration 15 mM of running buffer was chosen for further experiment.

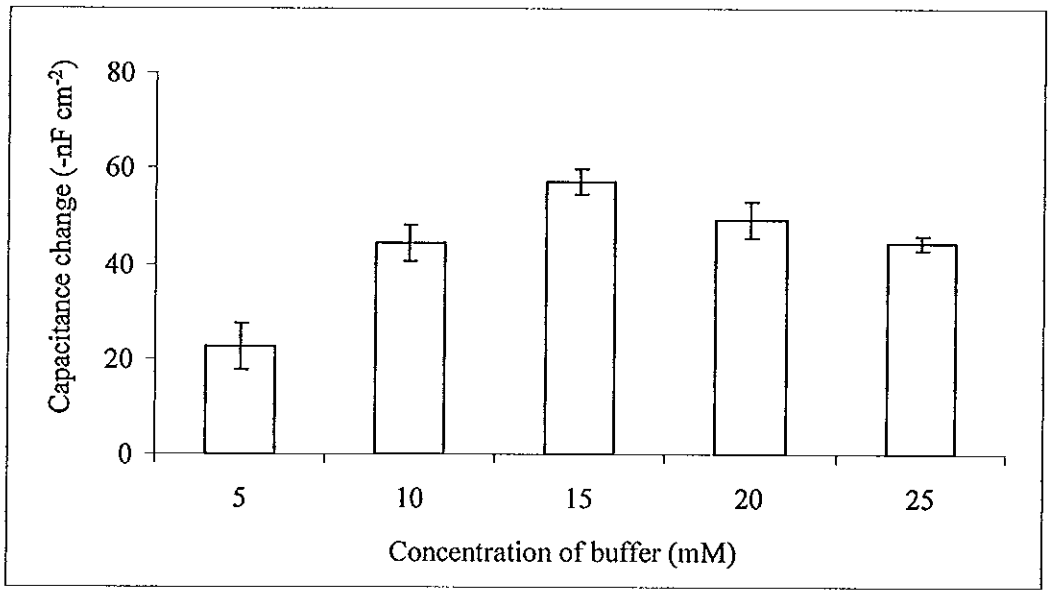

Figure 8.3 Response of capacitive immunosensor to pool positive sample (10,000 dilution factor) at different concentration of Tris-HCl pH 7.00.

8.4.3.2.2 pH

The influence of pH of 15 mM Tris-HCl buffer from 6.50-8.50 was studied. Figure 8.4a shows that the maximal capacitance change was found at 7.50. Therefore, pH ranging from 7.00 – 8.00 was further studied. The result showed that the highest response was pH 7.40 (Figure 8.4b). Since, the piezoelectric point (pI) of Bip D protein is 5.15 and pI of antibody (IgG) is 6.40-9.00 (Li *et al.*, 2002). At pH 7.40 Bip D protein had negative charge and *B. pseudomallei* antibody had positive charge and this help with the binding. Thus, 15 mM Tris-HCl pH 7.40 was selected for running buffer.

The optimum conditions of capacitive immunosensor are summarized in Table 8.2.

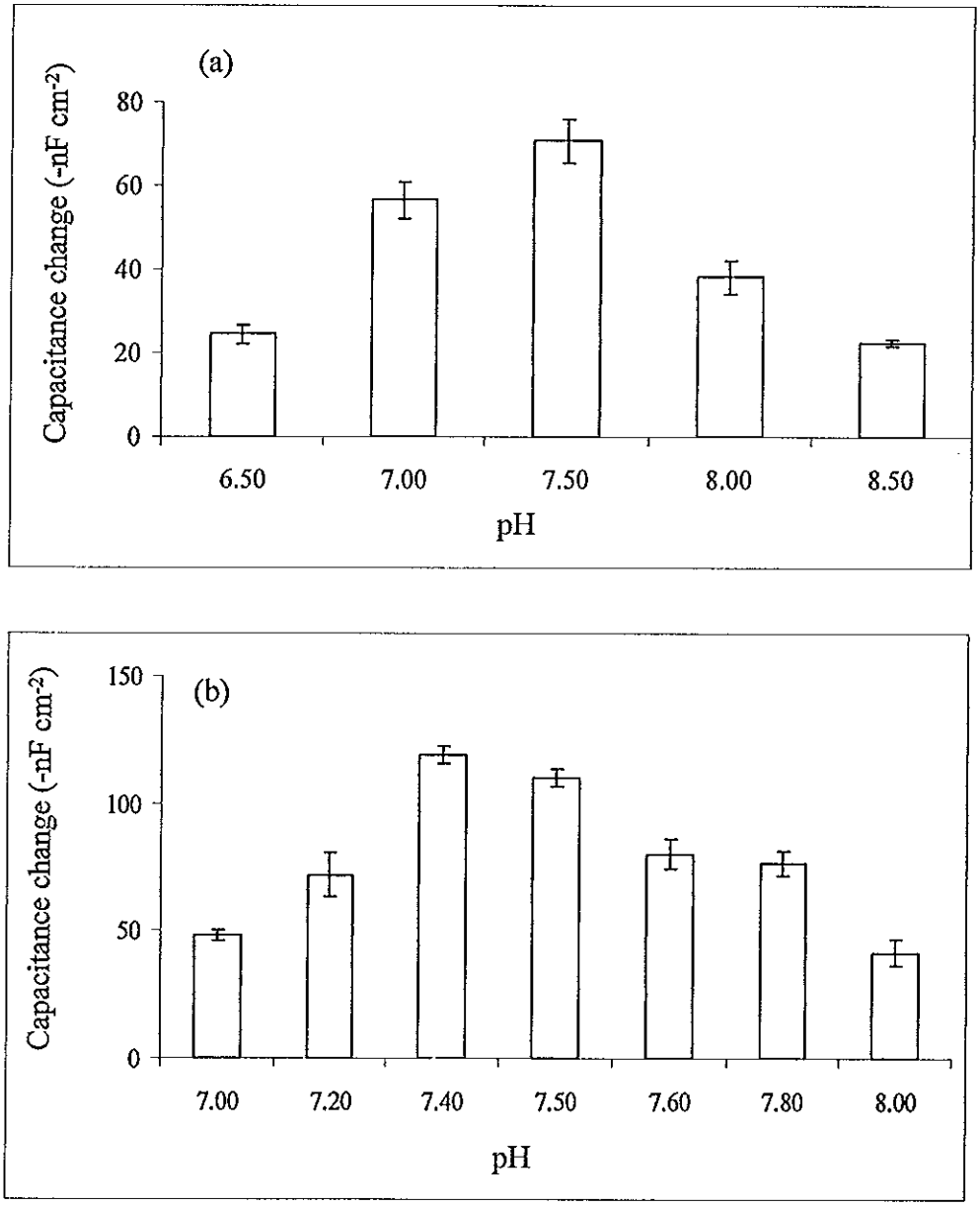

Figure 8.4 Effect of pH of 15 mM Tris-HCl buffer on response to pool positive sample (10,000 dilution factor).

Table 8.2 Tested and optimized values of the capacitive immunosensor system. Capacitance change obtained from the injection of to pool positive sample at 10,000 of dilution factor with 200 µl of sample volume and 50 µl min^{-1}.

Parameter of running buffer	Tested	Capacitance change ($-nF\ cm^{-2}$)	Analysis time* (min)	Optimum
Concentration of Tris-HCl pH 7.00 (mM)	5	23 ± 5	12	15
	10	44 ± 4	13	
	15	57 ± 3	15	
	20	49 ± 4	17	
	25	44 ± 2	29	
pH of 15 mM Tris-HCl (ranging from 6.50-8.50)	6.50	25 ± 2	15	7.50
	7.00	57 ± 5	15	
	7.50	71 ± 5	15	
	8.00	38 ± 4	15	
	8.50	23 ± 1	15	
pH of 15 mM Tris-HCl (ranging from 7.00-8.00)	7.00	48 ± 2	15	7.40
	7.20	72 ± 5	15	
	7.40	119 ± 4	15	
	7.50	110 ± 3	15	
	7.60	80 ± 6	15	
	7.80	76 ± 5	15	
	8.00	41 ± 5	15	

*Analysis time obtained from the time that required for the signal start changing after injection of pool positive sample to reach a steady state.

8.4.3.3 Dilution factor

Pooled positive and negative serum samples were diluted from 10,000 to 13,000 times with running buffer. High dilution factor of serum samples can reduce the matrix effect and also reduce sample volume. However, it causes a decrease of signal due to the low *B. pseudomallei* antibodies concentration. The results are shown in Figure 8.5. The signal increased as the dilution factor decreased. When the signals at 11,000 and 10,000 dilution times were compared, the 11,000 times provided 7 % less signal than the 10,000 times. However, at 11,000 times the signal between positive and negative can still be easily distinguished and lesser sample is required. Therefore, dilution factor of 11,000 times was selected.

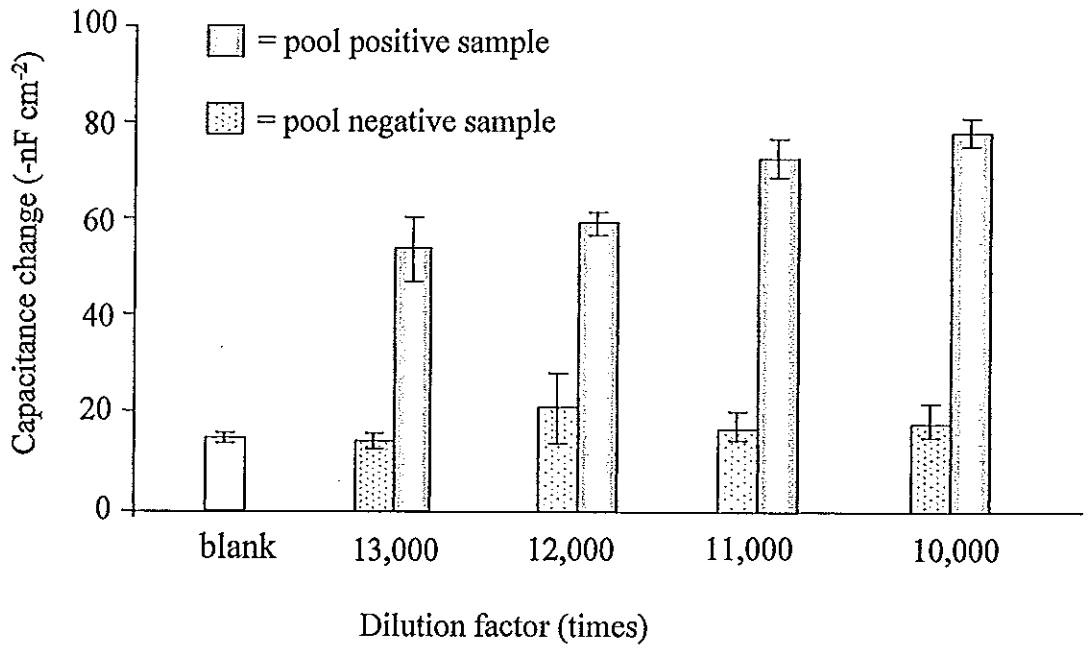

Figure 8.5 Effect of dilution factor on capacitance change to pool negative and pool positive serum sample.

8.4.3.4 Reuse of modified electrode

The reuse of electrode was studied at optimum conditions by continuously detecting the change of the capacitance at 11,000 times of dilution factor of pool

positive sample with subsequent regeneration by 25 mM NaOH to remove *B. pseudomallei* antibody from Bip D protein immobilized on the electrode. Figure 8.6 shows the percentage of capacitance change versus the cycles of regeneration. It maintained about 94% of the original capacitance change signal (28 times of regeneration) with an average of 94 ± 2 % after which the response declined more rapidly. That is, the modified electrode can be regenerated with good reusable for up to 28 times. The cyclic voltamogram of the modified electrode after the decrease of activity was tested and found to be similar to the one before the electrode was used. It indicated that self-assemble monolayer remained. Therefore, the decreasing of response may be caused by the loss of activity of Bip D protein because the self-assemble monolayer was not destroyed by regeneration solution.

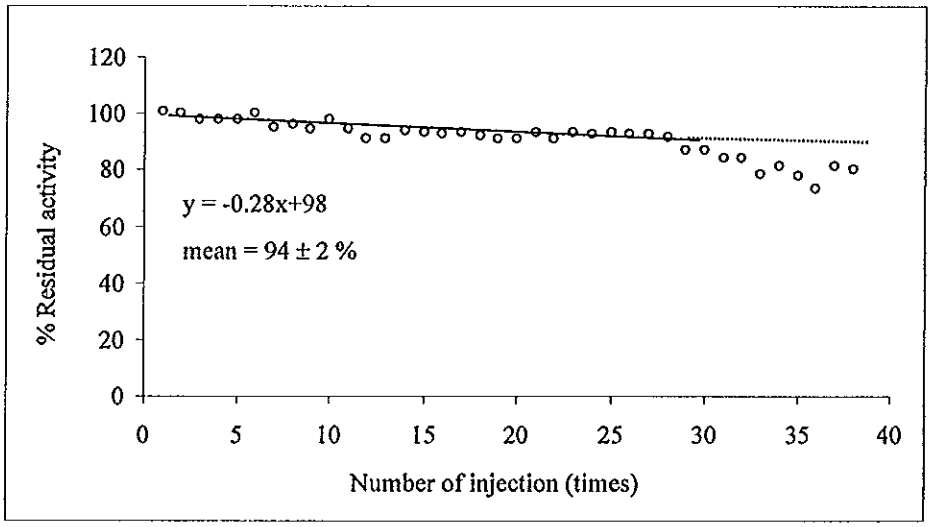

Figure 8.6 The reuse of the Bip D protein modified on electrode.

8.4.3.5 Individual real samples detection

Under optimum conditions of capacitive immunosensor system, fifteen samples of positive, negative and control serum were analyzed. All serum samples were diluted 11,000 times with 15 mM Tris-HCl pH 7.40 and 200 µl was injected into the flow-injection capacitive immunosensor system with a flow rate of 50 µl min^{-1}. Regeneration was carrier out by 200 µl of 25 mM NaOH to remove *B. pseudomallei* antibody from Bip D protein immobilized on the electrode. The performance of the

system was considered from differences between the signals of positive, negative and control serum samples. High performance system should provide significantly increasing of signal obtained from positive compared to negative and control serum sample. Figure 8.7 shows capacitance response obtained from control (number of 1-15), negative (number of 16-30) and positive (number of 30-45) serum samples. The result found that this capacitive system could separate between negative and positive serum sample at 32 –nF cm^{-2} of signal cut-off. This cut-off was taken as the mean of the maximum signal of negative or control serum samples plus two standard deviations (in this case it obtained from sample 2 signal = mean ± 2(SD) = 28 ± 2(2) – nF cm^{-2}) (Vuren and Paweska, 2009; Nagel *et al.*, 2008). This cut-off value can be used to identify the serum sample. If the obtained signal is higher than the cut-off it will be positive sample and if lower than the cut-off it will be negative sample. From these results, serum sample that provided signal higher than 32 –nF cm^{-2} was indicated as positive.

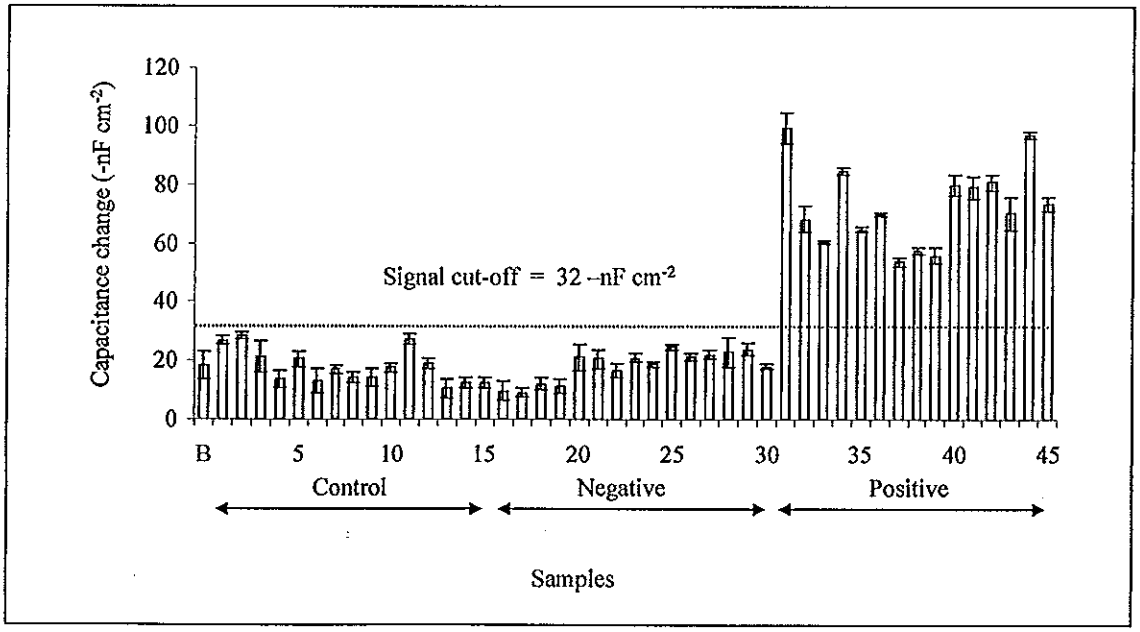

Figure 8.7 Capacitance response obtained from the analysis of blank (running buffer; B), control (number of 1-15), negative (number of 16-30) and positive (number of 30-45) serum samples.

Additionally, all results were statistically tested with Mann-Whitney Rank-Sum Test (Zar, 1983). In this test, the null hypothesis (there is no difference between the two samples) is rejected at a significance level ($\alpha < 0.05$) if the experimental value is higher than or equal to the critical values. First, the signals obtained from negative samples and control samples were compared. Table 8.3 showed that the null hypothesis is retained. There is no evidence differences between signals obtained from negative serum samples and control serum samples ($\alpha < 0.05$).

Table 8.3 The Mann-Whitney Rank-Sum Test the signal obtained from negative serum sample and control serum sample.

Sample	Capacitance signal (-nF cm^{-2})			
	Negative samples	Control samples	Rank of negative samples (R_1)	Rank of control samples (R_2)
1	10	27	2.5	28.5
2	9	28	1	30
3	12	21	6	21
4	11	14	4	10
5	21	20	21	18
6	21	13	21	8
7	16	17	12	13
8	21	14	21	10
9	19	14	16.5	10
10	25	18	27	14.5
11	21	27	21	28.5
12	22	19	24	16.5
13	23	10	25	2.5
14	24	12	26	6
15	18	12	14.5	6
	$n_1 = 15$	$n_2 = 15$	$\sum R_1 = 242.5$	$\sum R_2 = 222.5$
$^*U = n_1n_2 + [n_2(n_2+1)]/2 - R_2$				**122.5**
Critical values of Mann-Whitney at α=0.05, $n_1 = 15$ $n_2 = 15$				**161**

*U was calculated from small data that presented fewer sums of ranking samples.

Then the signals obtained from positive serum samples were compared with negative serum samples and the results are shown in Table 8.4. The null hypothesis is rejected, that is there is significant difference between positive serum samples and negative serum samples ($\alpha < 0.05$). From this statistic test and the signal obtains it

clearly shown that the signals of positive serum samples are significantly higher than the negative and control serum samples ($\alpha < 0.05$). Thus, this capacitive-based immunosensor would be efficiently employed as an alternative clinical method to determine *B. pseudomallei* antibody in serum samples.

Table 8.4 The Mann-Whitney Rank-Sum Test the signal obtained from negative serum sample positive serum sample.

Sample	Capacitance signal (-nF cm^{-2})			
	Negative samples	Positive samples	Rank of negative samples (R_1)	Rank of control samples (R_2)
1	10	99	2	30
2	9	68	1	21
3	12	60	4	19
4	11	85	3	28
5	21	65	9.5	20
6	21	70	9.5	22.5
7	16	54	5	16
8	21	57	9.5	18
9	19	56	7	17
10	25	80	15	26
11	21	79	9.5	25
12	22	81	12	27
13	23	70	13	22.5
14	24	97	14	29
15	18	73	6	24
	$n_1 = 15$	$n_2 = 15$	**$\sum R_1 = 120$**	$\sum R_2 = 345$
$^*U = n_1n_2 + [n_1(n_1+1)]/2 - R_1$				**225**
Critical values of Mann-Whitney at $\alpha=0.05$, $n_1 = 15$ $n_2 = 15$				**161**

*U was calculated from small data that presented fewer sums of ranking samples.

8.5 Conclusion

The developed flow- injection capacitive immunosensor system can be used to detect *B. pseudomallei* antibody in serum by immobilization of Bip D protein on the electrode. The performance of this system could separate between melioidosis and non-melioidosis patient serum sample with several advantages. First, the Bip D modified electrode has advantage in team of simple to prepare and one electrode could be reused up to 28 times (28 analysis) this helps to reduce the time and the cost of analysis compared to bacterial culture and immunological methods. This capacitive system also provided sensitive method to detect *B. pseudomallei* antibody because serum sample could be diluted up to 1:11,000 times higher than the immunoblotting method (1: 2,000 times) (Visutthi *et al.*, 2008). Finally, the main advantage of this method is rapid analysis for *B. pseudomallei* antibody. The results can be obtained more rapidly (15 min obtained result) than the bacterial culture assay (3-4 days obtained result) (Sirisinha *et al.*, 2000). Thus, this developed system can be use as an alternative analytical method for *B. pseudomallei* antibody analysis.

CHAPTER 9

Sensitivity Enhancement of Label –Free Surface Plasmon Resonance and Capacitive Immunosensors using Gold Nanoparticles

9.1 Introduction

High sensitive analytical method to detect low concentration analyte is now a necessity in several fields. For example, in clinical analysis the detection of tumor markers that exist in blood at trace levels can be used to indicate cancer (Wu *et al.* 2007a). Other areas that can also benefit from this type of high performance analytical methods are environmental (Kawazumi *et al.*, 2005; Soh *et al.*, 2003), and food safety (Hohensinner *et al.*, 2007; Xiulan *et al.*, 2006). One such method that can fulfill this role is immunosensor since it can provide rapid, specific, and sensitive analysis (Luppa *et al.*, 2001; Ricci *et al.*, 2007). Label-free immunosensor is particularly useful. Since it is simple to use, provides rapid analysis, and is low cost (Jiang *et al.*, 2008; Ramakrishnan and Sadana, 2002). However, in some cases the sensitivity of a label-free immunosensor may be insufficient to obtain good signal from a sample with low analyte concentration. Therefore, sensitivity enhancement methods are very important for label-free immunosensors.

Gold nanoparticles (AuNPs) with their unique properties, i.e. large surface-to-volume ratio, high catalytic efficiency, and strong adsorption ability of protein (Ren *et al.*, 2005) have played a significant role for the enhancement of sensitivity in biosensor technique. Biomolecule can adsorb on AuNPs surface by three basic phenomena: (a) charge attraction of the negatively charged particle to the positively charged protein domains, (b) hydrophobic interaction between particle and protein, and finally (c) self-assembled binding between sulphur and noble metal (Seydack, 2005). AuNPs have been incorporated for the detection of a number of molecules such as murine antibody (Huang *et al.*, 2006), hepatitis B virus surface antigen (Wang *et al.*, 2004), transferrin (Liu *et al.*, 2006), *Salmonella typhimurium* (Ko *et al.*, 2009) and trinitrotoluene (Kawaguchi *et al.*, 2008). They provide a better detection limit and

sensitivity because of the enhancement of the amount of immobilized biomolecules on the transducer surface.

In chapter 7, label-free surface plasmon resonance (SPR) and capacitive immunosensors were studied for direct detection of CA 125 by immobilization of antiobody directly on self-assemble monolayer (SAM), without using nanomaterial for sensitivity enhancement. In this work we are interested in the use of AuNPs for antibody immobilization and to see whether AuNPs can improve the sensitivity of SPR and capacitive immunosensors. SAM and polymer film were used to immobilize AuNPs to study whether AuNPs can be incorporated with different types of layer and can enhance their detection. For SPR system, AuNPs were incorporated on sensor surface via SAM because it can be easily formed. However, with the current set-up polymer film cannot be applied for the SPR system because this layer is achieved by electropolymerization which cannot be done with the SPR equipment. Therefore, polymer film was applied to immobilize AuNPs on gold electrode for the capacitive system since the electrode was modified outside the flow system and could be placed into an electrochemical cell for polymerization steps. Optimum amount of AuNPs was investigated. Cancer antigen 125 (M.W. = 200 kDa), human serum albumin (M.W. = 66 kDa), microcystin-LR (M.W = 995) and penicillin G (M.W. = 372) were tested to see the affect of molecular weight.

9.2 Experimental

9.2.1 Materials

Monoclonal anti-cancer antigen 125 (anti-CA 125) and cancer antigen (CA 125) from human were obtained from US biological (USA), monoclonal anti-microcystin-LR (anti-MCLR) and microcystin-LR (MCLR) from Alexis Biochemicals (Lausen, Switzerland), monoclonal anti-penicillinG (anti-Pen G) and penicillin G (Pen G) from US Biological (USA), and polyclonal anti-human serum albumin (Anti-HSA) and human serum albumin (HSA) from Dako, (Denmark). Chlorauric acid ($HAuCl_4$) solution and 1-dodeccanethiol ethanolic acid from Aldrich (Milwaukee, USA), sodium borohydride ($NaBH_4$) from Fluka Chemie AG (Buchs, Switzerland), trisodium citrate from Univar (Australia), glutaraldehyde 25% from

Fluka (USA), *para*-phenylenediamine from Sigma (USA), cysteamine from Fluka (Switzerland), ethanolamine from Merck (Darmstadt, Germany) and bovine serum albumin (BSA) from Fluka (Steinheim, Germany). All other chemicals used were of analytical grade. All buffers were prepared with water treated with a reverse osmosis-deionized system. Before used, the buffers were filtered through an Albet® nylon membrane filter (Albet, Spain), pore size 0.20 μm, with subsequent degassing.

9.2.2 Preparation of AuNPs

Glassware was cleaned by soaking in freshly prepared 10% HNO_3 (v/v) overnight and thoroughly rinsed with distilled water. AuNPs were prepared according to the literature with a little modification (Wang *et al.*, 2004). Briefly, five hundred milliliters of aqueous solution containing 0.25 mM $HAuCl_4$ solution and 0.38 mM trisodium citrate were prepared. Next, 1.0 ml of 0.125 M $NaBH_4$ solution was added into the gold solution under continuous stirring. Aqueous solution was then mixed and stirred vigorously overnight. The obtained AuNPs solution was then stored in a dark glass bottle at 4 °C for further use. The resulting solution of AuNPs was characterized with UV-vis spectrophotometer (U-1900, HITACHI, Japan) and transmission electron microscopy (TEM, JEM-2010. JEOL).

9.2.3 SPR immunosensor immobilization

The steps for gold disk cleaning followed the process described in chapter 7 (section 7.3.2.1). Cysteamine was used as SAM for immobilization on gold disk surface because it has amine group that AuNPs can be adsorbed on their amine group and also because of its short alkanethiol chain ($SHCH_2CH_2NH_2$). When AuNPs were immobilized on cyteamine monolayer the distance between gold surface and AuNPs would be less than using long alkanethiol. This helps making the layer to be within the evanescence wave and many works have used cysteamine incorporated with AuNPs (Ko *et al.*, 2009; Fu *et al.* 2007; Chah *et al.*, 2001).

Cysteamine-modified gold disk was prepared as shown in Figure 9.1, 250 μl of 1.0 mM cysteamine in ethanol solution was incubated on clean gold disk for 5 h to

form cysteamine monolayer (modified from Furuki *et al.*, 2001). Antibody immobilization steps followed these described by Limbut *et al.* (2006a,b) after rinsing with 1,000 µl of ethanol and 1,000 µl of distilled water to remove non-chemisorbed species. Amine groups of monolayer were activated with 5% (v/v) glutaraldehyde in 10 mM sodium phosphate buffer pH 7.00 for 20 min, thoroughly rinse the surface of modified gold disk with 1,000 µl of distilled water. Subsequently, 100 µl of antibody (500 µg ml^{-1} of anti-HSA (Sakai *et al.*, 1997), 20 µg ml^{-1} of MCLR (Loyprasert *et al.*, 2005) or 30 µg ml^{-1} of anti-CA 125 (He *et al.*, 2003) was incubated on the modified surface for 2 h. After 2 h the surface was rinsed with 1,000 µl of 15 mM phosphate buffer containing 150 mM NaCl pH 7.20. Any remaining groups were deactivated with 250 µl of 0.1 M ethanolamine pH 8.50 for 7 min. Finally, any pinholes were blocked with 250 µl of 1% (w/v) BSA for 1 h.

Cysteamine-modified gold disk incorporating AuNPs was prepared following the process shown in Figure 9.2 which was modified from the work of Gu *et al.* (2001). After the forming of cysteamine self-assembled monolayer the surface was incubated with AuNPs solution in darkness for 4 h. Subsequently, antibody (same concentration as without AuNPs immobilization) was placed on the modified surface for 2 h. In such a way, antibody–AuNPs–cysteamine-modified gold disk was obtained. Any remaining groups were deactivated and the surface was blocked as previously described.

Each immobilization step was monitored by SPR signal (AutoLab Spirit®, Eco Chemie B.V., Netherlands).

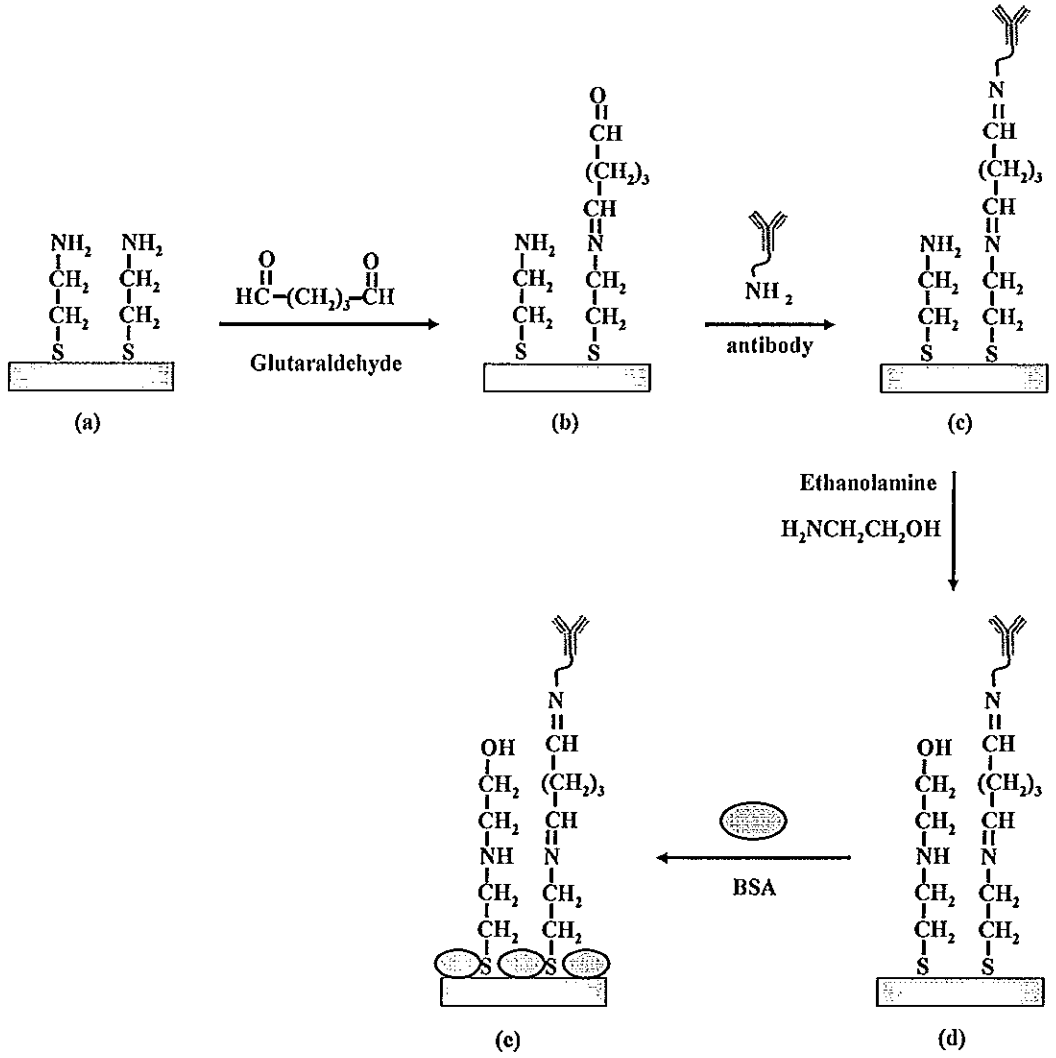

Figure 9.1 Schematic illustration for antibody immobilized covalently on a self-assemble cysteamine modified gold disk. (a) gold disk was modified with cysteamine, (b) amino groups of cysteamine are activated by glutaraldehyde, (c) covalent binding between aldehyde groups of the activated self-assemble monolayer and free amino groups of antibody, (d) remaining amine group deactived by ethanolamine and (e) block any pinholes on gold disk surface with BSA.

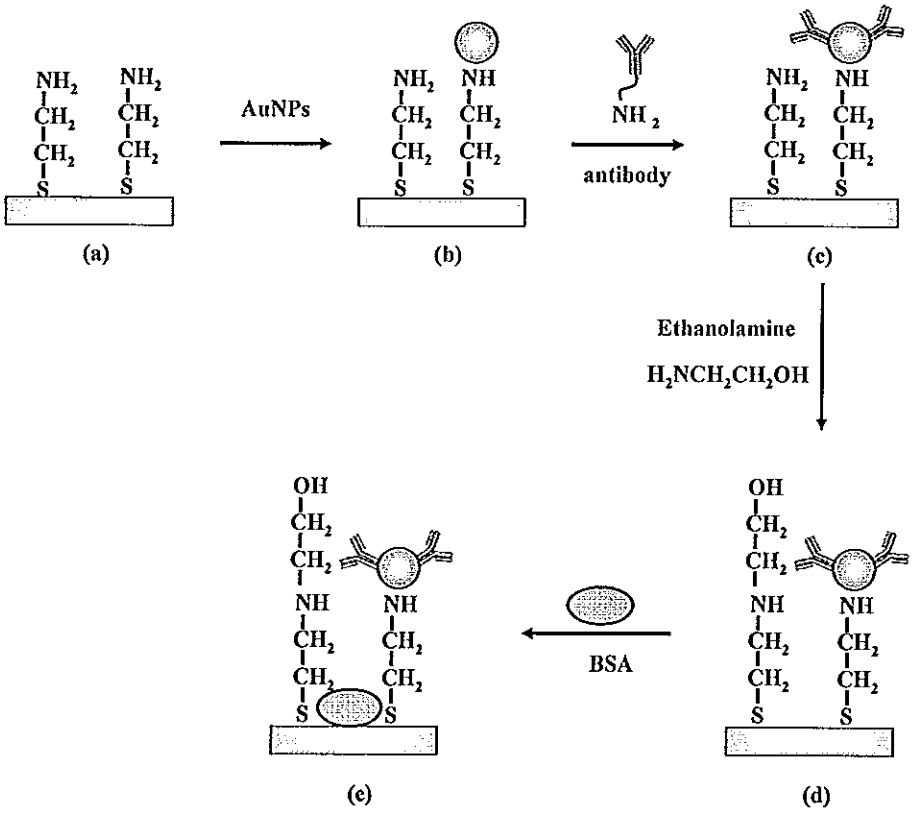

Figure 9.2 Schematic illustration for antibody immobilized onto gold disk via AuNPs. (a) gold disk was modified with cysteamine, (b) AuNPs were adsorbed on amino groups of cysteamine monolayer, (c) antibody was incubated on AuNPs surface, (d) modified surface were blocked with ethanolamine and (d) any pinholes were further block with BSA.

9.2.4 Capacitive immunosensor immobilization

Immobilization of antibody was modified from the work of Karalemus *et al.* (2000), Cheng *et al.* (2001) and Limbut *et al.* (2006a,b). *p*-phenylenediamine (*p*-PD) (Figure 9.3a) was used as monomer. Polymer-modified gold electrode was prepared following the process as shown in Figure 9.4. A thin film of polymer was coated on cleaned gold electrode surface by electropolymerization. The electropolymerization of *p*-phenylenediamine (*p*-PD) was performed in 20 ml of 5 mM *p*-PD in 10 mM acetate

solution (pH 5.18) with potential range from 0 to 0.8 V at a scan rate of 50 mV s^{-1} for 15 cycles by cyclic voltammetry. After electropolymerization of this polymer, poly (*p*-PD) chain as shown in Figure 9.3b and there are amine groups on the surface (Lakard *et al.*, 2003). These amine groups can be activated to immobilize antibody. Then this surface was activated with 1.0 ml of 5% (v/v) glutaraldehyde in 10 mM sodium phosphate buffer pH 7.00 at room temperature for 20 min to yield active aldehyde groups. It was rinsed with 10 ml of distilled water and then dried with nitrogen gas and finally, 20 µl of antibody (500 µg ml^{-1} of anti-HSA (Sakai *et al.*, 1997), 20 µg ml^{-1} of anti-MCLR (Loyprasert *et al.*, 2005), or 250 µg ml^{-1} of anti-Pen G (Thavarungkul *et al.*, 2007) was dropped on gold electrode surface and coupling reaction took place overnight at 4 °C. The electrodes were then washed with 10 ml of 10 mM phosphate buffer pH 7.00 to remove unbound antibody and then immersed in 1.0 ml of 0.1 M ethanolamine pH 8.50 for 7 min and washed with 10 ml of 10 mM phosphate buffer pH 7.00. Finally, this electrode was immersed in 1.0 ml of 10 mM 1-dodecanethiol ethanolic solution for 20 min to block any pinholes on the electrode surface.

Polymer-modified gold disk incorporating AuNPs was prepared by modification from the work of Silva *et al.* (2007) as shown in Figure 9.5. After the electrode was modified with polymer, it was immersed in AuNPs solution for 4 h at 4 °C in darkness and rinsed with 10 ml of distilled water. During this step AuNPs were adsorbed on the amine groups of the polymer layer. Afterward, 20 µl of antibody (the same concentration as without AuNPs) was dropped on the surface of AuNPs modified electrode and left overnight at 4 °C. Finally, this electrode was immersed in 1.0 ml of 10 mM 1-dodecanethiol ethanolic solution for 20 min.

The immobilization steps were monitored by cyclic voltammetry in 10 mM of $K_3[Fe(CN)_6$ solution. Electrochemical measurements were carried out using a potentiostat (Microautolab type III, Eco Chemie B.V., Netherlands) coupled to an electrochemical cell containing the modified working electrode, a custom made Ag/AgCl reference electrode and a platinum auxiliary electrode.

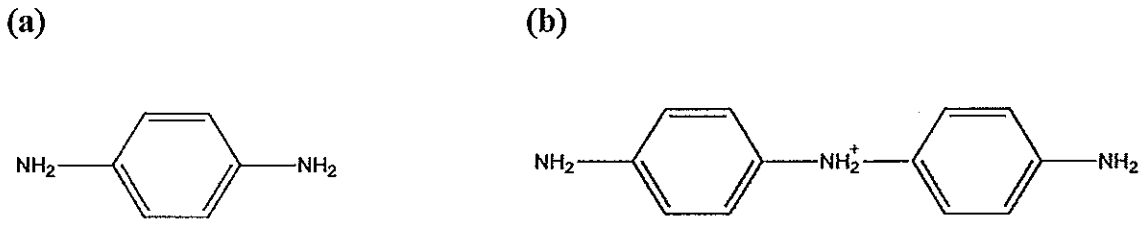

Figure 9.3 Structure of (a) *p*-phenylenediamine used as monomer and (b) after electropolymerization (Lakard *et al.*, 2003).

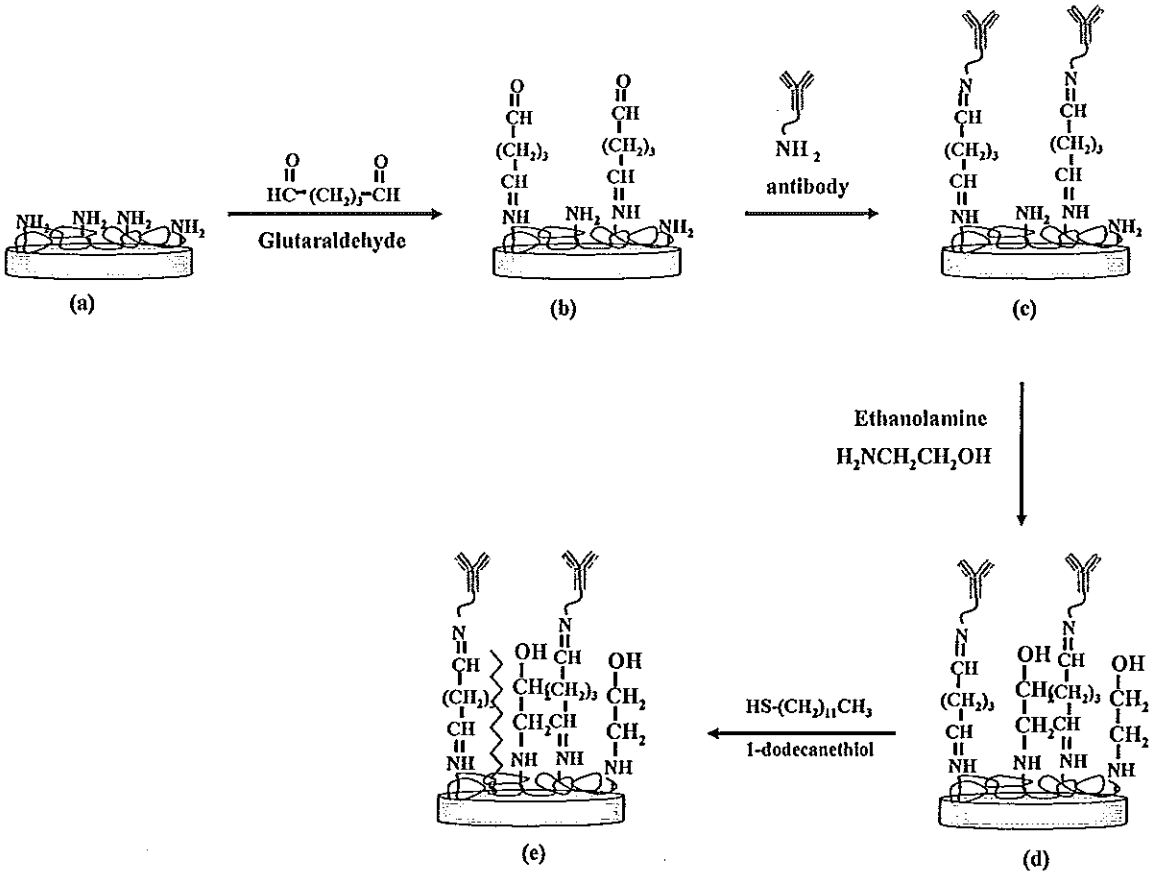

Figure 9.4 Schematic illustration of the immobilization of antibody onto gold electrode; (a) gold electrode covered with *p*-PD film, (b) glutaraldehyde was used to activate *p*-PD film, (c) glutaraldehyde-*p*-PD film was incubated in antibody (d) remaining amine groups were deactivated with ethanolamine and (e) 1-dodecanethiol was added to block.

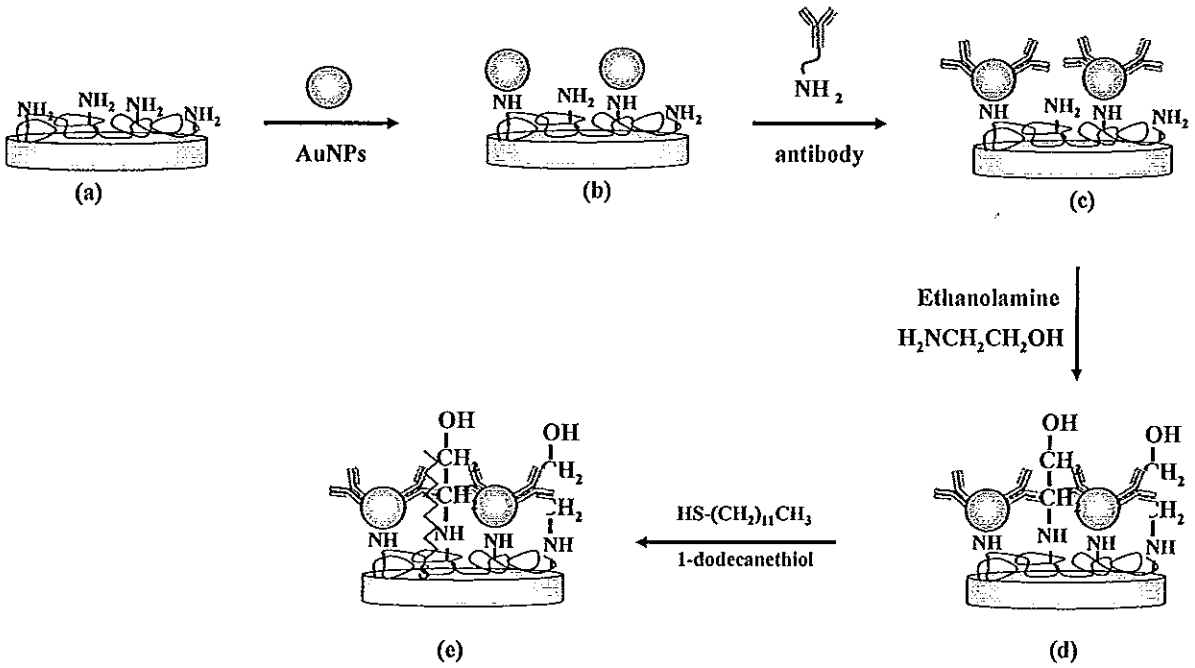

Figure 9.5 Schematic illustration of the immobilization of antibody onto gold electrode; (a) gold electrode covered with *p*-PD film (b) AuNPs was incubated on *p*-PD film (c) antibody was introduced to immobilize on polymer film and (d) antibody-AuNPs- *p*-PD film was blocked with ethanolamine and (e) with 1-dodecanethiol.

9.2.5 Flow-injection SPR system

The set-up of a flow-injection SPR immunosensor is described in section 7.3.2.2 (Figure 7.1). When antigen was injected into the flow cell it bound to immobilized antibody causing the increase of refractive index resulting in the increase of SPR angle.

9.2.6 Capacitive flow injection system

The flow injection capacitive immunosensor is described in section 7.3.3.2 (Figure 7.2). When antigen was injected into the flow cell it bound to immobilized antibody causing the increase of dielectric layer thickness and/or the change of dielectric behavior resulting in the decrease of total capacitance. The total capacitance was calculated as described in chapter 4 (section 4.2.2.1.2).

9.2.7 Optimization of amount of AuNPs immobilization for both SPR and capacitive immunosensors

The effect of amount of AuNPs that could be immobilized on the monolayer (SPR system) or polymer film (capacitive system) was studied. On one hand, dense AuNPs on amine groups of monolayer or polymer film can increase the signal due to more immobilized antibody. On the other hand, the number of amine groups on the monolayer or polymer film on the surface was limited and too much AuNPs cannot be immobilized. Optimization of the amount of AuNPs for both SPR and capacitive immunosensors followed the same procedure. The experiment was carried out using 2.0, 4.0, 6.0, 8.0, and 10.0 ml of AuNPs solution. Each of the AuNPs volume (except 2.0 ml) was centrifuged at 13,000 rpm for 30 min and the supernatant was removed until finally 2.0 ml of precipitation solution was obtained. That is, the AuNPs were concentrated by 2, 3, 4 and 5 times, respectively. The effect of the amount of AuNPs systems was studied by anti-HSA and HSA interaction. The calibration curves of standard HSA were studied from 10^{-8} to 10^{-5} for SPR and 10^{-16} to 10^{-10} M for capacitive system. Sensitivity (slope of calibration curve) obtained from the plot between SPR angle shift or capacitance change and concentrations of HSA for the five volumes of AuNPs (2.0, 4.0, 6.0, 8.0, 10.0 ml) were compared.

9.2.8 Surface coverage

Surface coverage was studied to determine the surface area of electrode by comparing the area of the reduction peak of electro-adsoption of oxygen atom on the AuNPs modified electrode and bare gold electrode (Sabatani *et al.*, 1987) (Figure 9.6). This experiment was carried out by cyclic votalmmetry technique in 100 mM phosphate buffer pH 7.40 with scan rate of 50 mV s^{-1}. The percentage of surface coverage was calculated by equation (9.1).

$$\% \text{ Surface coverage} = \frac{Q_{AuNPs} \times 100}{Q_{bare}} \qquad (9.1)$$

Where Q_{AuNPs} is the amount of electric charge exchanged during the electroadsorption of oxygen (coulombs cm^{-2}) of the modified AuNPs on gold electrode, and Q_{bare} is the amount of electric charge exchanged during the electroadsorption of oxygen (coulombs cm^{-2}) of the bare gold electrode.

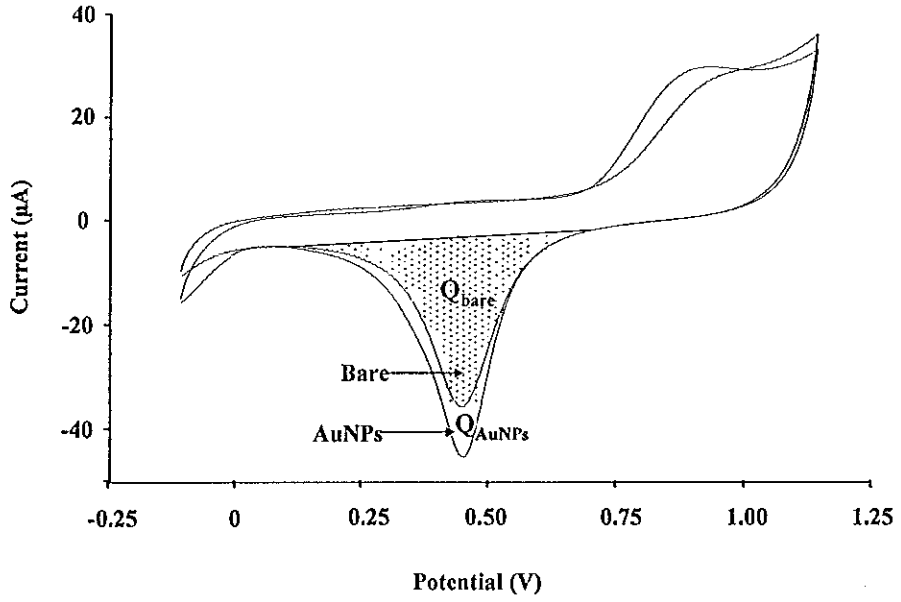

Figure 9.6 Cyclic votammograms of bare gold electrode and AuNPs modified electrode.

9.2.9 Immobilization yield

The amount of antibody was determined by silver binding method (Krystal, G., 1987; Krystal *et al.*, 1985; 1989). The quantity of antibody immobilized on electrode was determined by the difference between the concentration of the antibody in the solution before and after immobilization. In brief, 5.0 µl of sample was diluted to 50 µl with distilled water containing sodium dodecyl solfate (SDS) (0.2 % w/v) and Tween 20 (0.4 % w/v) to prevent passive adsorption of silver onto glass and plastic surfaces. Then this solution was diluted to 1.0 ml with distilled water. Next, 20 µl of 2.5% glutaraldehyde was added to each sample and then mixed with 200 µl of the ammoniacal silver solution. The reaction tubes were allowed to develop reaction at

room temperature for 10 min then stopped the color development by adding 40 µl of 30 mg l^{-1} sodium thiosulfate solution. Absorbance at 420 nm was measured and used to calculate the concentration from the calibration curve of standard antibody.

9.3 Results and discussion

9.3.1 Synthesis of AuNPs

AuNPs were prepared by reduction of $HAuCl_4$ using sodium citrate and $NaBH_4$ as reducing agents. Figure 9.7a shows the UV–vis spectrum of the ruby red solution produced after chemical reduction with sodium citrate and $NaBH_4$ indicated formation of AuNPs with a maximum absorption peak at λ = 506 nm. The size of AuNPs were measured by transmission electron microscope (TEM; JEM-2010, JEOL) operated at high vacuum mode with the voltage of 160 kV. Sample for TEM was prepared by droping AuNPs solution on a carbon-coated TEM copper grid and then let dry at room temperature. The TEM image (Figure 9.7b) and size distribution of AuNPs (Figure 9.7c) showed that the average size of AuNPs was 4.1±1.3 nm (n=120). The concentration of AuNPs was estimated to be 0.25 mM by assuming that $HAuCl_4$ was totally conversed to nanoparticles.

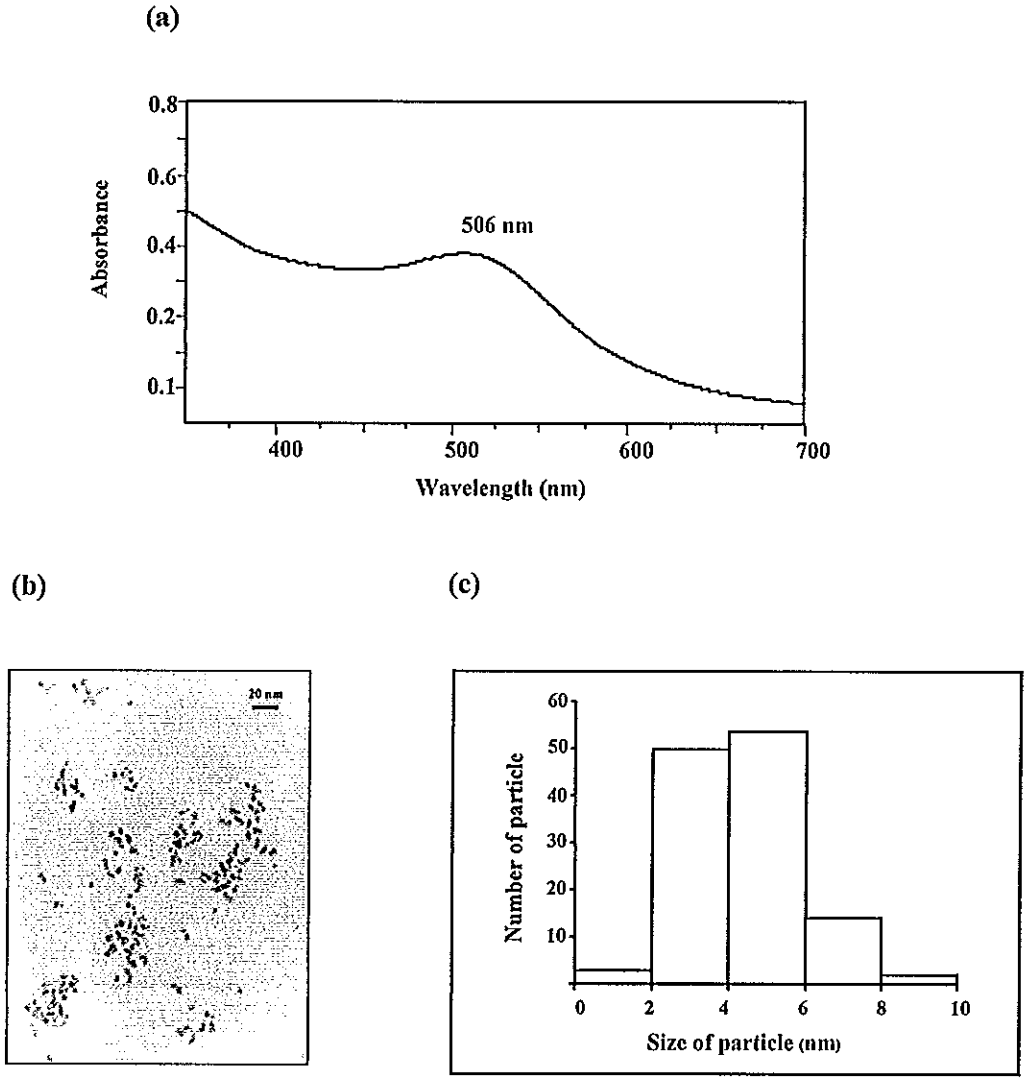

Figure 9.7 Characterizations of AuNPs by (a) UV–vis spectrum, (b) TEM image, and (c) histogram of size distribution.

9.3.2 Immobilization of antibody

9.3.2.1 SPR immunosensor system

SPR equipment was employed to follow the immobilization steps in real-time measurement as shown in Figure 9.8. For cysteamine modified gold disk, the first step was the injection of 250 µl of 0.1 mM cysteamine solution into the flow cell (a in Figure 9.8). After rinsing with ethanol and distilled water the SPR angle changed from the original θ_0 to θ_1 and θ_2, respectively. The increased from the original θ_0 to θ_2

is due to the formation of SAM on gold disk surface. Then this monolayer was activated with glutaraldehyde (point b). After 20 min of incubation, distilled water was added to remove unbounded material resulting in the decrease of SPR angle to a new base-line (θ_3). The increase of SPR angle from θ_2 to θ_3 was due to aldehyde group of glutaraldehyde reacting with amine groups of SAM to form a Schiff's base linkage. Next, anti-HSA was injected and incubated for 2 h (point c) and washed with 15 mM phosphate buffer containing 150 mM NaCl pH 7.20 to remove any weakly adsorbed antibody. This time the SPR angle increased to θ_4 due to the covalent binding between andehyde groups of glutaraldehyde and amine groups of antibody and then blocked with ethanolamine (θ_5). Finally, any pinholes were blocked by BSA (point d) for 1 h. The surface was washed with buffer until a stable base-line was obtained. The SPR angle increased from θ_6 to θ_7 because BSA was adsorbed on gold disk surface.

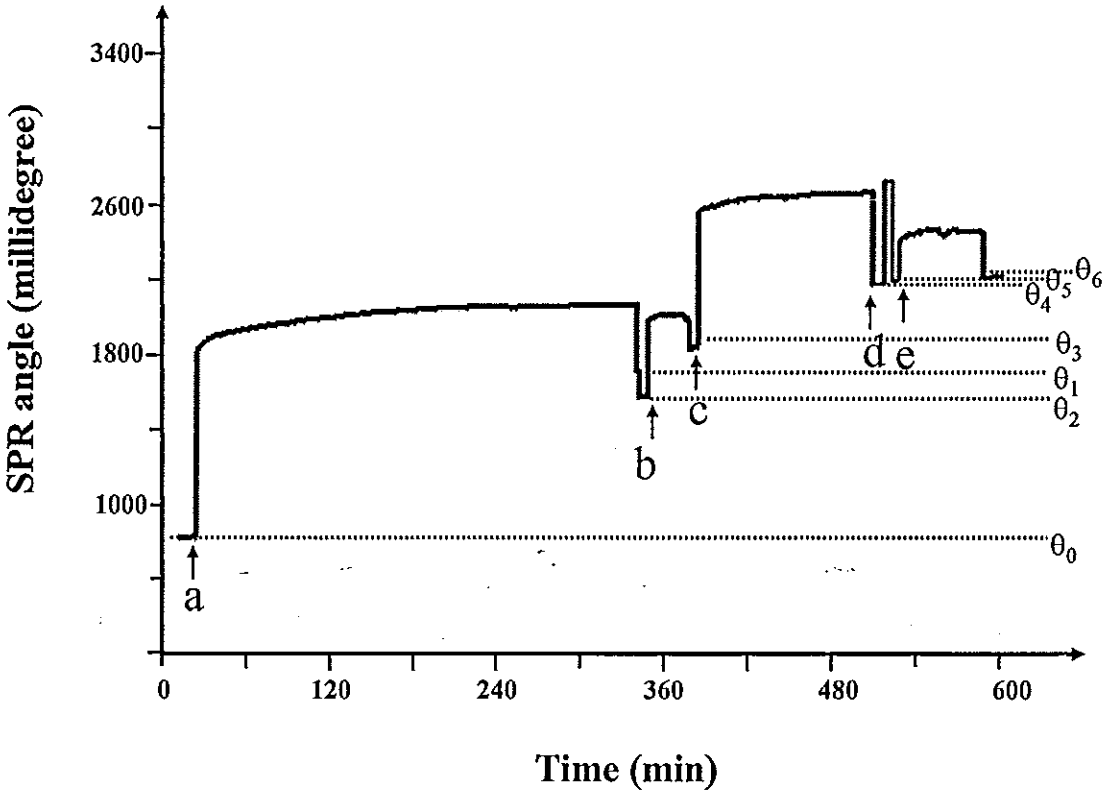

Figure 9.8 SPR sensorgram showing the change in SPR signal during anti-HSA immobilization steps. Arrows indicate injection of (a) cysteamine on cleaned gold disk, (b) glutaraldehyde , (c) anti-HSA, (d) ethanolamine and (e) BSA.

For cysteamine modified gold disk incorporating AuNPs, 250 µl of 0.1 mM cysteamine solution was injected into the flow cell (a in Figure 9.9). After 5 h this surface was then rinsed with ethanol (θ_1) and water (θ_2). Then AuNPs was added on SAM and incubated for 2 h (point b). After that distilled water was used to remove unbounded material and the SPR angle decreased to a new base-line (θ_3). Next, anti-HSA was injected and incubated for 2 h (point c) and then washed with 1,000 µl of 10 mM phosphate buffer containing 150 mM NaCl pH 7.20. The SPR angle then increased to θ_4. After the modified surface was treated with ethanolamine (point d) for 7 min the SPR angle increased to θ_5 and then blocked with BSA (point e) for 1 h and washed with buffer the SPR angle increased from θ_5 to θ_6.

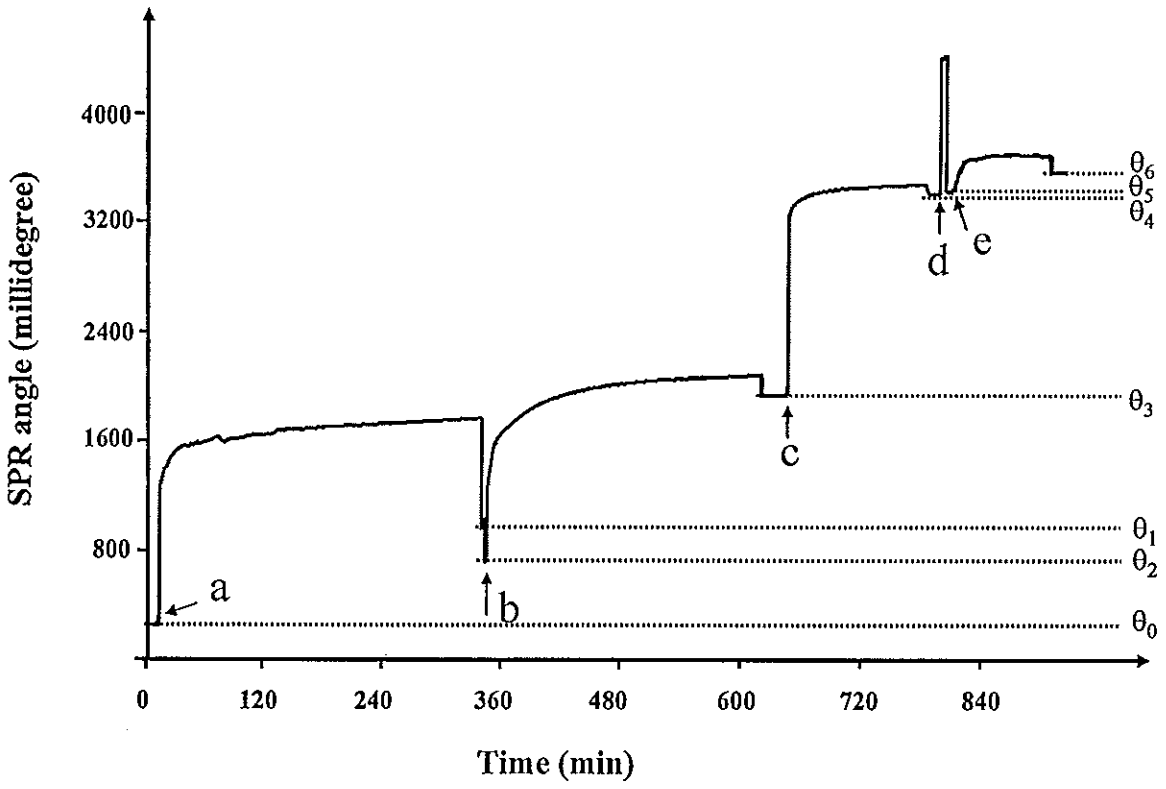

Figure 9.9 SPR sensorgram showing the change in SPR signal during anti-HSA immobilization steps. Arrows indicate injection of (a) cysteamine on cleaned gold disk, (b) AuNPs, (c) anti-HSA, (d) ethanolamine and (e) BSA.

9.3.2.2 Capacitive immunosensor system

9.3.2.2.1 Electropolymerization of *p*-PD

Figure 9.10 shows cyclic voltammograms of gold electrode during electropolymerization of *p*-PD. The anodic peak current decreases gradually after first scan and peak current dropped further with each scan. Finally, after 15 scans these were no current peak due to insulating of the polymer film on electrode surface.

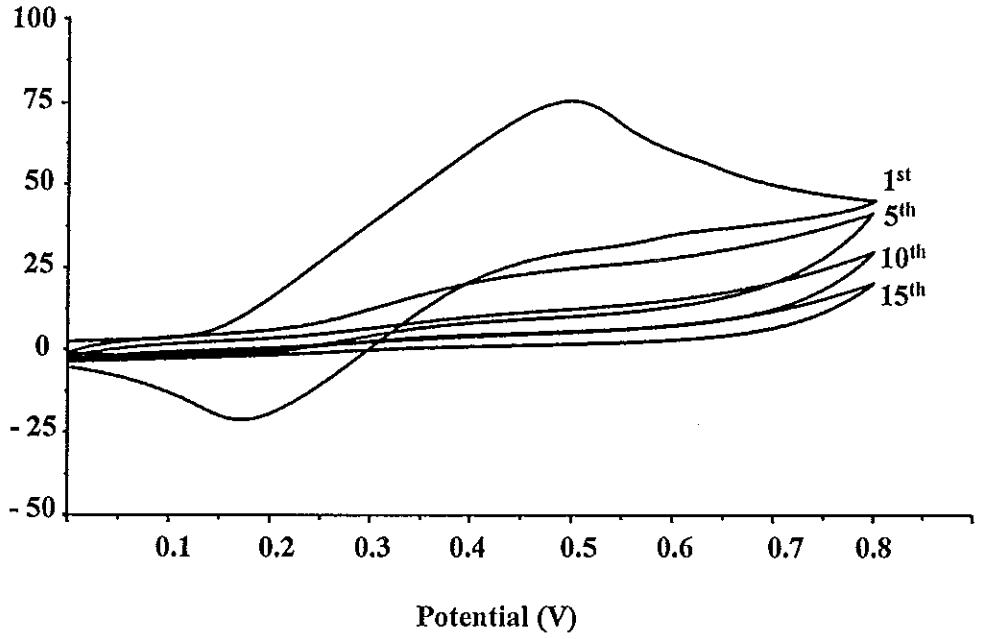

Figure 9.10 Cyclic voltammograms for the electropolymerization of 5 mM *p*-PD at a gold electrode in acetate buffer (pH 5.18) at scan rate 50 mV s^{-1}. The numbers shows the cycles.

9.3.2.2.2 Immobilization of antibody

Electrochemical characteristics of the modified electrode were monitored after each assembly step by cyclic voltammetry measurement. For the immobilization of polymer modified electrode, clean gold surface showed the oxidation and reduction peaks of the redox species in Figure 9.11 (curve a). When the electrode surface was covered with *p*-PD film, the redox peaks were much reduced (curve b). After the polymer modified electrode was immersed in glutaraldehyde solution the redox peaks

decreased further because aldehyde group of glutaraldehyde reacted with amine of polymer film (curve c). Further reduction of redox peaks were observed when antibody was immobilized on the electrode surface (curve d). When the surface was treated with ethanolamine the redox peak to decrease (cruve e) and finally blocked with 1-dodecanethiol the redox peaks disappeared (curve f).

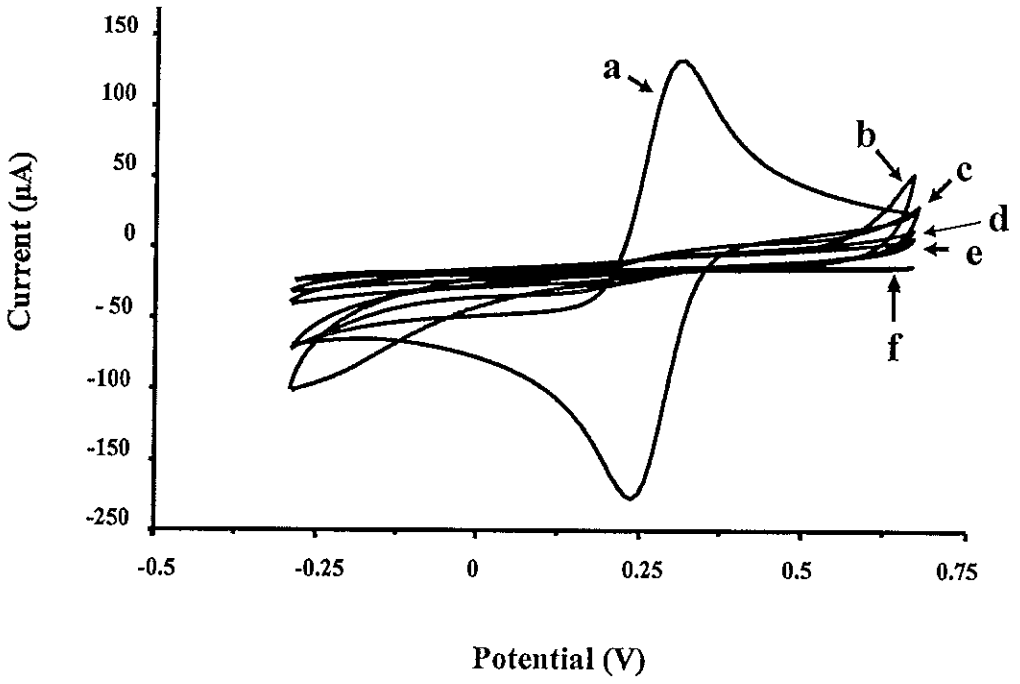

Figure 9.11 Cyclic voltammograms responses obtained in 10 mM $K_3Fe(CN)_6$ solution during the immobilization of anti-HSA (a) bare gold electrode (b) electropolymerization of *p*-PD (c) glytaraldehyde (d) anti-HSA, (e) ethanolamine and (e) 1-dodecanethiol.

For the AuNPs modified electrode (Figure 9.12). When AuNPs were deposited on the polymer layer, the peak currents of the redox couple increased (curve c). The reason is that the deposited AuNPs increase the effective surface area of the electrode. When the antibody was immobilized the redox peaks decreased (curve d) and blocked with ethanolamine (curve e). Finally, after treatment with 1-dodecanethiol the redox peaks disappeared (curve f).

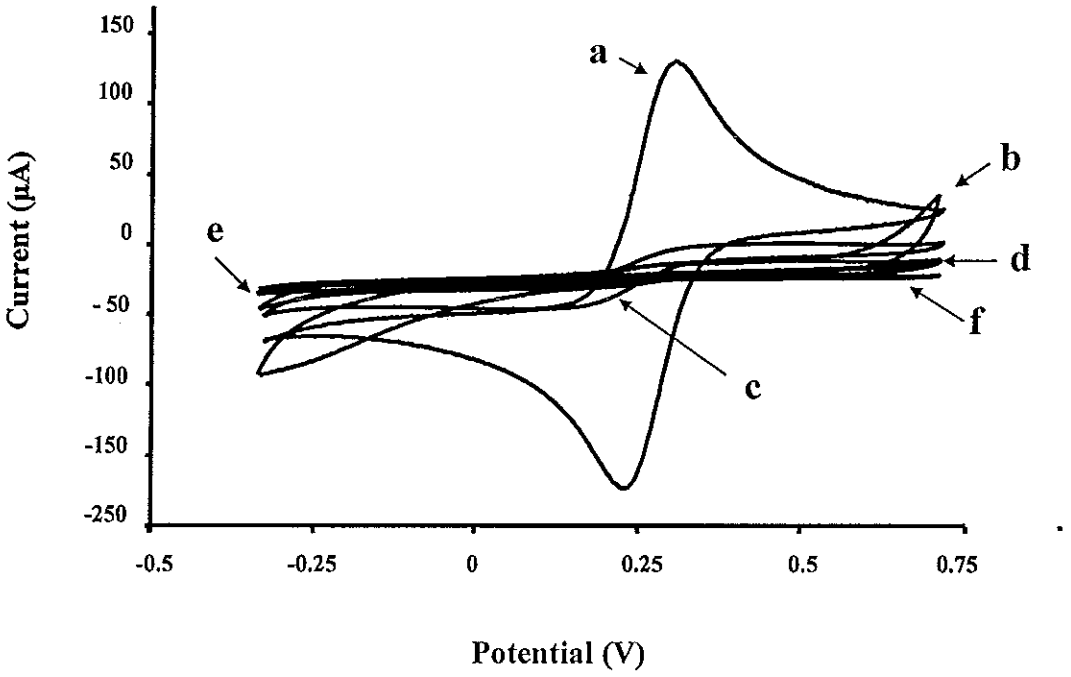

Figure 9.12 Cyclic voltammograms responses obtained in 10 mM $K_3Fe(CN)_6$ solution during the immobilization of anti-HSA (a) bare gold electrode, (b) electropolymerization of *p*-PD, (c) AuNPs, (d) anti-HSA, (e) ethanolamine and (f) 1-dodecanethiol.

9.3.3 Optimization of amount of AuNPs

9.3.3.1 Surface coverage

Determination of surface coverage was carried out by cyclic voltammetry technique but the immobilization of SPR system was done in situ. Since the flow cell that we used in SPR system cannot apply for electrochemical detection so, the surface coverage could not be studied. While, the immobilization of electrode for capacitive system was done outside the flow cell and it could be placed in an electrochemical cell to determine the surface coverage. Therefore, the effect of surface coverage was only studied for capacitive system. The percentage of surface coverage increased with the amount of AuNPs up to 6.0 ml then decreased (Figure 9.13). There has been report that AuNPs could be formed clusters when they stay closely (Daniel and Astruct, 2004). Therefore, it is possible that high density of AuNPs causing the formation of AuNPs cluster resulting in the decrease of surface area.

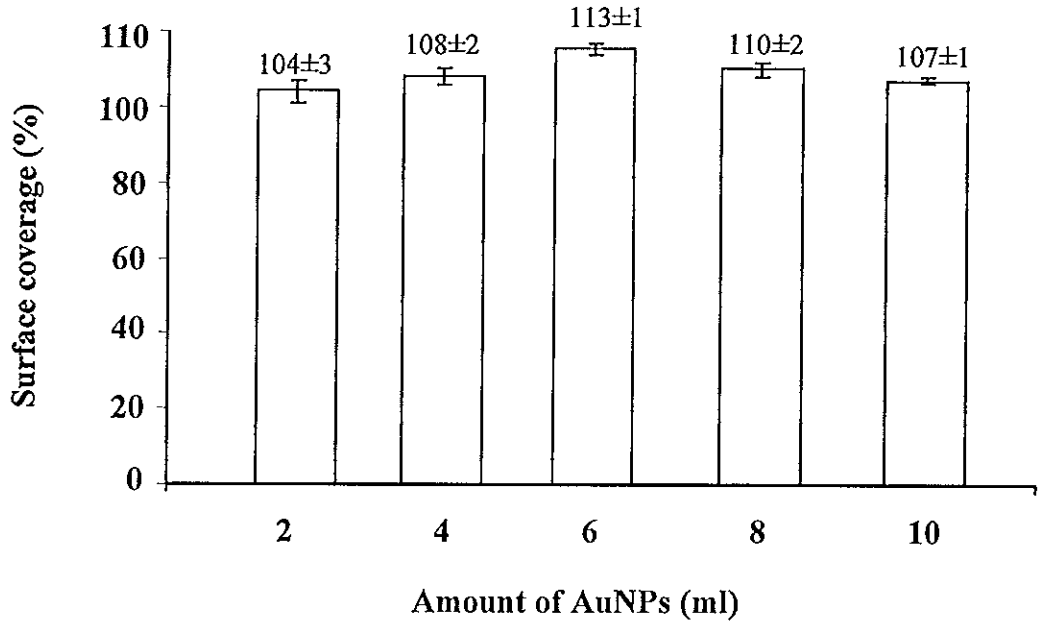

Figure 9.13 Effect of amount of AuNPs used in the modification of gold electrode via polymer film on effective electrode surface area.

9.3.3.2 Immobilization yield of antibody

Immobilization yield of antibody for SPR system was not studied. Since the immobilization was performed in situ so, it was difficult to collect the solution for the test. Therefore, determination of amount of antibody was only studied for the capacitive system. Anti-HSA immobilized on the modified electrode was determined by comparing the amount of antibody in the solution before and after immobilization. The immobilization yields of the modified electrode with different amount of AuNPs were shown in Figure 9.14. Six ml of AuNPs provided the highest immobilization yield. This corresponded well with its highest surface area (Figure 9.13). At longer amount of AuNPs the immobilization yield decreased corresponding to the decrease of surface coverage.

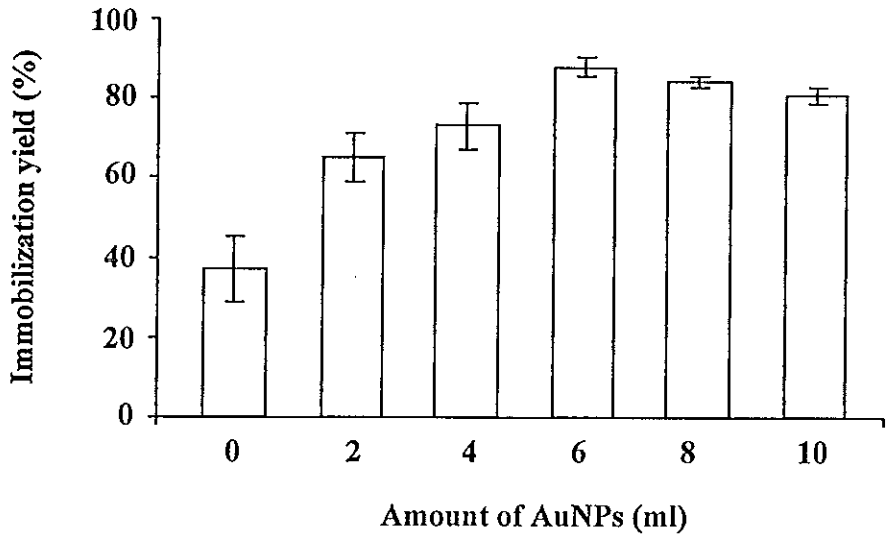

Figure 9.14 Effect of amount of AuNPs used in the modification of gold electrode via polymer film on effective immobilization yield.

9.3.3.3 Capacitive immunosensor

Figure 9.15 shows the effect of amount of AuNPs on the sensitivity (slope of calibration curve) of capacitive immunosensor response by injection of HSA at 10^{-16}, 10^{-14}, 10^{-12}, 10^{-10} mol l^{-1}. Sensitivity increased with amount of AuNPs from 2.0 to 6.0 ml due to the increase surface area and hence more antibodies could be immobilized on the surface. However, after 6.0 ml of AuNPs the sensitivity decreased since the surface area decreased and the amount of immobilized antibody also decreased. Therefore, 6.0 ml of AuNPs was selected for optimum condition of amount of AuNPs for further experiment.

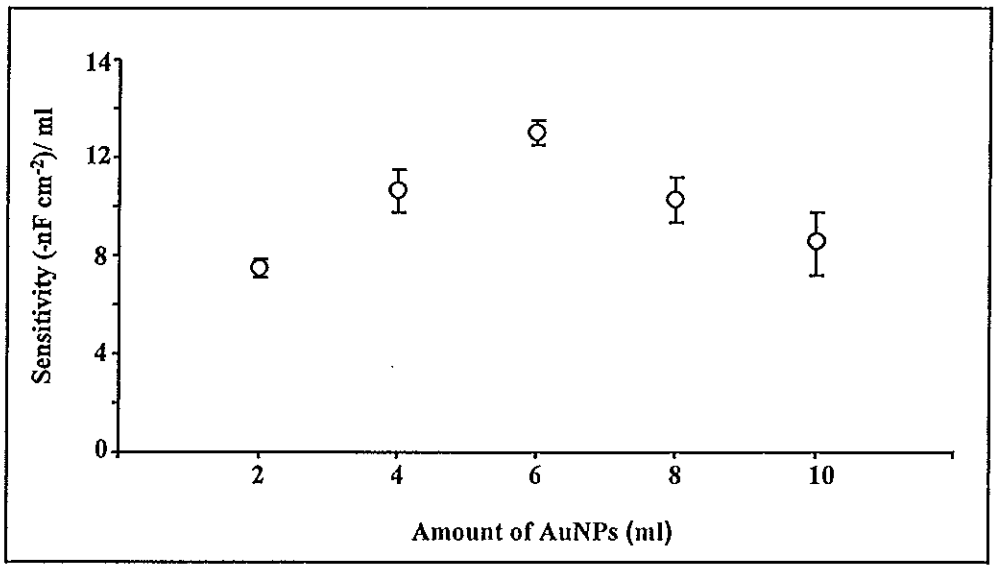

Figure 9.15 Sensitivity of immunosensors obtained from different amount of AuNPs.

9.3.3.4 SPR immunosensor

Calibration curve of standard HSA was performed at 10^{-8}, 10^{-7}, 10^{-6} and 10^{-5} mol l^{-1}. Sensitivity obtained from the plot between SPR angle shift and amount of AuNPs were compared (Figure 9.16). Similar results to the capacitive immunosensor were obtained. Thus, 6.0 ml of AuNPs was selected for optimum amount of AuNPs.

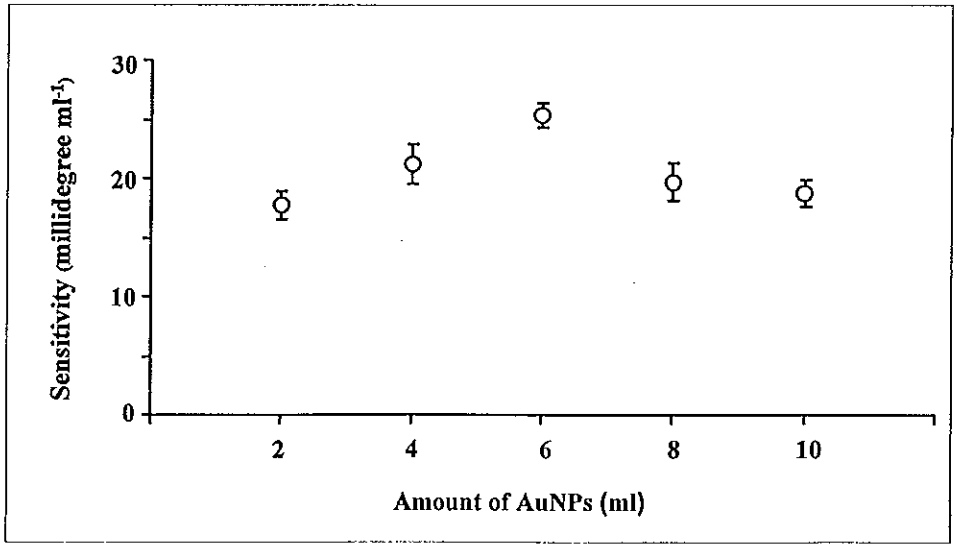

Figure 9.16 Sensitivity of immunosensors obtained from different amounts of AuNPs for SPR system.

9.3.4 Antigen detections

9.3.4.1 SPR immunosensors

The SPR immunosensors with (6 ml) and without AuNPs were used to detect CA 125, HSA and MCLR. The results are shown in Table 9.1. The use of AuNPs can enhance the sensitivity of SPR immunosensors for all tested antigens because the AuNPs could increase the amount of antibody and help shift the angle of plasmon resomance. The use of AuNPs could improve the linear range and limit of detection of CA 125 and HSA by two orders of magnitude but failed to do so for MCLR. This may be because CA 125 and HSA are large molecules (M.W = 200 kDa for CA 125 and M.W. = 66 kDa for HSA) and SPR detection is usually utilized and effective for the detection of large molecule (> 100 kDa) (Kawaguchi *et al.*, 2008). While, MCLR is a small molecule (M.W. = 995) and it is difficult to detect small molecule with SPR detection (Kawaguchi *et al.*, 2008). However, the use of AuNPs could enhance the sensitivity of detection.

According to previous work in chapter 7, anti-CA 125 was immobilized via self-assemble of 11- mercaptoundecanoic acid, which is normally employed in SPR detection (Bae *et al.*, 2005; Choi *et al.*, 2005; Oh *et al.*, 2003) while this work cysteamine was used as self-assemble monolayer. The use of 11- mercaptoundecanoic acid (LOD = 0.1 U ml^{-1}) provided lower detection limit than cysteamine monolayer (LOD = 1 U ml^{-1}). Because 11- mercaptoundecanoic acid has long chain alkane groups which are robust adsorption and close-packed formation on gold substrate more than short-chian (n< 10) (Love *et al.*, 2005), more antibody could be immobilized on the surface. This is the reasons of using 11- mercaptoundecanoic acid provided better detection limit than cysteamine monolayer. However, cysteamine monolayer incorporation with AuNPs could enhance LOD of CA 125 detection (0.01 U ml^{-1}) to be lower than when using the long chain thiol.

Table 9.1 SPR immunosensors performances for antigens detection.

Analyte	AuNPs Immobilization	Sensitivity	Linear range	LOD
CA 125	none	3.76 ± 0.02 (millidegree/ U ml^{-1})	1-40 (U ml^{-1})	1 (U ml^{-1})
	6 ml	4.21 ± 0.04 (millidegree/ U ml^{-1})	0.01-40 (U ml^{-1})	0.01 (U ml^{-1})
HSA	none	18.7 ± 0.2 (millidegree/ mol.l^{-1})	10^{-7}-10^{-5} (mol l^{-1})	10^{-7} (mol l^{-1})
	6 ml	25.3 ± 0.5 (millidegree/ mol.l^{-1})	10^{-9}-10^{-5} (mol l^{-1})	10^{-9} (mol l^{-1})
MCLR	none	0.022 ± 0.007 (millidegree/ mol l^{-1})	10^{-6}-10^{-3} (mol l^{-1})	10^{-6} (mol l^{-1})
	6 ml	0.05 ± 0.01 (millidegree/ mol l^{-1})	10^{-6}-10^{-3} (mol l^{-1})	10^{-6} (mol l^{-1})

9.3.4.2 Capacitive immunosensor

The results for capacitive immunosensor indicated that AuNPs can enhance both sensitivity and LOD for all the tested molecules (Table 9.2). The sensitivity of the modified electrode with AuNPs is better than the modified electrode without AuNPs by 2.6, 2.5 and 2.7 times for HSA, MCLR, and Pen G, respectively. These corresponded well with the higher immobilization yield of 2.7, 2.8 and 2.6 times, respectively (Table 9.3). The detection limit of HSA was lower than MCLR and Pen G due to their molecular weight. High molecular weight of antigen causes high capacitance change. Therefore, HSA with M.W. of 66 kDa provided lower limit of detection than MCLR (M.W = 995) and Pen G (M.W = 327). However, according to this reason MCLR should provide lower detection limit than Pen G an opposite result was obtained. From the SPR binding curve (section 9.3.4.1) it was observed that the binding of anti-MCLR and MCLR did not provide good response. This may be caused by the low activity of the anti-MCLR since it was obtained over 2 years ago.

For Pen G detection, this system without AuNPs provided the same detection limit of 10^{-15} mol l^{-1} as the impedimetric system of Thavarungkul *et al.* (2007). Using AuNPs, this system could improve the detection limit by one order of magnitude.

In addition, sensitivity enhancement using AuNPs of this work and silver nanoparticles (AgNPs) for MCLR detection (Loyprasert *et al.*, 2008) were compared. Modified electrode with AuNPs gave higher sensitivity than the modified electrode without AuNPs by 2.5 times. Only 1.7 times sensitivity enhancement is obtained from using AgNPs. The reasons might be because MCLR detection based on AuNPs was done under optimum amount of AuNPs and also particle size of AuNPs (4 nm) was smaller than AgNPs (40-60 nm). As we know that small size of nanoparticles provides large surface area and causes more antibody absorption on their surface compared to large particle size.

Table 9.2 The capacitive immunosensors performances for antigens detection.

Analyte	AuNPs Immobilization	Sensitivity	Linear range (M)	LOD (M)
HSA	none	3.9 ± 0.2 ($-nF\ cm^{-2}/\ mol\ l^{-1}$)	$10^{-16} - 10^{-10}$ ($mol\ l^{-1}$)	10^{-16} ($mol\ l^{-1}$)
	6 ml	10.5 ± 0.5 ($-nF\ cm^{-2}/\ mol\ l^{-1}$)	$10^{-18} - 10^{-10}$ ($mol\ l^{-1}$)	10^{-18} ($mol\ l^{-1}$)
MCLR	none	4.21 ± 0.04 ($-nF\ cm^{-2}/\ mol\ l^{-1}$)	$10^{-13} - 10^{-9}$ ($mol\ l^{-1}$)	10^{-13} ($mol\ l^{-1}$)
	6 ml	10.5 ± 0.5 ($-nF\ cm^{-2}/\ mol\ l^{-1}$)	$10^{-14} - 10^{-9}$ ($mol\ l^{-1}$)	10^{-14} ($mol\ l^{-1}$)
Pen G	none	2.7 ± 0.1 ($-nF\ cm^{-2}/\ mol\ l^{-1}$)	$10^{-14} - 10^{-8}$ ($mol\ l^{-1}$)	10^{-15} ($mol\ l^{-1}$)
	6 ml	7.2 ± 0.2 ($-nF\ cm^{-2}/\ mol\ l^{-1}$)	$10^{-15} - 10^{-9}$ ($mol\ l^{-1}$)	10^{-16} ($mol\ l^{-1}$)

Table 9.3 Immobilization yield of antibody.

Antibody	AuNPs immobilization	Immobilization yield (%)		
		1st experiment	2nd experiment	Average
HSA	none	34	32	33
	6 ml	88	91	90
MCLR	none	30	32	31
	6 ml	79	81	87
Pen G	none	35	32	33
	6 ml	89	86	88

9.4 Conclusions

This present work demonstrated the enhance performance of label-free SPR and capacitive immunosensors by optimization of AuNPs concentration. AuNPs were adsorbed on self-assemble monolayer and polymer layer modified gold substrate in SPR and capacitive system, respectively. Then AuNPs was used as platform to immobilize antibodies. High surface area of the assembled AuNPs could greatly increase surface area which leads to enhance the immobilization density of antibodies.

For detection, the use of AuNPs could improve LOD of large molecules *i.e.* CA 125 and HSA for SPR system. However, it could not improve LOD of small molecule (MCLR). However, for capacitive system, both LOD and sensitivity of all

antigens (HSA, MCLR and Pen G) could be improved by using AuNPs because this system is sensitive for various analyte sizes (Cheng *et al.*, 2001; Loyprasert *et al.*, 2008; Berggren *et al.*, 1999; Limbut *et al.*, 2006a,b).

For immobilization layer, this work showed that the use of AuNPs based on SAM or polymer film gave the same results, i.e. they could enhance the sensitivity. The AuNPs immobilized on polymer film provided higher improvement of sensitivity than SAM, since the amine groups of SAM are dense and partly imbedded in a two dimensional structure (Svobodova *et al.*, 2004). So immobilized antibody on AuNPs of SAM was less than on polymer with three dimensional matrix (Chegel *et al.*, 2002). In addition shorter preparation time was required for the polymer layer, i.e. 8 min compare to 5 h for SAM, making it more attractive. From the results it can be seen that these developed immunosensors with AuNPs could allow for the detection of several biomolecules in trace level concentration.

CHAPTER 10

Prussian blue Dispersed Sphere Catalytic Labels for Amplified Electronic Detection of DNA

10.1 Introduction

Deoxyribonucleic acid (DNA) is an important genetic material in organism and it is the basis of gene expression. Rapid detection, quantification, and sequencing of nucleic acids are crucial tasks in medial diagnostics (Hanaee *et al.*, 2007), environmental (Sun *et al.*, 2006), and basic research (Ding *et al.*, 2008c; Morio *et al.*, 2008; Selma *et al.*, 2008). A variety of techniques have been developed for DNA hybridization detection, including chemiluminescence (Ding *et al.*, 2008b), quartz crystal microbalance (Aung *et al.*, 2008), surface plasmon resonance (Wei *et al.*, 2009), and electrochemical technique (Li *et al.*, 2008a). Among these, electrochemical technique is very attractive owing to rapid detection of DNA hybridization with high sensitivity, inherent simplicity and miniaturization, and low cost (Wang, 2002).

Electrochemical monitoring of DNA hybridization has been proposed based on sandwich hybridization technique to detect DNA in low concentration scale especially amperometric technique (Lo *et al.*, 2008; Loaiza *et al.*, 2008; Ma *et al.*, 2009; Tong *et al.*, 2007). This techniquce provides high sensitivity, fast response, simple to use, and inexpensive (Ionescu *et al.*, 2007; Walsh and Dempsey, 2002; Zhang *et al.*, 2008b). For labeling, the use of enzyme tags has usually been applied. However, enzyme-based DNA detection often suffers from shortcoming associated with the limited stability and cost of the biocatalyst (Autheir *et al.*, 2001). Therefore, nanoparticle tags have been employed as catalytic labels instead of enzyme. Recently, platinum particles were used as catalytic labels for amperometric detection of DNA hybridization down to 10 pM level (Polsky *et al.*, 2006). Although platinum nanoparticle can overcome some of the problems associated with stability, it is not selective to hydrogen peroxide reduction in the presence of oxygen (Karyakin, 2001). Because this drawback, in the last decade Prussian blue has been preferred for

amperometric detection of hydrogen peroxide (Miao *et al.*, 2007; Miao *et al.*, 2007; Ricci and Palleschi, 2005).

PB is a ferriferrocyanide complex (Figure 10.1a) with well-known electrochemical properties (Koncki, 2002; Ricci and Palleschi, 2005). It exhibits excellent catalytic activity for the electrochemical reduction of hydrogen peroxide at low potentials, which is usually considered to be an "artificial peroxidase" (Figure 10.1b). The use of PB is suitable for application in affinity biosensor with many advantages such as low cost, high stability, and easy to synthesize (Ricci and Palleschi, 2005). For these reasons, a lot of attention was devoted to the use of PB in biosensors, including the detections of glucose (Wang *et al.*, 2009), d-amino acid (Wcislo *et al.*, 2007) and pesticides (Suprun *et al.*, 2005).

The loading of PB particles onto gold nanoparticles was shown recently to offer high catalytic activity towards the reduction of hydrogen peroxide (Miao *et al.*, 2007), but not in connection to bioaffinity assays. This work interested in the development of a new method to amplify electrical DNA detection using oligonucletides tagged with PB by embedded it into polystyrene (PS) beads, linked to the secondary DNA probe. To our knowledge, the modification of polymeric spheres with catalytic PB nanoparticles has not been reported.

(a)

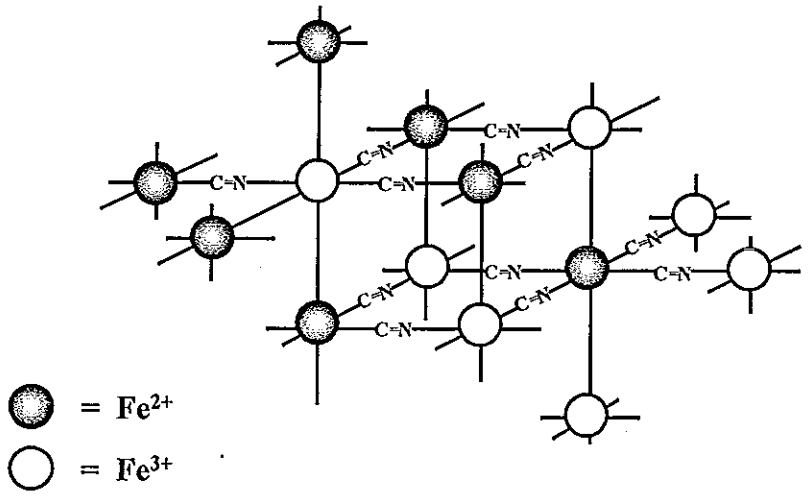

(b)

E_{app} = 0.0 V *vs* Ag/AgCl

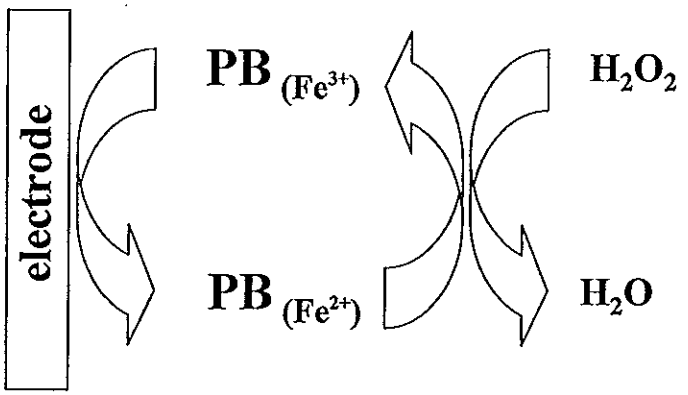

Figure 10.1 (a) Cubic structure of PB and (b) PB electrocatalyst of H_2O_2 reduction at 0.0 V *vs* Ag/AgCl (modified from Ricci and Palleschi, 2005; Koncki, 2002).

10.2 Experimental

10.2.1 Apparatus

Electrochemical measurements were performed with an AutoLab Potentiostat (Eco Chemie, Netherlands), controlled by the GPES software. Scanning electron microscopy (SEM) images of the PS and PS-PB beads were obtained with an XL30 SEM instrument (FEI Co., Hillsboro, OR). Ultraviolet-visible (UV-vis) absorption spectra were recorded in a 1 mm path-length cell coupled to a UV-2501 PC spectrophotometer (Shimadzu Scientific Instruments, Inc, CA). Fourier Transform Infrared (FT-IR) spectra were recorded using a Nicolet 6700 FT-IR (Thermo-Fisher, Madison, WI).

10.2.2 Materials

Potassium ferrocyanide ($K_4Fe(CN)_6$), iron(III)chloride ($FeCl_3$), potassium chloride (KCl), morpholineethanesulfonic acid (MES), N-(3-dimethylaminopropyl)-N-ethylcarbodiimide hydrochloride (EDC) and hydrogen peroxide were purchased from Sigma (St. Louis, MO). N-hydroxysulfosuccinimide (NHS) was obtained from Fluka (Buchs, Switzerland). Carboxylated polystyrene beads (1.04 mm diameter) were obtained from Bangs Laboratories (catalog number PC04N, Fishers, IN). DNA oligonucleotides were obtained from IDT Technologies (Corabille, IA). The following oligonucleotides were used:

Probe 1:

5'-SH-GAC CTAGTC CTT CCA ACAGC-3'

Probe 2:

5'-GGG TTTATG AAA AAC ACT TTT TTT TT-NH2-3'

Target:

5'-AAA GTG TTT TTC ATA AAC CCATTATCC AGG
ACT GTT TATAGC TGT TGG AAG GAC TAG GTC-3'

Noncomplementary DNA:

5'-TTC CTTAGC CCC CCC AGT GTG CAAGGG CAG
TGA AGACTT GAT TGTACA AAATAC GTT TTG-3'

All chemicals were analytical reagent grade and all solutions were prepared with double-distilled deionized water.

10.3 Methods

10.3.1 Analytical protocol

Figure 10.2 outlines the steps of the new microsphere-based bioelectronic sandwich assay. It involves co-immobilization of the DNA probe with 6-mercapto-1-hexanol on a gold surface (a), hybridization of the target DNA (b), binding of a secondary probe conjugated to PB-embedded PS spheres (c), and catalytic amperometric detection of hydrogen peroxide at the captured PS-PB spheres sections, such coupling of polymeric 'carrier' beads with the strong catalytic action of the PB 'artificial enzyme' was developed to detect DNA hybridization at low concentration.

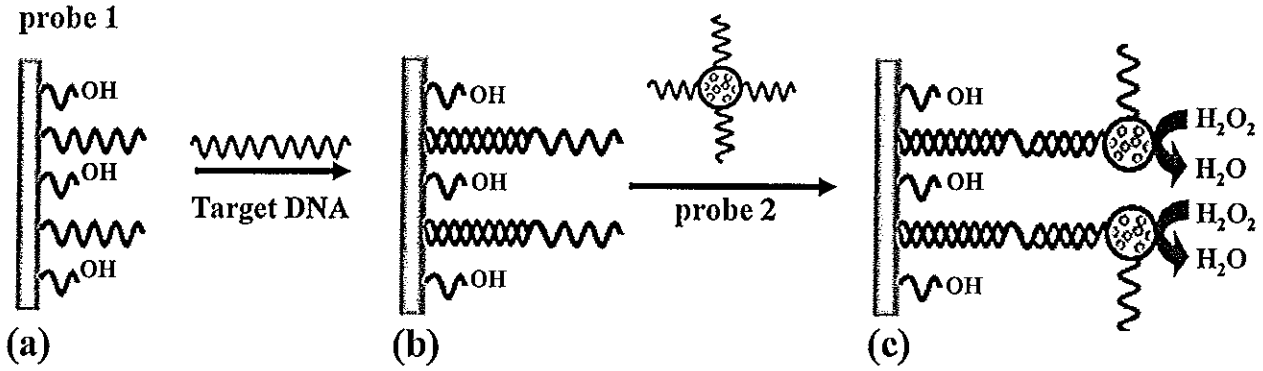

Figure 10.2 Schematic representation of the analytical protocol: (a) formation of monolayer of mixed monolayer of DNA probe on gold electrode: (b) hybridization with target DNA and (c) second hybridization with polystyrene-Prussian blue beads-labeled probe.

10.3.2 Preparation of PB nanoparticles

PB nanoparticles (ca. 15 nm in diameter) were prepared based on the method of Miao *et al.*, (2007). Briefly, seven-milliliter of deionized water, 1.0 ml of 10 mM KCl and 1.0 ml of 2.0 mM $K_4Fe(CN)_6$ were mixed with vigorous stirring. Then, 1.0

ml of 2.0 mM $FeCl_3$ was slowly added to the mixture for 40 min. The resulting dark-blue colloidal solution was centrifuged for 20 min at 13,000 rpm and the nanoparticles were collected in the precipitate.

10.3.3 Encapsulation of the PB nanoparticles within the PS beads

The PB nanoparticles were encapsulated into the PS beads by mixing rapidly 5.0 mg of the beads in 400 µl of a chloroform/butanol solvent mixture (15%/85% v/v). Six mg of PB nanoparticles were then added to the mixture, allowing the encapsulation to proceed for 40 min. The beads were then washed with 50 mM phosphate buffer (pH 6.00).

10.3.4 Effect of PB nanoparticles loading in PS beads

Amount of PB nanoparticles was optimized from 6.0 to 9.0 mg of PB in 5.0 mg of PS bead in 300 µl of 50 mM phosphate buffer pH 6.00. The procedure was carried out following 10.3.2. Then 20 µl of PS-PB beads was dropped on gold electrode surface and allowed to dry. This modified PS-PB beads electrode was then covered with 3 µl of 3% v/v Nafion solution and was used as the working electrode. Amperometric detection was carried out by addition of 0.1 mM of hydrogen peroxide in 0.1 M phosphate buffer/0.1 M KCl pH 6.00 solution at potential of 0.0 V at 50 mV/s scan rate.

10.3.5 Conjugation of the PB-PS beads with DNA-probe 2

The carboxylic groups of PB-PS beads were activated with 100 µl of 0.1 M NHS/ 0.4 M EDC solution for 30 min and centrifuged at 9,000 rpm for 5 min to link with NH_2-DNA. The modified beads were then incubated with 100 µl of 4 µM 3'NH_2 – DNA (probe 2) solution for 2 hours. Subsequently, the DNA linked PS-PB beads were centrifuged at 3,000 rpm for 3 min, washed twice with 50 mM phosphate buffer (pH 6.00) and suspended in 300 µl of the same phosphate buffer.

10.3.6 Immobilization, sandwich hybridization and detection

10.3.6.1 Immobilization of DNA probe (probe 1) on gold electrode

The surface of the gold disk electrode (2 mm in diameter; CH Instruments, Austin, TX) was cleaned by exposure to Piranha solution for 20 min and then rinsed with water. (Safety note: the Piranha solution should be handled with extreme caution.) The electrode was polished sequentially using alumina slurries of 3, 1 and 0.5 mm on a polishing pad. Its potential was then cycled between -0.3 to 1.5 V (vs. Ag/AgCl) in 1.0 M H_2SO_4 until a stable background voltammogram, typical of a clean gold surface, was observed. The oligonucleotide probe was immobilized onto the gold surface by exposing the electrode overnight to 50 µl of 1 mM thiolated-oligonucleotide probe 1 solution in 0.05 M phosphate buffer (pH 7.40). The DNA modified gold surface was then treated for 20 min in 0.1 M solution of 6-mercapto-1-hexanol (dissolved in water/ethanol, 1/4 (v/v)) followed by rinsing with deionized water.

10.3.6.2 Sandwich DNA hybridization

The oligonucleotide-probe modified gold electrode surface was incubated for 1 hour with 50 µl of the target DNA solution (in the hybridization buffer: 750 mM NaCl, 150 mM sodium citrate). The surface was then washed with the same buffer to remove the unbound DNA. Subsequently, the electrode was incubated for 1 hour with 50 µl of a solution containing the secondary DNA-linked PS-PB beads (0.83 mg/ µl) and then washed with the washing buffer (50 mM Tris-HCl, 0.1% Tween 20, pH 7.40).

10.3.6.3 Electrochemical detection

The three electrode system consisted of the DNA-modified gold working electrode, an Ag/AgCl reference electrode and a platinum wire counter electrode. The electrochemical response to the 10 mM hydrogen peroxide addition was monitored

amperometrically at a fixed potential of 0.0 V (*vs.* Ag/AgCl) using 3.0 ml cell containing 50 mM phosphate buffer/0.1 M KCl (pH 6.00) solution.

10.4. Results and Discussion

10.4.1 Characterizations of PS-PB beads

PB nanoparticles prepared in the reaction of $Fe(CN)_6^{4-}$ complex anion with Fe^{3+} cation (Miao *et al.*, 2007) were embedded into PS microspheres during the swelling of the beads by organic solvent. The PB embedded PS microspheres were characterized by scanning electron microscopic (SEM) and spectroscopic (UV-vis and FT-IR) measurements. Figure 10.3a compares SEM images of the PS microspheres before (A) and after swelling (B) in butanol/chloroform solution to the resulting PS-PB beads (C). While the initial surface of the PS beads is smooth, high degree of roughness is observed for the treated surface (A *vs.* B), reflecting the increased porosity associated with the swelling process. A similar treatment in the presence of the PB nanoparticles leads to a much smoother surface (C). This surface contains randomly distributed nonuniform globular microstructures corresponding to the Prussian blue. Such structures are not observed in the control experiment (without PB, B). Distinct PB nanoparticles cannot be observed under the low resolution of the SEM imaging.

The incorporation of PB into the PS spheres is also indicated by the UV-vis absorption spectra (Figure 10.3b). The 'naked' PS spheres display a broad absorption band around 400 nm (A). PB nanoparticles, in contrast, yield a single band around 710 nm (B), similar to that reported by Miao *et al.* (2007). The spectra of the PS-PB beads (C) show two absorption signals, around 400 and 710 nm, characteristic of both the PS and PB, respectively. Functional groups on the surface of PS-PB beads were characterized using FT-IR. The FT-IR spectra of the PS-PB spheres (Figure 10.3(C)) displayed a new band around 2100 nm (compare to PS beads alone (A)), characteristic of CN stretching (Kulesza *et al.*, 1996). It results from PB nanoparticles (B) which indicated they were embedded into the PS microspheres.

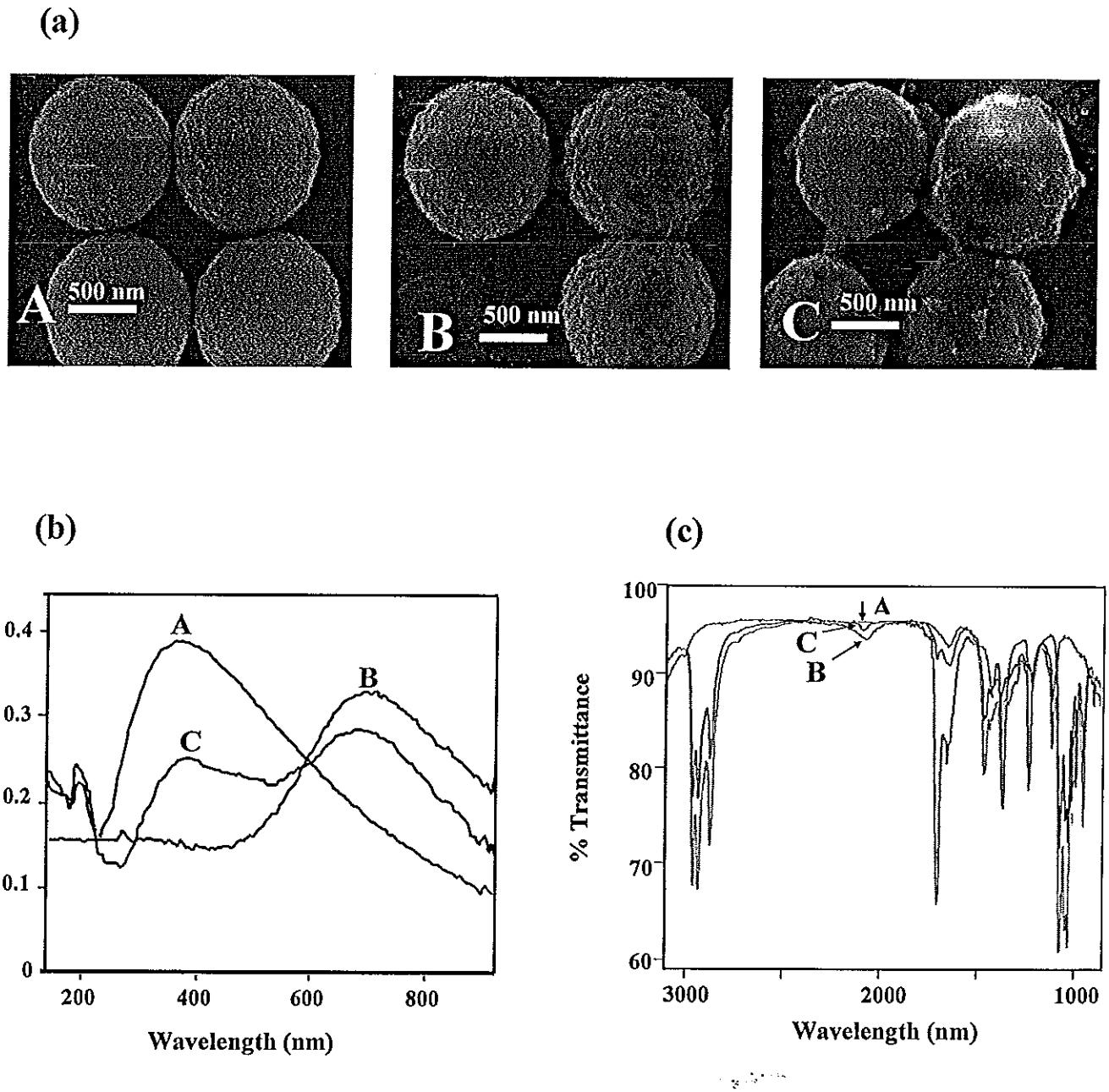

Figure 10.3 (a) SEM images of PS beads before (A) and after (B) swelling in a butanol/chloroform solution, and the resulting PS-PB beads (C), SEM parameters include an accelerating voltage of 30 kV with 50,000 magnification, (b) UV-vis absorption spectra of PS spheres (A), of PB nanoparticles (B), and of the PS-PB beads (C), Spectra were recorded in 50 mM phosphate buffer (pH 6.00), (c) FT-IR spectrum of PS (A), PB (B), and (C) incoporation of PS-PB solution in chloroform.

10.4.2 The effect of PB nanoparticles loading in PS bead

The influence of the PB loading (in the 'encapsulation' solution) was examined from the amperometric response to hydrogen-peroxide of a PS-PB modified gold electrode (Figure 10.4). The peroxide current increases rapidly with the level of PB in the 400 μl solution between 2.0 and 6.0 mg and levels off thereafter. All subsequent work was carried out using a 6.0 mg PB loading solution.

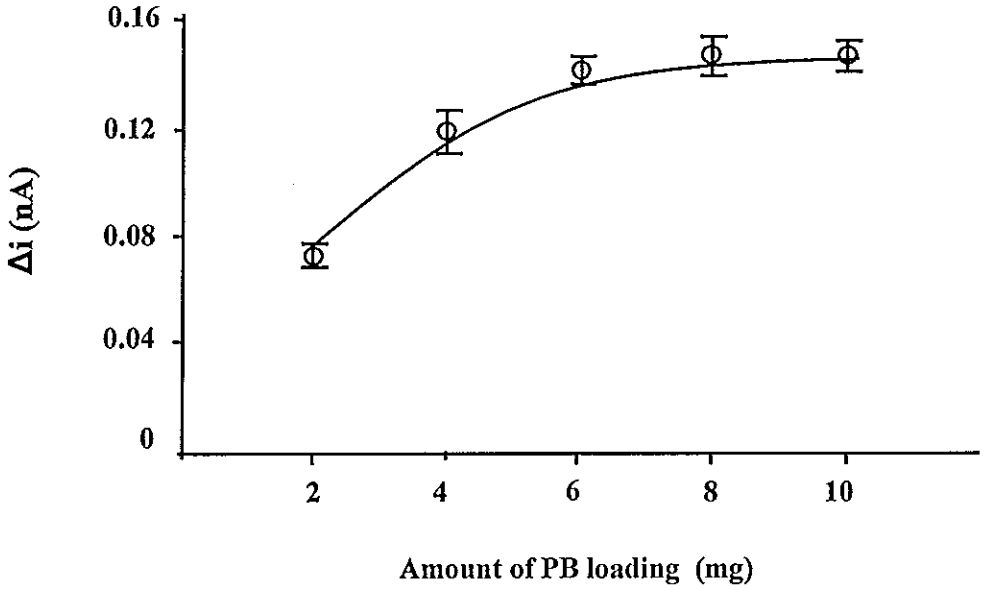

Figure 10.4 Effect of the loading of the PB particles on the PS beads on the amperometric response to 0.1 mM hydrogen peroxide.

10.4.3 Electrochemical response

The strong electrocatalytic activity of the PS-PB beads towards hydrogen peroxide was illustrated by using the catalytic spheres to modify the surface of a gold-disk electrode. The PS-PB modified electrode offers well-defined voltammetric (Figure 10.5) and amperometric (Figure 10.6) signals for hydrogen peroxide. Figure 10.5 compares cyclic voltammograms for hydrogen peroxide recorded at PS-(a) and PS-PB (b) sphere modified electrode. As expected, no peroxide response is observed

over the entire -0.1 to +0.5 V potential range in the absence of the embedded PB particles. In contrast, a well-defined voltammogram, characteristic of PB modified electrodes (Karyakin, 2001), is observed using the PS-PB coating.

The resulting PS-PB modified electrode offers a sensitive low-potential amperometric detection of hydrogen peroxide. Figure 10.6 shows typical current-time recordings for 0.1 mM additions of hydrogen peroxide obtained at 0.0 V (vs. Ag/AgCl) using the PS (a) and PS-PB (b) modified electrodes. The latter responds rapidly (ca. 20 s) to these peroxide additions and offers very favorable signal to-noise characteristics. In contrast, no response is observed at the PS-modified surface (a), reflecting the absence of the PB catalyst. The PS-PB beads modified electrode also exhibited high operational stability, as was indicated from its highly stable response for hydrogen peroxide over 30 successive runs.

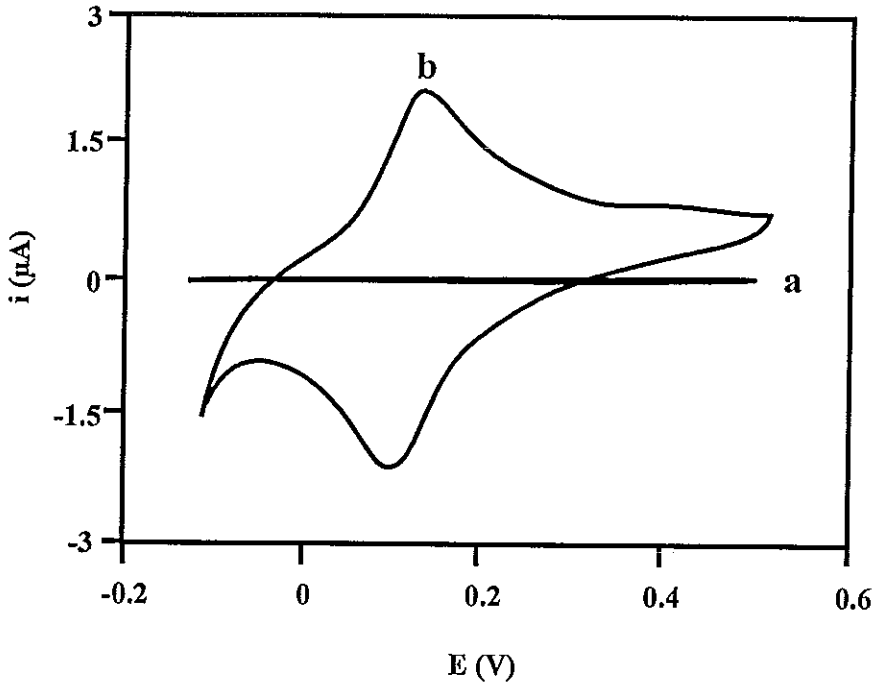

Figure 10.5 Cyclic voltammograms for 0.5 mM hydrogen peroxide at the PS (a) and PS-PB (b) modified electrodes.

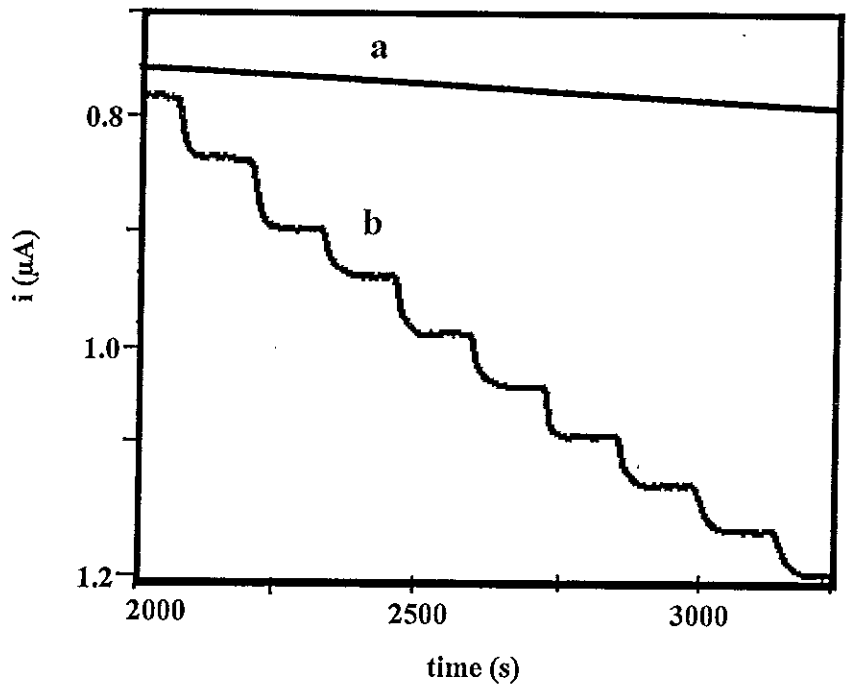

Figure 10.6 Amperometric response to successive additions of 0.1 mM hydrogen peroxide at the unmodified (a) and PS-PB modified (b) gold electrodes.

10.4.4 DNA hybridization detection

10.4.4.1 Effect of amine- DNA concentration

The response signal was detected by monitoring amine-DNA linked PS-PB beads which hybridized with target DNA on probe 1. When high amount of amine-DNA immobilized on PS-PB beads it can bind with target DNA more than low amount of amine-DNA immobilized on PS-PB beads resulting in high signal. Therefore, the influence of amine-DNA concentration was optimized to obtain optimum amount of amine-DNA immobilized on PS-PB beads. The effect of amine-DNA concentration on response current was examined from 2.0 to 8.0 μM with using 10^{-5} M of target DNA and 0.1 mg/μl of probe 2. Electrochemical measurements were performed using a 0.1 M phosphate buffer/0.1 M KCl (pH 6.00) solution, a potential of 0.0 V, and additions of 10 mM hydrogen peroxide. Figure 10.7 showed the signal increases with an increase of amine DNA concentration up to 4 μM. To obtain the maximum response, 4 μM was selected in subsequent work.

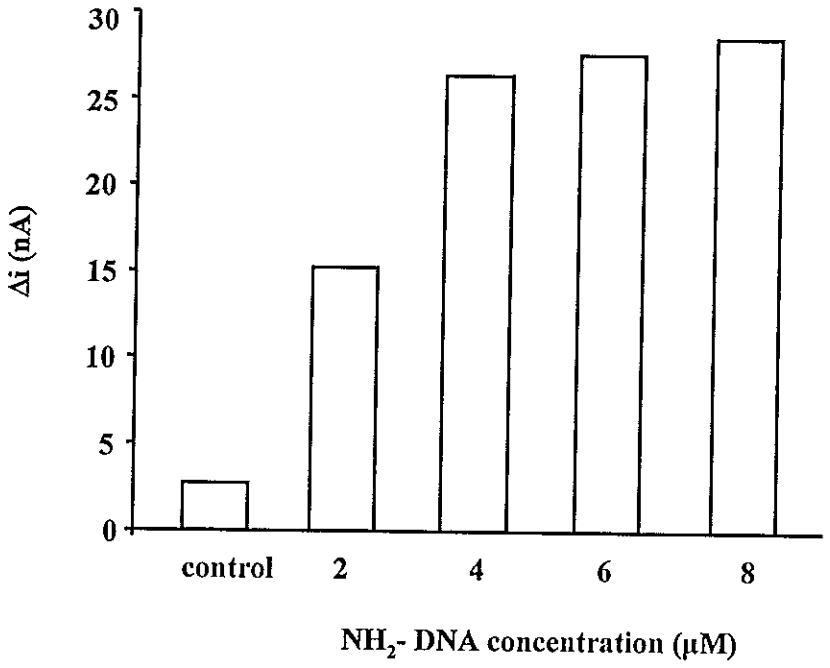

Figure 10.7 Effect of amine- DNA concentration.

10.4.4.2 Effect of amount of probe 2 (PS-PB-amine DNA)

An additional parameter that can affect the sandwich assay was probe 2 concentration. The amount of probe 2 from 0.05 to 0.3 mg/μl was studied for sandwich DNA hybridization detection with amperometric system by using 10^{-5} M of target DNA and 4 μM of anine-DNA. Electrochemical measurements were performed using a 0.1 M phosphate buffer/0.1 M KCl (pH 6.00) solution, a potential of 0.0 V, and additions of 10 mM hydrogen peroxide. Figure 10.8 shows the amperometric responses corresponded to the analysis of different concentration of probe 2. The response increased with probe 2 concentration until 0.2 mg/μl and this was selected as the concentration of probe 2.

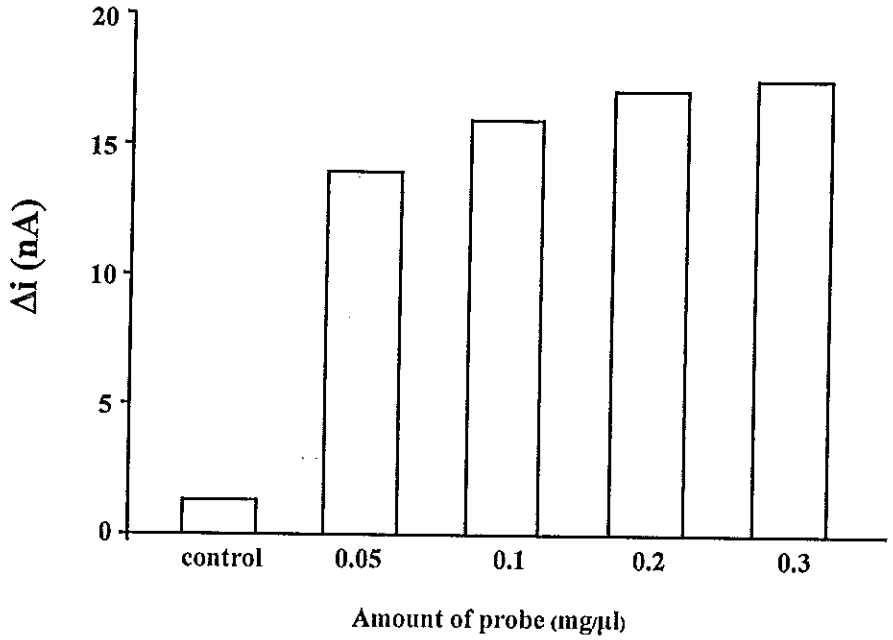

Figure 10.8 Effect of amount of probe 2.

10.4.4.3 Electrochemical performance

DNA hybridization assays were performed relied on a secondary nucleic-acid probe functionalized with the PS-PB microspheres and electrocatalytic detection of hydrogen peroxide by the captured PS-PB particles. Such use of PS-PB catalytic labels to amplify the detection of DNA hybridization is illustrated in Figure 10.9. Under optimum conditions, it displays amperometric hybridization signals for extremely low target DNA concentrations ranging from 1×10^{-13} to 1×10^{-10} M (Figure 10.9 a,b). Well defined current signals are observed for these picomolar concentrations of the target. A detection limit of 5×10^{-14} M target DNA can be estimated based on the signal-to-noise characteristics (S/N=3) of the response for the 1×10^{-13} M target. Such detection limit corresponds to 46 fg (2.5 amol) in the 50 μl samples. The present protocol is thus ca. 100 times more sensitive compared to the DNA electronic detection based on platinum-nanoparticle catalytic labels (Polsky *et al.*, 2006). A negligible signal is also observed in Figure 10.9a for a substantially (1000-fold) higher level of a noncomplementary oligomer. This small response is similar to that observed without the DNA target and reflects primarily the negligible

nonspecific adsorption of the probe-2/PS-PB conjugate. Such effective discrimination is attributed to hydrophilic character of the mixed monolayer of thiolated probe 1 and 6-mercapto-1-hexanol (Levicky *et al.*, 1998). The corresponding calibration plot of current vs. log [DNA] (Figure 10.9c) is linear over the 10^{-10} to 10^{-13} M range, with a correlation coefficient of 0.997. The amplified electrical signal is coupled to a relatively good reproducibility. The precision was estimated from a series of six successive trace measurements of 1×10^{-12} M target DNA.

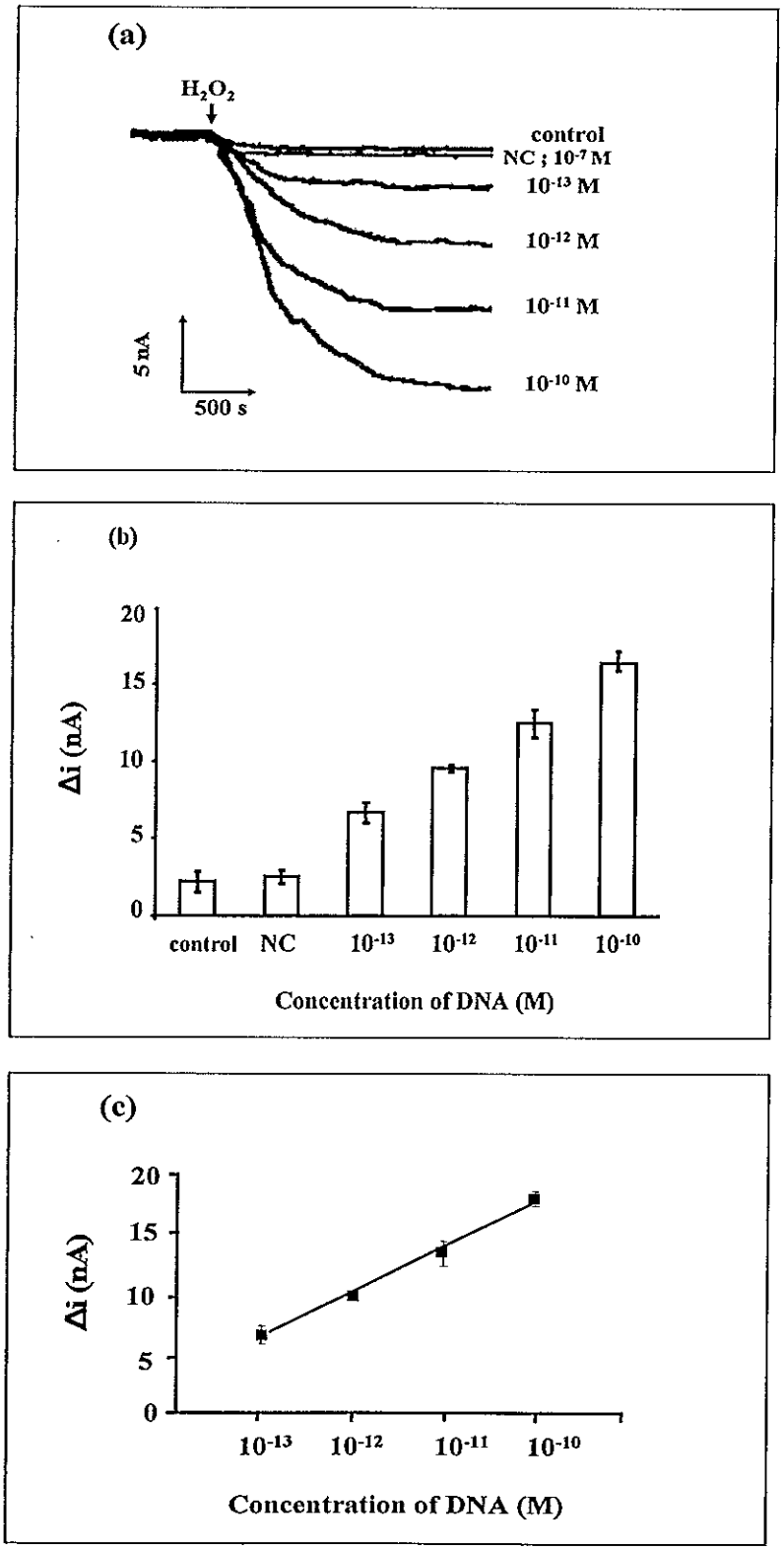

Figure 10.9 (a) Amperometric response to different concentrations of the target DNA and noncomplementary DNA.(b) Relative current signals for the different levels of the target DNA. (c) The calibration curve of DNA concentrations *vs* response.

10.5 Conclusions

This work demonstrated for the first time the use of PS-PB spheres as tags for highly sensitive bioelectronic detection of DNA hybridization. Such tags couple the amplification features of polymeric carrier beads with the powerful catalytic action of the PB 'artificial enzyme'. While the concept of PS-PB tags has been demonstrated for amplifying the transduction of DNA hybridization, it could be readily expanded for the monitoring of other target analytes such as proteins or glycans. The coupling of polymeric spheres with PB particles also holds great promise for surface coatings for improved oxidase-based enzyme electrodes and for enhancing the detection of different peroxide species ranging from hydrogen peroxide to peroxide explosives. Other catalytic labels (e.g., Pt nanoparticles (Polsky *et al.*, 2006)) could be coupled with the amplification features of polymeric carrier spheres and used for ultrasensitive monitoring of different biomolecular interactions.

CHAPTER 11

Conclusions

In this thesis, the development and evaluation of performance of SPR and electrochemical affinity biosensor systems have been described. These affinity biosensors were based on label-free and labeled assay for interested analytes.

In label-free assay, the detection was performed by SPR and capacitive transducers. Both affinity biosensors were carried out by immobilizing biological recognition element on gold substrate surface via self-assemble monolayer or polymer film. The interaction between target analytes and immobilized biological recognition element caused the increase of SPR angle or decrease of capacitance. Both principles of detection were used to analyse interested analytes as describes in chapters 7, 8 and 9.

First, a comparison between SPR and capacitive immunosensors was studied for a flow injection label-free detection of cancer antigen 125 (CA 125) in human serum. Both immunosensors were performed by immobilization of anti-CA 125 on gold substrate through a self-assemble monolayer. Under optimal conditions, SPR provided a detection limit of 0.1 U ml^{-1} while 0.05 U ml^{-1} was obtained for the capacitive system. Linearity for SPR was between 0.1 U ml^{-1} and 40 U ml^{-1} and 0.05-40 U ml^{-1} for capacitive system. Table 11.1 shows the comparison between analytical assays for CA 125 detection. The performances of these systems are much better than others in all aspects with no requirement of labels. Good agreement was obtained when CA 125 concentrations of human serum samples determined by both immunosensors systems were compared to conventional enzyme linked fluorescent assay (ELFA) method (P= 0.05).

Table 11.1 Comparison of analytical method for CA 125 detection.

Analytical method	Label (molecule)	Detection limit	Linear range
SPR (this work)	No	0.1 U ml^{-1}	0.1-40 U ml^{-1}
Capacitive (this work)	No	0.05 U ml^{-1}	0.05-40 U ml^{-1}
Chemiluminescent			
Fu *et al.*, 2008	Yes (ALP)	0.70 U ml^{-1}	1.0–50 U ml^{-1}
Amperometric			
Wu *et al.*, 2007c	Yes (HRP)	0.4 U ml^{-1}	0 - 25 U ml^{-1}
Wu *et al.*, 2007b	Yes (HRP)	1.8 U ml^{-1}	2 - 75 U ml^{-1}
Wu *et al.*, 2006	Yes (HRP)	1.73 U ml^{-1}	0 - 30 U ml^{-1}
Dai *et al.*, 2003	Yes (HRP)	1.29 U ml^{-1}	2 - 14 U ml^{-1}
Tang *et al.*, 2006	No	1.8 U ml^{-1}	10-30 U ml^{-1}

ALP = alkaline phosphatase; HRP = horseradish peroxidase

In the case where label-free capacitive immunosensor was applied for detection of *B. pseudomallei* antibody in serum samples of melioidosis and non-melioidosis patients. This capacitive immunosensor was achieved by immobilization of Bip D protein as biological recognition element on electrode surface to detect *B. pseudomallei* antibodies in serum samples. The optimized system could clearly separate between melioidosis and non-melioidosis patients. Comparing to other existing methods (Table 11.2) the develop technique is the most rapid, requiring only is 15 min for one analysis. It is also the most sensitive method, sample could be diluted up to 11,000 times.

Table 11.2 Comparison of analytical method for *B. pseudomallei* antibodies in serum samples detection.

Analytical method	Analysis time	Dilution
Capacitive immunosensor (this work)	**15 min**	**1:11,000**
Bacterial culture (Howard and Inglis, 2005)	3-4 days	No
Indirect hemagglutination antibody (Appassakij *et al.*, 1990)	3 h	1:160
PCR (Rattanathongkom *et al.*, 1997)	3.5 h	1:10
ELISA (Chantratita *et al.*, 2007)	2.5 h	1:4,000
Immunoblotting (Visutthi *et al.*, 2008)	3.5 h	1:2,000

PCR = polymerase chain reaction; ELISA = enzyme-linked immunosorbent assay

In addition, label-free affinity biosensor incorporation with AuNPs has also been studied for their high sensitivity detection based on SPR and capacitive principles detection. AuNPs were employed as platform to immobilize antibodies via SAM and polymer film. The concentration of AuNPs was optimized for both label-free SPR and capacitive immunosensors. Under optimal condition these systems were

applied to detect CA 125, HSA, MCLR and Pen G. For SPR system, AuNPs has been shown to enhance the sensitivity of all analytes detection. The use of AuNPs could improve the detection limit of CA 125 and HSA by two orders of magnitude but failed to do so for MCLR. Since, SPR is successful for large molecules (CA 125 and HSA) while this system is difficult to detect small molecule (MCLR). The measurement of small molecule can improve by sandwich assay to amplify original signal. For capacitive system, AuNPs could also enhance both sensitivity and LOD for all the tested molecules due to this technique well detection with different molecular weights of analytes. Therefore, AuNPs sensitivity enhancement of label-free SPR and immunosensors allowed detecting targeted analytes with low concentration.

Another type of affinity biosensor, labeled assay, was also investigated. It is based on the use of label to amplify signal which could help the systems to reach low detection limit. The polystyrene bead modified with Prussian-blue nanoparticles was developed for a labeled affinity biosensor for DNA detection. The amperometric measurement relies on sandwich assay where target DNA was bound to primary DNA on the gold electrode surface and secondary DNA labeled with polystyrene bead modified with PB nanoparticles. The use of polymeric spheres with PB particles could amplify the signal of for DNA detection down to the 50 fM level. Table 10.3 compares the performance of amperometric detection amplifies with PB-PS beads, in this work and other biosensors for DNA hybridization detection. Only the work of Liao *et al.* (2009) provided lower detection limit. Since the detection was carrier out by anodic stripping voltamogram which has preconcentration step of analyte onto the electrode prior to measurement and utra-low detection limit level can be achieved.

Table 11.3 Comparison of analytical method for DNA hybridization detection.

Analytical method	Label (molecule)	Detection limit	Linear range
Amperometric (This work)	**Yes (PB-PS bead)**	**50 fmol l^{-1}**	**10^{-13}-10^{-10} mol l^{-1}**
Piezoelectric			
Yao *et al.*, 2008	No	8.6 pg l^{-1}	N/A
SPR			
Jin *et al.*, 2009	No	50 ng ml^{-1}	50-400 ng ml^{-1}
Amperometric			
Mao *et al.*, 2008b	Yes (HRP)	0.1 nmol l^{-1}	0.1-1,000 nmol l^{-1}
Polsky *et al.*, 2006	Yes (Pt NPs)	1×10^{-11} mol l^{-1}	N/A
Sripping voltammetry			
Liao *et al.*, 2009	Yes (AuNPs)	0.35 amol l^{-1}	0.52–1,300 amol l^{-1}
Cai *et al.*, 2002a	Yes (AgNPs)	0.5 pmol l^{-1}	N/A

N/A = Not applicable

The performances of all SPR and electrochemical affinity biosensor systems are summarized in Table 10.4. The results showed that both SPR and electrochemical affinity biosensor can be applied for several analytes with high sensitivity, rapid analysis and good reproducibility. Therefore, these analytical methods can be applied as alternative method for other affinity binding analyzes.

Table 11.4 Performance of the surface plasmon resonance and electrochemical affinity biosensor systems for different analytes studied in this work.

Detection	Immobilized bioaffinity molecule	Analyte	Sensitivity of detection	Linear range	Detection limit	Reusable times	Analysis time
SPR	Anti-CA 125	CA 125	0.128±0.002 (milidegree/ Uml^{-1})	0.1-40 U ml^{-1}	0.1 U ml^{-1}	32	5 min
Capacitive	Anti-CA 125	CA 125	1.56±0.03 (milidegree/ Uml^{-1})	0.05-40 U ml^{-1}	0.05 U ml^{-1}	48	15 min
Capacitive	Bip D protein	*B. pseudomallei* antibody	11,000 times of dilution	-	30 –nF cm^{-2} (signal cut-off)	28	15 min
SPR	Anti-HSA using AuNPs	CA 125 HSA MCLR	4.21±0.04 (milidegree/ U ml^{-1}) 25.3 ± 0.5 (milidegree/ mol l^{-1}) 0.05 ± 0.01 (milidegree/ mol l^{-1})	0.01-40 U ml^{-1} 10^{-9}-10^{-5} mol l^{-1} 10^{-6}-10^{-3} mol l^{-1}	0.01 U ml^{-1} 10^{-9} mol l^{-1} 10^{-6} mol l^{-1}	No study No study No study	5 min 7 min 8 min
Capacitive	Anti-HSA using AuNPs	HSA MCLR Pen G	10.5 ± 0.5 (-nF cm^{-2}/ mol l^{-1}) 10.5 ±0.5 (-nF cm^{-2}/ mol l^{-1}) 7.2 ± 0.2 (-nF cm^{-2}/ mol l^{-1})	10^{-18}- 10^{-10} mol l^{-1} 10^{-14}-10^{-9} mol l^{-1} 10^{-15}-10^{-9} mol l^{-1}	10^{-18} mol l^{-1} 10^{-14} mol l^{-1} 10^{-15} mol l^{-1}	No study No study No study	15 min 20 min 15 min
Amperometric	DNA	DNA	3.7±0.2 (nA/mol l^{-1})	10^{-13}-10^{-10} mol.l^{-1}	10^{-13} mol.l^{-1}	No study	20 min

REFERENCES

Aizawa, H., Tozuka, M., Kurosawa, S., Kobayashi, K., Reddy, S.M. and Higuchi, M. 2007. Surface plasmon resonance-based trace detection of small molecules by competitive and signal enhancement immunoreaction. *Analytica Chimica Acta*. **591**: 191-194.

Alfonta, L., Singh, A.K., and Willner, I. 2001. Liposomes Labeled with Biotin and Horseradish Peroxidase: A Probe for the Enhanced Amplification of Antigen–Antibody or Oligonucleotide–DNA Sensing Processes by the Precipitation of an Insoluble Product on Electrodes. *Analytical Chemistry*. **73**: 91-102.

Armada, M. P. G., Losada, J., Zamora, M., Alonso, B., Cuadrado, I. and Casado, C. M. 2006. Electrocatalytical properties of polymethylferrocenyl dendrimers and their applications in biosensing. *Bioelectrochemistry*. **69**: 65-73.

Ambrosi, A., Merkoi, A. and Escosura-Muiz, A. 2008. Electrochemical analysis with nanoparticle-based biosystems. *TrAC Trends in Analytical Chemistry*. **27**: 568-584.

Andersson, K., Areskoug, D. and Hardenborg, E. 1999. Exploring buffer space for molecular interactions. *Journal of Molecular Recognition*. **12**: 310-315.

Andreescu, S.and Sadik, O.A. 2004. Trends and challenges in biochemical sensors for clinical and environmental monitoring. *Pure and Applied Chemistry*. **76**: 861–878.

Andreescu, S. and Luck, L.A. 2008. Studies of the binding and signaling of surface-immobilized periplasmic glucose receptors on gold nanoparticles: A glucose biosensor application. *Analytical Biochemistry*. **375**: 282-290.

Anthony, J. Killard, Brian. Deasy, Richard. O'Kennedy and Smyth M.R. 1995. Antibodies: production, functions and applications in biosensors. *trends in analytical chemistry*. **14**: 257-266.

Appassakij, H., Silpapojakul, K.R., Wansit, R. and Pornpatkul, M. 1990. Diagnostic value of the indirect hemagglutination test for melioidosis in an endemic area. *American Journal of Tropical Medicine and Hygiene*. **42**: 248-253.

Autheir, L., Grossiord, C. and Brossier, P. 2001. Gold nanoparticle-based quantitative electrochemical detection of amplified human cytomegalovirus DNA using disposable microband electrodes. *Analytical Chemistry.* **73**: 4450-4458.

Azek, F., Grossiord, C., Joannes, M., Limoges, B. and Brossier, P. 2000. Hybridization Assay at a Disposable Electrochemical Biosensor for the Attomole Detection of Amplified Human Cytomegalovirus DNA. *Analytical Biochemistry.* **284:** 107–113.

Babkina, S. S., Medyantseva, E. P., Budnikov, H. C. and Tyshlek, M. P. 1996. New Variants of Enzyme Immunoassay of Antibodies to DNA. *Analytical Chemistry.* **68**: 3827-3831.

Ballerstädt, R. and Ehwald, R. 1994. Suitability of aqueous dispersions of dextran and Concanavalin A for glucose sensing in different variants of the affinity sensor. *Biosensors and Bioelectronics.* **9**: 557-567.

Ballerstädt, R., Polak, A., Beuhler, A. and Frye, J. 2004. In vitro long-term performance study of a near-infrared fluorescence affinity sensor for glucose monitoring. *Biosensors and Bioelectronics.* **19**: 905-914.

Bange, A., Halsall, H. B. and Heineman, W. R. 2005. Microfluidic immunosensor systems. *Biosensors and Bioelectronics.* **20**: 2488-2503.

Bard, A.J. and Faulkner, L.R. 2001. Electrochemical methods; fundamentals and applications. New York, John Wiley & Sons, INC.

Bart, M., Stigter, E. C. A., Stapert, H. R., de Jong, G. J. and van Bennekom, W. P. 2005. On the response of a label-free interferon-[gamma] immunosensor utilizing electrochemical impedance spectroscopy. *Biosensors and Bioelectronics.* **21**: 49-59.

Belmont, A.S., Jaeger, S., Knopp, D., Niessner, R., Gauglitz, G. and Haupt, K. 2007. Molecularly imprinted polymer films for reflectometric interference spectroscopic sensors. *Biosensors and Bioelectronics.* **22**: 3267-3272.

Berggren, C. and Johansson, G. 1997. Capacitance Measurements of Antibody-Antigen Interactions in a Flow System. *Analytical Chemistry.* **69**: 3651 -3657.

Berggren, C., Staelhandske, P., Brundell, J. and Johansson, G. 1999. A Feasibility Study of a Capacitive Biosensor for Direct Detection of DNA Hybridization. *Electroanalysis*. **11**: 156-160.

Berggren, C., Bjarnason, B. and Johansson, G. 2001. Review; Capacitive Biosensors. *Electroanalysis*. **13**: 173-180.

Beusink, J.B., Lokate, A.M.C., Besselink, G.A.J., Pruijn, G.J.M. and Schasfoort, R.B.M. 2008. Angle-scanning SPR imaging for detection of biomolecular interactions on microarrays. *Biosensors and Bioelectronics*. **23**: 839-844.

Biomerieux® sa, VIDAS® CA 125 II™, France, 2004.

Birkert, O., Haake, H.M., A. Schotz, Mack, J.r., Brecht, A., Jung, G. and Gauglitz, G. 2000. A Streptavidin Surface on Planar Glass Substrates for the Detection of Biomolecular Interaction. *Analytical Biochemistry*. **282**: 200-208.

Bonanni, A., Esplandiu, M.J. and Valle. M. 2008. Signal amplification for impedimetric genosensing using gold-streptavidin nanoparticles. *Electrochimica Acta*. **53**: 4022-4029.

Bonroy, K., Frederix, F., Reekmans, G., Dewolf, E., Palma, R.D., Borghs, G., Declerck, P. and Goddeeris, B. 2006. Comparison of random and oriented immobilisation of antibody fragments on mixed self-assembled monolayers. *Journal of Immunological Methods*. **312**: 167-181.

Bontidean, I., Berggren, C., Johansson, G., Csoregi, E., Mattiasson, B., Lloyd, J.R., Jakeman, K.J. and Brown, N.L. 1998. Detection of Heavy Metal Ions at Femtomolar Levels Using Protein-Based Biosensors. *Analytical chemistry*. **70**: 4162-4169.

Bontidean, I., Lloyd, J.R., Hobman, J.L., Wilson, J.R., Csaregi, E., Mattiasson, B. and Brown, N.L. 2000. Bacterial metal-resistance proteins and their use in biosensors for the detection of bioavailable heavy metals. *Journal of Inorganic Biochemistry*. **79**: 225-229.

Bontidean, I., Ahlqvist. J., Mulchandani, A., Chen, W., Bae, W., Mehra, R.K., Mortari, A. and Caregi, E. 2003. Novel synthetic phytochelatin-based capacitive biosensor for heavy metal ion detection. *Biosensors and Bioelectronics*. **18**: 547-553.

Bosch, M.E., Sánchez, A.J. , Rojas, F.S. and Ojeda, C.B. 2007. Recent Development in Optical Fiber Belmont, A.S., Jaeger, S., Knopp, D., Niessner, R., Gauglitz, G. and Haupt, K. 2007. Molecularly imprinted polymer films for reflectometric interference spectroscopic sensors. *Biosensors and Bioelectronics.* **22**: 3267-3272.

Brecht, A., Gauglitz, G. and Polster, J. 1993. Interferometric immunoassay in a FIA-system: a sensitive and rapid approach in label-free immunosensing. *Biosensors and Bioelectronics.* **8**: 387-392.

Brecht, A., Piehler, J., Lang, G. and Gauglitz, G. 1995. A direct optical immunosensor for atrazine detection. *Analytica Chimica Acta.* **311**: 289-299.

Brosinger, F., Freimuth, H., Lacher, M., Ehrfeld, W., Gedig, E., Katerkamp, A., Spener, F.and Cammann, K. 1997a. A label-free affinity sensor with compensation of unspecific protein interaction by a highly sensitive integrated optical Mach-Zehnder interferometer on silicon. *Sensors and Actuators B: Chemical.* **44**: 350-355.

Brynda, E., Houska, M., Brandenburg, A. and Wikerst, A. 2002. Optical biosensors for real-time measurement of analytes in blood plasma. *Biosensors and Bioelectronics.* **17:** 665-675.

Buck, R.P., and Lindneri, E., 1994. Recommendations for nomenclature of ion-selective electrodes (IUPAC Recommendations 1994). *Pure and Applied Chemistry.* **66**: 2527-2536.

Byfield, M.P.and Abuknesha, R.A. 1994. Biochemical aspects of biosensors. *Biosensors & Bioelectronics.* **9**: 373-400.

Cai, H., Xu, Y., Zhu, N., He, P. and Fang, Y. 2002a. An electrochemical DNA hybridization detection assay based on a silver nanoparticle label. *Analyst.* **127**: 803–808.

Cai, H., Wang, Y., He, P. and Fang, Y. 2002b. Electrochemical detection of DNA hybridization based on silver-enhanced gold nanoparticle label. *Analytica Chimica Acta.* **469**: 165–172.

Carmon, K.S., Baltus, R.E. and Luck, L.A. 2005. A biosensor for estrogenic substances using the quartz crystal microbalance. *Analytical Biochemistry.* **345**: 277-283.

Campas, M. n. and Marty, J.L. 2007. Highly sensitive amperometric immunosensors for microcystin detection in algae. *Biosensors and Bioelectronics.* **22**: 1034-1040.

Caruso, F., Furlong, D.N., Niikura, K. and Okahata, Y. 1998. In-situ measurement of DNA immobilization and hybridization using a 27 MHz quartz crystal microbalance. *Colloids and Surfaces B: Biointerfaces.* **10**: 199-204.

Cao, C. and Sim, S. J. 2007. Signal enhancement of surface plasmon resonance immunoassay using enzyme precipitation-functionalized gold nanoparticles: A femto molar level measurement of anti-glutamic acid decarboxylase antibody. *Biosensors and Bioelectronics.* **22**: 1874-1880.

Casuso, I., Pla-Roca, M., Gomila, G., Samitier, J., Minic, J., Persuy, M.A., Salesse, R. and Pajot-Augy, E. 2008. Immobilization of olfactory receptors onto gold electrodes for electrical biosensor. *Materials Science and Engineering: C.* **28**: 686-691.

Chah, S., Hutter, E., Roy, D., Fendler, J. H. and Yi, J. 2001. The effect of substrate metal on 2-aminoethanethiol and nanoparticle enhanced surface plasmon resonance imaging. *Chemical Physics.* **272**: 127-136.

Chambers, J.P., Arulanandam, B.P., Matta, L.L., Weis, A. and Valdes, J.J. 2008. Biosensor recognition elements. *Current Issues in Molecular Biology.* **10**: 1-12.

Chang, Y.F., Chen, R.C., Lee, Y.J., Chao, S.C., Su, L.C., Li, Y.C., Chou, C. 2008. Localized surface plasmon coupled fluorescence fiber-optic biosensor for alpha-fetoprotein detection in human serum. *Biosensors and Bioelectronics.* In press.

Chantratita, N., Wuthiekanun, V., Thanwisai, A., Limmathurotsakul, D., Cheng, A.C., Chierakul, W., Day, N.P. J. and Peacock, S.J., 2007. Accuracy of Enzyme-Linked Immunosorbent Assay Using Crude and Purified Antigens for Serodiagnosis of Melioidosis. *Clinical and Vaccine immunology.* **14**: 110-111

Charles, P.T., Conrad, D.W., Jacobs, M.S., Bart, J.C. and Kusterbeck, A.W. 1995. Synthesis of a Fluorescent Analogue of Polychlorinated Biphenyls for Use in a Continuous Flow Immunosensor Assay. *Bioconjugate Chemistry.* **6**: 691.

Chegel, V., Shirshov, Y., Avilov, S., Demchenko, M. and Mustafaev, M. 2002. A novel aldehyde dextran sulfonate matrix for affinity biosensors. *Journal of biochemical and biophysical methods.* **50:** 201-216.

Chen, X., Zhang, X.E., Chai, Y.Q., Hu, W.P., Zhang, Z.P., Zhang, X.M. and Cass A.E. 1998. DNA optical sensor: a rapid method for the detection of DNA hybridization. *Biosensors and Bioelectronics.* **13:** 451-458.

Chen, J., Yan, F., Dai, Z. and Ju, H. 2005. Reagentless amperometric immunosensor for human chorionic gonadotrophin based on direct electrochemistry of horseradish peroxidase. *Biosensors and Bioelectronics.* **21**: 330-336.

Chen, H., Jiang, J.H., Huang, Y., Deng, T., Li, J.S., Shen, G.L. and Yu, R.Q. 2006a. An electrochemical impedance immunosensor with signal amplification based on Au-colloid labeled antibody complex. *Sensors and Actuators B: Chemical.* **117**: 211-218.

Chen, J., Tang, J., Yan, F. and Ju, H. 2006b. A gold nanoparticles/sol-gel composite architecture for encapsulation of immunoconjugate for reagentless electrochemical immunoassay. *Biomaterials.* **27**: 2313-2321.

Chen, Z.P., Peng, Z.F., Luo, Y., Qu, B., Jiang, J.H., Zhang, X.B. Shen, G.L. and Yu, R.Q. 2007. Successively amplified electrochemical immunoassay based on biocatalytic deposition of silver nanoparticles and silver enhancement. Biosensors and Bioelectronics. 23: 485–491.

Chen, J., Zhang, J., Huang, L., Lin, X. and Chen, G. 2008a. Hybridization biosensor using 2-nitroacridone as electrochemical indicator for detection of short DNA species of Chronic Myelogenous Leukemia. *Biosensors and Bioelectronics.* **24**: 349-355.

Chen, Z.P., Peng, Z.F., Jiang, J.H., Zhang, X.B., Shen, G.L. and Yu, R.Q. 2008b. An electrochemical amplification immunoassay using biocatalytic metal deposition coupled with anodic stripping voltammetric detection. *Sensors and Actuators B: Chemical.* **129**: 146-151.

Chen, S., Yuan, R., Chai, Y., Xu, Y., Min, L. and Li, N. 2008c. A new antibody immobilization technique based on organic polymers protected Prussian blue nanoparticles and gold colloidal nanoparticles for amperometric immunosensors. *Sensors and Actuators B: Chemical.* **135**: 236-244.

Chen, S.H., Wu, V. C. H., Chuang, Y.C. and Lin, C.S. 2008d. Using oligonucleotide-functionalized Au nanoparticles to rapidly detect foodborne pathogens on a piezoelectric biosensor. *Journal of Microbiological Methods.* **73**: 7-17.

Chen, S., Yuan, R., Chai, Y., Xu, Y., Min, L. and Li, N. 2008e. A new antibody immobilization technique based on organic polymers protected Prussian blue nanoparticles and gold colloidal nanoparticles for amperometric immunosensors. *Sensors and Actuators B.* **135**: 236–244.

Chen, P.R. and He, C. 2008. Selective recognition of metal ions by metalloregulatory proteins. *Current Opinion in Chemical Biology.* **12**: 214-221.

Cheng, Z., Wang, E. and Yang, X. 2001. Capacitive detection of glucose using molecularly imprinted polymers. *Biosensors & Bioelectronics.* **16**: 179-185.

Cheng, A.C. and Currie, B.J. 2005. Melioidosis: epidemiology, pathophysiology, and management. *Clinical microbiology reviews.* **18**: 383-416.

Cheng, A.C., Wuthiekanun, V., Limmathurotsakul, D., Chierakul, W. and Peacock, S.J. 2008. Intensity of exposure and incidence of melioidosis in Thai children. *Transactions of the Royal Society of Tropical Medicine and Hygiene.* **102/S1**: S37-S39.

Choi, J.W., Kang, D.Y., Jang, Y.H., Kim, H.H., Min. J. and Oh, B.K. 2008. Ultra-sensitive surface plasmon resonance based immunosensor for prostate-specific antigen using gold nanoparticle-antibody complex. *Colloids and Surfaces A: Physicochemical and Engineering Aspects.* **313-314**: 655-659.

Chou, S.F., Hsu, W.L., Hwang, J.M. and Chen, C.Y. 2004. Development of an immunosensor for human ferritin, a nonspecific tumor marker, based on surface plasmon resonance. *Biosensors and Bioelectronics.* **19**: 999-1005.

Chu, X., Fu, X., Chen, K., Shen, G.L. and Yu, R.Q. 2005a. An electrochemical stripping metalloimmunoassay based on silver-enhanced gold nanoparticle l abel. *Biosensors and Bioelectronics.* **20**: 1805–1812.

Chu, X., Xiang, Z.F., Fu, X., Wang, S.P., Shen, G.L., Yu, R.Q. 2005b. Silver-enhanced colloidal gold metalloimmunoassay for *Schistosoma japonicum* antibody detection. *Journal of Immunological Methods.* **301**: 77–88.

Chu, X., Zhao, Z.L., Shen, G.L. and Yu, R.Q. 2006. Quartz crystal microbalance immunoassay with dendritic amplification using colloidal gold immunocomplex. *Sensors and Actuators B.* **114**: 696–704.

Chumbimuni-Torres, K. Y., Dai, Z., Rubinova, N., Xiang, Y., Pretsch, E., Wang, J. and Bakker, E. 2006. Potentiometric Biosensing of Proteins with Ultrasensitive Ion-Selective Microelectrodes and Nanoparticle Labels. *Journal of the American Chemical Society.* **128**: 13676-13677.

Chumbimuni-Torres, K.Y., Dai, Z., Rubinova, N., Xiang, Y., Pretsch, E., Wang, J., and Bakker E. 2006. Potentiometric Biosensing of Proteins with Ultrasensitive Ion-Selective Microelectrodes and Nanoparticle Labels. *Journal of the American Chemical Society.* **130 (2):** 410-411.

Chung, J. W., Kim, S. D., Bernhardt, R. and Pyun, J. C. 2005. Application of SPR biosensor for medical diagnostics of human hepatitis B virus (hHBV). *Sensors and Actuators B: Chemical.* **111-112**: 416-422.

Chung, J.W., Bernhardt, R.and Pyun ,J.C. 2006. Additive assay of cancer marker CA 19-9 by SPR biosensor. *Sensors and Actuators B: Chemical.* **118:** 28-32.

Corbisier, P. and van der Lelie D. 1999. Whole cell- and protein-based biosensors for the detection of bioavailable heavy metals in environmental samples. *Analytica Chimica Acta.* **387**: 235-244.

Corso, C. D., Stubbs, D. D., Lee, S.H., Goggins, M., Hruban, R. H. and Hunt, W. D. 2006. Real-time detection of mesothelin in pancreatic cancer cell line supernatant using an acoustic wave immunosensor. *Cancer Detection and Prevention.* **30**: 180-187.

Csordas, A.T., Delwiche, M.J. and Barak, J.D. 2008. Nucleic acid sensor and fluid handling for detection of bacterial pathogens. *Sensors and Actuators B: Chemical.* **134**: 1-8.

Cui, R., Huang, H., Yin, Z., Gao, D. and Zhu, J.J. 2008. Horseradish peroxidase-functionalized gold nanoparticle label for amplified immunoanalysis based on gold nanoparticles/carbon nanotubes hybrids modified biosensor. *Biosensors and Bioelectronics.* **23**: 1666-1673.

Currie, B.J., Fisher, D.A., Howard, D.M., Burrow, J.N., Selvanayagam, S., Snelling, P.L. 2000. The epidemiology of melioidosis in Australia and Papua New Guinea. *Acta Tropica.* **74**: 121-127.

Dai, Z., Yan, F., Chen, J. and Ju, H. 2003. Reagentless Amperometric Immunosensors Based on Direct Electrochemistry of Horseradish Peroxidase for Determination of Carcinoma Antigen-125. *Analytical Chemistry.* **75**: 5429-5434.

Daniel, M.C. and Astruct, D. 2004. Gold Nanoparticles: Assembly, Supramolecular Chemistry, Quantum-Size-Related Properties, and Applications toward Biology, Catalysis, and Nanotechnology. *Chemical Reviews.* **104**: 293-346.

Deobagkar, D. D., Limaye, V., Sinha, S. and Yadava, R. D. S. 2005. Acoustic wave immunosensing of Escherichia coli in water. *Sensors and Actuators B: Chemical.* **104**: 85-89.

Dequaire, M., Degrand, C. and Limoges, B. 2000. An Electrochemical Metalloimmunoassay Based on a Colloidal Gold Label. *Analytical Chemistry.* **72**: 5521-5528.

Dharuman, V., Nebling, E., Grunwald, T., Albers, J., Blohm, L., Elsholz, B., Warl, R. and Hintsche, R. 2006. DNA hybridization detection on electrical microarrays using coulostatic pulse technique. *Biosensors and Bioelectronics.* **22**: 744-751.

Ding,Y., Wang, H., Shen, G. and Yu, R. 2005. Enzyme-catalyzed amplified immunoassay for the detection of *Toxoplasma gondii* -specific IgG using Faradaic impedance spectroscopy, CV and QCM. *Analytical Bioanalytical Chemistry.* **382**: 1491–1499.

Ding, Y., Liu, J., Wang, H., Shen, G. and Yu, R. 2007. A piezoelectric immunosensor for the detection of [alpha]-fetoprotein using an interface of gold/hydroxyapatite hybrid nanomaterial. *Biomaterials.* **28**: 2147-2154.

Ding, C., Zhong, H. and Zhang, S. 2008a. Ultrasensitive flow injection chemiluminescence detection of DNA hybridization using nanoCuS tags. *Biosensors and Bioelectronics.* **23**: 1314-1318.

Ding, Y., Lu, H., Shi, G., Liu, J., Shen, G. and Yu, R. 2008b. Cell-based immobilization strategy for sensitive piezoelectric immunoassay of total prostate specific antigen. *Biosensors and Bioelectronics.* **24**: 228-232.

Ding, C., Zhao, F., Zhang, M. and Zhang, S. 2008. Hybridization biosensor using 2,9-dimethyl-1,10-phenantroline cobalt as electrochemical indicator for detection of hepatitis B virus DNA. *Bioelectrochemistry.* **72**: 28-33.

Djellouli, N., Rochelet-Dequaire, M., Limoges, B., Druet, M. and Brossier, P. 2007. Evaluation of the analytical performances of avidin-modified carbon sensors based on a mediated horseradish peroxidase enzyme label and their application to the amperometric detection of nucleic acids. *Biosensors and Bioelectronics.* **22**: 2906-2913.

Dostalek, J., Homola, J., Miler, M. 2005. Rich information format surface plasmonre sonance biosensor based on array of diffraction gratings. *Sensors and Actuators B.* **107**: 154–161.

Drapp, B. , Piehler, J. , Brecht, A. , Gauglitz, G. , Luff, B.J. , Wilkinson, J.S. ,Ingenhoff, J. 1997. Integrated optical Mach-Zehnder interferometers as simazine immunoprobes. *Sensors and Actuators B.* **38-39**: 277-282.

Du, D., Yan, F., Liu, S. and Ju, H. 2003. Immunological assay for carbohydrate antigen 19-9 using an electrochemical immunosensor and antigen immobilization in titania sol-gel matrix. *Journal of Immunological Methods.* **283**: 67-75.

Du, D., Xu, X., Wang, S. and Zhang, A. 2007. Reagentless amperometric carbohydrate antigen 19-9 immunosensor based on direct electrochemistry of immobilized horseradish peroxidase. *Talanta.* **71**: 1257-1262.

Du, D., Ding, J., Tao, Y., Li, H. and Chen, X. 2008. CdTe nanocrystal-based electrochemical biosensor for the recognition of neutravidin by anodic stripping voltammetry at electrodeposited bismuth film. *Biosensors and Bioelectronics.* **24**: 863-868.

Dudak, F.C. and Boyacı, I.H. 2007. Development of an immunosensor based on surface plasmon resonance for enumeration of Escherichia coli in water samples. *Food Research International.* **40**: 803-807.

Duman, M., Saber, R. and Piskin, E. 2003. A new approach for immobilization of oligonucleotides onto piezoelectric quartz crystal for preparation of a nucleic acid sensor for following hybridization. *Biosensors and Bioelectronics.* **18**: 1355-1363.

Dungchai, W., Siangproh, W., Chaicumpa, W., Tongtawe, P. and Chailapakul. O. 2008. Salmonella typhi determination using voltammetric amplification of nanoparticles: A highly sensitive strategy for metalloimmunoassay based on a copper-enhanced gold label. *Talanta.* **77**: 727-732.

Dutra, R.F., Mendes, R.K., Lins da Silva, V. and Kubota, L.T. 2007a. Surface plasmon resonance immunosensor for human cardiac troponin T based on self-assembled monolayer. *Journal of Pharmaceutical and Biomedical Analysis.* **43**: 1744-1750.

Dutta, T., Garg, M. and Jain, N. K. 2008. Poly(propyleneimine) dendrimer and dendrosome mediated genetic immunization against hepatitis B. *Vaccine.* **26**: 3389-3394.

Duverger, E., Frison, N., Roche, A.C. and Monsigny, M. 2003. Carbohydrate-lectin interactions assessed by surface plasmon resonance. *Biochimie.* **85**: 167-179.

Eggins, B.R. 1996. *Biosensors: an introduction.* Chichester: John Wiley & Sons Ltd.

Endo, K., Matsuoka, Y., Nakashima, T., Fujli, S., Kunimatsu, M., Saga, T., Watanabe, Y., Kawamura, Y., Koizumi, M., Konishi, J., Torizuka, K. and Bast Jr., R. C. 1988. Development of a new sensitive IRMA for CA 125: mixed use of two monoclonal antibodies reaction with separate epitopes. . *Journal of Tumor Marker Oncology.* **3**: 65-71.

Endo, T., Okuyama, A., Matsubara, Y., Nishi, K., Kobayashi, M., Yamamura, S., Morita, Y., Takamura, Y., Mizukami, H. and Tamiya, E. 2005. Fluorescence-based assay with enzyme amplification on a micro-flow immunosensor chip for monitoring coplanar polychlorinated biphenyls. *Analytica Chimica Acta* **531**: 7-13.

Endo, T., Yamamura, S., Kerman, K. and Tamiya, E. 2008. Label-free cell-based assay using localized surface plasmon resonance biosensor. *Analytica Chimica Acta.* **614**: 182-189.

Epstein, J.R. and Walt, D.R. 2003. Fluorescence-based fibre optic arrays: a universal platform for sensing. *Chemical Society Review.* **32**: 203-214.

Erdem, A. 2007. Review: Nanomaterial-based electrochemical DNA sensing strategies. *Talanta.* **74**: 318-325.

Erskine, P.T., Knight, M.J., Ruaux, A., Mikolajek, H., Wong Fat Sang, N., Withers, J., Gill, R., Wood, S. P., Wood, M., Fox, G. C. and Cooper, J. B. High Resolution Structure of BipD: An Invasion Protein Associated with the Type III Secretion System of Burkholderia Pseudomallei. *Journal of Molecular Biology.* **363**: 125–136.

Eurachem Working Group, 1998. Fitness for Purpose of Analytical Methods: A Laboratory Guide to Method Validation and Related Topics Eurachem Guide, 1st English ed. 1.0. LGC (Teddington) Ltd.

Evtugyn, G. A., Eremin, S. A., Shaljamova, R. P., Ismagilova, A. R. and Budnikov, H. C. 2006. Amperometric immunosensor for nonylphenol determination based on peroxidase indicating reaction. *Biosensors and Bioelectronics.* **22**: 56-62.

Fernández-Sánchez, C., Gallardo-Soto, A. M., Rawson, K., Nilsson, O. and McNeil, C. J. 2004. Quantitative impedimetric immunosensor for free and total prostate specific antigen based on a lateral flow assay format. *Electrochemistry Communications.* **6**: 138-143.

Fernández-Sánchez, C., McNeil, C. J. and Rawson, K. 2005. Electrochemical impedance spectroscopy studies of polymer degradation: application to biosensor development. *TrAC Trends in Analytical Chemistry.* **24**: 37-48.

Feng, X., Castracane, J., Tokranova, N., Gracias, A., Lnenicka, G. and Szaro, B.G.2007a. A living cell-based biosensor utilizing G-protein coupled receptors: Principles and detection methods. *Biosensors and Bioelectronics.* **22**: 3230-3237.

Feng, K., Li, J., Jiang, J.H., Shen, G.L. and Yu, R.Q. 2007b. QCM detection of DNA targets with single-base mutation based on DNA ligase reaction and biocatalyzed deposition amplification. *Biosensors and Bioelectronics.* **22**: 1651-1657.

Feng, Y., Yang, T., Zhang, W., Jiang, C. and Jiao, K. 2008. Enhanced sensitivity for deoxyribonucleic acid electrochemical impedance sensor: Gold nanoparticle/polyaniline nanotube membranes. *Analytica Chimica Acta.* **616**: 144-151.

Fu, Z., Liu, H. and Ju, H. 2006. Flow-Through Multianalyte Chemiluminescent Immunosensing System with Designed Substrate Zone-Resolved Technique for Sequential Detection of Tumor Markers. *Analytical Chemistry.* **78:** 6999-7005.

Fu, E., Ramsey, S.A. and Yager, P. 2007. Dependence of the signal amplification potential of colloidal gold nanoparticles on resonance wavelength in surface plasmon resonance-based detection. *Analytica Chimica Acta.* **599**: 118–123.

Fu, Z., Yan, F., Liu, H., Lin, J. and Ju, H. 2008. A channel-resolved approach coupled with magnet-captured technique for multianalyte chemiluminescent immunoassay. *Biosensors and Bioelectronics.* **23**: 1422-1428.

Furuki, M., Kameoka, J., Craighead, H.G. and Isaacson, M.S. 2001. Surface plasmon resonance sensors utilizing microfabricated channels. *Sensors and Actuators B.* **79**: 63-69.

Gauglitz, G. 2005. Multiple reflectance interference spectroscopy measurements made in parallel for binding studies. *Review of Scientific Instruments* **76**, 06224-06222-10.

Gebbert, A., Alvarez-Icaza, M., Stocklein, W. and Schmid, R. D. 1992. Real-time monitoring of immunochemical interactions with a tantalum capacitance flow-through cell. *Analytical Chemistry.* **64**: 997-1003.

Geisler, J., Ekse, D., Helle, H., Duong, N. K. and Lanning, P. E. 2008. An optimised, highly sensitive radioimmunoassay for the simultaneous measurement of estrone, estradiol and estrone sulfate in the ultra-low range in human plasma samples. *The Journal of Steroid Biochemistry and Molecular Biology.* **109**: 90-95.

Gerard, M., Chaubey, A. and Malhotra, B.D. 2002. Application of conducting polymers to biosensors. *Biosensors and Bioelectronics.* **17**: 345-359.

Gilmore, G., Barnes, J., Ketheesan, N. and Norton, R. 2007. Use of Antigens Derived from *Burkholderia pseudomallei*, *B. thailandensis*, and *B. cepacia* in the Indirect Hemagglutination Assay for Melioidosis. *Clinical and vaccine immunology.* **14**: 1529-1531.

Gobi, K.V., Tanaka, H., Shoyama, Y. and Miura, N. 2005. Highly sensitive regenerable immunosensor for label-free detection of 2,4-dichlorophenoxyacetic acid at ppb levels by using surface plasmon resonance imaging. *Sensors and Actuators B: Chemical.* **111-112**: 562-571.

Gobi, K.V., Iwasaka, H. and Miura, N. 2007. Self-assembled PEG monolayer based SPR immunosensor for label-free detection of insulin. *Biosensors and Bioelectronics.* **22**: 1382-1389.

Gong, F.C., Tang, L., Shen, G.L. and Yu, R.Q. 2004. Fluorometric enzyme immunosensing system based on a renewable immunoreaction platform for the detection of *Schistosoma japonicum* antibody. *Talanta.* **62**: 735–740.

Gole, A., Dash, C., Ramakrishnan, V., Sainkar, S. R., Mandale, A. B., Rao, M. and Sastry, M. 2001. Pepsin–Gold Colloid Conjugates: Preparation, Characterization, and Enzymatic Activity. *Langmuir*. **17**: 1674-1679.

Gonzalez-Martinez, M.A., Puchades, R. and Maquieira, A. 2001.Comparison of Multianalyte Immunosensor Formats for On-Line etermination of Organic Compounds. *Analytical chemistry*. **73**: 4326-4332.

Green, R.J., Frazier, R.A., Shakeshe, K.M., Davies, M.C., Roberts, C.J., Tendler, S.J.2000. Review: Surface plasmon resonance analysis of dynamic biological interactions with biomaterials. *Biomaterials*. **21**: 1823-1835

Gu, H.Y., Yu, A.M., Chen, H.Y. 2001. Direct electron transfer and characterization of hemoglobin immobilized on a Au colloid–cysteamine-modified gold electrode. *Journal of Electroanalytical Chemistry*. **516**: 119–126.

Guo, S. and Dong, S. 2009. Biomolecule-nanoparticle hybrids for electrochemical biosensors. *TrAC Trends in Analytical Chemistry*. **28**: 96-109.

Gupta, G. and Kondoh, J. 2007. Tuning and sensitivity enhancement of surface plasmon resonance sensor. *Sensors and Actuators B: Chemical*. **122:** 381-388.

Gupta, G., Sugimoto, M., Matsui, Y., Kondoh, J. 2008. Use of a low refractive index prism in surface plasmon resonance biosensing. *Sensors and Actuators B*. **130**: 689–695.

Hanaee, H., Ghourchian, H. and Ziaee, A.A. 2007. Nanoparticle-based electrochemical detection of hepatitis B virus using stripping chronopotentiometry. *Analytical Biochemistry*. **370**: 195–200.

Hason, S., Pivonkova, H., Vetterl, V. and Fojta, M. 2008. Label-free sequence-specific DNA sensing using copper-enhanced anodic stripping of purine bases at boron-doped diamond electrodes. *Analytical chemistry*. **80**: 2391-2399.

Hassen, W.M. and Chaix, C., Abdelghani, A., Bessueille, F., Leonard, D. and Jaffrezic-Renault, N. 2008. An impedimetric DNA sensor based on functionalized magnetic nanoparticles for HIV and HBV detection. *Sensors and Actuators B: Chemica*l. **134**: 755-760.

He, Z., Gao, N. and Jin, W. 2003. Determination of tumor marker CA125 by capillary electrophoretic enzyme immunoassay with electrochemical detection. *Analytica Chimica Acta.* **497**: 75–81.

He, X., Yuan, R., Chai, Y., Zhang, Y. and Shi, Y. 2007. A new antibody immobilization strategy based on electro-deposition of gold nanoparticles and Prussian Blue for label-free amperometric immunosensor. *Biotechnology Letters.* **29**:149–155.

He, X., Yuan, R., Chai, Y. and Shi, Y. 2008. A sensitive amperometric immunosensor for carcinoembryonic antigen detection with porous nanogold film and nano-Au/chitosan composite as immobilization matrix. *Journal of Biochemical and Biophysical Methods.* **70**: 823-829.

He, P., Wang, Z., Zhang, L. and Yang, W. 2009. Development of a label-free electrochemical immunosensor based on carbon nanotube for rapid determination of clenbuterol. *Food Chemistry.* **112**: 707-714.

HedstrÖm, M., Galaev, I.Y. and Mattiasson, B. 2005. Continuous measurements of a binding reaction using a capacitive biosensor. *Biosensors and Bioelectronics.* **21**: 41–48.

Heideman, R.G., Kooyman, R.P. and Greve, J. 1993. Performance of a highly sensitive optical waveguide Mach-Zehnder interferometer immunosensor. *Sensors and Actuators B: Chemical.* **10:** 209-217.

Henry, J., Anand, A., Chowdhury, M., Cote, G., Moreir, R. and Good, T. 2004. Development of a nanoparticle-based surface-modified fluorescence assay for the detection of prion proteins. *Analytical Biochemistry.* **334**: 1–8.

Herrmann, S., Leshem, B., Landes, S., Rager-Zisman, B. and Marks, R.S. 2005. Chemiluminescent optical fiber immunosensor for the detection of anti-West Nile virus IgG. *Talanta.* **66:** 6-14.

Hoa, X.D., Kirk, A.G. and Tabrizian, M. 2007. Review: Towards integrated and sensitive surface plasmon resonance biosensors: A review of recent progress. *Biosensors and Bioelectronics.* **23**: 151–160.

Hohensinner, V., Maier, I. and Pittner, F. 2007. A gold cluster-linked immunosorbent assay': Optical near-field biosensor chip for the detection of allergenic [beta]-lactoglobulin in processed milk matrices. *Journal of Biotechnology.* **130**: 385-388.

Homola, J., Koudela, I. and Yee, S.S. 1999. Surface plasmon resonance sensors based on diffraction gratings and prism couplers: sensitivity comparison. *Sensors and Actuators B: Chemical.* **54:** 16-24.

Homola, J. 2008. Surface Plasmon Resonance Sensors for Detection of Chemical and Biological Species. *Chemical. Reviews.* **108 (2)**: 462-493.

Hong, B. and Kang, K.A. 2006. Biocompatible, nanogold-particle Fluorescence enhancer for fluorophore mediated, optical immunosensor. *Biosensors and Bioelectronics.* **21**: 1333–1338.

Hong, S., Kang, T., Oh, S., Moon, J., Choi, I., Choi, K. and Yi, J. 2008. Label-free sensitive optical detection of polychlorinated biphenyl (PCB) in an aqueous solution based on surface plasmon resonance measurements. *Sensors and Actuators B: Chemical.* **134:** 300-306.

Hong, C., Yuan, R., Chai, Y. and Zhuo, Y. 2009. Ferrocenyl-doped silica nanoparticles as an immobilized affinity support for electrochemical immunoassay of cancer antigen 15-3. *Analytica Chimica Acta.* **633**: 244-249.

Howard, K. and Inglis, T.J.J. 2005. Disinfection of Burkholderia pseudomallei in potable water. *Water Research.* **39**: 1085–1092.

Hsieh, B.Y., Chang, Y.F., Ng, M.Y., Liu, W.C., Lin, C.H., Wu, H.T.and Chou, C. 2007. Localized Surface Plasmon Coupled Fluorescence Fiber-Optic Biosensor with Gold Nanoparticles. *Analytical Chemistry.* **7(79)**: 3487-3493.

Hsieh, B.Y., Chang, Y.F., Ng, M.Y., Liu, W.C., Lin, C.H., Wu H.T. and Chou C. 2007. Localized Surface Plasmon Coupled Fluorescence Fiber-Optic Biosensor with Gold Nanoparticles. *Analytical Chemistry.* **79:** 3487-3493.

Hu, S.Q., Wu, Z.Y., Zhou, Y.M., Cao, Z.X., Shen, G.L. and Yu, R.Q. 2002. Capacitive immunosensor for transferrin based on an o-aminobenzenthiol oligomer layer. *Analytica Chimica Acta.* **458**: 297-304.

Hu, S.Q., Xie, J.W., Xu, Q.H., Rong, K.T., Shen, G.L. and Yu, R.Q. 2003. A label-free electrochemical immunosensor based on gold nanoparticles for detection of paraoxon. *Talanta.* **61**: 769-777.

Hu, S.Q., Xie, Z.M., Lei, C.X., Shen, G.L. and Yu, R.Q. 2005. The integration of gold nanoparticles with semi-conductive oligomer layer for development of capacitive immunosensor. *Sensors and Actuators B.* **106**: 641–647.

Huang, H., Liu, Z. and Yang, X. 2006. Application of electrochemical impedance spectroscopy for monitoring allergen-antibody reactions using gold nanoparticle-based biomolecular immobilization method. *Analytical Biochemistry.* **356**: 208-214.

Hun, X. and Zhang, Z. 2007. A novel sensitive staphylococcal enterotoxin C1 fluoroimmunoassay based on functionalized fluorescent core-shell nanoparticle labels. *Food Chemistry.* **105**: 1623–1629.

Iga, M., Seki, A. and Watanabe, K. 2004. Hetero-core structured fiber optic surface plasmon resonance sensor with silver film. *Sensors and Actuators B.* **101**: 368–372.

Ince, R. and Narayanaswamy, R. 2006. Analysis of the performance of interferometry, surface plasmon resonance and luminescence as biosensors and chemosensors. *Analytica Chimica Acta.* **569:** 1-20.

Indyk, H.E. 2009. Development and application of an optical biosensor immunoassay for [alpha]-lactalbumin in bovine milk. *International Dairy Journal.* **19:** 36-42.

Ionescu, R. E., Cosnier, S., Herzog, G., Gorgy, K., Leshem, B., Herrmann, S. and Marks, R. S. 2007. Amperometric immunosensor for the detection of anti-West Nile virus IgG using a photoactive copolymer. *Enzyme and Microbial Technology.* **40**: 403-408.

Ionescu, R. E., Cosnier, S., Herzog, G., Gorgy, K., Leshem, B., Herrmann, S. and Marks, R. S. 2007. Amperometric immunosensor for the detection of anti-West Nile virus IgG using a photoactive copolymer. *Enzyme and Microbial Technology.* **40**: 403-408.

Ivnitski, D., Abdel-Hamid, I., Atanasov, P., Wilkins, E. and Stricker, S. 2000. Application of Electrochemical Biosensors for Detection of Food Pathogenic Bacteria. *Electroanalysis.* **12**: 317-325.

Jena, B.K.and Raj, C. R. 2006. Electrochemical Biosensor Based on Integrated Assembly of Dehydrogenase Enzymes and Gold Nanoparticles. *Anaytical Chemistry.* **78 (18):** 6332-6339.

Jia, J., Wang, B., Wu, A., Cheng, G., Li, Z., and Dong, S. 2000. A Method to Construct a Third-Generation Horseradish Peroxidase Biosensor: Self-Assembling Gold Nanoparticles to Three-Dimensional Sol-Gel Network. *Analytical Chemistry.* **74**: 2217- 2223.

Jiang, X., Li, D., Xu, X., Ying, Y., Li, Y., Ye, Z. and Wang, J. 2008. Immunosensors for detection of pesticide residues. *Biosensors and Bioelectronics.* **23**: 1577-1587.

Jiang, D., Tang, J., Liu, B., Yang, P., Shen, X. and Kong, J. 2003. Covalently coupling the antibody on an amine-self-assembled gold surface to probe hyaluronan-binding protein with capacitance measurement. *Biosensor and Bioelectronic.* **18**: 1183-1191.

Jie, G., Huang, H., Sun, X. and Zhu, J.J. 2008. Electrochemiluminescence of CdSe quantum dots for immunosensing of human prealbumin. *Biosensors and Bioelectronics.* **23**: 1896-1899.

Jin, W., Lin, X., Lv, S., Zhang, Y., Jin, Q. and Mu, Y. 2009. A DNA sensor based on surface plasmon resonance for apoptosis-associated genes detection. Biosensors *and Bioelectronics.* **24**: 1266–1269.

Junhui, Z., Hong,C. and Ruifu, Y. 1997. DNA based biosensors.*Biotechnology Advances.* **15**: 43-58.

Jyoung, J.Y., Hong, S., Lee, W. and Choi, J.W. 2006. Immunosensor for the detection of Vibrio cholerae O1 using surface plasmon resonance. *Biosensors and Bioelectronics.* **21**: 2315-2319.

Kalogianni, D. P., Koraki, T., Christopoulos, T. K. and Ioannou, P. C. 2006. Nanoparticle-based DNA biosensor for visual detection of genetically modified organisms. *Biosensors and Bioelectronics.* **21**: 1069-1076.

Karube, I. and Nomura, Y. 2000. Enzyme sensors for environmental analysis. *Journal of Molecular Catalysis B: Enzymatic.* **10**: 177-181.

Karyakin, A. A., Karyakina, E. E. and Gorton, L. 2000. Amperometric Biosensor for Glutamate Using Prussian Blue-Based "Artificial Peroxidase" as a Transducer for Hydrogen Peroxide. *Analytical Chemistry.* **72**: 1720-1723.

Karyakin, A. A. 2001. Prussian Blue and Its Analogues: Electrochemistry and Analytical Applications. *Electroanalysis.* **13**: 813-819.

Kawazumi, H., Gobi, K. V., Ogino, K., Maeda, H. and Miura, N. 2005. Compact surface plasmon resonance (SPR) immunosensor using multichannel for simultaneous detection of small molecule compounds. *Sensors and Actuators B: Chemical.* **108**: 791-796.

Kawaguchi, T., Shankaran, D.R., Kim, S.J., Gobi, K.V., Matsumoto, K., Toko, K. and Miura, N. 2007. Fabrication of a novel immunosensor using functionalized self-assembled monolayer for trace level detection of TNT by surface plasmon resonance. *Talanta .***72**: 554-560.

Kawaguchi, T., Shankaran, D. R., Kim, S. J., Matsumoto, K., Toko, K. and Miura, N. 2008. Surface plasmon resonance immunosensor using Au nanoparticle for detection of TNT. *Sensors and Actuators B.* **133**: 467-472.

Kawde, A. N. and Wang, J. 2004. Amplified Electrical Transduction of DNA Hybridization Based on Polymeric Beads Loaded with Multiple Gold Nanoparticle Tags. *Electroanalysis.* **16**: 101-107.

Kerman, K., Morita, Y., Takamura, Y., Ozsoz, M. and Tamiya, E. 2004. Modification of *Escherichia coli* single-stranded DNA binding protein with gold nanoparticles for electrochemical detection of DNA hybridization. *Analytica Chimica Acta.* **510**: 169–174.

Kerman, K., Endo, T., Tsukamoto, M., Chikae, M., Takamura, Y. and Tamiya, E.2007. Quantum dot-based immunosensor for the detection of prostate-specific antigen using fluorescence microscopy. *Talanta.* **71**: 1494-1499.

Kerman, K., Saito, M., Tamiya, E., Yamamura, S. and Takamura, Y. 2008. Nanomaterial-based electrochemical biosensors for medical applications. *TrAC Trends in Analytical Chemistry.* **27**: 585-592.

Kim, M.G., Shin, Y.B., Jung, J.M., Ro, H.S. and Chung, B. H. 2005. Enhanced sensitivity of surface plasmon resonance (SPR) immunoassays using a peroxidase-catalyzed precipitation reaction and its application to a protein microarray. *Journal of Immunological Methods.* **297**: 125-132.

Kim, N., Park, I.S. and Kim, W.Y. 2007a. Salmonella detection with a direct-binding optical grating coupler immunosensor. *Sensors and Actuators B.* **121**: 606-615.

Kim, N., Park, I.S. and Kim, D.K. 2007b. High-sensitivity detection for model organophosphorus and carbamate pesticide with quartz crystal microbalance-precipitation sensor. *Biosensors and Bioelectronics.* **22**: 1593-1599.

Khlebtsov, N.G. 2004. Optical models for conjugates of gold and silver nanoparticles with biomacromolecules. *Journal of Quantitative Spectroscopy & Radiative Transfer.* **89**: 143–153.

Klotz, A., Brecht, A., Barzen, C., Gauglitz, G., Harris, R.D., Quigley, G.R., Wilkinson, J.S. and Abuknesha, R.A. 1998. Immunofluorescence sensor for water analysis. *Sensors and Actuators B: Chemical.* **51:** 181-187.

Knight, A.W. 1999. A review of recent trends in analytical applications of electrogenerated chemiluminescence. *trends in analytical chemistry.* **18:** 47-62.

Ko, S. and Grant, S.A. 2006. A novel FRET-based optical fiber biosensor for rapid detection of Salmonella typhimurium. *Biosensors and Bioelectronics.* **21:** 1283-1290.

Ko, S., Park, T.J., Kim, H.S., Kim, J.H. and Cho, Y.J. 2009. Directed self-assembly of gold binding polypeptide-protein A fusion proteins for development of gold nanoparticle-based SPR immunosensors. *Biosensors and Bioelectronics.* **24**: 2592–2597.

Kobayashi, Y., Nakamura, H., Sekiguchi, T., Takanami, R., Murata, T., Usui, T. and Kawagishi, H. 2005. Analysis of the carbohydrate binding specificity of the mushroom Pleurotus ostreatus lectin by surface plasmon resonance. *Analytical Biochemistry.* **336**: 87-93.

Koncki, R. 2002. Chemical Sensors and Biosensors Based on Prussian Blues. *Critical Reviews in Analytical Chemistry.* **32:** 79-96.

Kong, J. M., Zhang, H., Chen, X. T., Balasubramanian, N. and Kwong, D. L. 2008. Ultrasensitive electrical detection of nucleic acids by hematin catalysed silver nanoparticle formation in sub-microgapped biosensors. *Biosensors and Bioelectronics*. **24**: 787-791.

Krystal, G., Macdonald, C., Munt, B. and Ashwell, S. 1985. A method for quantitating nanogram amounts of soluble protein using the principle of silver binding. *Analytical Biochemistry*. **148**: 451-460.

Krystal, G. 1987. A silver-binding assay for measuring nanogram amounts of protein in solution. *Analytical Biochemistry*. **167**: 86-96.

Krystal, G., Lam, V. and Schrelben, W.E. 1989. Application of a silver-binding assay to the determination of protein in cerebrospinal fluid. *Clinical Chemistry*.**35**: 860-864.

Kulesza, P. J., Malik, M. A., Denca, A. and Strojek, J. 1996. In Situ FT-IR/ATR Spectroelectrochemistry of Prussian Blue in the Solid State. *Analytical Chemistry*. **68**: 2442-2446.

Kumbhat, S., Shankaran, D.R., Kim, S.J., Gobi, K.V., Joshi, V. and Miura, N. 2007. Surface plasmon resonance biosensor for dopamine using D3 dopamine receptor as a biorecognition molecule. *Biosensors and Bioelectronics*. **23**: 421-427.

Kurosawa, S., Park, J.W., Aizawa, H., Wakida, S.I., Tao, H. and Ishihara, K. 2006. Quartz crystal microbalance immunosensors for environmental monitoring. *Biosensors and Bioelectronics*. **22**: 473-481.

Kurtinaitiene, B., Ambrozaite, D., Laurinavicius, V., Ramanaviciene, A. and Ramanavicius, A. 2008. Amperometric immunosensor for diagnosis of BLV infection. *Biosensors and Bioelectronics*. **23**: 1547-1554.

La Belle, J.T., Gerlach, J.Q., Svarovsky, S. and Joshi, L. 2007. Label-free impedimetric detection of glycan-lectin interactions. *Analytical chemistry*. **79**: 6959-6964.

Lai, L.J., Yang, Y.W., Lin, Y.K., Huang, L.L. and Hsieh, Y.H. 2009. Surface characterization of immunosensor conjugated with gold nanoparticles based on cyclic voltammetry and X-ray photoelectron spectroscopy. *Colloids and Surfaces B: Biointerfaces*. **68**: 130-135.

Lakard, B., Herlem, G., Lakard, S. and Fahys, B. 2003. Ab initio study of the polymerization mechanism of poly(p-phenylenediamine). *Journal of Molecular Structure.* **638**: 177-187.

Lange, K., Griffin, G., Vo-Dinh, T. and Gauglitz, G. 2002. Characterization of antibodies against benzo[a]pyrene with thermodynamic and kinetic constants. *Talanta.* **56:** 1153-1161.

Länge, K., Herold, M., Scheideler, L., Geis-Gerstorfer, J., Wendel, H. and Gauglitz,G. 2004. Investigation of initial pellicle formation on modified titanium dioxide (TiO2) surfaces by reflectometric interference spectroscopy (RIfS) in a model system. *Dental Materials.* **20**: 814–822.

Laricchia-Robbio L. and Revoltella, R.P. 2004. Comparison between the surface plasmon resonance (SPR) and the quartz crystal microbalance (QCM) method in a structural analysis of human endothelin-1. *Biosensors and Bioelectronics.* **19**: 1753–1758.

Laschi, S., Mascini, M., Scortichini, G., Franek, M. and Mascini, M. 2003.Polychlorinated Biphenyls (PCBs) Detection in Food Samples Using an Electrochemical Immunosensor. *Journal of Agricultural and Food Chemistry.* **51**: 1816-1822.

Leca, B. and Blum, L.J. 2005. Biosensors for Protein Detection: A Review *Analytical Letters.* **38**: 1491-1517.

Lechuga, L.M., Lenferink, A.T., Kooyman, R.P., and Greve, J. 1995. Feasibility of evanescent wave interferometer immunosensors for pesticide detection: chemical aspects. *Sensors and Actuators B: Chemical.* **25**: 762-765.

Lee, Y.G. and Chang, K.S. 2005. Application of a flow type quartz crystal microbalance immunosensor for real time determination of cattle bovine ephemeral fever virus in liquid. *Talanta.* **65**: 1335-1342.

Leonard, P., Hearty, S., Quinn, J. and O'Kennedy, R. 2004. A generic approach for the detection of whole Listeria monocytogenes cells in contaminated samples using surface plasmon resonance. *Biosensors and Bioelectronics.* **19**: 1331-1335.

Leung, A., Shankar, P. M., Mutharasan, R. 2007. Review: A review of fiber-optic biosensors. *Sensors and Actuators B.* **125**: 688-703.

Leung, A., Shankar, P.M. and Mutharasan, R. 2008. Label-free detection of DNA hybridization using gold-coated tapered fiber optic biosensors (TFOBS) in a flow cell at 1310 nm and 1550 nm. *Sensors and Actuators B: Chemical.* **131**: 640-645.

Levicky, R., Herne, T.M., Tarlov, M.J. and Satija, S.K. 1998. Using Self-Assembly To Control the Structure of DNA Monolayers on Gold: A Neutron Reflectivity Study. *Journal of the American Chemical Society.* **120**: 9787-9792.

Levy, R. and Rusch, S. 2007. SPR waveguide sensor based on transition of modes at abrupt discontinuity. *Sensors and Actuators B.* **124**: 459–465.

Li, G., Stewart, R., Conlan, B., Gilbert, A., Roerth, P. and Nair, H. 2002. Purifification of human immunoglobulin G: a new approach to plasma fractionation. *Vox Sanguinis.* **83**: 332-338.

Li, J., He, X., Wu, Z., Wang, K., Shen, G. and Yu, R., 2003. Piezoelectric immunosensor based on magnetic nanoparticles with simple immobilization procedures. *Analytica Chimica Acta.* **481**: 191-198.

Li, J., Wu, Z., Wang, H., Shen, G. and Yu, R. 2005. A reusable capacitive immunosensor with a novel immobilization procedure based on 1,6-hexanedithiol and nano-Au self-assembled layers. *Sensors and Actuators B: Chemical.* **110**: 327-334.

Li, Y. J., Bi, L. J., Zhang, X. E., Zhou, Y. F., Zhang, J. B., Chen, Y. Y., Li, W. and Zhang, Z.P. 2006. Reversible immobilization of proteins with streptavidin affinity tags on a surface plasmon resonance biosensor chip. *Analytical Bioanalytical and Chemistry.* **386**: 1321-1326.

Li, A., Yang, F., Ma, Y. and Yang, X. 2007. Electrochemical impedance detection of DNA hybridization based on dendrimer modified electrode. *Biosensors and Bioelectronics.* **22**: 1716-1722.

Li, N., Zhao, H., Yuan, R., Peng, K. and Chai, Y. 2008a. An amperometric immunosensor with a DNA polyion complex membrane/gold nanoparticles-backbone for antibody immobilisation. *Electrochimica Acta.* **54**: 235-241.

Li, X. M., Yang, X.Y. and Zhang, S.S. 2008b. Electrochemical enzyme immunoassay using model labels. *Trends in Analytical Chemistry*. **27**(6): 543-553.

Li, Y.Y., Wang, J., Liu, G., Wu, H., Wai, C.M. and Lin, Y. 2008c. A nanoparticle label/immunochromatographic electrochemical biosensor for rapid and sensitive detection of prostate-specific antigen. *Biosensors and Bioelectronics*. **23**: 1659–1665.

Li, Y., Ren J., Nakajima, H., Kim, B.K., Soh, N., Nakano, K. and Imato, T. 2008d. Flow sandwich immunoassay for specific anti-OVA IgG antibody by use of surface plasmon resonance sensor. *Talanta*. **77**: 473-478.

Liang, W.B., Yuan, R., Chai, Y.Q., Li, Y. and Zhuo, Y. 2008. A novel label-free voltammetric immunosensor for the detection of [alpha]-fetoprotein using functional titanium dioxide nanoparticles. *Electrochimica Acta*. **53**: 2302-2308.

Liao, K.T., Cheng, J.T., Li, C.L., Liu, R.T. and Huang, H.J. 2009. Ultra-sensitive detection of mutated papillary thyroid carcinoma DNA using square wave stripping voltammetry method and amplified gold nanoparticle biomarkers. *Biosensors and Bioelectronics*. **24**: 1899–1904.

Liedberg, B., Nylander, C. and Lunstram, I. 1983. Surface plasmon resonance for gas detection and biosensing. *Sensors and Actuators*. **4**: 299-304.

Liedberg, B., Nylander, C. and LundstrÖm, I. 1995. Biosensing with surface plasmon resonance-how it all started. *Biosensors and Bioelectronics*. **10**: i-ix.

Limbut, W., Kanatharana, P., Mattiasson, B., Asawatreratanakul, P. and Thavarungkul, P. 2006a. A comparative study of capacitive immunosensors based on self-assembled monolayers formed from thiourea, thioctic acid, and 3-mercaptopropionic acid. *Biosensors and Bioelectronics*. **22**: 233-240.

Limbut, W., Kanatharana, P., Mattiasson, B., Asawatreratanakul, P. and Thavarungkul, P. 2006b. A reusable capacitive immunosensor for carcinoembryonic antigen (CEA) detection using thiourea modified gold electrode. *Analytica Chimica Acta*. **561**: 55-61.

Lin, H.C. and Tsai, W.C. 2003. Piezoelectric crystal immunosensor for the detection of staphylococcal enterotoxin B. *Biosensors and Bioelectronics.* **18**: 1479-1483.

Lin, J., Yan, F., Hu, X. and Ju, H. 2004. Chemiluminescent immunosensor for CA19-9 based on antigen immobilization on a cross-linked chitosan membrane. *Journal of Immunological Methods.* **291**: 165-174.

Lin, J. and Ju, H. 2005. Electrochemical and chemiluminescent immunosensors for tumor markers. *Biosensors and Bioelectronics.* **20**: 1461-1470.

Lin, Y.Y., Wang, J., Liu, G., Wu, H., Wai, C. M. and Lin, Y. 2008. A nanoparticle label/immunochromatographic electrochemical biosensor for rapid and sensitive detection of prostate-specific antigen. *Biosensors and Bioelectronics.* **23**: 1659-1665.

Lin, J., He, C., Zhang, L. and Zhang, S. 2009. Sensitive amperometric immunosensor for [alpha]-fetoprotein based on carbon nanotube/gold nanoparticle doped chitosan film. *Analytical Biochemistry.* **384**: 130-135.

Lin C. H., Chen H.Y., Yu C. J., Lu P.L., Hsieh C.H., Hsieh B.Y., Chang Y. F. and Chou, C. 2009. Quantitative measurement of binding kinetics in sandwich assay using a fluorescence detection fiber-optic biosensor. *Analytical Biochemistry.* **385**: 224–228.

Lisdat, F. and Schäfer, D. 2008. The use of electrochemical impedance spectroscopy for biosensing. *Analytical and Bioanalytical Chemistry.* **391**: 1555-1567.

Liu, X., Sun, Y., Song, D., Zhang, Q., Tian, Y., Bi, S. and Zhang, H. 2004. Sensitivity-enhancement of wavelength-modulation surface plasmon resonance biosensor for human complement factor 4. *Analytical Biochemistry.* **333**: 99–104.

Liu, X., S, Y., Song, D., Zhang, Q., Tian, Y. and Zhang, H. 2006. Enhanced optical immuosensor based on surface plasmon resonance for determination of transferring. *Talanta.* **68**: 1026–1031.

Liu, G., Lin, Y.Y., Wang, J., Wu, H., Wai, C.M. and Lin, Y. 2007. Disposable electrochemical immunosensor diagnosis device based on nanoparticle probe and immunochromatographic strip. *Analytical chemistry.* **79**: 7644-7653.

Liu, S., Zhang, X., Wu, Y., Tu, Y. and He, L. 2008a. Prostate-specific antigen detection by using a reusable amperometric immunosensor based on reversible binding and leasing of HRP-anti-PSA from phenylboronic acid modified electrode. *Clinica Chimica Acta.* **395**: 51-56.

Liu, Z., Yuan, R., Chai, Y., Zhuo, Y., Hong, C. and Yang, X. 2008b. Highly sensitive, reagentless amperometric immunosensor based on a novel redox-active organic–inorganic composite film. *Sensors and Actuators B.* **134**: 625–631.

Liu, G., Lin, Y.Y., Wang, J., Wu, H., Wai, C.M. and Lin, Y. 2008. Disposable Electrochemical Immunosensor Diagnosis Device Based on Nanoparticle Probe and Immunochromatographic Strip. *Analytical Chemistry.* **79**: 7644-7653.

Liu, S., Zhang, X., Wu, Y., Tu, Y. and He, L. 2008d. Prostate-specific antigen detection by using a reusable amperometric immunosensor based on reversible binding and leasing of HRP-anti-PSA from phenylboronic acid modified electrode. *Clinica Chimica Acta.* **395**: 51-56.

Liu, X. and Wong, D. K. Y. 2009. Picogram-detection of estradiol at an electrochemical immunosensor with a gold nanoparticleProtein G-(LC-SPDP)-scaffold. *Talanta.* **77**: 1437-1443.

Lo, P.-H., Kumar, S. A. and Chen, S.M. 2008. Amperometric determination of H_2O_2 at nano-TiO2/DNA/thionin nanocomposite modified electrode. *Colloids and Surfaces B: Biointerfaces.* **66**: 266-273.

Lojou, E. and Bianco, P. 2006. Assemblies of dendrimers and proteins on carbon and gold electrodes. *Bioelectrochemistry.* **69**: 237-247.

Long, F., He, M., Shi, H.C. and Zhu, A.N. 2008. Development of evanescent wave all-fiber immunosensor for environmental water analysis. *Biosensors and Bioelectronics.* **23**: 952-958.

Love, J. C., Estroff, L.A., Kriebel, J.K., Nuzzo, R.G. and. Whitesides, G.M. 2005.Self-Assembled Monolayers of Thiolates on Metals as a Form of Nanotechnology. *Chemistry Review*. **105**: 1103-1169.

Loyprasert, S., Thavarungkul, P., Asawatreratanakul, P., Wongkittisuksa, B., Limsakul, C. and Kanatharana, P. 2008. Label-free capacitive immunosensor for microcystin-LR using self-assembled thiourea monolayer incorporated with Ag nanoparticles on gold electrode. *Biosensors and Bioelectronics*. **24**: 78-86.

Lu, X., Bai, H., He, P., Cha, Y., Yang, G., Tan, L. and Yang, Y. 2008. A reagentless amperometric immunosensor for [alpha]-1-fetoprotein based on gold nanowires and ZnO nanorods modified electrode. *Analytica Chimica Acta*. **615**: 158-164.

Luo, J., Zhang, Q., Huang, Y., Liu, G. and Zhao, R. 2007. Quartz crystal microbalance biosensor for recombinant human interferon- detection based on antisense peptide approach. *Analytica Chimica Acta*. **590**: 91-97.

Lumley-Woodyear,T., Campbell C. N. and Heller A. 1996. Direct Enzyme-Amplified Electrical Recognition of a 30-Base Model Oligonucleotide. *Journal of the American Chemical Society*. **118 (23)**: 5504-5505.

Luppa, P.B., Sokoll, L.J. and Chan, D.W. 2001. Immunosensors-principles and applications to clinical chemistry. *Clinica Chimica Acta*. **314**: 1-26.

Lyon, L.A., Musick, M.D. and Natan, M.J. 1998. Colloidal Au-Enhanced Surface Plasmon Resonance Immunosensing. *Analytical Chemistry*. **70**: 5177-5183.

Lyon, L. A., Musick, M. D., Smith, P. C., Reiss, B. D., Pea, D. J. and Natan, M. J., 1999. Surface plasmon resonance of colloidal Au-modified gold films. *Sensors and Actuators B: Chemical*. **54**: 118-124.

Ma, L., Yuan, R., Chai, Y. and Chen, S. 2009. Amperometric hydrogen peroxide biosensor based on the immobilization of HRP on DNA-silver nanohybrids and PDDA-protected gold nanoparticles. *Journal of Molecular Catalysis B: Enzymatic*. **56**: 215-220.

Mackey, D., Killard, A. J., Ambrosi, A. and Smyth, M. R. 2007. Optimizing the ratio of horseradish peroxidase and glucose oxidase on a bienzyme electrode: Comparison of a theoretical and experimental approach. *Sensors and Actuators B: Chemical.* **122**: 395-402.

Mallat, E., Barcel, D., Barzen, C., Gauglitz, G. and Abuknesha, R. 2001. Immunosensors for pesticide determination in natural waters. *TrAC Trends in Analytical Chemistry.* **20**: 124-132.

Mannelli, I., Minunni, M., Tombelli, S. and Mascini, M. 2003. Quartz crystal microbalance (QCM) affinity biosensor for genetically modified organisms (GMOs) detection. *Biosensors and Bioelectronics.* **18**: 129-140.

Manera, M.G., Spadavecchia, J., Leone, A., Quaranta, F., Rella, R., Dell'atti, D., Minunni, M., Mascini, M. and Siciliano, P. 2008. Surface plasmon resonance imaging technique for nucleic acid detection. *Sensors and Actuators B: Chemical.* **130**: 82-87.

Mao, X., Yang, Su, X.L and Li, Y. 2006. A nanoparticle amplification based quartz crystal microbalance DNA sensor for detection of *Escherichia* coli O157:H7. *Biosensors and Bioelectronics.* **21**: 1178–1185.

Mao, X., Jiang, J., Luo, Y., Shen, G. and Yu, R. 2007. Copper-enhanced gold nanoparticle tags for electrochemical stripping detection of human IgG. *Talanta.* **73**: 420-424.

Mao, X., Baloda, M., Gurung, A.S., Lin, Y. and Liu, G. 2008a. Multiplex electrochemical immunoassay using gold nanoparticle probes and immunochromatographic strips. *Electrochemistry Communications.* **10**: 1636–1640.

Mao, X., Jiang, J., Xu, X., Chu, X., Luo, Y., Shen, G. and Yu, R. 2008b. Enzymatic amplification detection of DNA based on "molecular beacon" biosensors. *Biosensors and Bioelectronics.* **23**: 1555–1561.

Mark, G. 1996. A Practical Guide to Analytical Method Validation.*Analytical Chemistry.* **68**: 305A-309A.

Mark, S. S., Sandhyarani, N., Zhu, C., Campagnolo, C. and Batt, C. A. 2004. Dendrimer-functionalized self-assembled monolayers as a surface plasmon resonance sensor surface. *Langmuir.* **20**: 6808-6817.

Marazuela, M.D. and Moreno-Bondi, M.C. 2002. Fiber-optic biosensors – an overview. *Analytical and Bioanalytical Chemistry.* **372**: 664-682.

Marguerite, M., Pinto, M., Larry, H., Bernstein, M.D., Dennis, A., Brogan, M.P. Elaine, C. 1987. Immunoradiometric Assay of CA 725 in Effusions Comparison With Carcinoembryonic. Antigen. *Cancer.* **59**: 218-222.

Matsubara, K,, Kawata, S. and Minami, S. 1988. A compact surface plasmon resonance sensor for water in process. *Applied Spectroscopy.* **42**: 1375-131382.

Mauriz, E., Calle, A., Mancl, J.J., Montoya, A., Hildebrandt, A., Barcel, D. and Lechuga, L.M. 2007. Optical immunosensor for fast and sensitive detection of DDT and related compounds in river water samples. *Biosensors and Bioelectronics.* **22**: 1410-1418.

Mazumdar, S.D., Barlen, B., Kramer, T. and Keusgen, M. 2008. A rapid serological assay for prediction of Salmonella infection status in slaughter pigs using surface plasmon resonance. *Journal of Microbiological Methods.* **75**: 545-550.

Mcquarrie, S.A., Baum, R.P., Niesen, A., Madiyalakan, R., Korz, W., Sykes, T.R., Sykes, C.J., Hor, G., Mcwan, A.J. and. Noujaim, A.A. 1997. Pharmacokinetics and radiation dosimetry of 99Tcm-labelled monoclonal antibody B43.13 in ovarian cancer patients. *Nuclear Medicine Communications.* **18**: 878-886.

Mello, L.D. and Kubota, L.T. 2002. Review of the use of biosensors as analytical tools in the food and drink industries. *Food Chemistry.* **77**: 237-256.

Miao, Y., Chen, J., Wu, X. and Miao, J. 2007. Preparation and characterization of hybrid platinum/Prussian blue nanoparticles. *Colloids and Surfaces A: Physicochem. Eng. Aspects.* **295**:135-138.

Michalzik, M., Wendler, J., Rabe, J., Bottgenbach, S. and Bilitewski, U. 2005. Development and application of a miniaturised quartz crystal microbalance (QCM) as immunosensor for bone morphogenetic protein-2. *Sensors and Actuators B: Chemical.* **105**: 508-515.

Miller J.C. and Miller J.N. 2000. Statistics for Analytical Chemistry, 4 th ed., Harlow, England, pp.126-142.

Ming-Chung, Tseng., Chang, Y.P.and Chu, Y.H. 2007. Quantitative measurements of vancomycin binding to self-assembled peptide monolayers on chips by quartz crystal microbalance *Analytical Biochemistry*. **371**: 1-9.

Mitchell, J.S., Wu, Y., Cook, C.J. and Main, L. 2005. Sensitivity enhancement of surface plasmon resonance biosensing of small molecules. *Analytical Biochemistry*. **343**: 125–135.

Mizuta, Y., Onodera, T., Singh, P., Matsumoto, K., Miura, N. and Toko, K. 2008. Development of an oligo(ethylene glycol)-based SPR immunosensor for TNT detection. *Biosensors and Bioelectronics*. **24**: 191-197.

Mo, Z. Wang, H., Liang, Y., Liu, F. and Xu, Y. 2005. Highly reproducible hybridization assay of zeptomole DNA based on adsorption of nanoparticle-bioconjugate. *Analyst*. **130**: 1589–1594.

Morio, F., Corvec, S., Caroff, N., Le Gallou, F., Drugeon, H. and Reynaud, A. 2008. Real-time PCR assay for the detection and quantification of Legionella pneumophila in environmental water samples: Utility for daily practice. *International Journal of Hygiene and Environmental Health*. **211**: 403-411.

Mosiello, L., Nencini, L., Segre, L. and Span, M. 1997. A fibre-optic immunosensor for 2,4-dichlorophenoxyacetic acid detection. *Sensors and Actuators B: Chemical*. **39**: 353-359.

Nagel, T., Gajovic-Eichelmann, N., Tobisch, S., Schulte-Spechtel, U., Bier, F. 2008. Serodiagnosis of Lyme borreliosis infection using surface plasmon resonance. *Clinica Chimica Acta*. **394**: 110–113.

Nagel, T., Ehrentreich-Farster, E., Singh, M., Schmitt, K., Brandenburg, A., Berka, A. and Bier, F.F. 2008. Direct detection of tuberculosis infection in blood serum using three optical label-free approaches. *Sensors and Actuators B: Chemical*. **129**: 934-940.

Ngauy, V., Lemeshev, Y., Sadkowski, L. and Crawford, G. 2005. Cutaneous melioidosis in a man who was taken as a prisoner of war by the Japanese during World War II. *European journal of clinical microbiology*. **43**: 970-972.

Nguyen, C. T., Roy, G., Gauthier, C. and Galanis, N. 2007. Heat transfer enhancement using Al2O3-water nanofluid for an electronic liquid cooling system. *Applied Thermal Engineering.* **27**: 1501-1506.

Numnuam, A., Chumbimuni-Torres, K. Y., Xiang, Y., Bash, R., Thavarungkul, P., Kanatharana, P., Pretsch, E., Wang, J. and Bakker, E. 2008a. Aptamer-Based Potentiometric Measurements of Proteins Using Ion-Selective Microelectrodes. *Analytical Chemistry.* **80**: 707-712.

Numnuam, A., Chumbimuni-Torres, K. Y., Xiang, Y., Bash, R., Thavarungkul, P., Kanatharana, P., Pretsch, E., Wang, J. and Bakker, E. 2008b. Potentiometric Detection of DNA Hybridization. *Journal of the American Chemical Society.* **130**: 410-411.

Oh, B.K., Kim, Y.K., Lee, W., Bae, Y. M., Lee, W. H. and Choi, J.W. 2003. Immunosensor for detection of Legionella pneumophila using surface plasmon resonance. *Biosensors and Bioelectronics.* **18**: 605-611.

Qiang, Z., Yuan, R., Chai Y., Wang N., Zhuo Y., Zhang Y. and Li, X. 2006. A new potentiometric immunosensor for determination of [alpha]-fetoprotein based on improved gelatin-silver complex film. *Electrochimica Acta.* **51**: 3763-3768.

Oliveira, M.D., Correia, M.T., Coelho, L.C. and Diniz, F.B. 2008. Electrochemical evaluation of lectin-sugar interaction on gold electrode modified with colloidal gold and polyvinyl butyral. *Colloids and Surfaces B: Biointerfaces.* **66**: 13-19.

Okugaichi, A., Torigoe, K., Yoshimura, T. and Esumi, K. 2006. Interaction of cationic gold nanoparticles and carboxylate-terminated poly(amidoamine) dendrimers. *Colloids and Surfaces A: Physicochemical and Engineering Aspects.* **273**: 154-160.

Okuno, J., Maehashi, K., Kerman, K., Takamura, Y., Matsumoto, K. and Tamiya, E. 2007. Label-free immunosensor for prostate-specific antigen based on single-walled carbon nanotube array-modified microelectrodes. *Biosensors and Bioelectronics.* **22**: 2377-2381.

O'Sullivan, C.K. and Guilbault, G.G. 1999. Commercial quartz crystal microbalances theory and applications. *Biosensors & Bioelectronics.* **14**: 663-670.

Ordonez, S.S. and Fabregas, E. 2007. New antibodies immobilization system into a graphite–polysulfone membrane for amperometric immunosensors. *Biosensors and Bioelectronics*. **22**: 965–972

Ou, C., Chen, S., Yuan, R., Chai, Y. and Zhong, X. 2008. Layer-by-layer self-assembled multilayer films of multi-walled carbon nanotubes and platinum-Prussian blue hybrid nanoparticles for the fabrication of amperometric immunosensor. *Journal of Electroanalytical Chemistry*. **624**: 287-292.

Owen, T.W., Al Kaysi, R.O., Bardeen, C.J. and Cheng, Q. 2007. Microgravimetric immunosensor for direct detection of aerosolized influenza A virus particles. *Sensors and Actuators B: Chemical*. **126**: 691-699.

Pan, J. 2007. Voltammetric detection of DNA hybridization using a non-competitive enzyme linked assay. *Biochemical Engineering Journal*. **35**: 183-190.

Park, J.W., Lee, H.Y., Kim, J.M., Yamasaki, R., Kanno, T., Tanaka, H., Tanaka, H. and Kawai, T. 2004. Electrochemical detection of nonlabeled oligonucleotide DNA using biotin-modified DNA(ss) on a streptavidin-modified gold electrode. *Journal of Bioscience and Bioengineering*. **97**: 29-32.

Park, J., Kurosawa, S., Takai, M. and Ishihara, K. 2007. Antibody immobilization to phospholipid polymer layer on gold substrate of quartz crystal microbalance immunosensor. *Colloids and Surfaces B: Biointerfaces*. **55**: 164-172.

Park, I.S. and Kim, N. 2006. Development of a chemiluminescent immunosensor for chloramphenicol. *Analytica Chimica Acta*. **578**: 19-24.

Park, J.W., Kurosawa, S., Aizawa, H., God, Y., Takaic, M. and Ishihara, K. 2006.Piezoelectric immunosensor for bisphenol A based on signal enhancing step with 2-methacrolyloxyethyl phosphorylcholine polymeric nanoparticle. *Analyst*. **131**: 155–162.

Passamano, M. and Pighini, M. 2006. QCM DNA-sensor for GMOs detection. *Sensors and Actuators B: Chemical*. **118**: 177-181.

Pedroso, M.M., Watanabe, A.M., Roque-Barreira, M.C., Bueno, P.R. and Faria, R.C. 2008. Quartz Crystal Microbalance monitoring the real-time binding of lectin with carbohydrate with high and low molecular mass. *Microchemical Journal*. **89**: 153-158.

Peeters, S., Stakenborg, T., Reekmans, G., Laureyn, W., Lagae, L., Van Aerschot, A. and Van Ranst, M. 2008. Impact of spacers on the hybridization efficiency of mixed self-assembled DNA/alkanethiol films. *Biosensors and Bioelectronics.* **24**: 72-77.

Peh, W.Y., Reimhult, E., Teh, H. F., Thomsen, J.S. and Su, X. 2007. Understanding Ligand Binding Effects on the Conformation of Estrogen Receptor a-DNA Complexes: A Combinational Quartz Crystal Microbalance with Dissipation and Surface Plasmon Resonance Study. *Biophysical Journal.* **92**: 4415-4423.

Pei, R., Yang, X. and Wang, E. 2002. Enhanced surface plasmon resonance immunoassay for human complement factor 4. *Analytica Chimica Acta.* **453**: 173-179.

Pei, Z., Anderson, H., Aastrup, T. and RamstrÖm, O. 2005. Study of real-time lectin-carbohydrate interactions on the surface of a quartz crystal microbalance. *Biosensors and Bioelectronics.* **21**: 60-66.

Piehler, J., Brecht, A., Geckeler, K.E. and Gauglitz, G. 1996. Surface modification for direct immunoprobes. *Biosensors and Bioelectronics.* **11**: 579-590.

Piehler, J., Brecht, A., Valiokas, R., Liedberg, B. and Gauglitz, G. 2000. A high-density poly(ethylene glycol) polymer brush for immobilization on glass-type surfaces. *Biosensors and Bioelectronics.* **15**: 473-481.

Piehler, J. and Schreiber, G. 2001. Fast Transient Cytokine-Receptor Interactions Monitored in Real Time by Reflectometric Interference Spectroscopy. *Analytical Biochemistry.* **289**: 173-186.

Polsky, R., Gill, R., Kaganovsky, L. and Willner, I. 2006. Nucleic Acid-Functionalized Pt Nanoparticles:Catalytic Labels for the Amplified Electrochemical Detection of Biomolecules. *Analytical chemistry.* **78**: 2268-2271.

Preechaworapun, A., Dai, Z., Xiang, Y., Chailapakul, O. and Wang, J. 2008. Investigation of the enzyme hydrolysis products of the substrates of alkaline phosphatase in electrochemical immunosensing. *Talanta.* **76**: 424-431.

Prieto, F., Sepulveda, B., Calle, A., Llobera, A., Dominguez, C., Abad, A., Montoya,A. and Lechuga, L. M. 2003. An integrated optical interferometric nanodevice based on silicon technology for biosensor applications. *Nanotechnology*. **14**: 907–912.

Prieto, F., Sepulveda, B., Calle, A., Llobera, A., Dominguez, C.and Lechug, L.M. 2003. Integrated Mach-Zehnder interferometer based on ARROW structures for biosensor applications. *Sensors and Actuators B*. **92**: 151-158.

Proll, G., Steinle, L., Prall, F., Kumpf, M., Moehrle, B., Mehlmann, M.and Gauglitz, G. 2007. Potential of label-free detection in high-content-screening applications. *Journal of Chromatography A*. **1161**: 2-8.

R Development Core Team, 2006. R: A Language and Environment for Statistical Computing. R Foundation for Statistical Computing. R Development Core Team, Vienna, Austria, ISBN 3-900051-07-0.

Rabbany, S.Y., Donner, B.L. and Ligler, F.S. 1994. Optical Immunosensors. *Critical Reviews in Biomedical Engineering*. **22**: 307-346.

Rahman, M. A., Shiddiky, M. J. A., Park, J.S. and Shim, Y.B. 2007. An impedimetric immunosensor for the label-free detection of bisphenol A. *Biosensors and Bioelectronics*. **22**: 2464-2470.

Rajan, S. Chand and Gupta, B.D. 2007. Surface plasmon resonance based fiber-optic sensor for the detection of pesticide. *Sensors and Actuators B: Chemical*. **123**: 661-666.

Ramakrishnan, A. and Sadana, A. 2002. A kinetic study of analyte /receptor binding and dissociation for biosensor applications: a fractal analysis for two different DNA systems. *BioSystems*. **66**: 165-177.

Rao, T. P. and Kala, R. 2008. Potentiometric transducer based biomimetic sensors for priority envirotoxic markers—An overview. *Talanta*. **76**: 485-496.

Rattanathongkom A., Sermswan, R. W. and Wongratanacheewin, S., 1997. Detection of Burkholderia pseudomallei in blood samples using polymerase chain reaction. *Molecular and Cellular Probes*. **11**: 25–31.

Rashid, M.H., Bhattacharjee, R.R., Kota, A, Mandal, T.K. 2006. Synthesis of Spongy Gold Nanocrystals with Pronounced Catalytic Activities. *Langmuir*. **22**: 7141-7143.

Rebe Raz, S., Bremer, M.G., Giesbers, M.and Norde, W. 2008. Development of a biosensor microarray towards food screening, using imaging surface plasmon resonance. *Biosensors and Bioelectronics*. **24**: 552-557.

Ren, X., Meng, X. and Tang, F. 2005. Preparation of Ag-Au nanoparticle and its application to glucose biosensor. *Sensors and Actuators B: Chemical*. **110**: 358-363.

Ricard-Blum, S., Peel, L. L., Ruggiero, F. and Freeman, N. J. 2006. Dual polarization interferometry characterization of carbohydrate-protein interactions. *Analytical Biochemistry*. **352**: 252-259.

Ricci, F. and Palleschi, G. 2005. Sensor and biosensor preparation, optimisation and applications of Prussian Blue modified electrodes. *Biosensors and Bioelectronics*. **21**: 389-407.

Ricci, F., Volpe, G., Micheli, L. and Palleschi, G. 2007. A review on novel developments and applications of immunosensors in food analysis. *Analytica Chimica Acta*. **605**: 111-129.

Rodŕguez, À., Valera, E., RamÓn-AzcÓn, J., Sanchez, F. J., Marco, M. P. and CastaÓer, L. M. 2008. Single frequency impedimetric immunosensor for atrazine detection. *Sensors and Actuators B: Chemical*. **129**: 921-928.

Sabatani, E., Rubinstein, I., Moaz, R. and Sagiv, J. 1987. Organized self-assembling monolayers on electrodes, Part I. Octadecyl derivatives on gold. *Journal of Electroanalytical chem*istry. **219**: 365-371.

Safina, G., Lier, M. and Danielsson, B. 2008. Flow-injection assay of the pathogenic bacteria using lectin-based quartz crystal microbalance biosensor. *Talanta*. **77**: 468-472.

Sakai, G., Saiki, T., Miura, N. and Yamazoe, N. 1997. Evaluation of binding of human serum albumin (HSA) to monoclonal and polyclonal antibody by means of piezoelectric immunosensing technique. *Sensors and Actuators B*. **42**: 89-94.

Salama, O., Herrmann, S., Tziknovsky, A., Piura, B., Meirovich, M., Trakht, I., Reed, B., Lobel, L.I. and Marks, R.S. 2007. Chemiluminescent optical fiber immunosensor for detection of autoantibodies to ovarian and breast cancer-associated antigens. *Biosensors and Bioelectronics.* **22**: 1508-1516.

Santana, M.A., Santos, A.M., Oliveira, M.E., Oliveira, J.S., Baba, E.H., Santoro, M.M. and de Andrade, M.H. 2008. A novel and efficient and low-cost methodology for purification of Macrotyloma axillare (Leguminosae) seed lectin. *International Journal of Biological Macromolecules.* **43**: 352-358.

Sauerbrey, G.Z. 1959. Use of quartz vibration for weighing thin films on a microbalance. *Journal Physik.* **155**: 206-212.

Scholz, Z., 2002. *Electrochemical method: guide to experiments and applications.* New York: Verlag Berlin Heidelberg.

Selma, M. V., Martnez-Culebras, P. V. and Aznar, R. 2008. Real-time PCR based procedures for detection and quantification of Aspergillus carbonarius in wine grapes. *International Journal of Food Microbiology.* **122**: 126-134.

Serra, B., Gamella, M., Reviejo, A.J. and Pingarron, J.M. 2008. Lectin-modified piezoelectric biosensors for bacteria recognition and quantification. *Analytical and Bioanalytical Chemistry.* **391**: 1853-1860.

Seydack, M. 2005. Review; Nanoparticle labels in immunosensing using optical detection methods. *Biosensors and Bioelectronics.* **20**: 2454–2469.

Sharma, A. K. and Gupta, B. D. 2005. Fiber optic sensor based on surface plasmon resonance with nanoparticle films. *Photonics and Nanostructures - Fundamentals and Applications.* **3**: 30-37.

Sharma, V. K., Yngard, R. A. and Lin, Y. 2009. Silver nanoparticles: Green synthesis and their antimicrobial activities. *Advances in Colloid and Interface Science.* **145**: 83-96.

Shankaran, D.R., Gobi, K.V. and Miura, N. 2007. Recent advancements in surface plasmon resonance immunosensors for detection of small molecules of biomedical, food and environmental interest. *Sensors and Actuators B.* **121**: 158-177.

Shen, G., Liu, M., Cai, X. and Lu, J. 2008. A novel piezoelectric quartz crystal immnuosensor based on hyperbranched polymer films for the detection of [alpha]-Fetoprotein. *Analytica Chimica Acta.* **630**: 75-81.

Shew, B.Y., Cheng, Y.C. and Tsai, Y.H. 2008. Monolithic SU-8 micro-interferometer for biochemical detections. *Sensors and Actuators A: Physical.* **141**: 299-306.

Silva, M.G., Helali, S., Esseghaier, C., Suarez, C.E., Oliva, A., Abdelghani, A. 2004. An impedance spectroscopy method for the detection and evaluation of *Babesia bovis* antibodies in cattle. *Sensors and Actuators B.* **135**: 206–213.

Simonian, A. L., Good, T. A., Wang, S. S. and Wild, J. R. 2005. Nanoparticle-based optical biosensors for the direct detection of organophosphate chemical warfare agents and pesticides. *Analytica Chimica Acta.* **534**: 69-77.

Sirisinha, S., Anuntagool, N., Dharakul, T., Ekpo, P., Wongratanacheewin, S., Naigowit, P., Petchclai, B., Thamlikitkul, V. and Suputtamongkol, Y. (2000) Recent developments in laboratory diagnosis of melioidosis. *Acta Tropica.* **74**: 235-245.

Slavik, R., Homola, J. and Ctyroky, J. 1999. Single-mode optical fiber surface plasmon resonance sensor. *Sensors and Actuators B.* **54**: 74–79.

Soh, N., Tokuda, T., Watanabe, T., Mishima, K., Imato, T., Masadome, T., Asano, Y., Okutani, S., Niwa, O. and Brown, S. 2003. A surface plasmon resonance immunosensor for detecting a dioxin precursor using a gold binding polypeptide. *Talanta.* **60**: 733-745.

Song Y., Wang L., Ren C., Zhu G. and Li Z. 2006. A novel hydrogen peroxide sensor based on horseradish peroxidase immobilized in DNA films on a gold electrode. *Sensors and Actuators B.* **114**: 1001-1006.

Soykut, E.A., Dudak, F.C. and Boyaci, I.H. 2008. Selection of staphylococcal enterotoxin B (SEB)-binding peptide using phage display technology. *Biochemical and Biophysical Research Communications.* **370**: 104-108.

Su, X. and Li ,F.Y. 2001. Serological determination of *Helicobacter pylori* infection using sandwiched and enzymatically amplified piezoelectric biosensor. *Analytica Chimica Acta.* **429**: 27–36.

Suh J.S. and Moskovits M. 1986. Surface-enhanced Raman spectroscopy of amino acids and nucleotide bases adsorbed on silver. *Journal of the American Chemical Society.* **108**: 4711–4718.

Suni, I. I., 2008. Impedance methods for electrochemical sensors using nanomaterials. *TrAC Trends in Analytical Chemistry.* **27**: 604-611.

Sun, H., Zhang, Y. and Fung, Y. 2006. Flow analysis coupled with PQC/DNA biosensor for assay of *E. coli* based on detecting DNA products from PCR amplification. *Biosensors and Bioelectronics.* **22**: 506–512.

Suprun, E., Evtugyn, G., Budnikov, H., Ricci, F., Moscone, D. and Palleschi, G. 2005. Acetylcholinesterase sensor based on screen-printed carbon electrode modified with prussian blue. *Analytical Bioanalytical Chemistry.* **383**: 597-604.

Stillman, M.J. 1995. Metallothioneins. *Coordination Chemistry Reviews.* **144**: 461-511.

Stradiotto, N.R., Yamanaka, H. and Zanoni, M.V. 2003. Electrochemical sensors: A powerful tool in analytical chemistry. *Journal of the Brazilian Chemical Society.* **14**: 159-173.

Su X, The, H.F., Aung, K.M., Zong, Y. and Gao, Z. 2008. Femtomol SPR detection of DNA-PNA hybridization with the assistance of DNA-guided polyaniline deposition. *Biosensors and Bioelectronics.* **23**: 1715-1720.

Subrahmanyam, S., Piletsky, S.A. and Turner, A.P. 2002. Application of natural receptors in sensors and assays. *Analytical chemistry.* **74**: 3942-3951.

Suni, I.I. 2008. Impedance methods for electrochemical sensors using nanomaterials. *TrAC Trends in Analytical Chemistry.* **27**: 604-611.

Sung, J.H., Ko, H.J. and Park, T.H. 2006. Piezoelectric biosensor using olfactory receptor protein expressed in Escherichia coli. *Biosensors and Bioelectronics.* **21**: 1981-1986.

Suprun, E., Shumyantseva, V., Bulko, T., Rachmetova, S., Rad'ko, S., Bodoev, N. and Archakov, A. 2008. Au-nanoparticles as an electrochemical sensing platform for aptamer-thrombin interaction. *Biosensors and Bioelectronics.* **24**: 825-830.

Svobodova, L., Snejdarkova, M., Tothb, K., Gyurcsanyib, R.E. and Hianik T. 2004. Properties of mixed alkanethiol–dendrimer layers and their applications in biosensing. *Bioelectrochemistry*. **63**: 285– 289.

Svenso, S. 2008. Dendrimers as versatile platform in drug delivery applications. *European Journal of Pharmaceutics and Biopharmaceutics*. In press.

Taitt, C.R., Anderson, G.P. and Ligler, F.S. 2005. Evanescent wave fluorescence biosensors. *Biosensors and Bioelectronics*. **20**: 2470-2487.

Takae, S., Akiyama, Y., Yamasaki, Y., Nagasaki, Y. and Kataoka, K. 2005. Colloidal Au Replacement Assay for Highly Sensitive Quantification of Low Molecular Weight Analytes by Surface Plasmon Resonance. *Bioconjugate Chemistry*. **18**: 1241-1245.

Tan, F., Yan, F. and Ju, H. 2006. A designer ormosil gel for preparation of sensitive immunosensor for carcinoembryonic antigen based on simple direct electron transfer. *Electrochemistry Communications*. **8**: 1835-1839.

Tan, Y., Chu, X., Shen, G.L. and Yu, R.Q. 2009. A signal-amplified electrochemical immunosensor for aflatoxin B1 determination in rice. *Analytical Biochemistry*. **387**: 82–86.

Tang, D.P., Yuan, R., Chai, Y.Q., Zhong, X., Liu, Y., Dai, J.Y. and Zhang, L.Y.2004. Novel potentiometric immunosensor for hepatitis B surface antigen using a gold nanoparticle-based biomolecular immobilization method. *Analytical Biochemistry*. **333**: 345-350.

Tang, D., Yuan, R. and Chai., Y. 2006a. Electrochemical immuno-bioanalysis for carcinoma antigen 125 based on thionine and gold nanoparticles-modified carbon paste interface. *Analytica Chimica Acta*. **564**: 158-165.

Tang, D.Q., Zhang, D.J., Tang, D.Y. and Ai, H. 2006b. Amplification of the antigen-antibody interaction from quartz crystal microbalance immunosensors via back-filling immobilization of nanogold on biorecognition surface. *Journal of Immunological Methods*. **316**: 144-152.

Tang, H., Wang, Q., Xie, Q., Zhang, Y., Tan, L. abd Yao, S. 2007. Enzymatically biocatalytic precipitates amplified antibody–antigen interaction for super low level immunoassay: An investigation combined surface plasmon resonance with electrochemistry. *Biosensors and Bioelectronics*. **23**: 668–674.

Tang, H., Chen, J., Nie, L., Kuang, Y. and Yao, S. 2007. A label-free electrochemical immunoassay for carcinoembryonic antigen (CEA) based on gold nanoparticles (AuNPs) and nonconductive polymer film. *Biosensors and Bioelectronics*. **22**: 1061-1067.

Tang, D., Niessner, R. and Knopp, D. 2008a. Flow-injection electrochemical immunosensor for the detection of human IgG based on glucose oxidase-derivated biomimetic interface. *Biosensors and Bioelectronics*. In press.

Tang, D., Yuan, R. and Chai, Y. 2008b. Ultrasensitive Electrochemical Immunosensor for Clinical Immunoassay Using Thionine-Doped Magnetic Gold Nanospheres as Labels and Horseradish Peroxidase as Enhancer. *Analytical Chemistry*. **80**: 1582-1588.

Taverniers, I., Loose, M.D. and Bockstaele, E.V. 2004. Trends in quality in the analytical laboratory. II. Analytical method validation and quality assurance. *Trends in Analytical Chemistry*. **23**: 535-552.

Taylor, A.D., Ladd, J., Etheridge, S., Deeds, J., Hall, S. and Jiang, S. 2008. Quantitative detection of tetrodotoxin (TTX) by a surface plasmon resonance (SPR) sensor. *Sensors and Actuators B: Chemical*. **130**: 120-128.

Teles, F.R. and Fonseca, L.P. 2008a. Trends in DNA biosensors. *Talanta*. **77**: 606-623.

Terada, T., Nishikawa, M., Yamashita, F., Hashida, M. 2006. Analysis of the molecular interaction of glycosylated proteins with rabbit liver asialoglycoprotein receptors using surface plasmon resonance spectroscopy. *Journal of Pharmaceutical and Biomedical Analysis*. **41**: 966-972.

Teramura, Y. and Iwata, H. 2007. Label-free immunosensing for [alpha]-fetoprotein in human plasma using surface plasmon resonance. *Analytical Biochemistry*. **365**: 201-207.

Thavarungkul, P., Dawan, S., Kanatharana, P. and Asawatreratanakul, P. 2007. Detecting penicillin G in milk with impedimetric label-free immunosensor. *Biosensors and Bioelectronics*. **23**: 688-694.

Thévenot, D.R., Toth, K., Durst, R.A. and Wilso, G.S. 2001. Technical report:Electrochemical biosensors: recommended definitions and classification.*Biosensors and Bioelectronics*. **16**: 121-131.

Thompson, V.S. and Maragos, C.M. 1996. Fiber-Optic Immunosensor for the Detection of Fumonisin B1. *Journal of Agricultural and Food Chemistry*. **44**: 1041-1046.

Thurer, R., Vigassy, T., Hirayama, M., Wang, J., Bakker, E. and Pretsch, E. 2007. Potentiometric Immunoassay with Quantum Dot Labels. *Analytical Chemistry*. **79**: 5107-5110.

Tseng, M.C., Chang, Y.P. and Chu, Y.H. 2007. Quantitative measurements of vancomycin binding to self-assembled peptide monolayers on chips by quartz crystal microbalance. *Analytical Biochemistry*. **371**: 1-9.

Tsukruk, V. V., Rinderspacher, F. and Bliznyuk, V. N. 1997. Self-assembled multilayer films from dendrimers. *Langmuir*. **13**: X-2176.

Tomalia, D. A., Naylor, A. M. and Goddard Iii, W. A. 1990. Starbust dendrimers: Molecular-level control of size, shape, surface chemistry, topology, and flexibility from atoms to macroscopic matter. *Angewandte Chemie - International Edition in English*. **29**: 138-175.

Tong, Z., Yuan, R., Chai, Y., Chen, S. and Xie, Y. 2007. Amperometric biosensor for hydrogen peroxide based on Hemoglobin/DNA/Poly-2,6-pyridinediamine modified gold electrode. *Thin Solid Films*. **515**: 8054-8058.

Toyama, S., Shoji, A., Yoshida, Y., Yamauchi, S. and Ikariyama, Y. 1998. Surface design of SPR-based immunosensor for the effective binding of antigen or antibody in the evanescent field using mixed polymer matrix. *Sensors and Actuators B: Chemical*. **52**: 65-71.

Turiel, E., Fernandez, P., Prez-Conde, C., Gutirrez, A. M. and Camara, C. 1998. Flow-through fluorescence immunosensor for atrazine determination. *Talanta*. **47**: 1255-1261.

Uzawa, H., Ohga, K., Shinozaki, Y., Ohsawa, I., Nagatsuka, T., Seto, Y. and Nishida, Y. 2008. A novel sugar-probe biosensor for the deadly plant proteinous toxin, ricin. *Biosensors and Bioelectronics*. **24**: 923-927.

Valera, E., Raman-Azcan, J., Sanchez, F. J., Marco, M. P. and Rodfguez, A. 2008. Conductimetric immunosensor for atrazine detection based on antibodies labelled with gold nanoparticles. *Sensors and Actuators B: Chemical*. **134**: 95-103.

Varriale, A., Staiano, M., Rossi, M. and D'Auria, S. 2007. High-affinity binding of cadmium ions by mouse metallothionein prompting the design of a reversed-displacement protein-based fluorescence biosensor for cadmium detection. *Analytical chemistry*. **79**: 5760-5762.

Verma, N.and Singh, M., 2005. Biosensors for heavy metals. *BioMetals*. **18**: 121-129.

Vestergaard, M. d., Kerman, K. and Tamiya, E., 2007. An Overview of Label-free Electrochemical Protein Sensors. *Sensors and Actuators B*. **7**: 3442-3458.

Vig, A., Radoi, A., Munoz-Berbel, X., Gyemant, G., Marty, J.L. 2009. Impedimetric aflatoxin M1 immunosensor based on colloidal gold and silver electrodeposition. *Sensors and Actuators B*: Chemical.: In press.

Visutthi, M., Jitsurong, S. and Chotigeat, W. 2008. Production and purification of Burkholderia pseudomallei BipD protein. *The Southeast Asian journal of tropical medicine and public health*. **39**: 1-6.

Vornholt, W., Hartmann, M.and Keusgen, M. 2007. SPR studies of carbohydrate-lectin interactions as useful tool for screening on lectin sources. *Biosensors and Bioelectronics*. **22**: 2983-2988.

Vuren, P. J. and Paweska, J.T. 2009.Laboratory safe detection of nucleocapsid protein of Rift Valley fever virus in human and animal specimens by a sandwich ELISA. *Journal of Virological Methods*. **157**:15-24.

Walsh, D. A. and Dempsey, E. 2002. Comparison of electrochemical, electrophoretic and spectrophotometric methods for creatinine determination in biological fluids. *Analytica Chimica Acta*. **459:** 187-198.

Wang, J. 2000. *Analytical Electrochemitry* (2nd ed). New York: John, Wiley & Sons.

Wang, J., Xu, D., Kawde, A.N. and Polsky, R. 2001. Metal Nanoparticle-Based Electrochemical Stripping Potentiometric Detection of DNA Hybridization. *Analytical Chemistry.* **73(15):** 5576-5581.

Wang, J. 2002. Electrochemical nucleic acid biosensors. *Analytica Chimica Acta.* **469**: 63-71.

Wang. J., Liu, G. and Zhu, Q. 2003a. Indium Microrod Tags for Electrochemical Detection of DNA Hybridization. *Analytical chemistry.* **75**: 6218-6222.

Wang, J., Polsky, R., Merkoci, A. and Turner, K.L. 2003b. Electroactive Beads for Ultrasensitive DNA Detection. *Langmuir.* **19**: 989-991.

Wang, J., Liu, G. and Merkoçi, A. 2003c. Particle-based detection of DNA hybridization using electrochemical stripping measurements of an iron tracer. *Analytica Chimica Acta.* **482**: 149–155.

Wang, M., Wang, L., Wang, G., Ji, X., Bai, Y., Li, T., Gong, S. and Li, J. 2004.Application of impedance spectroscopy for monitoring colloid Au-enhanced antibody immobilization and antibody–antigen reactions. *Biosensors and Bioelectronics.* **19**: 575-582.

Wang, J.and Zhou, H. S. 2008.a Aptamer-Based Au Nanoparticles-Enhanced Surface Plasmon Resonance Detection of Small Molecules. *Analytical. Chemistry.* **80** (18): 7174-7178.

Wang, Z., Tu, Y. and Liu, S. 2008b. Electrochemical immunoassay for α-fetoprotein through a phenylboronic acid monolayer on gold. *Talanta.* **77**: 815–821.

Wang, S., Zhang, X., Mao, X., Zeng, Q., Xu, H., Lin, Y., Chen, W. and Liu, G. 2008c. Electrochemical immunoassay of carcinoembryonic antigen based on a lead sulfide nanoparticle label. *Nanotechnology.* **19**:12-19.

Wang, X., Gu, H., Yin, F. and Tu, Y. 2009. A glucose biosensor based on Prussian blue/chitosan hybrid film. *Biosensors and Bioelectronics.* **24**: 1527-1530.

Wcislo, M., Compagnone, D. and Trojanowicz, M. 2007. Enantioselective screen-printed amperometric biosensor for the determination of d-amino acids. *Bioelectrochemistry.* **71**: 91-98.

Weast, R.C., 1974. Hand book of chemistry and physics 55th edition. Ohio, CRC Press.

Wei, J., Mu Y., Song, D., Fang, X., Liu, X., Bu, L., Zhang, H., Zhang, G., Ding, J., Wang, W., Jin, Q. and Luo, G. 2003. A novel sandwich immunosensing method for measuring cardiac troponin I in sera. *Analytical Biochemistry.* **321**: 209-216.

Wei-Jie, S., Shi-Yun, A., Jin-Huan, L. and Lu-Sheng, Z. 2008. Electrochemical Biosensor Based on Dendrimer Immobilized Deoxyribonucleic Acid. *Chinese Journal of Analytical Chemistry.* **36**: 335-338.

Wei, X., Hao, Q., Zhou, Q., Wu, J., Lu, L., Wang, X.and Yang, X. 2008. Interaction between promethazine hydrochloride and DNA and its application in electrochemical detection of DNA hybridization. *Electrochimica Acta.* **53**: 7338-7343.

Wilder, J.L., Pavlik, E., Straughn, J.M., Kirby, T., Higgins, R.V., DePriest, P.D., Ueland, F.R., Kryscio, R.J., Whitley, R.J. and Nagell, J.V. 2003. Clinical implications of a rising serum CA-125 within the normal range in patients with epithelial ovarian cancer: a preliminary investigation[small star, filled]. *Gynecologic Oncology.* **89**: 233-235.

Wilson, M.S., and Nie, W. 2006. Multiplex Measurement of Seven Tumor Markers Using an Electrochemical Protein Chip. *Anaytical. Chemistry.* **78 (18)**: 6476-6483.

Wink, T., van Zuilen, S. J., Bult, A. and van Bennekom, W. P. 1998. Liposome-Mediated Enhancement of the Sensitivity in Immunoassays of Proteins and Peptides in Surface Plasmon Resonance Spectrometry. *Analytical Chemistry.* **70**: 827-832.

Wong, E.L. and Gooding, J.J. 2006. Charge Transfer through DNA: A Selective Electrochemical DNA Biosensor. *Analytical chemistry.* **78**: 2138-2144.

Wu, L., Chen, J., Du., D. and Ju, H. 2006. Electrochemical immunoassay for CA125 based on cellulose acetate stabilized antigen/colloidal gold nanoparticles membrane. *Electrochimica Acta.* **51**: 1208-1214.

Wu, B., Wang, Y., Li, J., Song, Z., Huang, J., Wang, X. and Chen, Q.

2006. An optical biosensor for kinetic analysis of soluble Interleukin-1 receptor I binding to immobilized Interleukin-1[alpha]. *Talanta.* **70**: 485-488.

Wu, J., Fu, Z., Yan, F. and Ju, H. 2007a. Biomedical and clinical applications of immunoassays and immunosensors for tumor markers. *TrAC Trends in Analytical Chemistry.* **26**: 679-688.

Wu, L., Yan, F. and Ju, H. 2007b. An amperometric immunosensor for separation-free immunoassay of CA125 based on its covalent immobilization coupled with thionine on carbon nanofiber. *Journal of Immunological Methods.* **322**: 12-19.

Wu, J., Zhang, Z., Fu, Z. and Ju, H. 2007c. A disposable two-throughput electrochemical immunosensor chip for simultaneous multianalyte determination of tumor markers. *Biosensors and Bioelectronics.* **23**: 114-120.

Xia, H., Wang, F., Huang, Q., Huang, J., Chen, M.i, Wang, J., Yao, C., Chen, Q., Cai, G. and Fu, W. 2008. Detection of *Staphylococcus epidermidis* by a Quartz Crystal Microbalance Nucleic Acid Biosensor Array Using Au Nanoparticle Signal Amplification. *Sensors.* **8**: 6453-6470.

Xiulan, S., Xiaolian, Z., Jian, T., Xiaohong, G., Jun, Z. and Chu, F. S. 2006. Development of an immunochromatographic assay for detection of aflatoxin B1 in foods. *Food Control.* **17**: 256-262.

Xu, H. and Kall, M. 2002. Modeling the optical response of nanoparticle-based surface plasmon resonance sensors. *Sensors and Actuators B.* **87**: 244–249.

Yan, G., Ju, H., Liang, Z. and Zhang, T. 1999. Technical and clinical comparison of two fully automated methods for the immunoassay of CA 125 in serum. *Journal of Immunological Methods.* **225**: 1-8.

Yang, L., Wei, W., Gao, X., Xia, J. and Tao, H. 2005. A new antibody immobilization strategy based on electrodeposition of nanometer-sized hydroxyapatite for label-free capacitive immunosensor. *Talanta.* **68**: 40-46.

Yang, L., and Li, Y. 2005. AFM and impedance spectroscopy characterization of the immobilization of antibodies on indium–tin oxide electrode through self-assembled monolayer of epoxysilane and their capture of *Escherichia coli* O157:H7. *Biosensors and Bioelectronics.* **20**: 1407–1416.

Yang, L., and Bashir, R. 2008. Electrical/electrochemical impedance for rapid detection of foodborne pathogenic bacteria. *Biotechnology Advances*. **26**: 135–150.

Yao, C., Zhu, T., Tang, J., Wu, R., Chen, Q., Chen, M., Zhang, B., Huang, J. and Fu, W. 2008. Hybridization assay of hepatitis B virus by QCM peptide nucleic acid biosensor. *Biosensors and Bioelectronics*. **23**: 879–885.

Yin, T., Wei, W., Yang, L., Gao, X. and Gao, Y. 2006. A novel capacitive immunosensor for transferrin detection based on ultrathin alumina sol-gel-derived films and gold nanoparticles. *Sensors and Actuators B: Chemical*, **117**: 286-294.

Yingying, Z., Jiancheng L., Chunyong W. and Zhenhua L. 2008. Considerations for improving the performance of surface plasmon resonance biosensors. Paper presented to the BioMedical Engineering and Informatics: New Development and the Future - Proceedings of the 1st International Conference on BioMedical Engineering and Informatics, BMEI 2008.

Ymeti, A., Kanger, J.S., Wijn, R., Lambeck, P.V. and Greve, J. 2002. Development of a multichannel integrated interferometer immunosensor. *Sensors and Actuators B: Chemical*. **83**: 1-7.

Yu, H., Yan, F., Dai, Z. and Ju, H. 2004. A disposable amperometric immunosensor for [alpha]-1-fetoprotein based on enzyme-labeled antibody/chitosan-membrane-modified screen-printed carbon electrode. *Analytical Biochemistry*. **331**: 98-105.

Yu, Q., Chen, S., Taylor, A.D., Homola, J., Hock, B. and Jiang, S. 2005. Detection of low-molecular-weight domoic acid using surface plasmon resonance sensor. *Sensors and Actuators B*. **107**: 193-201.

Yuan, R., Zhang, L., Li, Q., Chai, Y. and Cao, S. 2005. A label-free amperometric immunosenor based on multi-layer assembly of polymerized o-phenylenediamine and gold nanoparticles for determination of Japanese B encephalitis vaccine. *Analytica Chimica Acta*. **531**: 1-5.

Yuan, J., Oliver, R., Aguilar, M.I. and Wu, Y. 2008. Surface Plasmon Resonance Assay for Chloramphenicol. *Analytical Chemistry*. **80**: 8329–8333.

Yuk, J.S., Lee, M.J., Kim, U.R. and Ha, K.S. 2007. Analysis of blood proteins on protein arrays with a spectral surface plasmon resonance biosensor. *Current Applied Physics*. 7: 102-107.

Zar, J.H. 1984. Two-Sample Rank Testing. (Second Edition), Biostatistical Analysis. Prentice-Hall, USA, pp. 138-140.

Zeng, H., Wang, H., Chen, F., Xin, H., Wang, G., Xiao, L., Song, K., Wu, D., He, Q. and Shen, G. 2006. Development of quartz-crystal-microbalance-based immunosensor array for clinical immunophenotyping of acute leukemias. *Analytical Biochemistry.* **351**: 69-76.

Zeng, D., Wang, J., Yin, L., Zhang, Y., Zhang, Y., Zhou, F. 2007. Sequence-specific analysis of oligodeoxynucleotides by precipitate-amplified surface plasmon resonance measurements. Frontiers in Bioscience. **12**: 5117-5123.

Zezza, F., Pascale, M., Mul,G. and Visconti, A. 2006. Detection of Fusarium culmorum in wheat by a surface plasmon resonance-based DNA sensor. *Journal of Microbiological Methods*. **66**: 529-537.

Zhang, X.R., Baeyens, W.R., Garcèa-Campanìa, A.M. and Ouyang, J. 1999. Recent developments in chemiluminescence sensors. *trends in analytical chemistry.* **18**: 384-391.

Zhang, C., Zhang, Z.Y., Yu, B.B. and Zhang X.R. 2002. Application of the biological conjugate between antibody and colloid Au nanoparticles as analyte to inductively coupled plasma mass spectrometry. *Analytical. Chemistry*. **74**: 96–99.

Zhang, S., Wang, N., Niu, Y. and Sun, C. 2005. Immobilization of glucose oxidase on gold nanoparticles modified Au electrode for the construction of biosensor. *Sensors and Actuators B*. **109**: 367–374.

Zhang, Y., Xu, M., Wang, Y., Toledo, F. and Zhou, F. 2007. Studies of metal ion binding by apo-metallothioneins attached onto preformed self-assembled monolayers using a highly sensitive surface plasmon resonance spectrometer. *Sensors and Actuators B: Chemical*. **123**: 784-792.

Zhang, B., Jiang, Y., Kuang, H., Yao, C., Huang, Q., Xu, S., Tang, D. and Fu, W. 2008a. Development of a spiral piezoelectric immunosensor based on thiol self-assembled monolayers for the detection of insulin. *Journal of Immunological Methods.* **338**: 7-13.

Zhang, L., Liu ,Y. and Chen, T. 2008b. A mediatorless and label-free amperometric immunosensor for detection of h-IgG. *International Journal of Biological Macromolecules.* **43**: 165-169.

Zhang, Y., Wang, H., Yan, B., Zhang, Y., Li, J., Shen, G.and Yu, R. 2008c. A reusable piezoelectric immunosensor using antibody-adsorbed magnetic nanocomposite. *Journal of Immunological Methods.* **332**: 103-111.

Zhao W., Xu J.J. and Chen H.Y. 2006. Electrochemical Biosensors Based on Layer-by-Layer Assemblies. *Electroanalysis.* **18**: 1737 – 1748.

Zhao, G., Xing, F. and Deng, S. 2007. A disposable amperometric enzyme immunosensor for rapid detection of Vibrio parahaemolyticus in food based on agarose/Nano-Au membrane and screen-printed electrode. *Electrochemistry Communications.* **9**: 1263-1268.

Zhong, Z., Li, M., Xiang, D., Dai, N., Qing, Y., Wang, D. and Tang, D. 2009. Signal amplification of electrochemical immunosensor for the detection of human serum IgG using double-codified nanosilica particles as labels. *Biosensors and Bioelectronics.* **24**: 2246–2249.

Zhou, C., Pivarnik, P., Auger, S., Rand, A.and Letcher, S. 1997. A compact fiber-optic immunosensor for Salmonella based on evanescent wave excitation. *Sensors and Actuators B: Chemical.* **42**: 169-175.

Zhu, N., Zhang, A., Wang, Q., He, P. and Fang, Y. 2004. Electrochemical detection of DNA hybridization using methylene blue and electro-deposited zirconia thin films on gold electrodes. *Analytica Chimica Acta.* **510**: 163-168.

Zhu, N., Chang, Z., He, P. and Fang, Y. 2005. Electrochemical DNA biosensors based on platinum nanoparticles combined carbon nanotubes. *Analytica Chimica Acta.* **545**: 21–26.

Zhuo, Y., Yuan, R., Chai, Y., Zhang, Y., Li, X., Zhu, Q., Wang, N. 2005

An amperometric immunosensor based on immobilization of hepatitis B surface antibody on gold electrode modified gold nanoparticles and horseradish peroxidase. *Analytica Chimica Acta.* **548**: 205–210.

Zhuo, Y., Yuan, P.X., Yuan, R., Chai, Y.Q. and Hong, C.L. 2009. Bienzyme functionalized three-layer composite magnetic nanoparticles for electrochemical immunosensors. *Biomaterials.* **30**: 2284–2290.

Ziegler, C.and Gopel, W. 1998. Biosensor development. *Current Opinion in Chemical Biology.* **2** : 585-591.

APPENDICES

APPENDIX A

Full Paper

Prussian Blue Dispersed Sphere Catalytic Labels for Amplified Electronic Detection of DNA

Sirilwan Suwansa-ard,[a,b] *Yun Xiang,*[a] *Ralph Bash,*[a] *Panote Thavarungkul,*[b] *Proespichaya Kanatharana,*[b] *Joseph Wang*[a]*

[a] Biodesign Institute, Departments of Chemical Engineering and Chemistry and Biochemistry, Arizona State University, Tempe, AZ 85287, USA
*e-mail: joseph.wang@asu.edu
[b] Faculty of Science, Prince of Songkla University, Hat Yai, Songkhla 90112, Thailand

Received: September 5, 2007
Accepted: October 22, 2007

Abstract
A highly sensitive electrochemical DNA hybridization assay using Prussian blue (PB)-modified polymeric spheres as the oligonucleotide labeling tag is described. The sandwich assay relies on a secondary nucleic-acid probe functionalized with polystyrene beads loaded with numerous Prussian blue nanoparticles. The very strong catalytic activity of the captured PB 'artificial peroxidase' tag towards the reduction of hydrogen peroxide, along with the encapsulation of numerous catalytic particles onto polymeric beads, allows amperometric detection of the DNA target down to the 50 fM level (2.5 amol). Imaging and spectroscopic measurements are used to characterize the PB-tagged polystyrene beads. Such coupling of PB catalytic labels with polymeric carrier beads offers great promise for amplified transduction of different biomolecular interactions.

Keywords: DNA hybridization, Prussian blue, Amplification, Microspheres

DOI: 10.1002/elan.200704063

Dedicated to Professor Ernö Pretsch on the Occasion of His Retirement from ETH Zürich

1. Introduction

The development of electrochemical DNA biosensors has been the subject of considerable effort [1–3]. Such devices offer great promise for nucleic acid assays with features that include high sensitivity, inherent miniaturization, low cost, independence of sample turbidity or optical path length, minimal power demands, and high compatibility with modern microfabrication technologies. Electrochemical hybridization biosensors commonly rely on the conversion of the base-pair recognition event into a useful current signal [1–3]. Such electronic transduction of DNA hybridization events has commonly been achieved in connection to electroactive indicators, enzyme tracers or nanoparticle tags [1–3].

Achieving very high sensitivity is a major goal in electrochemical detection of DNA hybridization. This commonly requires innovative approaches that couple different amplification platforms and amplification processes [4]. While the use of enzyme tags has been extremely attractive for this purpose, enzyme-based DNA assays often suffer from shortcomings associated with the limited stability and cost of the biocatalyst. Recent work by Polsky et al. [5] illustrated that nanoparticle tags can be used as catalytic labels, in a manner analogous to the use of enzyme tracers. For example, nucleic-acid functionalized platinum particles were shown to be useful for amplifying the detection of DNA hybridization down to the 10 pM level.

Here we report on an attractive method for amplifying the electrochemical detection of biomolecular interactions based on nucleic-acid polystyrene (PS) beads modified with Prussian-blue (PB) particles. PB is well recognized as the most attractive electrocatalyst for the reduction of hydrogen peroxide [6]. The favorable catalytic behavior of PB resembles that of commonly used peroxidase tags, and hence PB has often been denoted as 'artificial enzyme peroxidase' [7]. Such use of catalytic 'artificial enzyme' labels also addresses stability and cost limitations inherent to the use of enzyme tags.

In the present study, we coupled the powerful catalytic action of PB with the amplification features of polymeric 'carrier' spheres [4, 8], by embedding PB nanoparticles within polystyrene (PS) spheres (linked to the secondary DNA probe). To our knowledge, the modification of polymeric spheres with catalytic PB nanoparticles has not been reported. The loading of PB particles onto gold nanoparticles was shown recently to offer high catalytic activity towards the reduction of hydrogen peroxide [9], but not in connection to bioaffinity assays. Figure 1 outlines the steps of the new microsphere-based bioelectronic sandwich assay. It involves co-immobilization of the DNA probe with 6-mercapto-1-hexanol on a gold surface (a), hybridization of the target DNA (b), binding of a secondary probe con-

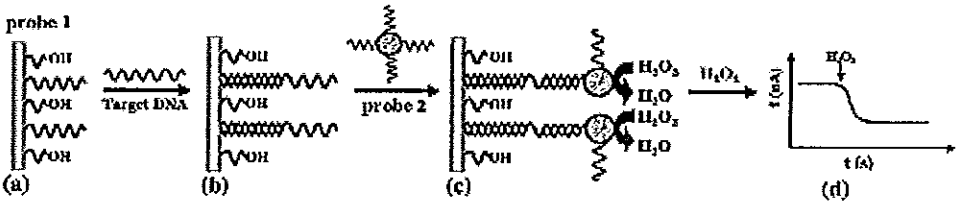

Fig. 1. Schematic representation of the analytical protocol. a) Formation of a mixed monolayer of the thiolated DNA probe (probe 1) and 6-mercapto-1-hexanol on the gold electrode. b) Hybridization of probe 1 with the target DNA. c) Hybridization of the captured DNA target with the PS-PB beads-labeled probe 2. d) Amperometric detection of hydrogen peroxide at the captured PB-loaded particles.

jugated to PB-embedded PS spheres (c), and catalytic amperometric detection of hydrogen peroxide at the captured PS-PB spheres (d). As illustrated in the following sections, such coupling of polymeric 'carrier' beads with the strong catalytic action of the PB 'artificial enzyme' leads to a remarkably sensitive bioelectronic detection of DNA hybridization down to the amol level.

2. Experimental

2.1. Apparatus

Electrochemical measurements were performed with an AutoLab Potentiostat (Eco Chemie, Netherlands), controlled by the GPES software. Scanning electron microscopy (SEM) images of the PS and PS-PB beads were obtained with an XL30 SEM instrument (FEI Co., Hillsboro, OR). Ultraviolet-visible (UV-vis) absorption spectrums were recorded in a 1 mm path-length cell coupled to a UV-2501 PC spectrophotometer (Shimadzu Scientific Instruments, Inc, CA). Fourier Transform Infrared (FT-IR) spectra were recorded using a Nicolet 6700 FT-IR (Thermo-Fisher, Madison, WI).

2.2. Reagents

Potassium ferrocyanide ($K_4Fe(CN)_6$), iron(III)chloride ($FeCl_3$), potassium chloride (KCl), morpholineethanesulfonic acid (MES), *N*-(3-dimethylaminopropyl)-*N*-ethylcarbodiimide hydrochloride (EDC) and hydrogen peroxide were purchased from Sigma (St. Louis, MO). *N*-hydroxysulfosuccinimide (NHS) was obtained from Fluka (Buchs, Switzerland). Carboxylated polystyrene beads (1.04 μm diameter) were obtained from Bangs Laboratories (catalog number PC04N, Fishers, IN). DNA oligonucleotides were obtained from IDT Technologies (Corabille, IA). The following oligonucleotides were used:

Probe 1:
5'-SH-GAC CTA GTC CTT CCA ACA GC-3'
Probe 2:
5'-GGG TTT ATG AAA AAC ACT TTT TTT TT-NH_2-3'
Target:
5'-AAA GTG TTT TTC ATA AAC CCA TTA TCC AGG ACT GTT TAT AGC TGT TGG AAG GAC TAG GTC-3'
Noncomplementary DNA:
5'-TTC CTT AGC CCC CCC AGT GTG CAA GGG CAG TGA AGA CTT GAT TGT ACA AAA TAC GTT TTG-3'

All chemicals were analytical reagent grade and all solutions were prepared with double-distilled deionized water.

2.3. Preparation of Prussian Blue Nanoparticles

Prussian blue nanoparticles (ca. 15 nm in diameter) were prepared based on the method of Miao et al. [9]. Briefly, seven-milliliter of deionized water, 1 mL of 10 mM KCl and 1 mL of 2 mM $K_4Fe(CN)_6$ were mixed with vigorous stirring. Then, 1 mL of 2 mM $FeCl_3$ was slowly added to the mixture for 40 min. The resulting dark-blue colloidal solution was centrifuged for 20 min at 13,000 rpm and the nanoparticles were collected in the precipitate.

2.4. Encapsulation of the PB Nanoparticles within the PS Beads

The PB nanoparticles were encapsulated into the PS beads by mixing rapidly 5 mg of the beads in 400 μL of a chloroform/butanol solvent mixture (15%/85% v/v). Six mg of PB nanoparticles were then added to the mixture, allowing the encapsulation to proceed for 40 min. The beads were then washed with 50 mM phosphate buffer (pH 6.0).

2.5. Conjugation of the PB-PS Beads with the Probe 2 DNA

The PB-PS beads were incubated in 100 μL of 0.1 M NHS/0.4 M EDC (in 0.1 M MES buffer, pH 5.5) solution, for 30 min and centrifuged at 9000 rpm for 5 min. The beads were then incubated with 100 μL of a 4 μM 3'NH_2 – DNA (probe 2) solution for 2 hours. Subsequently, the DNA-linked PS-PB beads were centrifuged at 3000 rpm for 3 min

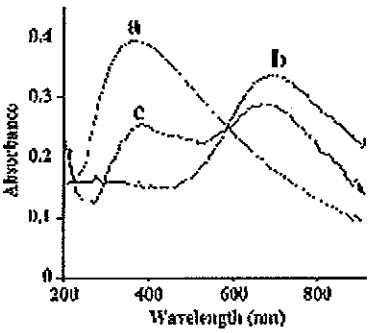

Fig. 3. UV-vis absorption spectra of PS spheres (a), of PB nanoparticles (b), and of the PS-PB beads (c). Spectra were recorded in 50 mM phosphate buffer (pH 6.0).

around 710 nm (b), similar to that reported by Miao [9]. The spectra of the PS-PB beads (c) show two absorption signals, around 400 and 710 nm, characteristic of both the PS and PB, respectively. The FTIR spectra of the PS-PB spheres (not shown) displayed a new band around 2100 nm (compare to PS beads alone), characteristic of CN stretching [10]. The influence of the PB loading (in the 'encapsulation' solution) was examined from the amperometric response to hydrogen-peroxide of a PS-PB modified gold electrode (Fig. 4A). The peroxide current increases rapidly with the level of PB in the 400 µL solution between 2 and 6 mg and levels off thereafter. All subsequent work was carried out using a 6 mg PB loading solution. On-going studies examine the surface loading and coverage of PB on (and within) the PS spheres, and the extent of coverage over the surface vs. internal encapsulation within the swelling-induced nanopores.

The strong electrocatalytic activity of the PS-PB beads towards hydrogen peroxide was illustrated by using the catalytic spheres for modifying the surface of a gold-disk electrode (Fig. 4, B and C). The PS-PB modified electrode offers well-defined voltammetric (B) and amperometric (C) signals for hydrogen peroxide. Figure 2B compares cyclic voltammograms for hydrogen peroxide recorded at PS-(a) and PS-PB (b) sphere modified electrode. As expected, no peroxide response is observed over the entire −0.1 to +0.5 V potential range in the absence of the embedded PB particles. In contrast, a well-defined voltammogram, characteristic of PB modified electrodes [6], is observed using the PS-PB coating (ΔE_p of 40 mV, $E_{p,c}$ = 130 mV, $E_{p,a}$ = 170 mV). The resulting PS-PB modified electrode offers a sensitive low-potential amperometric detection of hydrogen peroxide. Figure 4C shows typical current-time recordings for 100 µM additions of hydrogen peroxide obtained at 0.0 V (vs. Ag/AgCl) using the PS-(a) and PS-PB (b) modified electrodes. The latter responds rapidly (ca. 20 s) to these peroxide additions and offers very favorable signal-to-noise characteristics. In contrast, no response is observed at the PS-modified surface (a), reflecting the absence of the PB catalyst. The PS-PB beads modified electrode also exhibited high operational stability, as was indicated from its highly stable response for hydrogen peroxide over 30 successive runs (not shown).

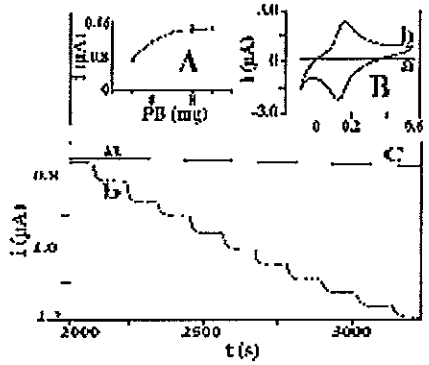

Fig. 4. Electrocatalytic behavior of the PS-PB modified electrode. A) Effect of the loading of the PB particles on the PS beads on the amperometric response to 0.1 mM hydrogen peroxide. B) Cyclic voltammograms for 0.5 mM hydrogen peroxide at the PS-(a) and PS-PB (b) modified electrodes. C) Amperometric response to successive additions of 0.1 mM hydrogen peroxide at the unmodified (a) and PS-PB modified (b) gold electrodes. Operating potential (A), 0.0 V; scan rate (B), 50 mV/s. Electrolyte, 0.1 M KCl. Surface modification protocol, see Section 2.7.

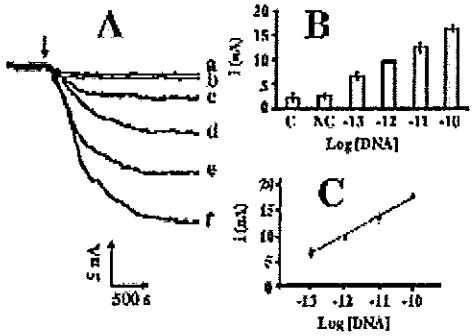

Fig. 5. A) Amperometric response to different concentrations of the target DNA: 0 (a), 1×10^{-12} M (c), 1×10^{-13} M (d), 1×10^{-11} M (e) and 1×10^{-10} M (f), along with the response to 1×10^{-9} M of a noncomplementary DNA (b). B) Relative current signals for the different levels of the target DNA (shown in A). C) The corresponding semi-log calibration plot over the 1×10^{-13}–1×10^{-10} M range of the DNA target. Hybridization buffer: 750 mM NaCl, 150 mM sodium citrate; hybridization time, 1 h. Electrochemical measurements were performed using a 0.1 M phosphate buffer/0.1 M KCl (pH 6.0) solution, a potential of 0.0 V, and additions of 10 mM hydrogen peroxide.

Subsequent DNA hybridization assays have relied on a secondary nucleic-acid probe functionalized with the PS-PB microspheres and electrocatalytic detection of hydrogen peroxide by the captured PS-PB particles. Such use of PS-PB catalytic labels for amplifying the detection of DNA hybridization is illustrated in Figure 5. This figure displays amperometric hybridization signals for extremely low target DNA concentrations ranging from 1×10^{-15} to 1×10^{-10} M (Fig. 5A, c–f). Well defined current signals are observed for these picomolar concentrations of the target. A detection limit of 5×10^{-14} M target DNA can be estimated based on the signal-to-noise characteristics ($S/N = 3$) of the response for the 1×10^{-13} M target (c). Such detection limit corresponds to 46 fg (2.5 amol) in the 50 μL samples. The present protocol is thus ca. 100 times more sensitive compared to the DNA electronic detection based on platinum-nanoparticle catalytic labels [5]. A negligible signal is also observed in Figure 5 for a substantially (1000-fold) higher level of a noncomplementary oligomer (b). This small response is similar to that observed without the DNA target (a) and reflects primarily the negligible nonspecific adsorption of the probe-2/PS-PB conjugate. Such effective discrimination is attributed to hydrophilic character of the mixed monolayer of thiolated probe 1 and 6-mercapto-1-hexanol [11]. The corresponding calibration plot of current vs. log [DNA] (Fig. 5C) is linear over the 10^{-10} to 10^{-15} M range, with a correlation coefficient of 0.997. The amplified electrical signal is coupled to a relatively good reproducibility. The precision was estimated from a series of six successive trace measurements of 1×10^{-12} M target DNA that yielded reproducible current signals, with a *RSD* of 11%.

4. Conclusions

We have demonstrated for the first time the use of PS-PB spheres as tags for highly sensitive bioelectronic detection of DNA hybridization. Such tags couple the amplification features of polymeric carrier beads with the powerful catalytic action of the PB 'artificial enzyme'. While the concept of PS-PB tags has been demonstrated for amplifying the transduction of DNA hybridization, it could be readily expanded for the monitoring of other target analytes such as proteins or glycans. The coupling of polymeric spheres with PB particles also holds great promise for surface coatings for improved oxidase-based enzyme electrodes and for enhancing the detection of different peroxide species ranging from hydrogen peroxide to peroxide explosives. Other catalytic labels (e.g., Pt nanoparticles [5]) could be coupled with the amplification features of polymeric carrier spheres and used for ultrasensitive monitoring of different biomolecular interactions.

5. Acknowledgements

This work was supported by the National Science Foundation (Grants CHE 0506529) and National Institutes of Health (Award Numbers 1U01AI075565, EB002189 and R01A 1056047-04). S. S. acknowledges a fellowship from the Thailand Research Fund (Royal Golden Jubilee Ph.D. Program).

6. References

[1] E. Palecek, M. Fojta, *Anal. Chem.* **2001**, *73*, 75A.
[2] J. Wang, *Anal. Chim. Acta* **2002**, *469*, 63.
[3] A. Merkoci, *Electroanalysis* **2007**, *19*, 739.
[4] J. Wang, *Small* **2005**, *1*, 1036.
[5] R. Pokky, R. Gill, L. Kagancsky, I. Willner, *Anal. Chem.* **2006**, *78*, 2268.
[6] A. A. Karyakin, *Electroanalysis* **2001**, *13*, 813.
[7] A. A. Karyakin, E. E. Karyakina, L. Gorton, *Anal. Chem.* **2000**, *72*, 1720.
[8] J. Wang, R. Pokky, A. Merkoci, K. L. Turner, *Langmuir* **2003**, *19*, 989.
[9] Y. Miao, J. Chen, X. Wu, J. Miao, *Colloids Surf. A, Physicochem. Eng.* **2007**, *295*, 135.
[10] P. J. Kulesza, M. A. Malik, A. Denca, J. Strojek, *Anal. Chem.* **1996**, *68*, 2442.
[11] R. Levicky, T. Herne, M. Tarlov, S. Satija, *J. Am. Chem. Soc.* **1998**, *120*, 9787.

APPENDIX B

Comparison of surface plasmon resonance and capacitive immunosensors for cancer antigen 125 detection in human serum samples

Siriwan Suwansa-ard[a,b,c], Proespichaya Kanatharana[a,b,c],Punnee Asawatreratanakul[a,d] BooncharoenWongkittisuksa[a,e], Chusak Limsakul[a,e], Panote Thavarungkul[a,b,f,*]

[a]*Trace Analysis and Biosensor Research Center, Prince of Songkla University, Hat Yai, Songkhla 90112, Thailand*

[b]*Center for Innovation in Chemistry, Faculty of Science, Prince of Songkla University, Hat Yai, Songkhla 90112, Thailand*

[c]*Department of Chemistry, Faculty of Science, Prince of Songkla University, Hat Yai, Songkhla 90112, Thailand*

[d]*Department of Biochemistry, Faculty of Science, Prince of Songkla University, Hat Yai, Songkhla 90112, Thailand*

[e]*Department of Electrical Engineering, Faculty of Engineering, Prince of Songkla University, Hat Yai, Songkhla 90112,Thailand*

[f]*Department of Physics, Faculty of Science, Prince of Songkla University, Hat Yai, Songkhla 90112, Thailand*

Corresponding author at: Department of physics, Faculty of Science, Prince of Songkla University, Hat Yai, Songkhla 90112, Thailand. Tel: +66-74-288753, Fax: +66-74-212817.

E-mail : panote.t@psu.ac.th (P.Thavarungkul).

Abstract

This paper presents a comparison between surface plasmon resonance (SPR) and capacitive immunosensors for a flow injection label-free detection of cancer antigen 125 (CA 125) in human serum. Anti-CA 125 was immobilized on gold surface through a self-assemble monolayer. Parameters affecting the responses of each system were optimized. Under optimal conditions, SPR provided a detection limit of 0.1 U ml^{-1} while 0.05 U ml^{-1} was obtained for the capacitive system. Linearity for SPR was between 0.1 U ml^{-1} and 40 U ml^{-1} and 0.05-40 U ml^{-1} for capacitive system. These immunosensors were applied to analyze CA 125 concentrations in human serum samples and compared with conventional enzyme linked fluorescent assay (ELFA). Both systems showed good agreement with ELFA ($P<0.05$). Moreover, these immunosensors were very stable and provided good reproducible responses after regeneration, up to 32 times for SPR and 48 times for capacitive system with relative standard deviation lower than 4 %. The SPR immunosensor provided advantages in term of fast response and real-time monitoring while capacitive immunosensor offered a sensitive and cost effective method for CA 125 detection.

Keywords: surface plasmon resonance; capacitance; label-free immunosensor;

cancer antigen 125

1. Introduction

Cancer antigen 125 (CA 125) is a tumor marker for ovarian cancer. It is present in 80 % of nonmucinous for ovarian cancer and circulates in the serum of patients (Endo et al., 1988). For healthy human, the concentration levels of CA 125 are lower than 35 U ml^{-1} (Wilder et al., 2003). The determination of CA 125 level in human serum is very useful to clinical diagnoses since it can give information of the disease stage, monitoring the progress of ovarian cancer patients following cytoreductive surgery and chemotherapy.

For clinical laboratory, CA 125 levels are often measured by radiometric (Marguerite et al., 1987; Mcquarrie et al., 1997) and enzyme immunoassay (Dai et al., 2003; Wu et al., 2007; Yan et al., 1999; VIDAS® CA 125 II™). These conventional immunoassays are time consuming, required several separation steps and special equipped laboratories and/or skilful personnel (He et al., 2003; Lin and Ju, 2005). In view of these development of an alternative specific method for the determination of CA 125 which is relatively easy to operate is interesting. One approach is immunosensor.

Immunosensors combine the natural specificity of antibody and antigen reaction with high sensitivity of various physical transducers. Most immunosensors for CA 125 are labeled with enzyme (Dai et al., 2003; Fu et al., 2008; Wu et al., 2007) and the analysis procedure requires several steps (Bange et al., 2005). Label-free immunosensor is more attractive since it directly detects changes in physical properties owing to the antibody-antigen binding on the transducer surface. For label-free, there was only one report on the analysis of CA 125 by using differential pulse voltammetry, provided a detection limit of 1.8 U ml^{-1} and a linear range of 10-30 U ml^{-1} (Tang et al., 2006).

Several transducers have been developed for label-free immunosensors. Capacitive and surface plasmon resonance transducers have recently attracted a lot of interest especially for direct detection of biomolecular interactions (Berggren and Johansson, 1997; Dudak and Boyaci, 2007; Limbut et al., 2006b; Loyprasert et al., 2008; Mazumdar et al., 2008; Teramura and Iwata, 2007; Yin et al., 2006). SPR biosensor has become particularly powerful because of its high surface sensitivity, real-time monitoring, and kinetic analysis (Campagnolo et al., 2004; Toyama et al.,

1998) while the main advantages of capacitive biosensor are its high sensitivity, simple to operate, and relatively inexpensive.

In the present work, we employed both surface plasmon resonance and capacitive transducers for the direct detection of CA 125 using anti-CA 125 immobilized on a gold surface by self-assembled monolayer. Parameters affecting the response of both transducers were optimized then their performances were compared. To show real application, human serum samples were tested by both systems under optimum conditions. The results were then compared to enzyme linked fluorescent assay (ELFA). To the best of our knowledge this is the first time SPR and capacitive systems are investigated for direct detection of CA 125. This is also the first time that the performances of these two systems were compared under optimum conditions and applied to detect analyte concentration in real samples.

2. Experimental

2.1 Materials

Monoclonal anti-cancer antigen 125 (anti-CA 125) and cancer antigen (CA 125) from human were obtained from US biological (USA), anti-alpha-fetoprotein antibody (anti-AFP) and alpha-fetoprotein (AFP) were obtained from Dako (Denmark) and anti-human carcinoembryonic antigen (anti-CEA), carcinoembryonic antigen (CEA) obtained from Sigma (St. Louis, USA), 11-mercaptoundecanoic acid from Aldrich (MO, USA), N-(3-Dimethylaminopropyl)-N-ethylcarbodiimide hydrochloride (EDC), N-Hydroxysuccinimide (NHS) from Aldrich (Steinheim, Germany), 1-dodeccanethiol ethanolic acid from Aldrich (Milwaukee, USA), ethanolamine from Merck (Darmstadt, Germany), bovine serum albumin (BSA) from Fluka (Steinheim, Germany). All other chemicals used were of analytical grade. All buffers were prepared with distilled water treated with a reverse osmosis-deionized system. Before used, the buffers were filtered through an Albet® nylon membrane filter (Albet, Spain), pore size 0.20 μm, with subsequent degassing.

2.2 SPR immunosensor

2.2.1 Anti- CA 125 immobilization

A gold disk (ϕ = 2.5 cm.; 50 nm thick gold-coated BK-7 glass plate, Eco Chemie B.V., Netherlands) was cleaned with piranha solution (3:1 mixture of H_2SO_4 and H_2O_2), thoroughly rinsed with water, ethanol and dried in a stream of nitrogen gas. The glass side of this gold disk was adhered to the prism via a matching oil with the same refractive index (n = 1.518) and placed inside the holding block of the SPR equipment (AutoLab Spirit®, Eco Chemie B.V., Netherlands) with the gold surface facing upward. A custom built flow cell was screwed into place, on top of the gold disk, leaving a space of 10 µl (ϕ = 3 mm) where solution can pass through the gold surface. Immobilization steps were monitored by SPR detection, controlled by Autolab SPR version 4.2.1 software. The freshly cleaned disk was incubated in 150 mM 11- mercaptoundecanoic acid solution for 5 h. During this time self-assembled monolayer was formed on the gold surface. These optimum values of concentration and incubation time were obtained from prior tests when the angle shift of the self assembled layer of 11- mercaptoundecanoic acid on gold disk surface reach a steady value. For the coupling of anti-CA 125, the surface was activated with 0.2 M EDC/ 0.05 M NHS for 50 min, the optimum activation time. Then, 30 µg $ml^{-1}$of anti-CA 125 in 10 mM Tris-HCl pH 7.50 was incubated on this surface and then with ethanolamine pH 8.50 for 7 min to block the remaining reactive sites. Finally any pinholes on the surface were blocked with 1% BSA for 1 h.

2.2.2 SPR system

All SPR experiments were performed using SPR AutoLab. Solution was delivered using a syringe pump (Kd Scientific, USA) into the SPR flow injection system, equipped with a custom build flow cell. Standard CA 125, serum sample, and regeneration solution were loaded with a sample injector (Valco, USA). The flow cell was maintained at 25°C by a circulating water bath (Grant Instrument, UK). A monochromatic p-polarized laser (λ = 670 nm) was directed through prism onto the gold disk. The interaction between immobilized anti-CA 125 on the gold disk and CA 125 antigen was measured as the SPR angle shift by a photodiode detector among a dynamic range of 4,000 millidegree.

2.3 Capacitive immunosensor

2.3.1 Anti-CA 125 immobilization

Gold rod electrode (ϕ=3 mm, 99.99 % purity) was cleaned and treated followed the steps described by Limbut et al. (2006a,b). Immobilization of capacitive immunosensor followed the same steps as the immobilization of SPR immunosensor except the time allowed for self-assemble monolayer and the chemical used in the blocking step. The gold rod electrode was immersed in 150 mM of 11-mercaptoundecanoic acid solution for 15 min to form monolayer. This optimum value was obtained by determining percentage of surface coverage of 11-mercaptoundecanoic acid formation on electrode surface (Limbut et al., 2006a). For the blocking step, 10 mM of 1-dodeccanethiol ethanolic acid was applied for 20 min. The electrochemical behavior of each immobilization step was studied by cyclic voltammetry (Eco Chemie μ-autolab B.V., Netherland, and software package GPES 4.7). A reduction of redox peaks after each immobilization step indicated the existence of an additional layer on the electrode surface. After the final blocking step the redox peaks disappeared.

2.3.2 Capacitive system

The reaction cell (10 μl) of the capacitive flow system consisted of an anti-CA 125 modified gold working electrode, a custom made Ag/AgCl reference electrode and a stainless steel tube auxiliary electrode. They were connected to a potentiostat (ML 160, AD Instruments, Australia). Carrier buffer was flowed through the system using a peristaltic pump (Gilson, France). Standard CA 125, serum sample, and regeneration solution were injected into the flow cell by a sample injector (Valco, USA). The capacitance was measured using a potentiostatic step method (Berggren et al., 1998). The current responses obtained from the application of 50 mV potential pulses were used to calculate the capacitance followed the procedures described by Limbut et al. (2006a,b). In brief the logarithm of the current response was plotted *versus* time, the capacitance of the layer covering the electrode was obtained from the slope and plotted as a function of time.

2.4 Optimization of the flow injection SPR and capacitive immunosensors

Parameters affecting the performances of both SPR and capacitive immunosensors (Table 1) were optimized. Initial conditions were 300 µl of 15 U ml^{-1} of CA 125 with 10 mM phosphate buffer pH 7.20 at a flow rate of 10 µl min^{-1} for SPR and 200 µl of 5 U $ml^{-1}$of CA 125 with 10 mM Tris-HCl pH 7.20 at a flow rate of 100 µl min^{-1} for the capacitive system (Wu et al., 2006). The response was the average of three injections. The optimization was performed by changing a single parameter while keeping other parameters constant. The optimum operating condition was considered by balancing between the signal and analysis time for one analysis.

2.5 Selectivity

To investigate the selectivity of the immunosensor, carcinoembryonic antigen (CEA) and α-1-fetoprotein (AFP), two other tumor markers indicating ovarian cancer (Wu et al., 2007), were tested.

2.6 Determination of CA 125 in real samples

Human serum samples were obtained from Hat Yai Hospital, Songkhla, Thailand. The efficiency of the two immunosensor systems were tested by detecting CA 125 in these samples and compared with ELFA technique (obtained from the Hospital).

3. Results and discussion

3.1 SPR response

When CA 125 was injected into the flow system it bound to anti-CA 125 on the surface of modified gold disk and the refractive index increased resulting in the increase of SPR (Fig. 1 (a)). When the signal reached a steady state (after 5 min) 300 µl of regeneration solution was injected with a flow rate of 100 µl min^{-1} to dissociate the binding between antibody and antigen. This caused the reduction of SPR angle due to the lower refractive index of regeneration solution compared to the running buffer (Weast, 1974; Yu *et al.*, 2005). When the running

buffer was flowed again the signal returned to a steady base-line, then a new CA 125 was injected. The response was detected by measurement of SPR angle change ($\Delta\theta$).

3.2 Capacitive response

The binding of the injected CA 125 to the immobilized anti-CA 125 caused the increase of dielectric layer thickness and/or the change of dielectric behavior resulting in the decrease of total capacitance (Fig.1(b)). The time required for the signal to reach a steady state was 15 min. The capacitance response was measured by detecting the change in capacitance before and after antigen-antibody interaction (ΔC). The surface was then regenerated with regeneration solution to remove CA 125 binding. The increase of signal after regeneration solution injection was because the regeneration solution has higher ionic strength than the running buffer (Limbut et al., 2006b; Jiang, et al., 2003; Berggren et al., 1998).

3.3 Optimization of the flow injection systems

3.3.1 Regeneration solution

The reusability of the sensor surface is the main advantage of immunosensors over other immunological methods, e.g. ELISA. The breaking of the non-covalent binding between anti-CA 125 and CA 125 using regeneration solution is essential for the repeated use of the sensor. Several types of regeneration solutions were tested; i.e., acidic (glycine-HCl buffer and HCl) (Loyprasert et al., 2008; Thavarungkul et al., 2007), basic (NaOH) (Li et al., 2006) and salt ($MgCl_2$) (Andersson et al., 1999). For SPR systems the experiments were done by using 300 µl of regeneration solution with 100 µl min^{-1} flow rate and 300 µl of sample solution with 10 µl min^{-1} flow rate. While for capacitive system 200 µl with 100 µl min^{-1} flow rate were applied for both regeneration and sample solution. These are optimum values obtained from the other study in our laboratory (unpublished data). These parameters were later optimized for the present systems (see 3.4.3 and 3.4.4).

The efficiency was determined by residual activity of the immobilized anti-CA 125 monitored from the change in response due to the binding between CA 125 before ($\Delta\theta_1$ or ΔC_1) and after regeneration ($\Delta\theta_2$ or ΔC_2) (Fig. 1) as follows:

$$\% \text{ Residual activity} = \frac{\Delta\theta_2 (or \Delta C_2) \times 100}{\Delta\theta_1 (or \Delta C_1)} \quad (1)$$

The highest residual activity of both transducers was from HCl pH 2.50 (SPR = 93±3 %, capacitive = 94±2 %). The influence of different pH of HCl solution was then studied. Residual activity increased from pH 2.80 to 2.60 then decreased. This may be because low pH can destroy the SAM layer (Jiang et al., 2003). Therefore, pH 2.60 was selected (SPR = 96±2 %, capacitive = 98±3 %).

3.3.2 Running buffer solution

Investigation of running buffer was carried out using the same sample volume and flow rate as in 3.3.1. The influence of three types of buffer commonly used in immunosensor system was studied (Table 1). For SPR system, calibration curve of standard CA 125 at 10, 15, 20, and 25 U ml^{-1} (preliminary study indicated linear range at these concentrations) was performed. While for capacitive system, standards CA 125 from 5 to 20 U ml^{-1} were studied. Sensitivity (slope of calibration curve) obtained from the plot between SPR angle shift or capacitance change and concentrations of CA 125 for the three running buffer were compared. Sodium phosphate saline buffer and Tris-HCl buffer provided the lowest base-line for SPR and capacitive immunosensor systems, respectively. Hence, they gave the highest sensitivity (SPR = 0.042±0.001 millidegree/U ml^{-1}, capacitive = 4.1±0.1 –nF cm^{-2}/U ml^{-1}).

The influence of pH of running buffer was then investigated from 7.00 to 7.80 by using 10 U ml^{-1} of CA 125 in 10 mM of sodium phosphate saline for SPR and 5 U ml^{-1} of CA 125 in 10 mM of Tris-HCl for capacitive system. These concentrations were selected since they can give relatively high signal. Other parameters were the same as for the study of types of buffer. The highest response was at pH 7.20 for both systems, 3.3±0.1 millidegree for SPR and 56±3 –nF cm^{-2} for capacitive.

Buffer concentrations were also studied (Table 1) since ionic strength of solution is also a factor that affect the association and dissociation affinity binding (Shankaran et al., 2007). The maximum responses were obtained at 15 mM for both immunosensor systems (SPR = 3.5±0.1 millidegree, capacitive = 73±1 –nF cm^{-2}).

3.4.3 Flow rate

The influence of the flow rate was investigated. The responses for both systems increased when the flow rate decreased because slower flow rate allowed CA 125 to retain longer in the flow cell to bind with anti-CA 125. However, for SPR the response between 10 µl min^{-1} (5.3±0.2 millidegree) and 15 µl min^{-1} (4.8±0.2 millidegree), were not much different (9 %) but the time required to reach a steady state of 15 µl min^{-1} was much shorter, 5 min compared to 8 min. Therefore, 15 µl min^{-1} was selected. Similarly, 100 µl min^{-1} (66±1 –nF cm^{-2}) was chosen for capacitive immunosensor because the response was only 3 % lower than 50 µl min^{-1} (68±3 –nF cm^{-2}), but the time was much shorter, 15 compared to 25 min.

3.4.4 Sample volume

The variation of response with the injected sample volume was studied (Table 1). Initially the response increased with the volume. However, antigen-antibody binding also depends on the amount of anti-CA 125 immobilized on the surface. So, too much CA 125 for the same amount of anti-CA 125 cannot increase the response. The response reached a plateau at 300 µl for SPR (5.1±0.5 millidegree) and 250 µl for capacitive system (74±1 –nF cm^{-2}). These values were then chosen for further experiments.

Optimum conditions of the two flow injection immunosensors are summarized in Table 1. Under these optimum conditions the time required for the change in signal to reach a steady state was 5 min for SPR and 15 min for capacitive system.

3.5 Linear range and detection limit

Different concentrations of CA 125 were tested by the SPR and capacitive systems under their optimum conditions, each concentration was injected 3 times. Since the calibration curve (Fig. 2) has similar shape to the calibration plot of

ion selective electrode the limit of detection was determined followed IUPAC Recommendation 1994 (Buck and Lindneri, 1994). For SPR the linear range was between 0.1 and 40 U ml^{-1} (Fig. 2) with a detection limit of 0.1 U ml^{-1} (Fig. 2 inset). Similar calibration curve was obtained for the capacitive system with slightly wider linear range, 0.05-40 U ml^{-1} ($y(-nF\ cm^{-2}) = (1.56\pm0.03)x + (41.8 \pm 0.3)$ (U ml^{-1}), $r = 0.998$) and a lower detection limit, 0.05 U ml^{-1}. Both immunosensors provided detection limits much lower than the 35 U ml^{-1} which is the concentration of CA 125 in normal human blood. The detection limits of present work are much lower than enzyme-labeled immunosensors; 1.29, 1.73, and 4 U ml^{-1} (Dai et al., 2003, Wu et al., 2006, VIDAS ® CA 125 II ™).

3.6 Selectivity of SPR and capacitive immunosensors

CEA and AFP were used to evaluate the selectivity of both immunosensors because they are important tumor markers responsible for clinical diagnosis such as lung, pancreas, ovaries, and other types of tumor (Wu et al., 2007). Fig. 3 shows that CEA and AFP gave much lower responses than CA 125, the same response as blank (running buffer; 0.69 ± 0.05 millidegree) and lower than the response at the detection limit of CA 125 (4.3 ± 0.1 millidegree). While the responses to CA 125 increased with concentration. Similar results were obtained for the capacitive system. Therefore, their presence would not interfere with these systems. Thus, both immunosensors have good selectivity to CA 125 analysis.

3.7 Reproducibility

The reproducibility was tested by continuously injecting the same concentration of standard CA 125 (10 U ml^{-1} for SPR and 5 U ml^{-1} for capacitive system) with subsequent regeneration. Then percentage of residual activity was calculated. The result found that for SPR immunosensor during 32 times of regeneration (2 days) the percentage of residual activity maintained an average of 96 ± 4 (4 % RSD) after which the response decrease rapidly. For capacitive immunosensor the percentage of residual activity gave an average of 97 ± 3 (3 % RSD) for 48 times of regeneration cycle (3 days). Both immunosensors provided good reproducibility with RSD lower than 4% for sensing surface detection of CA 125.

In the SPR system, the base-line of the system when the response decreased was similar to the one before the modified electrode was first used. For the capacitive system cyclic voltamogram of the modified electrode after the decrease of activity was tested and found to be similar to the one before the electrode was used. These indicated that the SAM layer remained intact. Therefore, the decreasing of response is probably caused by the loss of activity of anti-CA 125 because the self-assemble monolayer was not destroyed by regeneration solution.

The lesser number of reuse for SPR sensor (32 times) when compared to the capacitive system (48 times) may be because in the SPR system the immobilized antibody was exposed to the regeneration solution slightly longer (3 min) than in the capacitive system (2.5 min).

3.8 Matrix effect

Ten human serum samples were obtained from Hat Yai Hospital, Thailand. For SPR, the linear range was 0.1 – 40 U ml^{-1} and 0.05 - 40 U ml^{-1} for capacitive system. Since the concentration of CA 125 in blood of healthy human is lower than 35 U ml^{-1}, analysis of the human serum sample can be diluted at least 100 times. To study the matrix effect, the calibration curves of spiked (obtained from spiking CA 125 into real sample) and standard (obtained from spiking CA 125 into running buffer) were done for all ten samples. Different concentration of standard CA 125 were spiked into serum samples and then diluted with running buffer at 100 and 1000 times. The slope of standard solution curve and the spiked curve were compared by using two-way ANOVA (analysis of variance), calculated by R software (R development Core Team, 2006). If there is no significant difference, it indicates that the matrix has no effect on response of the immunosensors. For example, the calibration equation of one sample for SPR system was $y = (2.24\pm 0.18)x + (1.99\pm1.54)$ for standard solution and $y = (2.21\pm 0.15)x + (4.29\pm1.25)$ for spiked sample. Both slopes were statistically tested and showed that they were no significant difference ($P<0.05$). The results found that for every sample at 100 times dilution the matrix already has no effect. Therefore, all samples, after dilution, can be directly analyzed by using standard calibration curve.

3.9 Real samples

Ten serum samples were analyzed by using SPR and capacitive immunosensors and the results were compared with an enzyme linked fluorescent assay (VIDAS® CA 125 II™), a conventional method in clinical laboratory used by Hat Yai Hospital. In brief, this method is based on a sandwich enzyme immunoassay. Secondary antibodies were labeled with alkaline phosphate to catalyze the hydrolysis of 4-methyl umbelliferyl phosphate substrate into a fluorescent product (4-methyl umbelliferone) the fluorescent of which is measured at 450 nm.

Calibration curves of the immunosensors were first constructed using standard solution between 0.1 and 1.5 U ml^{-1} for SPR and between 0.05 and 1.5 U ml^{-1} for capacitive immunosensors. Samples were diluted with running buffer at 100 and 1000 times. The immunosensors responses of each sample were used to determine CA 125 concentration from the calibration curve of CA 125 standard and multiplied by the dilution factor. The results are shown in Table 2. The two immunosensors results were compared to ELFA method by Wilcoxon singned rank test (Triola, 1998). There is no evidence for systematic differences between the results obtained from both immunosensors and the enzyme linked fluorescent method ($P<0.05$). That is, the concentration determined by both immunosensors and enzyme linked fluorescent are in good agreement.

3.10 Recovery

To further validate the systems, the recovery was studied by spiking all serum samples with different concentrations of CA 125, 5-1500 U ml^{-1} for the capacitive system and 10-1500 U ml^{-1} for SPR. Percentage of recovery was calculated by the following equation

$$\text{Recovery (\%)} = \frac{C_1 - C_2}{C_3} \times 100 \qquad (2)$$

Where, C_1 = concentration determined in fortified (or spiked) sample, C_2 = concentration determined in unfortified sample and C_3 = concentration of fortification (Eurachem Working group, 1998). Average recoveries were between 81 and 110 %

with R.S.D. between 2 and 12 %. These are acceptable since the lowest concentration tested was 5 U ml^{-1} or 33 ppb (1 mg = 150 kU) and the acceptable recovery of 100 ppb level is 80-110 % and RSD is 15-22.6 % (Taverniers et al., 2004).

Limit of quantification (LOQ) was determined by considering the lowest concentration of analyte with acceptable accuracy and precision (Taverniers et al., 2004). For SPR it was studied by spiking 10 U ml^{-1} into 5 real samples (1 sample was repeated 3 times), diluted 100 times to 0.1 U ml^{-1} (LOD) or 0.7 ppb and determined the recovery and precision. Acceptable recovery and precision at 1 ppb were 40-120 % and % RSD $\leq$ 30 (Taverniers et al., 2004). The recovery of SPR at 0.1 U ml^{-1} was 97±9 % (% RSD = 10) which are very well within the acceptable range. Therefore, LOQ of SPR could be said to be 0.1 U ml^{-1}. Similar test was carried out with the capacitive system and found the LOQ to be 0.05 U ml^{-1} or 0.3 ppb (recovery = 95±9 %, % RSD = 10). Thus, the present methods could satisfy the requirements for determining CA 125 in human serum in clinical diagnosis.

Conclusions

In this paper we presented two sensitive and accurate immunosensors for measuring CA 125 in human serum samples with no requirement of labeling. The comparison between surface plasmon resonance and capacitive immunosensors were carried out with the same immobilization technique. The analytical performances of both techniques were evaluated at their optimum conditions. The SPR method was superior in terms of real-time monitoring making it easy to follow and monitor the immobilization and optimization steps. It also required less time for the steady response (5 min for SPR and 15 min for capacitive) and regeneration (5 min for SPR and 12 min for capacitive). Whereas, the capacitive system showed a slightly lower limit of detection (0.05 U ml^{-1}) than SPR (0.1 U ml^{-1}). The instrument is also less complicated with lower cost and the gold rod electrode can be reuse. However, our capacitive system cannot provide real-time response, the capacitance have to be calculated afterwards. Therefore, future development of a real-time capacitive system may help to improve certain aspect of this system such as real-time detection, easy to follow optimization steps and simpler data interpretation. Both immunosensors allow

sensitive and accurate CA 125 determinations compared with the current clinical method. These two immunosensors have the advantages of very low detection limit and permitting a label-free analysis of CA 125. Similar performances were obtained from both SPR and capacitive techniques. This is different from the findings of Labib et al. (2009). In their work SPR system provided higher detection limit than the capacitive system by three order of magnitude. This may be because SPR parameters were not optimized, lower concentration of antibody was employed and/or their analyte has a relatively low molecular weight (cholera toxin; M.W. = 85 kDa). SPR detection is usually utilized for the detection of large molecule (> 100 kDa) (Kawaguchi et al., 2008). The good performance of SPR in our work may due to the large molecule of CA 125 (200 kDa). However, for label-free detection of small molecules (M.W. < 1000) capacitive system may be more useful (Cheng et al., 2001; Loyprasert et al., 2008). Further comparison between the two systems for the detection of small molecules would be an interesting study. In conclusion, these SPR and capacitive-based immunosensors were highly efficient for the clinical determination of CA 125 levels in human serum samples.

Acknowledgements

This project was supported by The Royal Golden Jubilee Ph.D. Program (RGJ) supported by The Thailand Research Fund, Center for Innovation in Chemistry (PERCH-CIC), Trace Analysis and Biosensor Research Center, Graduate School and Faculty of Science, Prince of Songkla University, Hat Yai, Thailand.

References

Andersson, K., Areskoug, D., Hardenborg, E., 1999. J. Mol. Recognit. 12, 310-315.

Bange, A., Halsall, H.B., Heineman, W.R., 2005. Biosens. Bioelectron. 20, 2488-2503.

Berggren, C., Johansson, G., 1997. Anal. Chem. 69, 3651 -3657.

Berggren C., Bjarnason B., Johansson G., 1998. Biosens. Bioelectron. 13, 1061–1068.

Biomerieux® sa, VIDAS® CA 125 II™, France, 2004.

Buck, R.P., Lindneri, E., 1994. Pure Appl. Chem. 66(12), 2527-2536.

Campagnolo, C., Meyers, K. J., Ryan, T., Atkinson, R. C., Chen, Y. T., Scanlan, M. J.,Ritter, G., Old, L. J., Batt, C. A., 2004. J. Biochem. Biophys. Methods. 61, 283-298.

Cheng, Z., Wang, E., Yang, X., 2001. Biosens. Bioelectron. 16, 179-185.

Dai, Z., Yan, F., Chen, J., Ju. H., 2003. Anal. Chem. 75, 5429-5434.

Dudak, F.C., Boyaci, I.H., 2007. Food. Res. Int. 40, 803-807.

Eurachem Working Group, 1998. Fitness for Purpose of Analytical Methods: A Laboratory Guide to Method Validation and Related Topics Eurachem Guide,1st English ed. 1.0. LGC (Teddington) Ltd.

Endo, K., Matsuoka, Y., Nakashima, T., Fujli, S., Kunimatsu, M., Saga, T., Watanabe, Y., Kawamura, Y., Koizumi, M., Konishi, J., Torizuka, K., Bast, R.C., 1988. J. Tumor. Marker. Oncol. 3, 65-71.

Fu, Z., Yan, F., Liu, H., Lin, J., Ju, H., 2008. Biosens. Bioelectron. 23, 1422-1428.

He, Z., Gao, N., Jin, W., 2003. Anal. Chim. Acta. 497, 75-81.

Jiang, D., Tang, J., Liu, B., Yang, P., Shen, X., Kong, J., 2003. Biosens. Bioelectron. 18, 1183-1191.

Kawaguchi, T., Shankaran, D.R., Kim, S.J., Matsumoto, K., Toko, K., Miura N., 2008. Sensor. Actuat. B-Chem. 133, 467-472.

Labib, M., HedstrÖm, M., Amin, M., Mattiasson, B., 2009. Anal.Chim.Acta. 634, 255-261.

Li, Y.J., Bi, L.J., Zhang, X.E., Zhou, Y.F., Zhang, J.B., Chen, Y.Y., Li, W., Zhang. Z.P, 2006. Anal. Bioanal. Chem. 386, 1321-1326.

Limbut, W., Kanatharana, P., Mattiasson, B., Asawatreratanakul ,P., Thavarungkul, P., 2006a. Biosens. Bioelectron. 22(2), 233-240.

Limbut, W., Kanatharana, P., Mattiasson, B., Asawatreratanakul ,P., Thavarungkul, P., 2006b. Anal. Chim. Acta. 561, 55-61.

Lin, J., H., Ju. 2005. Biosensors. Bioelectron. 20, 1461-1470.

Loyprasert, S., Thavarungkul, P., Asawatreratanakul, P., Wongkittisuksa, B., Limsakul,C., Kanatharana, P., 2008. Biosensors. Bioelectron. 24, 78-86.

Marguerite, M., Pinto, M., Larry, H., Bernstein, M.D., Dennis, A., Brogan, M.P., Elaine, C., 1987. Cancer. 59, 218-222.

Mazumdar, S.D., Barlen, B., Kramer, T., Keusgen, M., 2008. J. Microbiol. Meth. 75, 545-550.

Mcquarrie, S.A., Baum, R.P., Niesen, A., Madiyalakan, R., Korz, W., Sykes, T.R., Sykes, C.J., Hor, G., Mcewan, A.J.B., Noujaim, A.A., 1997. Nucl. Med. Commun. 18, 878-886.

R Development Core Team, 2006. R: A Language and Environment for Statistical Computing. R Foundation for Statistical Computing. R Development Core Team, Vienna, Austria, ISBN 3-900051-07-0.

Shankaran D.R., Gobi K. V., Miura N. 2007. Sensor. Actuators B. 121, 158-177.

Tang, D., Yuan, R., Chai, Y., 2006. Anal, Chim. Acta. 564, 158-165.

Taverniers, I., Loose, M.D., Bockstaele, E.V., 2004. TrAC. Trends. Anal. Chem. 23, 535-552.

Teramura, Y., Iwata, H., 2007. Anal. Biochem. 365, 201-207.

Thavarungkul, P., Dawan, S., Kanatharana, P., Asawatreratanakul, P., 2007. Biosensors. Bioelectron. 23, 688-694.

Toyama, S., Shoji A., Yoshida, Y., Yamauchi, S., Ikariyama, Y., 1998. Sensor. Actuat. B. Chem. 52, 65-71.

Triola, M.F., 1998. In: Triola, M.F. (Ed.), Wilcoxon Signed-rank Test for Two 498 Dependents Samples. Addison–Wesley, USA, pp. 655–668.

Weast, R.C., 1974. Hand book of chemistry and physics 55th edition. Ohio, CRC Press.

Wilder, J.L., Pavlik, E., Straughn, J.M., Kirby, T., Higgins, R.V., DePriest, P.D., Ueland, F.R., Kryscio, R.J., Whitley, R.J., Nagell J.V., 2003. Gynecol. Oncol. 89, 233-235.

Wu, J., Fu, Z., Yan, F., Ju, H., 2007. TrAC. Trends. Anal. Chem. 26, 679-688.

Wu, L., Chen, J., Du, D., Ju, H. 2006. Electrochim. Acta. 51, 1208-1214.

Yan, G., Ju, H., Liang, Z., Zhang, T., 1999. J. Immunol. Methods. 225, 1-8.

Yin, T., Wei, W., Yang, L., Gao, X., Gao, Y., 2006. Sensors. Actuat. B. Chem. 117, 286-294.

Yu, Q., Chen, S., Taylor, A.D., Homola, J., Hock, B., Jiang, S., 2005. Sensor. Actuat. B-Chem.107. 193–201. 2005.

Table 1

Tested and optimum conditions of regeneration solution and the flow injection SPR and capacitive immunosensor systems developed to determine CA 125

Parameters	Transducer			
	SPR		Capacitive	
	Tested	Optimum	Tested	Optimum
Regeneration				
Type	25 mM $MgCl_2$ HCl pH 2.50 50 mM glycine-HCl pH 2.50 NaOH pH 10.00	HCl pH 2.50	25 mM $MgCl_2$ 50 mM glycine-HCl NaOH pH 10.00 HCl pH 2.50	pH 2.50
pH of HCl	2.20, 2.40, 2.60, 2.80	2.60	2.20, 2.40, 2.60, 2.80	2.60
Buffer solution				
Type	10 mM Na-PBS pH 7.20 15 mM Na- PBS pH 7.20 15 mM K-PBS pH 7.20 15 mM Tric-HCl pH 7.20	10 mM Na-PBS pH 7.20	15 mM Na-PBS pH 7.20 10 mM K-PBS pH 7.20 10 mM Tric-HCl pH 7.20	
pH	7.00, 7.20, 7.40, 7.60, 7.80	7.20	7.00, 7.20, 7.40, 7.60, 7.80	7.20
Concentration (mM)	5, 10, 15, 20, 25	15	5, 10, 15, 20, 25	15
Flow rate ($\mu l\ min^{-1}$)	5, 10, 15, 20, 25	15	30, 50, 100, 150, 200	100
Sample volume (μl)	200, 250, 300, 350 400	300	150, 200, 250, 300 350	250

Na-PBS= sodium phosphate saline, K-PBS=potassium phosphate saline

Table 2

Comparison of CA 125 concentrations in human serum samples obtained from SPR and capacitive immunosensors with conventional method in hospitals (mean ± SD, n=3)

Sample	CA 125 concentration (U ml^{-1}) (RSD)		
	ELFA	SPR	Capacitive
1	114	115 ± 1 (1%)	118 ± 2 (2%)
2	85	83 ± 1 (1%)	82 ±2 (2%)
3	106	109.2 ± 0.4 (0.4%)	108 ± 3 (3%)
4	177	175 ± 4 (2%)	177 ±5 (3%)
5	33	30 ± 1 (3%)	33 ± 1 (3%)
6	113	115 ± 2 (2%)	110 ± 2 (2%)
7	99	98 ± 2 (2%)	101 ± 4 (4%)
8	32	33 ± 1 (3%)	30 ± 1 (3%)
9	662	658 ± 26 (4%)	663 ± 30 (5%)
10	31	28 ± 1 (4%)	29.5 ± 0.3 (1%)

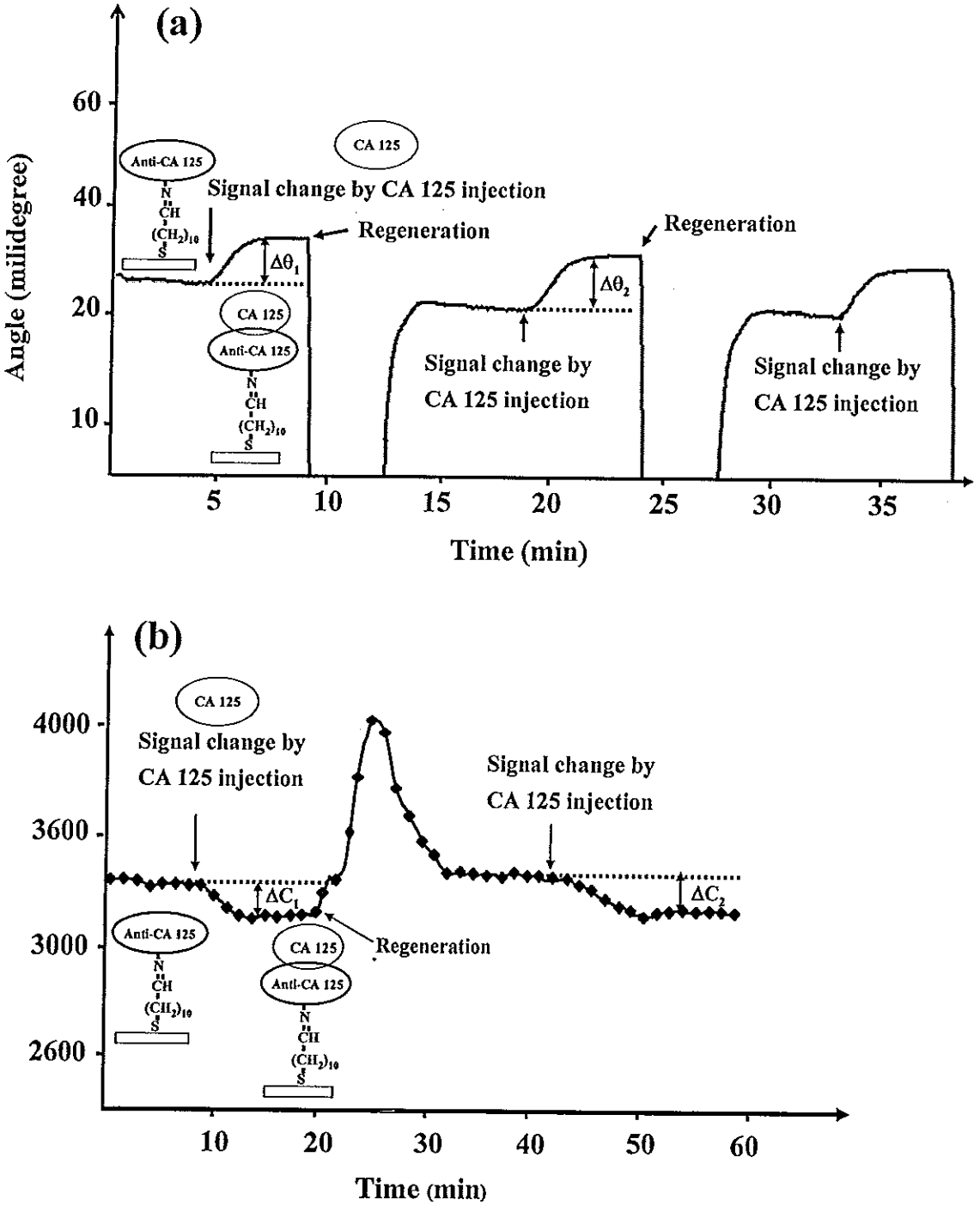

Fig. 1 (a) SPR sensorgram obtained from the injections of 10 U ml^{-1} CA 125 over the immobilized anti-CA 125 resulting in the increase of SPR angle ($\Delta\theta$). (b) Capacitive signal obtained from the injections of 5 U ml^{-1} CA 125, causing the capacitance to decrease (ΔC).

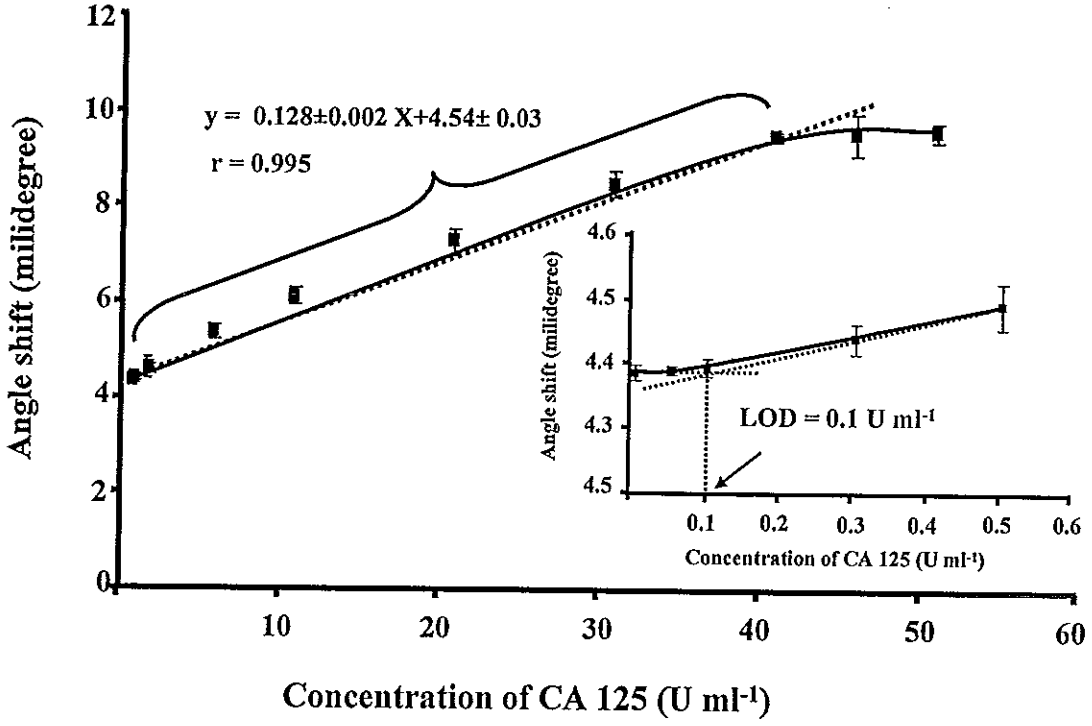

Fig. 2 Calibration curve for CA 125 obtained with the label-free immunosensor under optimal conditions of SPR immunosensor.

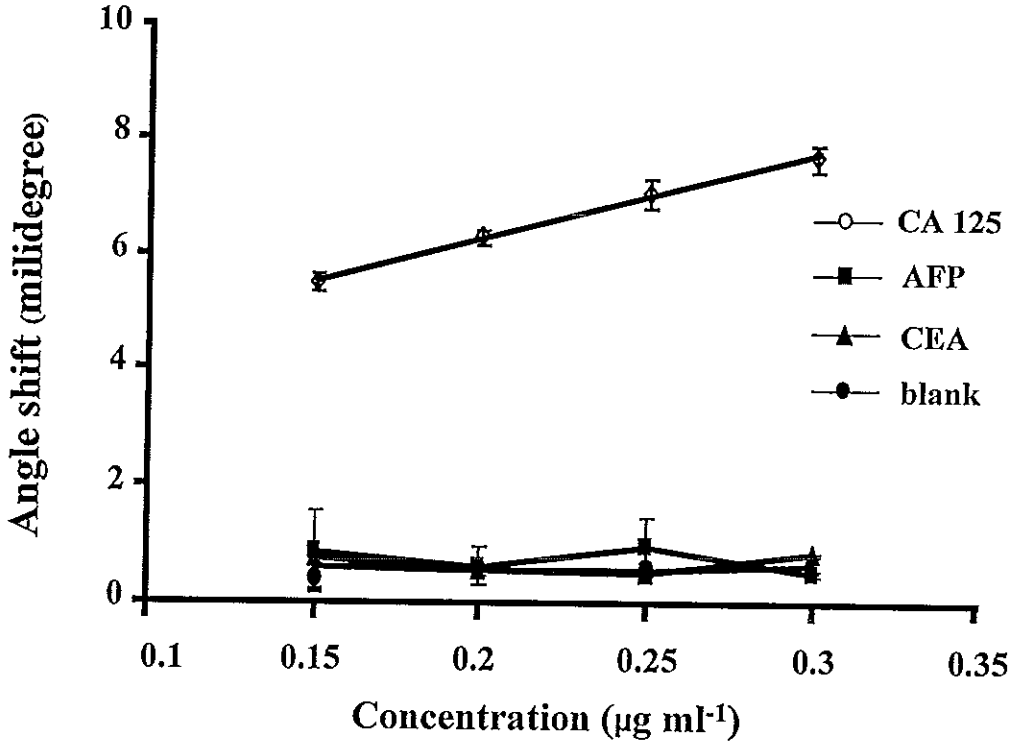

Fig.3. Response change *vs* the concentration of CA 125, CEA, AFP, and blank (running buffer) in SPR system. Binding between anti-CA 125 and CA 125 was dissociated with HCl pH 2.60 before injection of a new CA 125.

VITAE

Name Miss Siriwan Suwansa-ard

Student ID 4823016

Education Attainment

Degree	Name of Institution	Year of Graduation
Bachelor of Science (Education), Second Class Honors	Prince of Songkla University	2000
Master of Science (Analytical Chemistry)	Prince of Songkla University	2003

Scholarship Award during Enrolment

1. The Royal Golden Jubilee Ph.D. Program (RGJ) supported by The Thailand Research Fund
2. Center for Innovation in Chemistry (PERCH-CIC)
3. Rajamangala University of Technology Thanyaburi

List of Publications and Proceedings

Publications

1. Siriwan Suwansa-ard, Yun Xiang, Ralph Bash, Panote Thavarungkul, Proespichaya Kanatharana, Joseph Wang. 2008. Prussian Blue Dispersed Sphere Catalytic Labels for Amplified Electronic Detection of DNA. *Electroanalysis* **20**(3): 308 – 312.
2. Siriwan Suwansa-ard, Proespichaya Kanatharana, Punnee Asawatreratanakul, BooncharoenWongkittisuksa, Chusak Limsakul, Panote Thavarungkul. 2009. Comparison of surface plasmon resonance and capacitive immunosensors for cancer antigen 125 detection in human serum samples. *Biosensor and Bioelectronic*. In press.

Proceedings

Oral Presentations

1. Siriwan Suwansa-ard, Yun Xiang, Ralph Bash, Panote Thavarungkul, Proespichaya Kanatharana, Joseph Wang. 2008. Prussian-Blue Dispersed Polymeric Sphere Catalytic Labels for Amplification of DNA Detection. RGJ-Ph.D Congree IX. Jomtein Plam Beach Pattaya, Chonburi. 4^{th}-6^{th} April, 2008.

Poster Presentations

1. Suchera Loyprasert, Siriwan Suwansa-ard, Supaporn Dawan, Proespichaya Kanatharana, Panote Thavarungkul. 2008. Nanoparticles-Enhanced Capacitive Detection of Affinity Binding. 1^{st} Regional Electrochemistry Meeting of South-East Asia REMSEA, National University of Singapore, 5^{th} – 7^{th} August, 2008.
2. Siriwan Suwansa-ard, Proespichaya Kanatharana, Punnee Asawatreratanakul, Panote Thavarungkul. 2009. Label-free surface plasmon resonance immunosensor for human serum albumin detection. Pure and Applied Chemistry International Conference PACCON 2009, Naresuan University, Phitsanulok, Thailand. 14^{th}-16^{th} January, 2009.
3. Siriwan Suwansa-ard, Proespichaya Kanatharana, Punnee Asawatreratanakul, Panote Thavarungkul. 2009. Label-free surface plasmon resonance immunosensor for cancer antigen 125 detection in human serum samples. The International Congress for Innovation in Chemistry PERCH-CIC Congress VI., Jomtein Plam Beach Hotel & Resort, Pattaya, Thailand. 3^{rd}-6^{th} May, 2009.